

*In situ* forming hydrogels for  
intra-articular delivery of celecoxib:  
from polymer design to *in vivo* studies

**Audrey Petit**

2014

The printing of this thesis was partly financially supported by:

Ingell Labs

Branching Tree

Corbion

Utrecht Institute for Pharmaceutical Sciences (UIPS)

***In situ* forming hydrogels for intra-articular delivery of celecoxib:  
from polymer design to *in vivo* studies**

by Audrey Petit

PhD thesis with summary in Dutch and French

Department of Pharmaceutics, Utrecht University, The Netherlands

Ingell BV, The Netherlands

May 2014

ISBN: 978-94-6203-563-8

Copyright © 2014 Audrey Petit. All rights reserved. No parts of this thesis may be reproduced or transmitted in any form or by any means, without written permission by the author and the publisher holding the copyrights of the published articles.

Cover and invitation card designed by Martin Dubiez

Printed by CPI – Royal Wöhrmann - Zutphen

***In situ* forming hydrogels for  
intra-articular delivery of celecoxib:  
from polymer design to *in vivo* studies**

*In situ* vormende hydrogelen voor  
de afgifte van celecoxib in gewrichten:  
van polymeerontwerp naar *in vivo* experimenten  
(met een samenvatting in het Nederlands)

Hydrogels formés *in situ* pour  
la délivrance intra-articulaire de célécoxib:  
de la conception des polymères aux études *in vivo*  
(avec un résumé en français)

**Proefschrift**

ter verkrijging van de graad van doctor aan de Universiteit Utrecht op gezag  
van de rector magnificus, prof.dr. G.J. van der Zwaan, ingevolge het besluit  
van het college voor promoties in het openbaar te verdedigen op woensdag 7  
mei 2014 des middags te 4.00 uur

door

**Audrey Petit**

geboren op 5 juni 1980 te Baccarat, Frankrijk

**Promotor:**

Prof.dr.ir. W.E. Hennink

**Co-promotoren:**

Dr.ir. T. Vermonden

Dr. L.G.J. de Leede

*‘Le premier était de ne recevoir jamais aucune chose pour vraie, que je ne la connusse évidemment être telle : c’est-à-dire, d’éviter soigneusement la précipitation et la prévention ; et de ne comprendre rien de plus en mes jugements, que ce qui se présenterait si clairement et si distinctement à mon esprit, que je n’eusse aucune occasion de le mettre en doute.*

*Le second, de diviser chacune des difficultés que j’examinerais, en autant de pour celles qu’il se pourrait, et qu’il serait requis pour les mieux résoudre.*

*Le troisième, de conduire par ordre mes pensées, en commençant par les objets les plus simples et les plus aisés à connaître, pour monter peu à peu, comme par degrés, jusqu’à la connaissance des plus composés ; et supposant même de l’ordre entre ceux qui ne se précèdent point naturellement les uns les autres.*

*Et le dernier, de faire partout des dénombrements si entiers, et des revues si générales, que je fusse assuré de ne rien omettre.’*

**Descartes**

**Discours de la méthode**

*Pour bien conduire sa raison, et chercher la vérité dans les sciences*  
(1637)



## Table of contents

<b>CHAPTER 1</b>	General introduction	9
<b>CHAPTER 2</b>	Modulating rheological and degradation properties of temperature-responsive gelling systems composed of blends of a PCLA-PEG-PCLA triblock copolymer and its fully hexanoyl-capped derivative	25
<b>CHAPTER 3</b>	Effect of polymer composition on rheological and degradation properties of temperature-responsive gelling systems composed of acyl-capped PCLA-PEG-PCLA	61
<b>CHAPTER 4</b>	<i>In situ</i> forming acyl-capped PCLA-PEG-PCLA triblock copolymer-based hydrogels	105
<b>CHAPTER 5</b>	Celecoxib-loaded acetyl-capped PCLA-PEG-PCLA thermogels: <i>in vitro</i> and <i>in vivo</i> release behaviour and intra-articular biocompatibility	139
<b>CHAPTER 6</b>	Sustained intra-articular release of celecoxib from <i>in situ</i> forming gels made of acetyl-capped PCLA-PEG-PCLA triblock copolymers in horses	175
<b>CHAPTER 7</b>	Summary and perspectives	207
<b>APPENDICES</b>	Nederlandse samenvatting Résumé français Curriculum vitae List of publications Acknowledgments	223







## CHAPTER 1

# General introduction



## **1. Local and sustained drug delivery**

The majority of drugs, being developed and marketed by the pharmaceutical industry are formulated as immediate-release tablets or capsules for oral administration [1-5]. Besides, there is a large number of drugs or drug candidates that have potential efficacy in therapies, but poor effects are often observed after oral administration due to a low bioavailability and the rate and extent at which the drugs are deposited in the target tissues. Another issue regarding the oral delivery route of drugs is the clinical safety. Toxicity is often observed due to high systemic concentrations required to obtain a therapeutic effective drug concentration at the target side, while frequent administrations to maintain the local drug concentration at sufficient level for prolonged periods lead to fluctuating plasma levels and a lack of patient compliance [1].

Drug delivery systems (DDSs) that release the loaded active pharmaceutical ingredients (APIs) in a controlled and sustained manner with less adverse effects have been developed and account for ~80 new approvals by the Food and Drug Administration (FDA) per year [1,6-9]. Furthermore, DDSs made of poly(lactide-*co*-glycolide) (PLGA) in the form of injectable depots or microspheres have entered the market and led to important pharmaceutical products like Lupron Depot<sup>®</sup>, Zoladex<sup>®</sup>, Decapeptyl<sup>®</sup>, Eligard<sup>®</sup>, Enantone<sup>®</sup>, Trenantone<sup>®</sup>, Nutropin Depot<sup>®</sup>, Sandostatin LAR<sup>®</sup> and Profact<sup>®</sup> [7].

Over the last decades, DDSs that are easy to inject have been developed for local delivery to reach high local effective drug concentrations and less systemic absorption, hence less adverse effects. The administration routes can be, amongst others, subcutaneous (s.c.), intramuscular, intra-tumoral, intra-ocular, and intra-articular (i.a.). So, local delivery can serve in cancer treatments, inflammation treatments, anaesthesia, and regenerative treatments of cartilage, bone and nerve tissues when combined with tissue engineering constructs to deliver growth factors [8-16].

## **2. Osteoarthritis and local and sustained drug delivery**

### *2.1. Clinical manifestations, epidemiology and pathogenesis*

Osteoarthritis (OA) is a common joint disease of which the symptoms are pain and loss of joint functionality, mainly involving hips or knees and

leading to walking-disability [17-19]. OA prevalence increases with risk factors such as demographic (age, gender, ethnicity), and genetic factors, but also with modifiable factors like obesity and joint injury [17,20-22]. Because of ageing of the population and increasing prevalence of obesity, the OA prevalence is rapidly increasing [20,23,24]. In the United States population, the lifetime risk of developing symptomatic knee and hip OA has been estimated recently at ~45 % [25] and ~25 % [26], respectively.

The pathogenesis of OA is complex and multifactorial, and is likely a combination of different genetic, biochemical and biomechanical factors leading to a high degree of degradation of the cartilage [19,27]. This degradation has been linked to a disequilibrium between anabolic and catabolic processes in the joint, by for instance the upregulation of catabolic enzymes such as matrix metalloproteinases (MMPs) and aggrecanases, and the expression of pro-inflammatory cytokines such as interleukin 1B (IL-1B) and tumour necrosis factor  $\alpha$  (TNF- $\alpha$ ) [27-31].

Mainly because the pathogenesis of OA is poorly understood, there are no disease modifying osteoarthritic drugs (DMOADs) available yet [32,33], and consequently OA is presently a non-curable disease, which often requires total joint replacement surgery [27].

## *2.2. Palliative treatments of osteoarthritis*

Because OA patients experience pain associated with joint inflammation [27,34], current treatments are mainly based on oral administration of pain medication like Celebrex®, which are tablets of the non-steroidal anti-inflammatory drug (NSAID) celecoxib, which inhibits the enzyme cyclooxygenase 2 (COX-2) [20,27,34-38]. Oral administration of Celebrex® does not target specifically the diseased joints but acts systemically and thereby leads to side-effects like toxicity on the myocardial muscle [37,39-41].

I.a. injection of Kenalog® (an aqueous suspension containing triamcinolone acetonide, a corticosteroid) allows for local delivery into the diseased joints while minimizing systemic exposure [42]. However, this formulation provides limited effects since the rapid turnover of the drug in the synovial fluid leads to sub-therapeutic local drug concentrations after ~1 week [20,43]. Therefore, multiple i.a. injections are required [44-46], which can cause cartilage and joint damage [20,37,46]. Better performing local

DDSs for OA should provide sustained drug concentrations for longer duration, and thus require less frequent administrations [47,48].

### *2.3. Experimental treatment of osteoarthritis with drug delivery systems*

Injectable DDSs developed for controlled i.a. release are mainly based on liposomes or polymeric nano-/micro-particles [49-54], but they show limitations that hinder their clinical applicability (e.g., low encapsulation efficiency, high burst, incomplete drug recovery, non-straightforward pharmaceutical manufacturing). A highly concentrated solution (400 mg/ml) of celecoxib in poly(ethylene glycol) 400 (PEG<sub>400</sub>) is presently under investigation as an *in situ* forming depot for injection into equine joint cavities [55]. After injection in an aqueous medium like the synovial fluid, PEG<sub>400</sub> is diluted in the medium and celecoxib precipitates/crystallizes; hence, its sustained release is achieved by slow dissolution of the drug depot/crystals [55]. Even though local celecoxib concentrations in time after i.a. injection have not been evaluated, this *in situ* forming system shows the potential as depot material for i.a. delivery but does not provide possibilities to modulate release rates and durations. Also, the administration of the system led to granulomatous synovitis 10 days after injection, which warrants investigations on better performing systems to guarantee better tolerability.

## **3. *In situ* forming gels based on polyester/PEG copolymers**

### *3.1. Mechanism of sol-to-gel transition*

DDSs based on block copolymers of polyester and PEG that form *in situ* depots are under investigation for biomedical and pharmaceutical applications because of their ease of injection (due to low viscosity and homogeneity), their tolerability after s.c. injection and their biodegradability [56-61]. One stimulus for the formation of *in situ* depots is a temperature trigger: the DDSs are sols at room temperature and upon injection in the body at 37 °C they transform into gels. The mechanism responsible for the sol-to-gel transition of aqueous systems based on polyester/PEG block copolymers has been unravelled with <sup>13</sup>C NMR spectroscopy [58,62-67]. In the sol state, the polyester/PEG copolymers form micelles with a hydrophobic polyester core and a hydrated PEG shell. These micelles are flower-like micelles if the copolymers are ABA triblock copolymers with PEG as B-block

flanked by two hydrophobic polyester A-blocks. In the gel state, significant phase mixing between the PEG- and polyester-blocks occurs. Thereby, the shell-core structure of the micelles is partially destroyed and hydrophobic interactions are enhanced leading to aggregation of the micelles and mesoscopical phase-separation. As the temperature further increases, hydrophobic interactions are further enhanced causing phase-separation at a macroscopic level [58,67-71].

### 3.2 Drug release and clinical applications

Aqueous systems based on polyester/PEG block copolymers offer possibilities for the encapsulation of drugs and ease of modulation of their release kinetics [72-74]. In particular, they have been shown to be suitable for the solubilisation of hydrophobic drugs [72-75] like, for instance, the anticancer drug paclitaxel [72]. A temperature-responsive gelling system based on poly(lactide-*co*-glycolide)-*b*-poly(ethylene glycol)-*b*-poly(lactide-*co*-glycolide) (PLGA-PEG-PLGA) has already found clinical applications for the release of this drug [76]. The release of paclitaxel from this system is mediated by a combination of diffusion and chemical polymer degradation, which takes approximately six weeks *in vitro* as well as *in vivo* [72-74].

For some applications, longer release durations are however required, and to slow down hydrolysis and increase the degradation duration, PLGA blocks have been replaced by poly( $\epsilon$ -caprolactone-*co*-lactide) (PCLA) blocks. Systems based on PCLA-PEG-PCLA are indeed stable for longer time depending on the ratio of caproyl units (CL) to lactoyl units (LA). For instance, systems composed of PCLA blocks containing 70 mol% CL showed complete degradation in about six months [77,78].

### 3.3. Acylation of hydroxyl-terminated polyester-PEG-polyester copolymers

Interestingly, modification of the terminal hydroxyl groups of polyester-PEG-polyester copolymers allows modulating the sol-to-gel transition temperature [67,79]. As an example, Jo and co-workers [79] reported the effect of modifying the terminal hydroxyl end groups of PCLA-PEG-PCLA, with hexanoyl and lauroyl aliphatic groups. Whereas a system of hydroxyl triblock copolymer of 20 wt% in water was transparent sols until 40 °C, the fully acylated triblock copolymer was insoluble in water. It was further

shown that, depending on the degree of acylation, temperature-responsive gelling systems can be prepared: acylated triblock copolymer with 50% hexanoyl modification in water of 20 wt% had a sol-to-gel transition at 30 °C making this system suitable as injectable system for biomedical applications. Investigations on the effect of the acylation degree on the degradation time and mechanism have yet to be carried out.

#### 4. Aim and outline of this thesis

The aim of the work described in this thesis is to design an *in situ* forming gel based on acylated poly( $\epsilon$ -caprolactone-*co*-lactide)-*b*-poly(ethylene glycol)-*b*-poly( $\epsilon$ -caprolactone-*co*-lactide) (PCLA-PEG-PCLA) for the local and sustained release of celecoxib in the joint cavity, which can be used for the treatment of OA. Celecoxib is a registered drug for the oral treatment of OA for which daily administration is required and concerns on its toxicity on the myocardial muscle have risen [37, 40-41]. Celecoxib is therefore the drug of choice for preparing DDSs for sustained and local release in the treatment of OA. In particular, the focus of this thesis is on the design of a celecoxib-loaded gel with good tolerability after i.a. administration as well the ability for local and sustained release of celecoxib for more than 10 days, which would allow less frequent administration than the systems currently available for the i.a. treatment of OA [20,42,55].

**Chapter 2** describes a novel approach to tailor the sol-to-gel transition temperature and degradation properties of temperature-responsive gelling systems. Blending uncapped (i.e. hydroxyl-terminated) and fully hexanoyl-capped PCLA-PEG-PCLA triblock copolymers having the same backbone composition results in a practical method to modulate gel properties of the systems. *In vitro* degradation of these systems at 37 °C and pH 7.4 occurs by gel dissolution while enrichment of the residual gels in CL is caused by preferential leaching out of CL-poor polymer chains.

**Chapter 3** investigates the parameters to modulate degradation properties of aqueous systems composed of acylated PCLA-PEG-PCLA. Subtle changes in the polymer composition, and in particular in the CL content, have significant effect on the degradation/dissolution properties. In addition, it is demonstrated that degradation of the systems is retarded by crystallization of the CL-rich domains and degradation/dissolution time of

the gels can be varied between 3 and 9 months depending on the CL sequence length.

**Chapter 4** describes the end capping of PCLA-PEG-PCLA with triiodobenzoyl groups as an approach to prepare a radiopaque *in situ* forming gel. This chapter shows that the *in situ* forming gel containing a triiodobenzoyl-capped polymer is *in vivo* visible for 90 and 30 days after s.c. and i.a. administration in rats, respectively. Although *in vitro* and s.c. degradation occurs for similar duration, *in vitro* degradation occurs exclusively by dissolution whereas *in vivo* likely enzymatic degradation is involved as well. Also, it is demonstrated that 50  $\mu$ l of a similar gel based on acetyl-capped PCLA-PEG-PCLA is well tolerated after i.a. injection.

**Chapter 5** describes the use of temperature-responsive gelling systems composed of an acetyl-capped PCLA-PEG-PCLA polymer to release celecoxib in a sustained manner *in vitro* as well as *in vivo*. Celecoxib-releasing systems are prepared with different drug loadings and it is demonstrated that the release is mediated by polymer dissolution *in vitro* and hence can be modulated by the polymer composition. In addition, this chapter shows that after single s.c. injection in rats, celecoxib plasma concentrations are detectable for 4-8 weeks, and that after single i.a. injection of 50  $\mu$ l, the system is well tolerated as no signs of cartilage damage are observed.

**Chapter 6** describes the use of celecoxib-loaded systems for i.a. delivery of celecoxib in equine joint cavities. The systems are loaded with two doses of celecoxib (50 mg/g and 260 mg/g), and sterilized by autoclaving without significant polymer hydrolysis and have low endotoxin content. After i.a. administration of 2 ml, the systems induce a transient inflammation for 72 hours of a similar extent than that of the commercially available hyaluronic acid gel, Hyonate®. Importantly, no indication of cartilage degradation is observed, and thus the gels are well tolerated. Celecoxib is detected in synovial fluid for 4 weeks after injection while in plasma its concentration is, depending on the drug loading, 150 to 330 times lower than in synovial fluid for the first 3 days after administration and thereafter dropped below the detection limit.

This thesis is concluded with a summarizing discussion (**Chapter 7**). With the chapters of this thesis as guiding principle, the use of *in situ*



forming gels based on acylated PCLA-PEG-PCLA triblock copolymers for i.a. delivery of drugs is discussed. Furthermore, future perspectives of these hydrogel systems for treatment of OA are discussed.

## References

- [1] Kidane A, Bhatt PP. Recent advances in small molecule drug delivery. *Curr Opin Chem Biol* 2005;9:347-351.
- [2] Han C, Wang B. Factors that impact the developability of drug candidates: an overview. In: B Wang, TJ Siahaan, R Soltero (Eds.), *Drug Delivery: Principles and Applications*, John Wiley & Sons, Inc. 2005:1-14.
- [3] Prentis RA, Lis Y, Walker SR. Pharmaceutical innovation by the seven UK-owned pharmaceutical companies (1964-1985). *Br J Clin Pharmacol* 1988;25:387-396.
- [4] Kola I, Landis J. Can the pharmaceutical industry reduce attrition rates? *Nat Rev Drug Discov* 2004;3:711-716.
- [5] Kwong E, Higgins J, Templeton AC. Strategies for bringing drug delivery tools into discovery. *Int J Pharm* 2011;412:1-7.
- [6] Couto S, Perez-Breva L, Saraiva P, Cooney CL. Lessons from innovation in drug-device combination products. *Adv Drug Deliv Rev* 2012;64:69-77.
- [7] Wischke C, Shwendeman SP. Principles of encapsulating hydrophobic drugs in PLA/PLGA microparticles. *Int J Pharm* 2008;364:298-327.
- [8] Allen TM, Cullis PR. Drug delivery systems: entering the mainstream. *Science* 2004;303:1818-1822.
- [9] Barenholz YC. Doxil® - the first FDA-approved nano-drug: lessons learned. *J Control Release* 2012;160:117-134.
- [10] Bhattarai N, Gunn J, Zhang M. Chitosan-based hydrogels for controlled, localized drug delivery. *Adv Drug Deliv Rev* 2010;62:83-99.
- [11] Weiniger CF, Golovanevski L, Domb AJ, Ickowicz D. Extended release formulations for local anaesthetic agents. *Anaesthesia* 2012;67:906-916.
- [12] Woodrow AK, Bennett KM, Lo DD. Mucosal vaccine design and delivery. *Annu Rev Biomed Eng* 2012;14:17-46.
- [13] Wachsmann P, Lamprecht A. Polymeric nanoparticles for the selective therapy of inflammatory bowel disease. *Methods Enzymol* 2012;508:377-397.
- [14] Patel T, Zhou J, Piepmeier JM, Saltzman WM. Polymeric nanoparticles for drug delivery to the central nervous system. *Adv Drug Deliv Rev* 2012;64:701-705.

- [15] Beck-Broichsitter M, Merkel OM, Kissel T. Controlled pulmonary drug and gene delivery using polymeric nano-carriers. *J Control Release* 2012;161:214-224.
- [16] Wolinsky JB, Colson YL, Grinstaff MW. Local drug delivery strategies for cancer treatment: gels, nanoparticles, polymeric films, rods, and wafers. *J Control Release* 2012;159:14-26.
- [17] Busija L, Bridgett L, Williams SRM, Osborne RH, Buchbinder R, March L, Fransen M. Osteoarthritis. *Best Pract Res Clin Rheumatol* 2010;24:757-768.
- [18] Dillon CF, Rasch EK, Gu Q, Hirsch R. Prevalence of knee osteoarthritis in the United States: arthritis data from the Third National Health and Nutrition Examination Survey 1991-94. *J Rheumatol* 2006;33:2271-2279.
- [19] Goldring MB, Otero M. Inflammation in osteoarthritis. *Curr Opin Rheumatol* 2011;23:471-478.
- [20] Hunter DJ. In the clinic. Osteoarthritis. *Ann Intern Med* 2007;147:ITC18-1-ITC18-16.
- [21] Suri P, Morgenroth DC, Hunter DJ. Epidemiology of osteoarthritis and associated comorbidities. *P M R* 2012;4:S10-S19.
- [22] Zhang Y, Jordan JM. Epidemiology of osteoarthritis. *Rheum Dis Clin North Am* 2008;34:515-529.
- [23] Praemer A, Furner S, Rice DP. Musculoskeletal conditions in the United States. *Amer Acad of Orthopaedic Surgeons*; 1 edition 1999.
- [24] Praemer A, Furner S, Rice D. Musculoskeletal system; Wounds and injuries. *Amer Acad of Orthopaedic Surgeons*; 1 edition 1992.
- [25] Murphy L, Schwartz TA, Helmick CG, Renner JB, Tudor G, Koch G, Dragomir A, Kalsbeek WD, et al. Lifetime risk of symptomatic knee osteoarthritis. *Arthritis Rheum* 2008;59:1207-1213.
- [26] Murphy LB, Helmick CG, Schwartz TA, Renner JB, Tudor G, Koch GG, et al. One in four people may develop symptomatic hip osteoarthritis in his or her lifetime, *Osteoarthritis Cartilage* 2010;18:1372-1379.
- [27] van der Kraan PM. Osteoarthritis year 2012 in review: biology. *Osteoarthritis Cartilage* 2012;20:1447-1450.

*Chapter 1*

---

- [28] Wang M, Shen J, Jin H, Im H, Sandy J, Chen D. Recent progress in understanding molecular mechanisms of cartilage degeneration during osteoarthritis. *Ann N Y Acad Sci* 2011;1240:61-69.
- [29] Beekhuizen M, Bastiaansen-Jenniskens YM, Koevoet W, Saris DBF, Dhert WJA, Creemers LB, et al. Osteoarthritic synovial tissue inhibition of proteoglycan production in human osteoarthritic knee cartilage: establishment and characterization of a long-term cartilage-synovium coculture. *Arthritis Rheum* 2011;63:1918-1927.
- [30] Fukai A, Kamekura S, Chikazu D, Nakagawa T, Hirata M, Saito T, et al. Lack of a chondroprotective effect of cyclooxygenase 2 inhibition in a surgically induced model of osteoarthritis in mice. *Arthritis Rheum* 2012;64:198-203.
- [31] Yoo S, Park B, Yoon H, Lee J, Song J, Kim HA, et al. Calcineurin modulates the catabolic and anabolic activity of chondrocytes and participates in the progression of experimental osteoarthritis. *Arthritis Rheum* 2007;56:2299-2311.
- [32] Matthews GL, Hunter DJ. Emerging drugs for osteoarthritis. *Expert Opin Emerging Drugs* 2011;16:479-491.
- [33] Buckwalter JA, Stanish WD, Rosier RN, Schenck RC Jr, Dennis DA, Coutts RD. The increasing need for nonoperative treatment of patients with osteoarthritis. *Clin Orthop Relat Res* 2001;385:36-45.
- [34] de Lange-Brokaar BJE, Ioan-Facsinay A, van Osch GJVM, Zuurmond A, Schoones J, Toes REM, et al. Synovial inflammation, immune cells and their cytokines in osteoarthritis: a review. *Osteoarthritis Cartilage* 2012;20:1484-1499.
- [35] Argoff CE. Recent developments in the treatment of osteoarthritis with NSAIDs. *Curr Med Res Opin* 2011;27:1315-1327.
- [36] Ross SM. Osteoarthritis of the knee: an integrative therapies approach. *Holist Nurs Pract* 2011;25:327.
- [37] Recommendations for the medical management of osteoarthritis of the hip and knee: 2000 update. *Arthritis Rheum* 2000;43:1905-1915.
- [38] Hochberg MC. Osteoarthritis year 2012 in review: clinical. *Osteoarthritis Cartilage* 2012;20:1465-1469.
- [39] Altman RD, Barthel HR. Topical Therapies for Osteoarthritis. *Drugs* 2011;71.

- [40] Roth SH, Anderson S. The NSAID dilemma: managing osteoarthritis in high-risk patients. *Phys Sportsmed* 2011;39:62.
- [41] Gong L, Thorn CF, Bertagnolli MM, Grosser T, Altman RB, Klein TE. Celecoxib pathways: pharmacokinetics and pharmacodynamics. *Pharmacogenet Genomics* 2012;22:310-318.
- [42] Bahadir C, Onal B, Dayan V, Güner N. Comparison of therapeutic effects of sodium hyaluronate and corticosteroid injections on trapeziometacarpal joint osteoarthritis. *Clin Rheumatol* 2009;28:529-533.
- [43] Xavier A. Injections in the treatment of osteoarthritis. *Best Pract Res Clin Rheumatol* 2001;15:609-626.
- [44] Jiang D, Zou J, Huang L, Shi X, Zhu X, Wang G, Yang H. Efficacy of intra-articular injection of celecoxib in a rabbit model of osteoarthritis. *Int J Mol Sci* 2010;11:4106-4113.
- [45] Céleste C, Ionescu M, Poole AR, Laverty S. Repeated intra-articular injections of triamcinolone acetonide alter cartilage matrix metabolism measured by biomarkers in synovial fluid. *J Orthop Res* 2005;23:602-610.
- [46] Bellamy N, Campbell J, Robinson V, Gee T, Bourne R, Wells G. Intra-articular corticosteroid for treatment of osteoarthritis of the knee (Review). *Cochrane Database Syst Rev* 2006;19:CD005328.
- [47] Gerwin N, Hops C, Lucke A. Intra-articular drug delivery in osteoarthritis. *Adv Drug Deliv Rev* 2006;58:226-242.
- [48] Edwards SHR. Intra-articular drug delivery: The challenge to extend drug residence time within the joint. *Vet J* 2011;190:15-21.
- [49] Liggins RT, Cruz T, Min W, Liang L, Hunter WL, Burt HM. Intra-articular treatment of arthritis with microsphere formulations of paclitaxel: biocompatibility and efficacy determinations in rabbits. *Inflammation Res* 2004;53:363-372.
- [50] Tunçay M, Çaliş S, Kaş HS, Ercan MT, Peksoy I, Hincal AA. Diclofenac sodium incorporated PLGA (50:50) microspheres: formulation considerations and *in vitro/in vivo* evaluation. *Int J Pharm* 2000;195:179-188.
- [51] Mountziaris P, Sing D, Chew S, Tzouanas S, Lehman E, Kasper F, et al. Controlled release of anti-inflammatory siRNA from biodegradable polymeric microparticles

- intended for intra-articular delivery to the temporomandibular joint. *Pharm Res* 2011;28:1370-1384.
- [52] Thakkar H, Sharma RK, Mishra AK, Chuttani K, Murthy RSR. Efficacy of chitosan microspheres for controlled intra-articular delivery of celecoxib in inflamed joints. *J Pharm Pharmacol* 2004;56:1091-1099.
- [53] Butoescu N, Jordan O, Doelker E. Intra-articular drug delivery systems for the treatment of rheumatic diseases: a review of the factors influencing their performance. *Eur J Pharm Biopharm* 2009;73:205-218.
- [54] Panusa A, Selmin F, Rossoni G, Carini M, Cilurzo F, Aldini G. Methylprednisolone-loaded PLGA microspheres: a new formulation for sustained release via intra-articular administration. A comparison study with methylprednisolone acetate in rats. *J Pharm Sci* 2011;100:4580-4586.
- [55] Larsen SW, Frost AB, Østergaard J, Thomsen MH, Jacobsen S, Skonberg C, et al. *In vitro* and *in vivo* characteristics of celecoxib *in situ* formed suspensions for intra-articular administration. *J Pharm Sci* 2011;100:4330-4337.
- [56] van Tomme SR, Storm G, Hennink WE. *In situ* gelling hydrogels for pharmaceutical and biomedical applications. *Int J Pharm* 2008;355:1-18.
- [57] Nguyen MK, Lee DS. Injectable biodegradable hydrogels. *Macromol Biosci* 2010;10:563-579.
- [58] Yu L, Ding J. Injectable hydrogels as unique biomedical materials. *Chem Soc Rev* 2008;37:1473-1481.
- [59] Li Y, Rodrigues J, Tomás H. Injectable and biodegradable hydrogels: gelation, biodegradation and biomedical applications. *Chem Soc Rev* 2012;41:2193-2221.
- [60] Vermonden T, Censi R, Hennink WE. Hydrogels for protein delivery. *Chem Rev* 2012;112:2853-2888.
- [61] Park MH, Joo MK, Choi BG, Jeong B. Biodegradable thermogels. *Acc Chem Res* 2012;45:424-433.
- [62] Hwang MJ, Suh JM, Bae YH, Kim SW, Jeong B. Caprolactonic poloxamer analog: PEG-PCL-PEG. *Biomacromolecules* 2005;6:885-890.

- [63] Jeong B, Kibbey MR, Birnbaum JC, Won Y, Gutowska A. Thermogelling biodegradable polymers with hydrophilic backbones: PEG-*g*-PLGA. *Macromolecules* 2000;33:8317-8322.
- [64] Jeong B, Wang L, Gutowska A. Biodegradable thermoreversible gelling PLGA-*g*-PEG copolymers. *Chem Commun* 2011:1516-1517.
- [65] Lee DS, Shim MS, Kim SW, Lee H, Park I, Chang T. Novel thermoreversible gelation of biodegradable PLGA-*block*-PEO-*block*-PLGA triblock copolymers in aqueous solution. *Macromol Rapid Commun* 2011;22:587-592.
- [66] Yu L, Chang G, Zhang H, Ding J. Temperature-induced spontaneous sol-gel transitions of poly(D,L-lactic acid-*co*-glycolic acid)-*b*-poly(ethylene glycol)-*b*-poly(D,L-lactic acid-*co*-glycolic acid) triblock copolymers and their end-capped derivatives in water. *J Polym Sci A Polym Chem* 2007;45:1122-1133.
- [67] Yu L, Zhang H, Ding J. A subtle end-group effect on macroscopic physical gelation of triblock copolymer aqueous solutions. *Angew Chem Int Ed Engl* 2006;45:2232-2235.
- [68] Moretton M, Chiappetta D, Sosnik A. Cryoprotection-lyophilization and physical stabilization of rifampicin-loaded flower-like polymeric micelles. *J R Soc Interface* 2012;9:487-502.
- [69] Gong C, Shi S, Wu L, Gou M, Yin Q, Guo Q, et al. Biodegradable *in situ* gel-forming controlled drug delivery system based on thermosensitive PCL-PEG-PCL hydrogel. Part 2: sol-gel-sol transition and drug delivery behaviour. *Acta Biomater* 2009;5:3358-3370.
- [70] Bae SJ, Suh JM, Sohn YS, Bae YH, Kim SW, Jeong B. Thermogelling poly(caprolactone-*b*-ethylene glycol-*b*-caprolactone) aqueous solutions. *Macromolecules* 2005;38:5260-5265.
- [71] Jeong B, Bae YH, Kim SW. Thermoreversible gelation of PEG-PLGA-PEG triblock copolymer aqueous solutions. *Macromolecules* 1999;32:7064-7069.
- [72] Zentner GM, Rathi R, C Shih, McRea JC, Seo M, Oh H, et al. Biodegradable block copolymers for delivery of proteins and water-insoluble drugs. *J Control Release* 2001;72:203-215.
- [73] Qiao M, Chen D, Ma W, Liu Y. Injectable biodegradable temperature-responsive PLGA-PEG-PLGA copolymers: synthesis and effect of copolymer composition on the drug release from the copolymer-based hydrogels. *Int J Pharm* 2005;294:103-112.

- [74] Gao Y, Ren F, Ding B, Sun N, Liu X, Ding W, et al. A thermo-sensitive PLGA-PEG-PLGA hydrogel for sustained release of docetaxel. *J Drug Target* 2011;19:516-527.
- [75] Nagarajan R, Barry M, Ruckenstein E. Unusual selectivity in solubilization by block copolymer micelles. *Langmuir* 1986;2:210-215.
- [76] Elstad NL, Fowers KF. OncoGel® (ReGel®/paclitaxel) - clinical applications for a novel paclitaxel delivery system. *Adv Drug Deliv Rev* 2009;61:785-794.
- [77] Bramfeldt H, Sarazin P, Vermette P. Characterization, degradation, and mechanical strength of poly(D,L-lactide-*co*-caprolactone)-poly(ethylene glycol)-poly(D,L-lactide-*co*-caprolactone). *J Biomed Mater Res A* 2007;83A:503-511.
- [78] Zhang Z, Ni J, Chen L, Yu L, Xu J, Ding J. Biodegradable and thermoreversible PCLA-PEG-PCLA hydrogel as a barrier for prevention of post-operative adhesion. *Biomaterials* 2011;32:4725-4736.
- [79] Jo S, Kim J, Kim SW. Reverse thermal gelation of aliphatically modified biodegradable triblock copolymers. *Macromol Biosci* 2006;6:923-928.





## CHAPTER 2

**Modulating rheological and degradation properties of temperature-responsive gelling systems composed of blends of a PCLA-PEG-PCLA triblock copolymer and its fully hexanoyl-capped derivative**

Audrey Petit<sup>1,2</sup>, Benno Müller<sup>1</sup>, Peter Bruin<sup>1</sup>, Ronald Meyboom<sup>1</sup>, Martin Piest<sup>1</sup>, Loes MJ Kroon-Batenburg<sup>3</sup>, Leo GJ de Leede<sup>1</sup>, Wim E Hennink<sup>2</sup> and Tina Vermonden<sup>2</sup>

<sup>1</sup> InGell Labs BV, Groningen, The Netherlands

<sup>2</sup> Department of Pharmaceutics, Utrecht Institute for Pharmaceutical Sciences, Utrecht University, Utrecht, The Netherlands

<sup>3</sup> Department of Crystal and Structural Chemistry, Bijvoet Center for Biomolecular Research, Utrecht University, Utrecht, The Netherlands

## Chapter 2

### Blends

## Abstract

In this study, the ability to modulate rheological and degradation properties of temperature-responsive gelling systems composed of aqueous blends of a poly( $\epsilon$ -caprolactone-*co*-lactide)-*b*-poly(ethylene glycol)-*b*-poly( $\epsilon$ -caprolactone-*co*-lactide) (PCLA-PEG-PCLA) triblock copolymer (i.e. uncapped) and its fully capped derivative was investigated. Uncapped and capped PCLA-PEG-PCLA triblock copolymers, abbreviated as degree of modification 0 and 2 (DM0 and DM2, respectively), were composed of identical PCLA- and PEG-blocks but different end groups: namely hydroxyl- and hexanoyl-end groups.

DM0 was synthesized by ring opening polymerization of L-lactide and  $\epsilon$ -caprolactone in toluene using PEG as initiator and tin (II) 2-ethylhexanoate as the catalyst. A portion of DM0 was subsequently reacted with an excess of hexanoyl chloride in solution to yield DM2. The cloud point and phase behaviour of DM0 and DM2 in buffer as well as that of their blends were determined by light scattering in diluted state and by vial tilting and rheological measurements in concentrated state. Degradation/dissolution properties of temperature-responsive gelling systems were studied *in vitro* at pH 7.4 and 37 °C.

The cloud points of DM0/DM2 blends were ratio-dependent and could be tailored from 15 to 40 °C for blends containing 15 to 100 wt% DM0. Vial tilting and rheological experiments showed that, with solid contents between 20 and 30 wt%, DM0/DM2 blends (15/85 to 25/75 wt/wt) had a sol-to-gel transition temperature at 10-20 °C, whereas blends with less than 15 wt% DM0 formed gels below 4 °C and the ones with more than 25 wt% DM0 did not show a sol-to-gel transition up to 50 °C. Complete degradation of temperature-responsive gelling systems took ~100 days, independent of the DM0 fraction and the initial solid content. Analysis of residual gels in time by GPC and  $^1\text{H}$  NMR showed no chemical polymer degradation, but indicated gel degradation by dissolution. Preferential dissolution of lactoyl-rich polymers induced enrichment of the residual gels in caproyl-rich polymers. To the best of our knowledge, degradation of temperature-responsive gelling systems by dissolution has not been reported or hypothesized as being the consequence of acylation of polymers.

In conclusion, blending of PCLA-PEG-PCLA triblock polymers composed

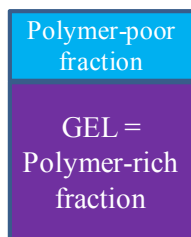
of identical backbones but different end groups provides for a straightforward preparation of temperature-responsive gelling systems with well-characterized rheological properties and potential in drug delivery. Furthermore, acylation of triblock copolymers may allow for the design of bioerodible systems with control over degradation by polymer dissolution.

DM0=   $\xrightarrow{\text{in buffer}}$  MICELLES up to 40 °C

$\downarrow$   
+ excess  
hexanoyl chloride

DM2=   $\xrightarrow{\text{in buffer}}$  AGGREGATES

DM0 (15-25 wt%)  
+  
DM2 (85-75 wt%)  $\xrightarrow{\text{in buffer}}$  MICELLES up to 15 °C  
 $\downarrow$   
@ 20-30 wt% in buffer  
and @ 37 °C



GEL DEGRADATION  
BY DISSOLUTION  
(with preferential leaching  
of LA-rich polymer chains)

## 1. Introduction

Hydrogels composed of copolymers containing polyester and PEG are of general interest for biomedical and pharmaceutical applications as they are biocompatible and biodegradable, while also possessing properties of injectability, crystallinity, network mesh size that are easy to modulate [1-6]. Triblock copolymers made of PEG as middle block flanked by two aliphatic polyester blocks form, in aqueous medium, flower-like micelles in the low concentration range [7]. At higher concentrations and above critical gel temperature, these polymers rearrange to form viscoelastic hydrogels [8,9]. Such temperature-responsive gelling systems are developed as injectable drug delivery depots and, in particular, an aqueous system containing poly(lactide-*co*-glycolide)-*b*-poly(ethylene glycol)-*b*-poly(lactide-*co*-glycolide) (PLGA-PEG-PLGA) triblock copolymers, loaded with paclitaxel, has already found clinical applications in oncology [10]. Paclitaxel is essentially located in the hydrophobic domains of the system and its release is mediated by a combination of diffusion and chemical polymer degradation, which takes around six weeks *in vitro* as well as *in vivo* to degrade completely [11-13].

When designing temperature-responsive gelling systems for drug delivery, it is important to understand and to be able to modulate rheological and release/degradation properties. Rheological properties can be modulated by polymer composition and molecular weight ( $M_n$ ) of the building blocks [8,14]. In particular, temperature-responsive gelling systems ideally fulfill two requirements: (i) liquid at room temperature for ease of handling and injection, and (ii) viscoelastic at 37 °C to form hydrogel depots upon administration, which requires a sol-to-gel transition temperature between 20 and ~30-35 °C. The sol-to-gel transition temperature depends on the hydrophilic/hydrophobic balance of the copolymers (i.e.  $M_n$  of PEG as well as  $M_n$  and type of polyester). Moreover, the composition of polymers also governs the release/degradation properties of temperature-responsive gelling systems, which is of key importance in modulating the mobility/diffusion of loaded drug molecules.

Blending in water of PLGA-PEG-PLGA copolymers made of PLGA blocks with different  $M_n$ 's was shown to be a practical method to prepare temperature-responsive gelling systems with easy to modulate rheological properties and complete degradation taking four to eight weeks [15,16]. For

some clinical applications, longer degradation times are desired, which can be achieved by decreasing the rate of hydrolysis through the use of PCLA instead of PLGA. Degradation of systems composed of PCLA-PEG-PCLA copolymers depends on the ratio of caproyl units (CL) to lactoyl units (LA), and systems containing 70/30 mol/mol CL/LA ratio showed complete degradation occurring after six months [17,18].

Interestingly, modification of hydroxyl-end groups of polyester-PEG-polyester triblock copolymers also allows for modulation of rheological properties [19]. As an example, Jo and co-workers [20] modified hydroxyl-end groups of PCLA-PEG-PCLA copolymers, with hexanoyl and lauroyl aliphatic groups. At 20 wt% in water, a hydroxyl-terminated PCLA-PEG-PCLA copolymers was transparent sols until at least 40 °C and a fully acylated one aggregated, whereas a polymer bearing 50 % hexanoyl modification showed a sol-to-gel transition at 30 °C, suitable for biomedical applications.

In this study, we investigated a novel approach to modulate the rheological and degradation properties of temperature-responsive gelling systems. We hypothesized that blending, in aqueous medium, of uncapped (i.e. hydroxyl-terminated) and capped (i.e. fully hexanoyl-modified) PCLA-PEG-PCLA triblock copolymers made of identical PCLA- and PEG-blocks would allow modulation of the phase behaviour, gel properties and degradation rate of temperature-responsive gelling systems.

## 2. Experiments and protocols

### 2.1. Materials

Except L-lactide (obtained from Purac Biochem, The Netherlands), all chemicals were obtained from Aldrich and used as received.

### 2.2. Synthesis of uncapped and fully hexanoyl-capped PCLA-PEG-PCLA

The synthesis of uncapped and fully hexanoyl-capped PCLA-PEG-PCLA triblock copolymers, abbreviated as degree of modification 0 and 2 (DM0 and DM2) respectively, was performed essentially as previously described by Jo and co-workers [20]. Briefly, in a three-neck round-bottom flask equipped with a Dean Stark trap and a condenser, 50 g PEG<sub>1500</sub> (33 mmol), 12 g L-lactide (83 mmol), 48 g  $\epsilon$ -caprolactone (421 mmol) and 150 ml toluene were introduced and, while stirring, heated to reflux under nitrogen atmosphere.

The solution was azeotropically dried by distilling off ~65 ml toluene/water. Next, it was cooled to ~90 °C and 0.7 ml tin(II) 2-ethylhexanoate (1.7 mmol) was added. Ring-opening polymerization was carried out at 110-120 °C overnight under nitrogen atmosphere. Subsequently, the solution was cooled to room temperature and aliquoted in two equal portions of ~90 g.

To obtain DM2, 100 ml of dichloromethane and 10 ml of triethylamine (99 mmol) were added to one of the portions. At 0 °C, while stirring, 10 ml hexanoyl chloride (74 mmol, ratio hexanoyl/PEG = 4/1 mol/mol) was added dropwise and acylation was allowed to proceed for 3 hours. Dichloromethane was removed under vacuum at 60-65 °C, and ethyl acetate (100 ml) was added. Triethylamine hydrochloride salts were removed by filtration.

DM0 and DM2 were precipitated by addition of 900 ml of a 1:1 mixture of hexane and diethyl ether. Upon storage at -20 °C, DM0 and DM2 separated as waxy solids, from which the non-solvents containing unreacted monomers and hexanoyl chloride could be decanted easily. Finally, precipitated DM0 and DM2 were dried in vacuo and obtained in good yield (51 g and 49 g, respectively).

### 2.3. <sup>1</sup>H NMR analysis

<sup>1</sup>H NMR analysis of DM0 and DM2 dissolved in CDCl<sub>3</sub> was performed using a Varian Oxford, operating at 300 MHz. <sup>1</sup>H NMR spectra were referenced to the signal of chloroform at 7.26 ppm:

5.25-4.95 (*I*<sub>5.1</sub>, 1H, -CO-CH(CH<sub>3</sub>)-O-); 4.35-4.15 (2H, -PEG-O-CH<sub>2</sub>-CH<sub>2</sub>-O-CO- and 1H, -CO-CH(CH<sub>3</sub>)-OH); 4.15-3.95 (2H, -C-(CH<sub>2</sub>)<sub>4</sub>-CH<sub>2</sub>-O-CO-); 3.85-3.25 (-O-CH<sub>2</sub>-CH<sub>2</sub>-O- and 2H, -CO(CH<sub>2</sub>)<sub>4</sub>-CH<sub>2</sub>-OH); 2.85 (1H, -CO-CH(CH<sub>3</sub>)-OH); 2.50-2.35 (*I*<sub>2.4</sub>, 2H, -CO-CH(CH<sub>3</sub>)-O-CO-CH<sub>2</sub>-(CH<sub>2</sub>)<sub>3</sub>-C-); 2.35-2.20 (*I*<sub>2.3</sub>, 2H, -O-CO-CH<sub>2</sub>-(CH<sub>2</sub>)<sub>4</sub>-O-CO-CH<sub>2</sub>-(CH<sub>2</sub>)<sub>3</sub>-C-); 1.80-1.25 (2H, -CO-CH<sub>2</sub>-CH<sub>2</sub>-CH<sub>2</sub>-C-; 3H, -CO-CH(CH<sub>3</sub>)-O- and 2H, -CO-CH<sub>2</sub>-CH<sub>2</sub>-CH<sub>2</sub>-CH<sub>2</sub>-CH<sub>2</sub>); 0.95-0.70 ppm (*I*<sub>0.8</sub>, 3H, -CO-(CH<sub>2</sub>)<sub>4</sub>-CH<sub>3</sub>-) [20-23].

Since the peak belonging to -CO-(CH<sub>2</sub>)<sub>4</sub>-CH<sub>2</sub>-OH of terminal CL and -O-CH<sub>2</sub>-CH<sub>2</sub>-OH of unreacted PEG overlap with the peak belonging to -C-O-CH<sub>2</sub>-CH<sub>2</sub>-O-C- of PEG at 3.85-3.25 ppm, the shift reagent trichloroacetylisocyanate (TCAI) was used to react with free hydroxyl-end groups of CL and PEG and to form -CH<sub>2</sub>-O-C(O)-NH-C(Cl)<sub>3</sub> urethane-containing moieties. The protons belonging to -CH<sub>2</sub>-O-C(O)-NH-C(Cl)<sub>3</sub> of

CL, PEG and LA have chemical shifts around 1 ppm higher than that of the initial hydroxyl moieties (4.6, 4.4 and 5.2 ppm, respectively) [24].

After addition of an excess of TCAI, the composition of DM0 and DM2 was established from the integral of signals belonging to methine protons of LA subdivided in four quadruplets ( $I_{5.1}$ ), methylene protons of PEG ( $I_{3.6}$  at 3.72-3.55 ppm), methylene protons of CL subdivided in two triplets ( $I_{2.4} + I_{2.3}$ ), and methyl protons of hexanoyl-end group ( $I_{0.8}$ ). Signals of TCAI-reacted moieties are relatively small, as DM0 only contains a few protons adjacent to hydroxyl-end groups. The equation used to calculate the composition of DM0 and DM2 is given in the appendices (Equation A.1 to A.12).

#### 2.4. Gel permeation chromatography analysis (GPC)

$M_n$  of DM0 and DM2 were determined by GPC using an Agilent system Series 100 equipped with three Varian columns (PLgel, 5 $\mu$ m, 500 $\text{\AA}$ , 300  $\times$  7.5 mm). Detection was performed with a light scattering detector. PEGs of different molecular weights were used for calibration. The eluent was THF, the elution rate was 1 ml/min, and the column temperature was 30  $^{\circ}\text{C}$ . The concentration of the samples was 20 mg/ml in THF and the injection volume was 50  $\mu$ l.

#### 2.5. Differential scanning calorimetry analysis (DSC)

Thermal properties of DM0, DM2 and PEG<sub>1500</sub> were determined by DSC (TA Instruments DSC Q2000 apparatus). Samples of  $\sim$ 10 mg in closed aluminium pans were heated from room temperature to 60  $^{\circ}\text{C}$  with a heating rate of 5  $^{\circ}\text{C}/\text{min}$  and a nitrogen flow rate of 50 ml/min. Next, the samples were cooled to -90  $^{\circ}\text{C}$  with the same cooling rate, followed by a second heating cycle at the same heating rate to 60  $^{\circ}\text{C}$ . Using the second heat run, the glass transition temperature ( $T_g$ ) was determined as the midpoint of heat capacity change and the melting enthalpy ( $\Delta H$ ) as the integral of the endothermic area.

#### 2.6. X-ray diffraction (XRD)

X-ray diffraction patterns were recorded for PEG<sub>1500</sub> and DM0 using a Bruker X8-Proteum with Helios mirrors using  $\text{CuK}\alpha$  radiation



( $\lambda = 0.15418 \text{ \AA}$ ) on a Platinum-135 CCD detector. The patterns were recorded at a sample-to-detector distance of 60 mm. Separate blank patterns were recorded to allow subtraction of air- and capillary wall-scattering. The two-dimensional X-ray scattered intensities were transformed into one-dimensional intensity with  $2\theta$  as x-axis.

### *2.7. Preparation of blends*

DM0 and DM2 were separately dissolved in 15 ml ethyl acetate at a concentration of 500 mg/ml. The solutions were mixed to achieve specific ratios and the obtained mixtures were transferred to 11-cm Petri dishes. The solvent was removed under nitrogen flow for 48 hours ( $^1\text{H}$  NMR analysis indicated a residual ethyl acetate content of less than 0.5%).

### *2.8. Dynamic light scattering (DLS)*

DLS measurements were performed using a Malvern CGS-3 multiangle goniometer with a JDS Uniphase 22mW He-Ne laser operating at 632.8 nm at a  $90^\circ$  angle. Polymer concentrations were 1, 10 and 100 mg/ml in phosphate buffer (50 mM, 0.07 mM NaCl, 0.02%  $\text{NaN}_3$ , pH 7.4). The samples were cooled to  $5^\circ\text{C}$  and temperature was increased to  $50^\circ\text{C}$  at a rate of  $1^\circ\text{C}/\text{min}$ . The change in solvent viscosity with temperature was corrected by the software.

### *2.9. Cloud Point (CP) determination*

CP of DM0 and DM2 as well as that of their blends (prepared as described in section 2.7) were measured using an UV spectrometer with temperature control (Shimadzu UV2450). 10 ml phosphate buffer was added to 20 mg polymers (concentration of 2 mg/ml). The samples were incubated for 10 min at  $4^\circ\text{C}$  and subsequently the absorbance at 650 nm was measured while the samples were heated to  $50^\circ\text{C}$  with a heating rate of  $1^\circ\text{C}/\text{min}$ .

### *2.10. Vial tilting and rheological characterization*

Phosphate buffer was added to 500 mg DM0 or its blends with DM2 (prepared as described in section 2.7) in screw-capped vials of 1-cm diameter to yield systems at the desired solid content (ranging from 20 to 30 wt%). The samples were heated for 15 min at  $50^\circ\text{C}$  to allow melting of the polymers and

vortexed. The samples were placed at 4 °C for 48 hours to allow formation of homogeneous systems.

Vial tilting was used to visually characterize sol and gel state [8,14]. Vial tilting was performed at 4 °C and at 37 °C after 30 min incubation. Immobility, after 10 min with vials upside, was used to discriminate between mobile sols and immobile gels.

Rheological characteristics were monitored by oscillatory temperature- and time-sweep experiments using a TA AR-G2 rheometer equipped with a Peltier plate (1 ° steel cone, 20 mm diameter with solvent trap) at 0.5 % strain and 7 Hz frequency. The solvent trap of the Peltier plate was filled with water to prevent dehydration of the samples during measurement. For temperature-sweep measurements, the plates of the rheometer were pre-cooled to 4 °C and subsequently 70 µl sample was introduced between the plates. The sample was heated from 4 to 50 °C with a heating rate of 1 °C/min. For time-sweep measurements, samples were incubated overnight at 37 °C. Polymer-rich fractions of the phase-separated systems were introduced between the plates of the rheometer, pre-heated to 37 °C, and then measured for 5 min.

### *2.11. Degradation behaviour*

Blends with 25 wt% solid content and 75 wt% phosphate buffer containing different DM0/DM2 ratios (15, 20 and 25 wt% DM0) as well as blends containing 20 wt% DM0 with varying solid contents (20, 25 and 30 wt%) were used to study the degradation properties of gels in physiological conditions (37 °C, pH 7.4). Sols (300 µl) were transferred via a syringe to glass vials (8.2 × 40 mm). This handling was performed at 4 °C, temperature at which the sols were homogeneous. The vials were placed at 37 °C to allow gel formation. After 30 min, 700 µl phosphate buffer was added. At predetermined time points, the buffer was removed, the weight of residual gels was measured, and fresh buffer was added. In addition, samples were freeze-dried for further analysis (dry weight determination and analysis by GPC and <sup>1</sup>H NMR using an excess of TCAI). Dry weight was determined by weighing residual gels after freeze-drying. Solid content is defined as the ratio between dry and wet weights and corresponds to the concentration of polymer in residual gels.

### 3. Results and discussion

#### 3.1. Synthesis and characterization of uncapped and capped copolymers

The synthesis of PCLA-PEG-PCLA triblock copolymers (abbreviated as DM0) was performed by ring opening polymerization of L-lactide and  $\epsilon$ -caprolactone in solution using PEG<sub>1500</sub>-diol as macroinitiator and tin(II) 2-ethylhexanoate as catalyst (yield 93 %). Subsequently, acylation of hydroxyl-end groups of DM0 using an excess of hexanoyl chloride resulted in the formation of DM2 (yield 89 %). <sup>1</sup>H NMR spectra of DM0 and DM2 are shown in Figure A.1 of the appendices. The characteristic peaks at 5.25-4.95, 3.65-3.55, 2.50-2.10 and 0.95-0.70 ppm correspond to methine protons of LA, methylene protons of PEG, methylene protons of CL [21,22], and methyl protons of hexanoyl-end groups [20], respectively. Because of overlap of the peaks belonging to methylene protons of PEG and methylene protons of hydroxyl CL at 3.65-3.55 ppm, the integral of the peaks was performed using the spectra of DM0 and DM2 after addition of an excess of TCAI. Figure A.2 shows the peak of protons belonging to  $-\text{O}-\text{CH}(\text{CH}_3)-\text{O}-\text{C}(\text{O})-\text{NH}-\text{C}(\text{Cl})_3$  of LA with a chemical shift  $\sim 5.2$  ppm; the peaks of protons belonging to  $-\text{CH}_2-\text{O}-\text{C}(\text{O})-\text{NH}-\text{C}(\text{Cl})_3$  of CL and PEG are difficult to distinguish as they are relatively small and have chemical shifts around 4.2-4.6 ppm, which partially overlap with the peaks of protons belonging to  $-\text{PEG}-\text{O}-\text{CH}_2-\text{CH}_2-\text{O}-\text{CO}-$  at 4.35-4.15 ppm.

The composition of DM0 and DM2 was determined according to Equation A.1 to A.11. The molar ratio of CL to LA (defined in Equation A.7),  $k$ , was 1.6, which corresponds to 71 wt% CL, in accordance with the feed of 80 wt%. Each PCLA block, which is composed on average of 6.0 CL ( $\sim 700$  g/mol) and 3.8 LA, i.e. 1.9 lactide ( $\sim 300$  g/mol), has a  $M_n$  of  $\sim 1000$  g/mol. The weight ratio of PCLA to PEG (PCLA/PEG) of DM0 and DM2 (composed of one PEG<sub>1500</sub> block as middle block flanked by two PCLA<sub>1000</sub> blocks), was thus 1.3, which is in accordance with the feed ratio of 1.2. The average block length of the CL sequences was estimated according to Equation A.12 and shown to be 4.8 CL indicating not complete randomization of LA and CL. DM0 was prepared at 110-120 °C with tin(II) 2-ethylhexanoate as the catalyst and also Kricheldorf et al. have shown that this procedure results in not fully random polymers [25].

**Table 1:** Characteristics of uncapped and fully hexanoyl-capped PCLA-PEG-PCLA triblock copolymers.

<i>Polymer</i>	<i>HO-PCLA-PEG-PCLA-OH</i>	<i>Hex-PCLA-PEG-PCLA-Hex</i>
<i>Abbreviation</i>	<i>DM0</i>	<i>DM2</i>
PEG feed [g]		50 g
$\epsilon$ -caprolactone feed [g]		48 g
Lactide feed [g]		12 g
Hexanoyl chloride feed [g]	-	10
Aimed $M_n$ [g/mol]	3200	3500
Yield [%]	93	89
PCLA/PEG <sup>a)</sup>		1.3
CL [wt%] <sup>b)</sup>		71
DM <sup>c)</sup>	0	2.0
$M_n^d$ [g/mol]	3300	3500
PDI <sup>e)</sup>	1.27	1.24

<sup>a)</sup> weight ratio of PCLA to PEG determined by <sup>1</sup>H NMR

<sup>b)</sup> weight ratio of  $\epsilon$ -caprolactone to L-lactide determined by <sup>1</sup>H NMR

<sup>c)</sup> number of end groups per triblock copolymer determined by <sup>1</sup>H NMR

<sup>d)</sup> number average molecular weight determined by GPC, relative to PEG standards

<sup>e)</sup> polydispersity ( $= M_w/M_n$ ) determined by GPC

### 3.2. Thermal properties of DM0 and DM2 determined by DSC

The melting and crystallization behaviour of DM0, DM2 and PEG<sub>1500</sub> was determined by DSC (Figure A.4 in the appendices). The thermograms of DM0 and DM2 showed a single  $T_g$  around -60 °C, which is close to that of poly( $\epsilon$ -caprolactone) (PCL) [26,27] and can therefore be ascribed to the  $T_g$  of CL-rich PCLA. The thermogram of PEG<sub>1500</sub> showed a melting endotherm at 45 °C and no  $T_g$ , likely because of high crystallinity as reflected by a  $\Delta H$  of

202 J/g. The thermograms of DM0 and DM2 were very similar to each other and showed broad melting endotherms from 0 to 40 °C ( $\Delta H$  of DM0 and DM2 were 60 J/g and 48 J/g, respectively), which can either be ascribed to melting of PCLA (high  $M_n$  PCL has a melting temperature between 40 and 70 °C [26,27], and depending on  $M_n$ , oligo( $\epsilon$ -caprolactone) have melting temperature between -25 and 31 °C [28]) or to melting of PEG [29-31] (see the thermogram of PEG in Figure A.4). X-ray diffraction analysis convincingly showed that the crystallinity of DM0 can be exclusively attributed to PEG (Figure A.5 in the appendices), even though one could expect PCLA to be crystalline taking into account the average CL-sequence length of 4.8 CL [25,32]. Based on  $\Delta H$  of PEG and PEG content of DM0 and DM2 (according to  $^1\text{H}$  NMR: 43 wt% and 40 wt%, respectively), one would expect a  $\Delta H$  of DM0 and DM2 due to the melting of PEG of  $\sim 87$  J/g and  $\sim 81$  J/g, respectively. The lower observed  $\Delta H$  values (60 and 48 J/g for DM0 and DM2, respectively) is likely due to the imperfect crystallinity of PEG because of partial miscibility with PCLA [33,34].

### *3.3. Influence of temperature on the polymers and blends in diluted state*

DLS analysis showed that DM2 at 10 mg/ml in buffer at 4 °C formed large aggregates in the micrometer range (data not shown). Conversely, under similar conditions, DM0 formed stable and transparent dispersions and DLS measurements showed the presence of micelles of 10 nm with a small size distribution (as reflected by a PDI of 0.15) at temperatures below 40 °C (Figure 1). Because of the ABA architecture of DM0, the micelles are likely flower-like micelles with a shell formed by B loops (PEG) anchored by A blocks (PCLA) in the micellar core [2,7,35,36].

Above 40 °C, the micellar dispersion of DM0 became turbid and structures in the mesoscopic range were formed due to aggregation/precipitation (Figure 1A). Micellar dispersions of polyester/PEG block copolymers with temperature-dependent aggregation/precipitation have been observed previously [37-39]. Figure 1B shows the CP of DM0/DM2 blends with varying DM0 fractions (the corresponding temperature-turbidity curves are shown in Figure A.6 of the appendices). With increasing DM0 fraction, and thus hydrophilicity, the CP increases, which is in line with previous studies [19,32]. The driving force for micellar aggregation is the dehydration of PEG

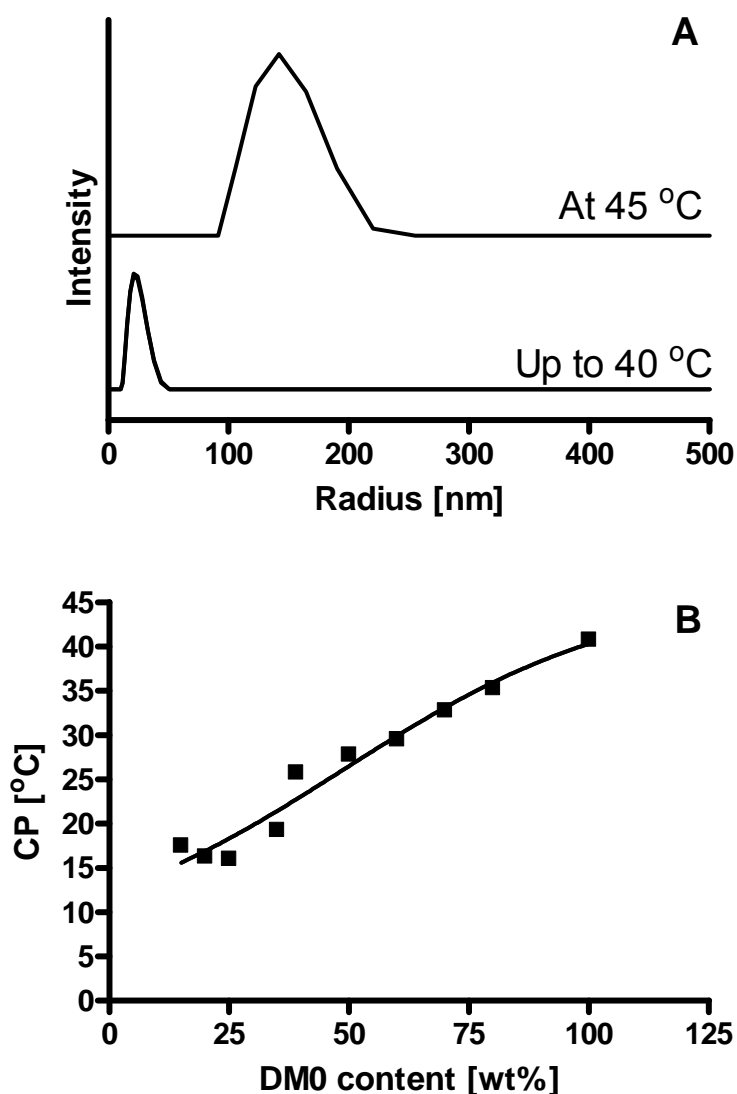


**Figure 1:** Behaviour of dilute aqueous micellar suspensions with temperature. 1A shows the radius of micelles (lower lines) and that of the aggregates (upper line) measured by DLS of DM0 at 10 mg/ml. 1B shows the cloud point of DM0/DM2 blends at 2 mg/ml.

upon increasing temperature leading in turn to increasing hydrophobic polymer-polymer interactions [9,19,32,40]. In line with this proposal,  $^{13}\text{C}$  NMR analysis on similar systems has shown that the core-shell structure of micelles composed of PEG-polyester copolymers is partially destroyed above the CP [38], due to phase mixing of PEG and polyester [3,32,40].

We also measured micellar dispersions of DM0 at 1 mg/ml and 100 mg/ml with DLS and it appeared that the size of micelles at 5 °C was in the same

range (10 nm) as measured at 10 mg/ml. However, above CP, the aggregates, formed at 100 mg/ml, settled down very rapidly leading to formation of white gel-like pellets: sol-to-gel transition at concentrations above the critical gel concentration was also shown to originate from aggregation/precipitation [19,38-41].

### *3.4. Rheological properties of aqueous DM0/DM2 blends*

Figure 2A shows photographs of a sample with a solid content of 25 wt% containing a DM0/DM2 blend (20 wt% DM0 fraction). At 4 °C, the sample was a turbid sol, whereas it formed an immobile opaque gel at 37 °C. Samples containing less than 15 wt% DM0 were already immobile gels at 4 °C whereas samples containing more than 25 wt% DM0 were still sols at 37 °C. Compositions ranging from 15 to 25 wt% DM0 are thus the most interesting ones for application as injectable drug delivery depots since they are liquid in the low temperature range and form gels at 37 °C. Figure 2B shows the temperature-dependent storage and loss moduli ( $G'$  and  $G''$ , respectively) of samples with a solid content of 25 wt% in buffer containing DM0 only and a DM0/DM2 blend (20 wt% DM0). The DM0 sample showed only little variations of its moduli between 4 and 50 °C: this sample remained a sol. On the other hand, the DM0/DM2 sample showed a  $G''/G'$  cross-over point ( $\tan \delta = 1$ ) at 15 °C, which is in the range of the CP determined by light scattering (Figure 1B). Above 20-25 °C, the system phase-separated and both moduli slightly decreased, an observation that can likely be ascribed to an artifact in the measurement due to loss of contact between the plates of the rheometer and the gel.

The mechanism behind the sol-to-gel transition in systems similar to those investigated in the present study have previously been unravelled with  $^{13}\text{C}$  NMR [3,9,14,19,39,41,42]. In the sol state, polyester/PEG copolymers form micelles with a hydrophobic polyester core and a hydrated PEG shell. In the gel state and at elevated temperatures, PEG is dehydrated and polymer-polymer interactions become stronger, resulting in phase mixing and consequently disruption of the organised shell-core structure of the micelles, leading to aggregation/precipitation and mesoscopic phase-separation. As the temperature further increases, hydrophobic polymer-polymer interactions are enhanced causing phase-separation to a macroscopic level [3,9,19]. In the case

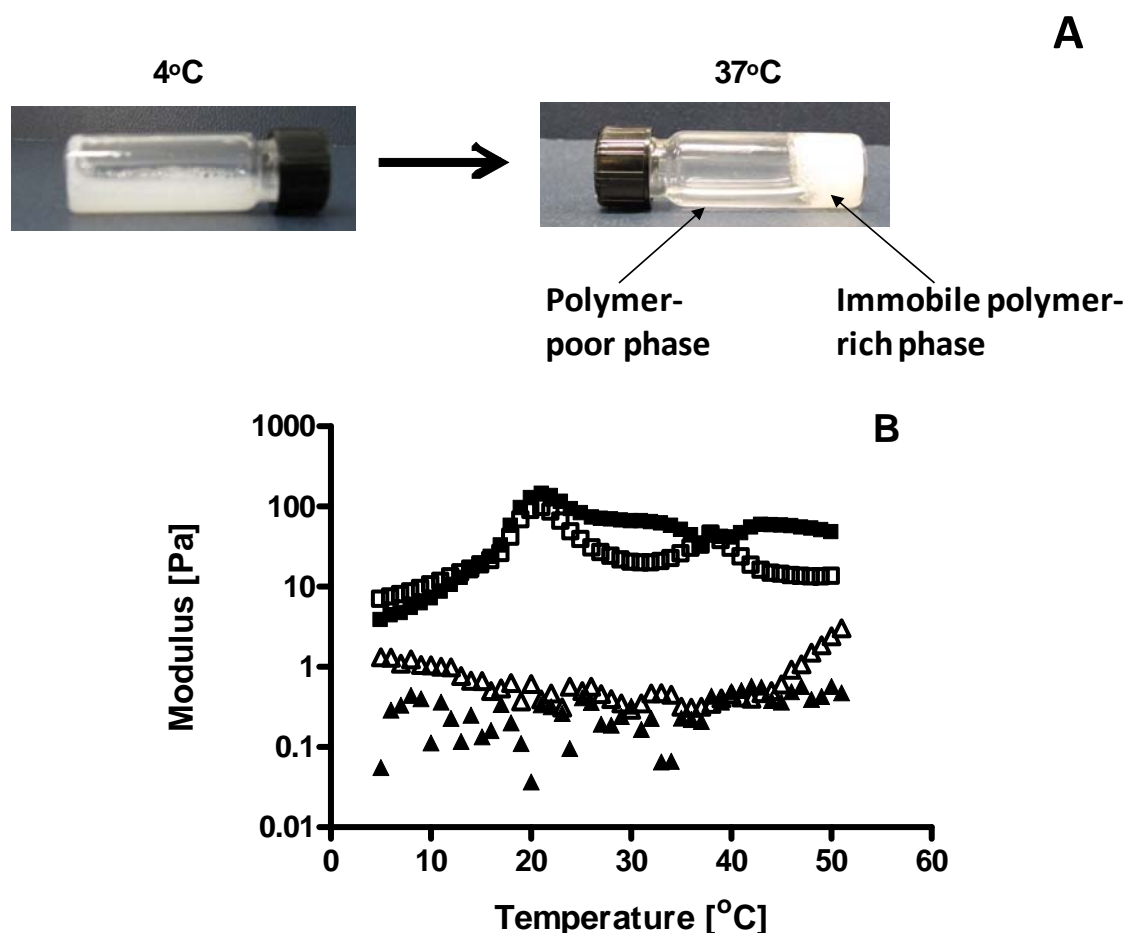


**Figure 2:** Behaviour of concentrated aqueous micellar suspensions with temperature. 2A shows photographs of a 25 wt% sample containing DM0/DM2 blend (20/80 w/w) after 30 min at 4 and 37 °C. 2B shows rheological temperature sweep measurements of 25 wt% samples containing DM0 (triangles) and a DM0/DM2 blend 20/80 w/w (squares). The closed and open symbols represent  $G'$  and  $G''$ , respectively.

of flower-like micelles, aggregation of the micelles is additionally facilitated by the presence of inter-micellar bridges [3,9,14,19,37-42].

To gain additional insight into the influence of the DM0 weight fraction on the moduli of aqueous DM0/DM2 blends at 37 °C, samples with 25 wt% solid content and varying DM0/DM2 ratios were incubated overnight at 37 °C resulting in phase-separated systems (~80 vol% polymer-rich fraction and ~20 vol% polymer-poor fraction). The moduli of polymer-rich fractions at 37 °C were measured and the results suggest that for blends containing less



than 25 wt% DM0,  $G'$  was larger than  $G''$  with moduli in the range of 1 to 10 kPa (Figure 3).  $\tan \delta$  increased with increasing DM0 fraction mainly because  $G''$  increased and, hence, the systems became less elastic and more viscous liquid-like. These results show that blending of DM0 and DM2 is a practical approach to modulate the sol-to-gel transition temperature of aqueous DM0/DM2 blends. It should be stressed that in Figure 3, only the polymer-rich fractions were measured which explains the higher modulus values compared to that measured during the temperature-sweep measurements as depicted in Figure 2.

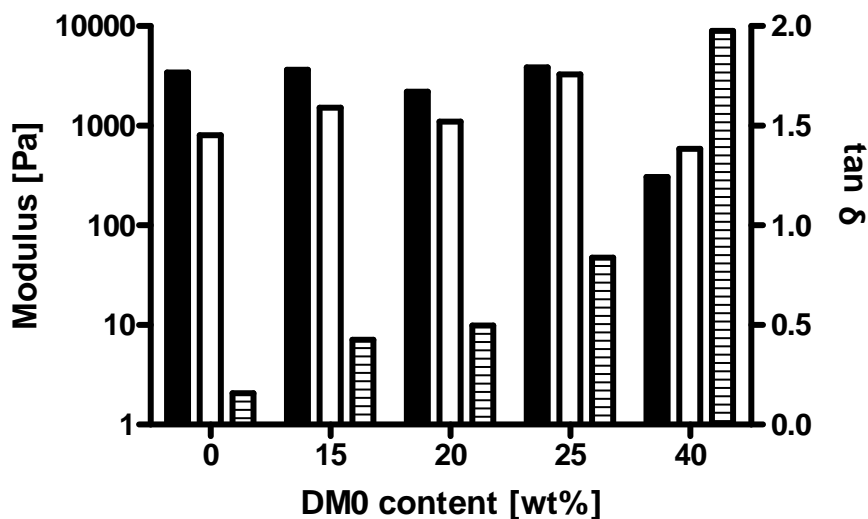


**Figure 3:** Rheological properties of the polymer-rich fractions of DM0/DM2 blends after phase separation at 37 °C showing  $G'$  (black),  $G''$  (white) and  $\tan \delta$  (striped).

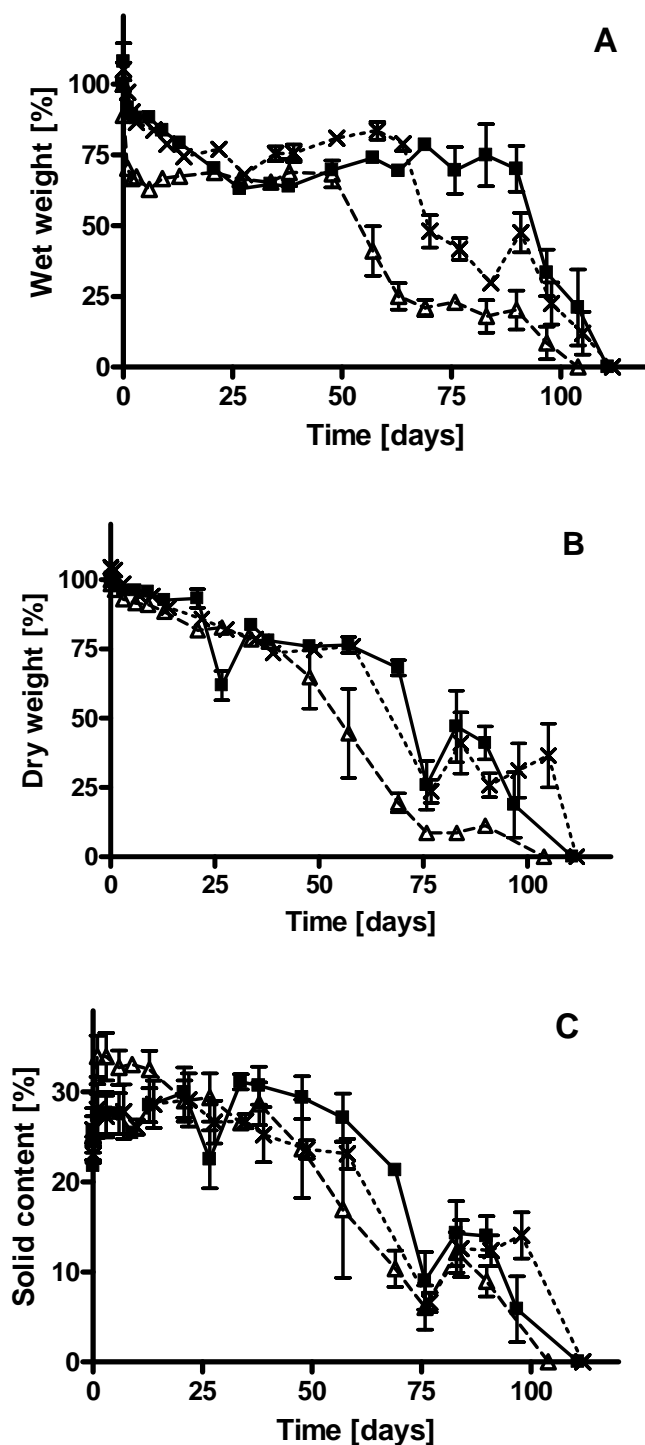
### 3.5. *In vitro* degradation of gels with varying ratios and solid contents

Gel degradation was investigated at 37 °C in phosphate buffer (pH 7.4). Figure 4A shows the wet weight, in time, of residual gels with an initial solid content of 25 wt% and varying DM0/DM2 ratios (15, 20 and 25 wt% DM0). Independent of the DM0/DM2 ratio, gels showed significant decrease in wet weight during the first phase of the experiment, which can be ascribed to phase separation (Figure 2A). The extent of the initial decrease in wet weight of the gels was dependent on the DM0 fraction: gels containing 25 wt% DM0 had a more rapid decrease in wet weight than gels containing 15 and 20 wt% DM0. This initial wet weight loss was accompanied by a decrease in dry

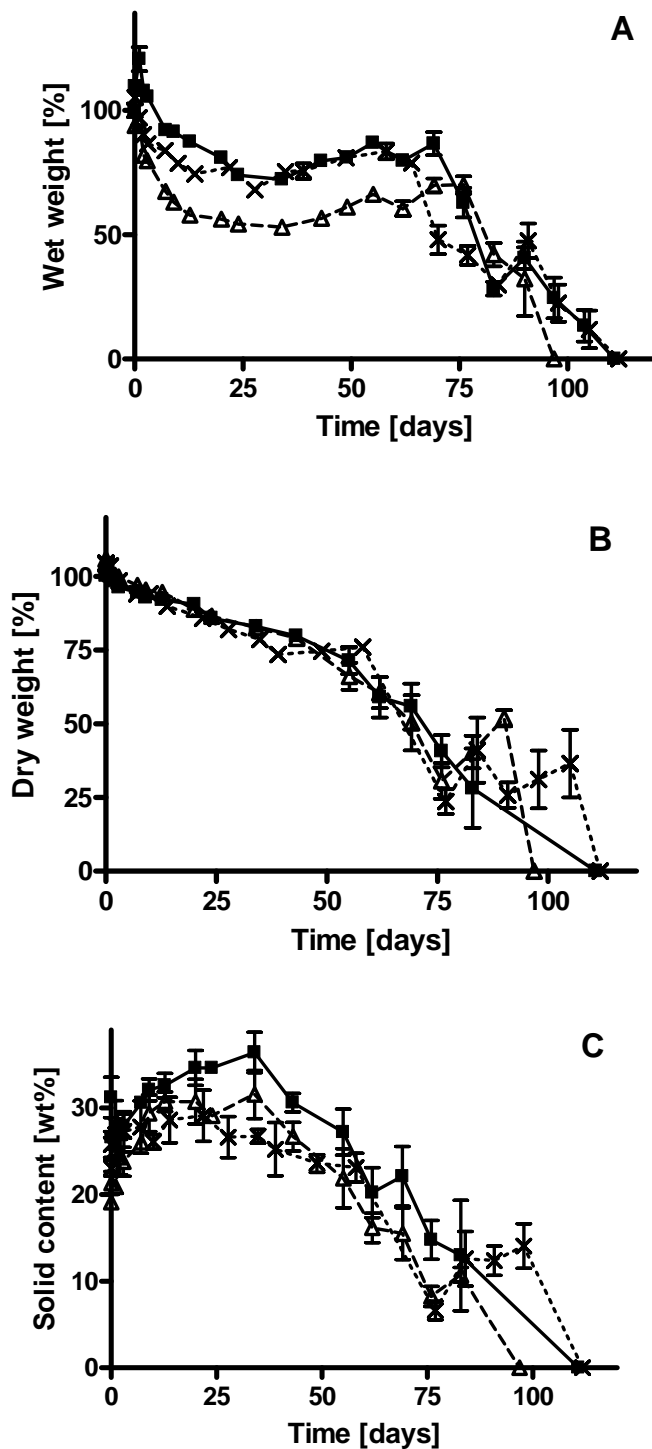
weight, which was however ratio-independent (Figure 4B). With increasing the DM0 fraction, the hydrophilicity of the gels increases, and one would expect a less extended phase separation and more water absorption, resulting in an increase in wet weight. However, the increase in the DM0 fraction also leads to formation of weaker gels, i.e. higher  $\tan \delta$  (Figure 3). Therefore, gels with high DM0 fractions might be more prone to damage due to external factors such as mechanical stress induced by buffer refreshment, offering a possible explanation for the faster decrease in wet weight observed. After 25 days, no further gel shrinking occurred and a value of about 70-80 % of the initial wet weight was reached. The residual gels then contained ~80 % of the initial polymer weight (see Figure 4B), meaning a solid content of 30 wt% (calculated using the data of Figure 4A and 4B, see Figure 4C). Upon further incubation, the dry weight decreased linearly, but the solid content remained relatively constant until day 50. At day 50, 70 and 90 for gels containing 25, 20 and 15 wt% DM0 respectively, the wet weight dropped substantially until complete degradation at ~100-110 days, independent on the DM0 fraction. The difference in time, depending on the DM0/DM2 ratio before the drop in wet weight, is also observed for the dry weight and is in line with the difference in hydrophilicity of the systems.

Figure 5 shows the degradation of gels with a fixed DM0/DM2 ratio (20 wt% DM0 fraction) and varying initial solid contents of 20, 25 and 30 wt%. As described previously for the effect of the DM0/DM2 ratio (Figure 4), the gels showed a significant decrease in wet weight during the first phase of the experiment, which can again be ascribed to phase separation. After 25 days, no further gel shrinking occurred. Upon further incubation, the dry weight decreased linearly, but the solid content remained relatively constant until day 40. Thereafter, wet weight, dry weight and solid content dropped until complete degradation at ~100-110 days, independent of the initial solid content. Degradation of the gels in ~100-110 days is in line with degradation times found for other systems containing PCLA-PEG-PCLA triblock copolymers with a molar ratio CL/LA close to  $k = 1.6$  [17].

GPC analyses were carried out to estimate the  $M_n$  of the residual polymer chains. The chromatograms showed a single peak with a  $M_n$  increasing slightly in time from 3700 to 3900 g/mol at day ~90-100 (Figure 6). These results suggest that no chemical polymer degradation took place during incubation of



**Figure 4:** Degradation of gels (25 wt% in buffer) composed of DM0/DM2 15/85 (squares), 20/80 (crosses) and 25/75 (triangles) in time at 37 °C. 4A shows the wet weight of the gels. 4B shows the dry weight of the gels. 4C shows the solid content of the gels. Experiments were performed at 37 °C (pH 7.4). Error bars represent standard deviation (n = 3).



**Figure 5:** Degradation of gels (DM0/DM2 20/80 w/w) with an initial solid content of 30 wt% (squares), 25 wt% (crosses) and 20 wt% (triangles) in time at 37 °C. 5A shows the wet weight of the gels. 5B shows the dry weight of the gels. 5C shows the solid content of the gels. Experiments were performed at 37 °C in phosphate buffer (pH 7.4). Error bars represent standard deviation ( $n = 3$ ).

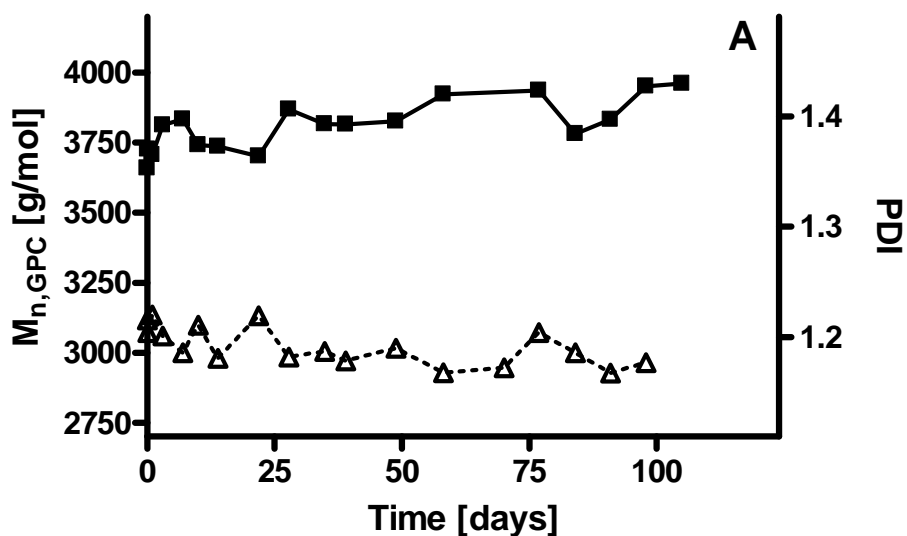


**Figure 6:** Degradation of the gel (DM0/DM2 20/80 w/w) with an initial solid content of 25 wt% in time at 37 °C showing the  $M_n$  (squares) and PDI (triangles) of the residual gels as determined by GPC.

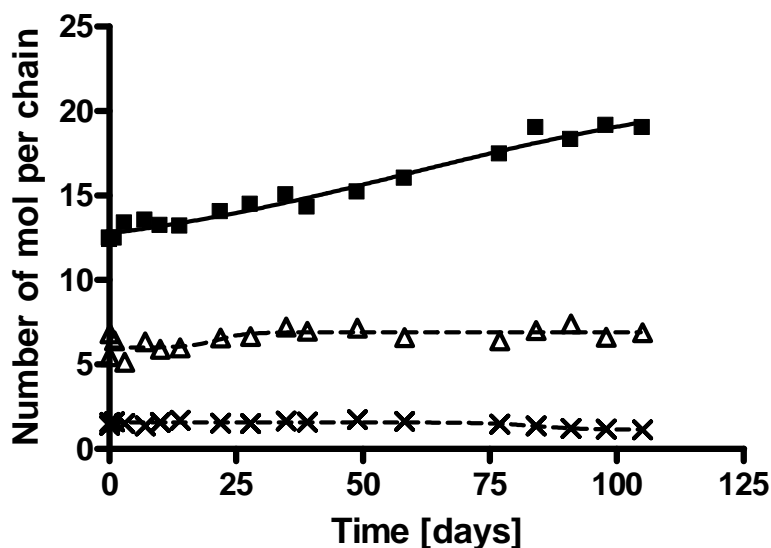


**Figure 7:** Number of CL (squares), LA (triangles) and hexanoyl group (crosses) per polymer chain, estimated by  $^1\text{H}$  NMR after addition of an excess TCAI, during degradation in residual gels containing DM0/DM2 (20 wt% DM0) with an initial solid content of 25 wt% polymer in buffer. Experiments performed at 37 °C in phosphate buffer (pH 7.4).

the gels at 37 °C in phosphate buffer pH 7.4 and this finding was confirmed by  $^1\text{H}$  NMR analysis after addition of an excess of TCAI, which showed no significant formation of hydroxyl-terminated moieties (Figure A.7) and no variations in the ratio of the peaks belonging to  $-\text{LA-O-CO-CH}_2-(\text{CH}_2)_4-$  and  $-\text{CL-O-CO-CH}_2-(\text{CH}_2)_4-$  of CL or hexanoyl-end groups (at 2.50-2.35 and 2.35-2.20 ppm, respectively). As mentioned previously, the degradation time of our systems matches those reported in literature, however it is normally induced by chemical polymer degradation [17,18,43]. Chemical polymer degradation of polyester is caused by cleavage of ester bonds occurring randomly along polyester chains. Compared to high molecular weight polyesters, mPEG-oligo(polyester) copolymers, having a relatively high amount of hydroxyl chain ends located at the hydrophobic-hydrophilic interface (e.g., micelle core-water phase interface), degrade mainly by chain end cleavage, i.e. backbiting [44-46]. End capping of mPEG-oligo(polyester) polymers protects polyester chains from chain end cleavage as no hydroxyl-end groups are located inside the hydrophobic micellar cores, hence end capping slows down chemical polymer degradation [43-46]. For instance, the half life of benzoyl-capped mPEG<sub>750</sub>-PCL containing 5 CL was estimated to be 25 years in buffer [44]. This finding is in line with the observed chemical stability of our gels for at least 100 days, which consist of polymers with ~10 ester bonds containing 75 mol% CL-CL ester bonds while 75 to 85 % of the chains are end-capped [16,17,23,47]. As a consequence, gel degradation observed for our systems (see Figure 4 and 5) occurs by polymer dissolution instead of polymer hydrolysis.

Figure 7 shows that  $^1\text{H}$  NMR analysis revealed enrichment in CL of the residual gels whereas the LA/PEG and hexanoyl/PEG molar ratios remained constant in time. The CL/LA molar ratio, k initially of 1.6, increased to approximately 2.7 in 100-110 days; at day ~100, the PEG/CL molar ratio, initially of 0.08, was 0.05, hence a decrease of ~35%. Enrichment in the most hydrophobic component of polyester/PEG block copolymers in time during degradation is in line with previous studies on similar systems, but is generally associated with chemical polymer degradation [16,17,23,47]. In the case of chemical polymer degradation, short polyester/PEG triblock copolymers, PEG-polyester diblock copolymers, PEG-diol, (un)capped polyesters are formed (because of backbiting, cleavage of ester bonds and

random chain scission in polyesters) and, depending on their hydrophilicity, partially leach out of gels, which leads in turn to an enrichment of the residues in hydrophobic moieties. Chemical polymer degradation translates thus in the formation of significant amounts of hydroxyl-terminated moieties in the residual gels, which, as mentioned previously (see also Figure A.7) was not observed in this study. This suggests that degradation in time occurred by dissolution with preferential leaching of triblock copolymers rich in LA leading to CL-enriched residues. The most hydrophilic (high LA content) polymers have thus the highest tendency to dissolve out of gels, leaving longer and more hydrophobic copolymers (high CL content).

#### **4. Conclusions**

In this study, the physical properties of blends composed of a PCLA-PEG-PCLA triblock copolymer (DM0) and its fully hexanoyl-capped derivative (DM2) in buffer were investigated. The self-assembly of DM0 into micelles was assessed by DLS. The cloud point of DM0/DM2 blends in buffer was ratio-dependent and could be tailored from 15 to 40 °C. DM0/DM2 blends containing 15 to 25 wt% DM0 with solid content between 20 to 30 wt% were sols at low temperature and viscoelastic gels at 37 °C. Gel degradation of the temperature-responsive gelling systems proceeded by dissolution in ~100 days, independent of the DM0/DM2 ratio and the initial solid content. To the best of our knowledge, this is the first study that demonstrates that temperature-responsive gelling systems based on acylated triblock copolymers rather dissolve than hydrolyse during degradation with a preferential leaching out of CL-poor polymer chains.

Systems based on blends of PCLA-PEG-PCLA copolymers and their hexanoyl end-capped derivatives have therefore potential as injectable systems for the controlled release of drugs. The mixing ratio allows to accurately preparing temperature-responsive gelling systems and gel degradation by dissolution brings opportunities for further development.

#### **Acknowledgements**

Mike de Leeuw and Dr. Theo Flipsen are gratefully acknowledged for their support and valuable discussions. Polyvation BV and Jan Wever particularly are thanked for carrying out the GPC measurements. Mies J van Steenbergen

is thanked for the technical support for the different apparatus used in this study. Dr. Nathaniel I Martin is thanked for English editing.



## References

- [1] van Tomme SR, Storm G, Hennink WE. *In situ* gelling hydrogels for pharmaceutical and biomedical applications. *Int J Pharm* 2008;355:1-18.
- [2] Nguyen MK, Lee DS. Injectable biodegradable hydrogels. *Macromol Biosci* 2010;10:563-579.
- [3] Yu L, Ding J. Injectable hydrogels as unique biomedical materials. *Chem Soc Rev* 2008;37:1473-1481.
- [4] Li Y, Rodrigues J, Tomás H. Injectable and biodegradable hydrogels: gelation, biodegradation and biomedical applications. *Chem Soc Rev* 2012;41:2193-2221.
- [5] Vermonden T, Censi R, Hennink WE. Hydrogels for protein delivery. *Chem Rev* 2012;112:2853-2888.
- [6] Park MH, Joo MK, Choi BG, Jeong B. Biodegradable thermogels. *Acc Chem Res* 2012;45:424-433.
- [7] Moretton M, Chiappetta D, Sosnik A. Cryoprotection-lyophilization and physical stabilization of rifampicin-loaded flower-like polymeric micelles. *J R Soc Interface* 2012;9:487-502.
- [8] Shim MS, Lee HT, Shim WS, Park I, Lee H, Chang T, et al. Poly(D,L-lactic acid-*co*-glycolic acid)-*b*-poly(ethylene glycol)-*b*-poly(D,L-lactic acid-*co*-glycolic acid) triblock copolymer and thermoreversible phase transition in water. *J Biomed Mater Res* 2002;61:188-196.
- [9] Yu L, Chang G, Zhang H, Ding J. Temperature-induced spontaneous sol-gel transitions of poly(D,L-lactic acid-*co*-glycolic acid)-*b*-poly(ethylene glycol)-*b*-poly(D,L-lactic acid-*co*-glycolic acid) triblock copolymers and their end-capped derivatives in water. *J Polym Sci A Polym Chem* 2007;45:1122-1133.
- [10] Elstad NL, Fowers KD. OncoGel® (ReGel®/paclitaxel) - clinical applications for a novel paclitaxel delivery system. *Adv Drug Deliv Rev* 2009;61:785-794.
- [11] Zentner GM, Rathi R, Shih C, McRea JC, Seo M, Oh H, et al. Biodegradable block copolymers for delivery of proteins and water-insoluble drugs. *J Control Release* 2001;72:203-215.
- [12] Kim YJ, Choi S, Koh JJ, Lee M, Ko KS, Kim SW. Controlled release of insulin from injectable biodegradable triblock copolymer. *Pharm Res* 2001;18:548-550.

- [13] Choi S, Kim SW. Controlled release of insulin from injectable biodegradable triblock copolymer depot in ZDF rats. *Pharm Res* 2003;20:2008-2010.
- [14] Lee D, Shim M, Kim S, Lee H, Park I, Chang T. Novel thermoreversible gelation of biodegradable PLGA-*block*-PEO-*block*-PLGA triblock copolymers in aqueous solution. *Macromol Rapid Commun* 2001;22:587-592.
- [15] Yu L, Zhang Z, Zhang H, Ding J. Mixing a sol and a precipitate of block copolymers with different block ratios leads to an injectable hydrogel. *Biomacromolecules* 2009;10:1547-1553.
- [16] Yu L, Zhang Z, Zhang H, Ding J. Biodegradability and biocompatibility of thermoreversible hydrogels formed from mixing a sol and a precipitate of block copolymers in water. *Biomacromolecules* 2010;11:2169-2178.
- [17] Bramfeldt H, Sarazin P, Vermette P. Characterization, degradation, and mechanical strength of poly(D,L-lactide-*co*- $\epsilon$ -caprolactone)-poly(ethylene glycol)-poly(D,L-lactide-*co*- $\epsilon$ -caprolactone). *J Biomed Mater Res A* 2007;83A:503-511.
- [18] Zhang Z, Ni J, Chen L, Yu L, Xu J, Ding J. Biodegradable and thermoreversible PCLA-PEG-PCLA hydrogel as a barrier for prevention of post-operative adhesion. *Biomaterials* 2011;32:4725-4736.
- [19] Yu L, Zhang H, Ding J. A subtle end-group effect on macroscopic physical gelation of triblock copolymer aqueous solutions. *Angew Chem Int Ed Engl* 2006;45:2232-2235.
- [20] Jo S, Kim J, Kim SW. Reverse thermal gelation of aliphatically modified biodegradable triblock copolymers. *Macromol Biosci* 2006;6:923-928.
- [21] Jiang Z, Deng X, Hao J. Thermogelling hydrogels of poly( $\epsilon$ -caprolactone-*co*-D,L-lactide)-poly(ethylene glycol)-poly( $\epsilon$ -caprolactone-*co*-D,L-lactide) and poly( $\epsilon$ -caprolactone-*co*-L-lactide)-poly(ethylene glycol)-poly( $\epsilon$ -caprolactone-*co*-L-lactide) aqueous solutions. *J Polym Sci A Polym Chem* 2007;45:4091-4099.
- [22] Yavuz H, Babaç C, Tuzlakoglu K, Piskin E. Preparation and degradation of L-lactide and  $\epsilon$ -caprolactone homo and copolymer films. *Polym Degrad Stab* 2002;75:431-437.
- [23] Buwalda SJ, Dijkstra PJ, Calucci L, Forte C, Feijen J. Influence of amide versus ester linkages on the properties of eight-armed PEG-PLA star block copolymer hydrogels. *Biomacromolecules* 2009;11:224-232.

- [24] Vos R, Goethals EJ. End group analysis of commercial poly(ethylene glycol) monomethyl ether's. *Polym Bull* 1986;15:547-549.
- [25] Kricheldorf HR, Bornhorst K, Hachmann-Thiessen H. Bismuth(III) n-hexanoate and tin(II) 2-ethylhexanoate initiated copolymerizations of  $\epsilon$ -caprolactone and L-lactide. *Macromolecules* 2005;38:5017-5024.
- [26] Hao J, Keller T, Cai K, Klemm E, Bossert J, Jandt KD. The effect of D,L-lactidyl/ $\epsilon$ -caproyl weight ratio and chemical microstructure on surface properties of biodegradable poly(D,L-lactide)-*co*-poly( $\epsilon$ -caprolactone) random copolymers. *Adv Eng Mater* 2008;10:B23-32.
- [27] van de Velde K, Kiekens P. Biopolymers: overview of several properties and consequences on their applications. *Polym Test* 2002;21:433-442
- [28] Carstens MG, Bevernage JJL, van Nostrum CF, van Steenberg MJ, Flesch FM, Verrijk R, et al. Small oligomeric micelles based on end group modified mPEG-oligocaprolactone with monodisperse hydrophobic blocks. *Macromolecules* 2007;40:116-122.
- [29] Sánchez-Soto P, Ginés J, Arias M, Novák C, Ruiz-Conde A. Effect of molecular mass on the melting temperature, enthalpy and entropy of hydroxy-terminated PEO. *J Therm Anal Calorim* 2002;67:189-197.
- [30] Ginés JM, Arias MJ, Rabasco AM, Novák C, Ruiz-Conde A, Sánchez-Soto PJ. Thermal characterization of polyethylene glycols applied in the pharmaceutical technology using differential scanning calorimetry and hot stage microscopy. *J Therm Anal Calorim* 1996;46:291-304.
- [31] Craig DQM, Newton JM. Characterisation of polyethylene glycols using differential scanning calorimetry. *Int J Pharm* 1991;74:33-41.
- [32] Carstens MG, van Nostrum CF, Ramzi A, Meeldijk JD, Verrijk R, de Leede LL, et al. Poly(ethylene glycol)-oligolactates with monodisperse hydrophobic blocks: preparation, characterization, and behavior in water. *Langmuir* 2005;21:11446-11454.
- [33] Na Y, He Y, Shuai X, Kikkawa Y, Doi Y, Inoue Y. Compatibilization effect of poly( $\epsilon$ -caprolactone)-*b*-poly(ethylene glycol) block copolymers and phase morphology analysis in immiscible poly(lactide)/poly( $\epsilon$ -caprolactone) blends. *Biomacromolecules* 2002;3:1179-1186.

- [34] Tsuji H, Yamada T, Suzuki M, Itsuno S. Part 7. Effects of poly(L-lactide-*co*- $\epsilon$ -caprolactone) on morphology, structure, crystallization, and physical properties of blends of poly(L-lactide) and poly( $\epsilon$ -caprolactone). *Polym Int* 2003;52:269-275.
- [35] de Graaf AJ, Boere KWM, Kemmink J, Fokkink RG, van Nostrum CF, Rijkers DTS, et al. Looped structure of flowerlike micelles revealed by  $^1\text{H}$  NMR relaxometry and light scattering. *Langmuir* 2011;27:9843-9848.
- [36] Booth C, Attwood D. Effects of block architecture and composition on the association properties of poly(oxyalkylene) copolymers in aqueous solution. *Macromol Rapid Commun* 2000;21:501-527.
- [37] Gong C, Shi S, Wu L, Gou M, Yin Q, Guo Q, et al. Biodegradable *in situ* gel-forming controlled drug delivery system based on thermosensitive PCL-PEG-PCL hydrogel. Part 2: Sol-gel-sol transition and drug delivery behavior. *Acta Biomater* 2009;5:3358-3370.
- [38] Bae SJ, Suh JM, Sohn YS, Bae YH, Kim SW, Jeong B. Thermogelling Poly(caprolactone-*b*-ethylene glycol-*b*-caprolactone) aqueous solutions. *Macromolecules* 2005;38:5260-5265.
- [39] Hwang MJ, Suh JM, Bae YH, Kim SW, Jeong B. Caprolactonic poloxamer analog: PEG-PCL-PEG. *Biomacromolecules* 2005; 2011;6:885-890.
- [40] Jeong B, Bae YH, Kim SW. Thermoreversible gelation of PEG-PLGA-PEG triblock copolymer aqueous solutions. *Macromolecules* 1999;32:7064-7069.
- [41] Jeong B, Kibbey MR, Birnbaum JC, Won Y-Y, Gutowska A. Thermogelling biodegradable polymers with hydrophilic backbones: PEG-*g*-PLGA. *Macromolecules* 2000;33:8317-8322.
- [42] Jeong B, Wang L-Q, Gutowska A. Biodegradable thermoreversible gelling PLGA-*g*-PEG copolymers. *Chem Commun* 2001:1516-1517.
- [43] Shim WS, Kim J, Park H, Kim K, Chan Kwon I, Lee DS. Biodegradability and biocompatibility of a pH- and thermo-sensitive hydrogel formed from a sulfonamide-modified poly( $\epsilon$ -caprolactone-*co*-lactide)-poly(ethylene glycol)-poly( $\epsilon$ -caprolactone-*co*-lactide) block copolymer. *Biomaterials* 2006;27:5178-5185.
- [44] Carstens MG, van Nostrum CF, Verrijck R, de Leede LGJ, Crommelin DJA, Hennink WE. A mechanistic study on the chemical and enzymatic degradation of PEG-oligo( $\epsilon$ -caprolactone) micelles. *J Pharm Sci* 2008;97:506-518.

- [45] van Nostrum CF, Veldhuis TFJ, Bos GW, Hennink WE. Hydrolytic degradation of oligo(lactic acid): a kinetic and mechanistic study. *Polymer* 2004;45:6779-6787.
- [46] Geng Y DD, Discher DE. Hydrolytic degradation of poly(ethylene oxide)-*block*-polycaprolactone worm micelles. *J Am Chem Soc* 2005;127:12780-12781.
- [47] Jeong B, Bae YH, Kim SW. *In situ* gelation of PEG-PLGA-PEG triblock copolymer aqueous solutions and degradation thereof. *J Biomed Mater Res* 2000;50:171-177.

## Appendices

### Equation

**Equation A.1:** Theoretical number of methylene protons in PEG<sub>1500</sub> per mole,  $I_{PEG}$

$$I_{PEG} = 4 \times \left( \frac{M_{PEG}}{M_{EG}} \right) = 136 \text{ with } M_{PEG} = 1500 \text{ g/mol and } M_{EG} = 44 \text{ g/mol.}$$

**Equation A.2:** Number of methylene protons in PEG at 3.72-3.55 ppm,  $I_{3.6}$

This value was determined by adding an excess of TCAI to PEG<sub>1500</sub>. The formation of  $\text{Cl}_3\text{C-NH-C(O)-(O-CH}_2\text{-CH}_2)_n\text{-O-C(O)-NH-CCl}_3$  led to the formation of a new peak at 4.40ppm ( $I_{4.4}$ , 4H,  $\text{Cl}_3\text{C-NH-C(O)-O-CH}_2\text{-CH}_2\text{-O-}$ ) [24].

$I_{3.6} = 122$  for  $I_{4.4} = 4$ . This value is in agreement with the expected value of  $136 - 4 = 132$  H (as determined in Equation A.1.).

**Equation A.3:** Number of CL-CL bonds per mol PEG

This value is estimated from the spectrum of DM0 since  $\text{-C(O)-CH}_2\text{-(CH}_2)_3\text{-CH}_3$  of the end groups of DM2 has a chemical shift at 2.50-2.20 ppm.

$$n_{CL-CL} = \frac{I_{2.2}}{2} \text{ for normalized } I_{3.6} = 122.$$

**Equation A.4:** Number of CL-LA bonds per mol PEG

This value is estimated from the spectrum of DM0 since  $\text{-C(O)-CH}_2\text{-(CH}_2)_3\text{-CH}_3$  of the end groups of DM2 has a chemical shift at 2.50-2.20 ppm.

$$n_{CL-LA} = \frac{I_{2.3}}{2} \text{ for normalized } I_{3.6} = 122.$$

**Equation A.5:** Number of CL per polymer chain

$$n_{CL} = n_{CL-CL} + n_{CL-LA}.$$

**Equation A.6:** Number of LA per polymer chain

This value is estimated from the spectrum of DM2 since  $\text{-C(O)-CH(CH}_3\text{)-OH}$  of DM0 has a chemical shift at 4.30-4.20 ppm.

$$n_{LA} = I_{5.1} \text{ for normalized } I_{3.6} = 122.$$

**Equation A.7:** Molar ratio CL/LA

$$k = \frac{n_{CL}}{n_{LA}}.$$

**Equation A.8:** Number average molecular weight of PCLA

$$M_{n,PCLA} = n_{CL} \times 114 + n_{LA} \times 72 .$$

**Equation A.9:** Weight CL content

$$CL(wt\%) = 100 \times \left[ \frac{(n_{CL} \times 114)}{M_{n,PCLA}} \right] .$$

**Equation A.10:** Weight ratio PCLA/PEG

$$PCLA/PEG = \frac{M_{n,PCLA}}{M_{PEG}} .$$

**Equation A.11:** Degree of Modification

$$DM(mol) = \frac{I_{0.8}}{3} \text{ for normalized } I_{3.6} = 122 .$$

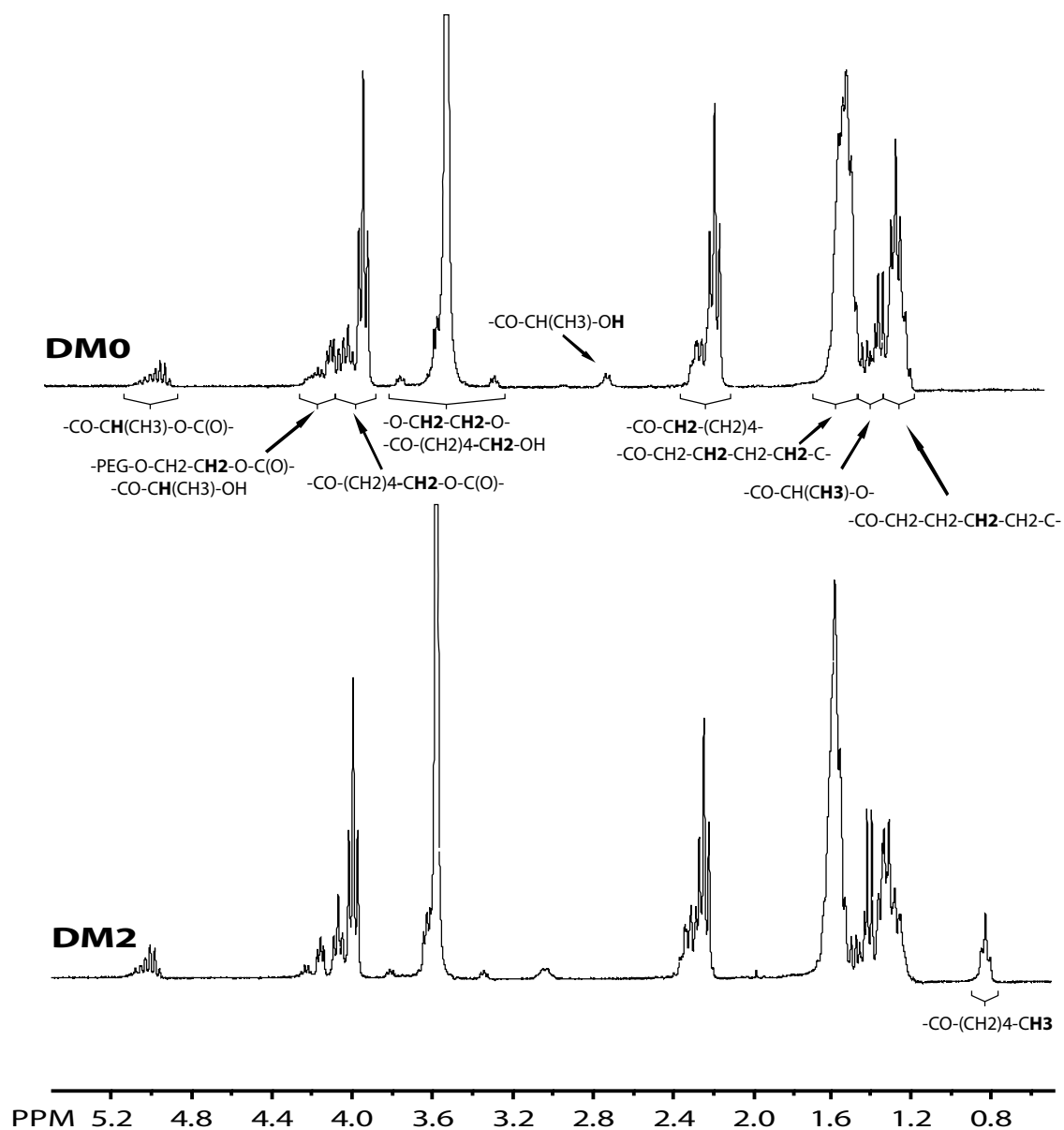
**Equation A.12:** Number average molecular weight

$$M_{n,NMR} = M_{PEG} + M_{n,PCLA} + (99 \times DM) .$$

**Equation A.13:** Average length of the CL blocks

$$L_{CL} = (n_{CL-CL} / n_{LA-CL}) + 1 .$$

Figure

Figure A.1:  $^1\text{H}$  NMR spectra of DM0 and DM2 in  $\text{CDCl}_3$ .



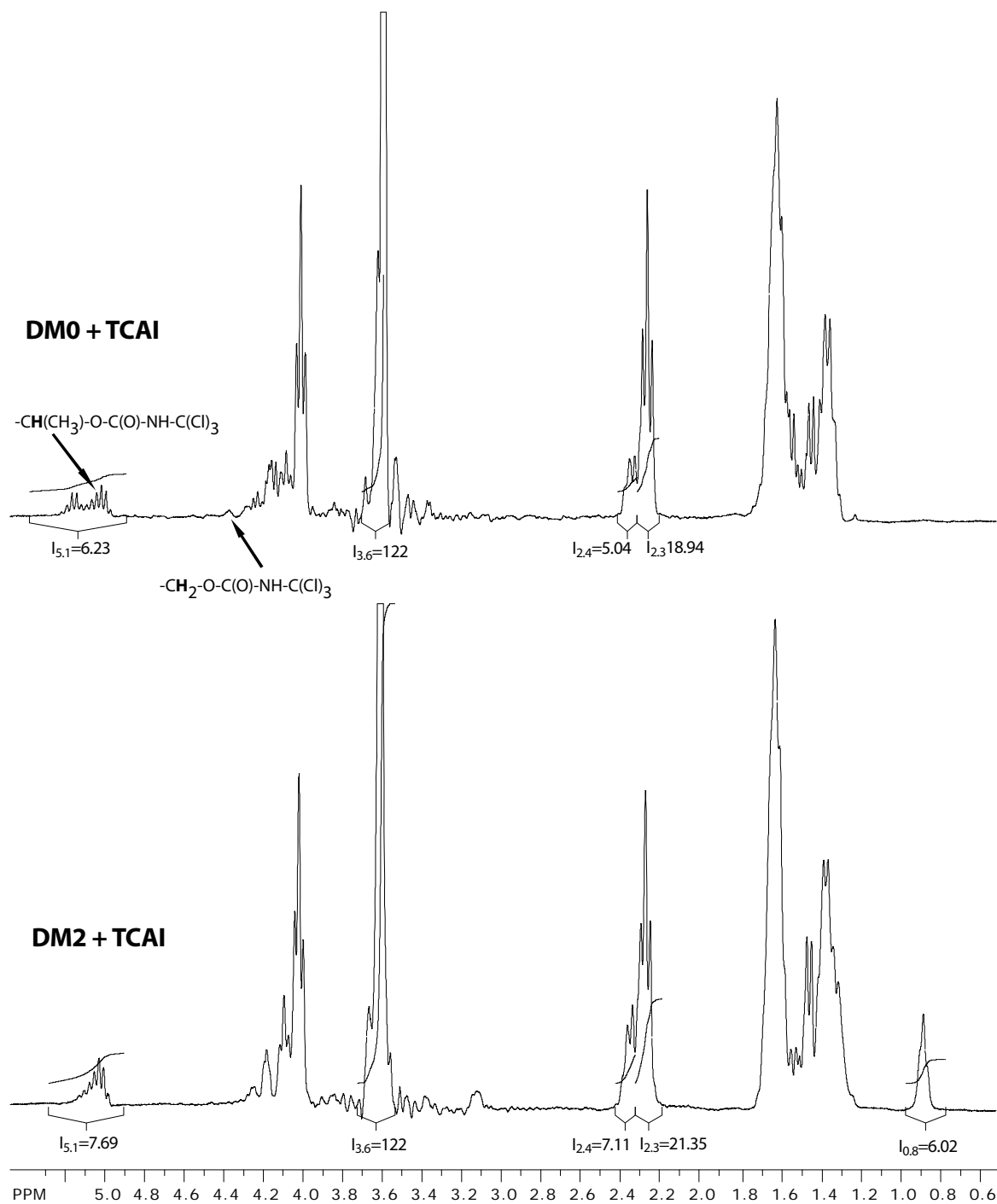


Figure A.2: Integrated spectra of DM0 and DM2 after addition of an excess of TCAI.

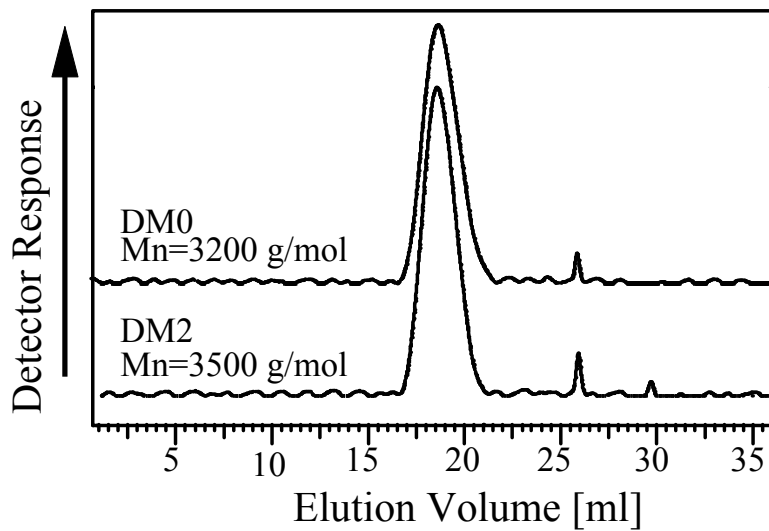


Figure A.3: GPC chromatograms of the DM0 and DM2.

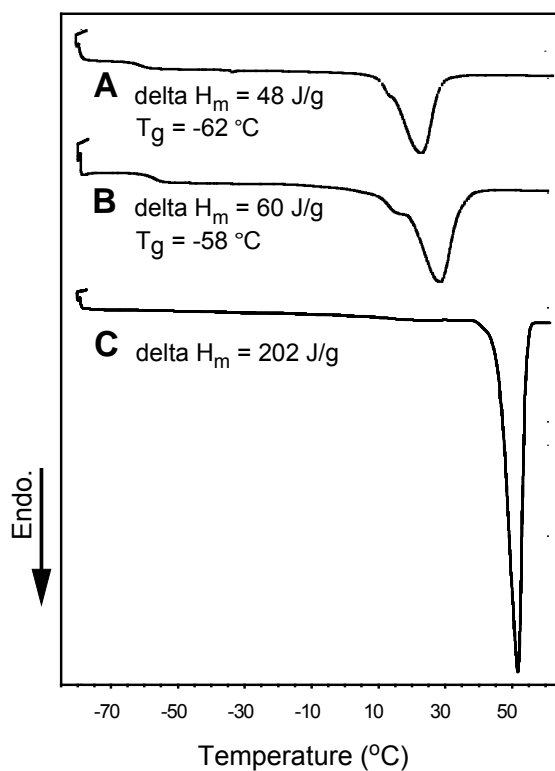


Figure A.4: DSC thermograms (second heating) of DM2 (A), DM0 (B) and PEG1500 (C). Glass transition ( $T_g$ ) and melting enthalpy ( $\Delta H$ ) are the average of two measurements.

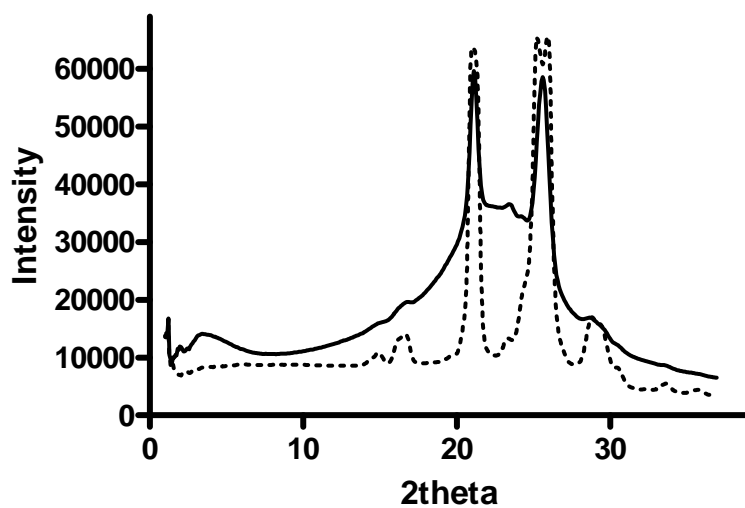


Figure A.5: X-ray diffraction patterns of PEG<sub>1500</sub> (dotted line) and DM0 (continue line) polymers.

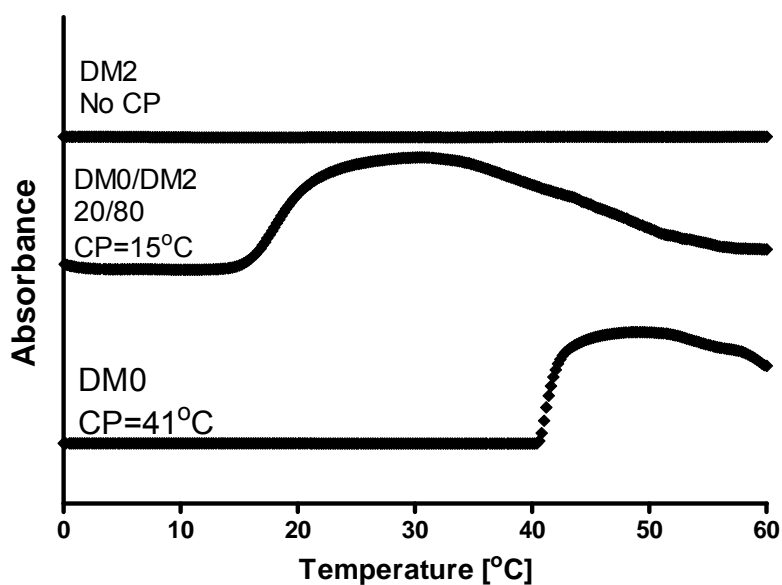
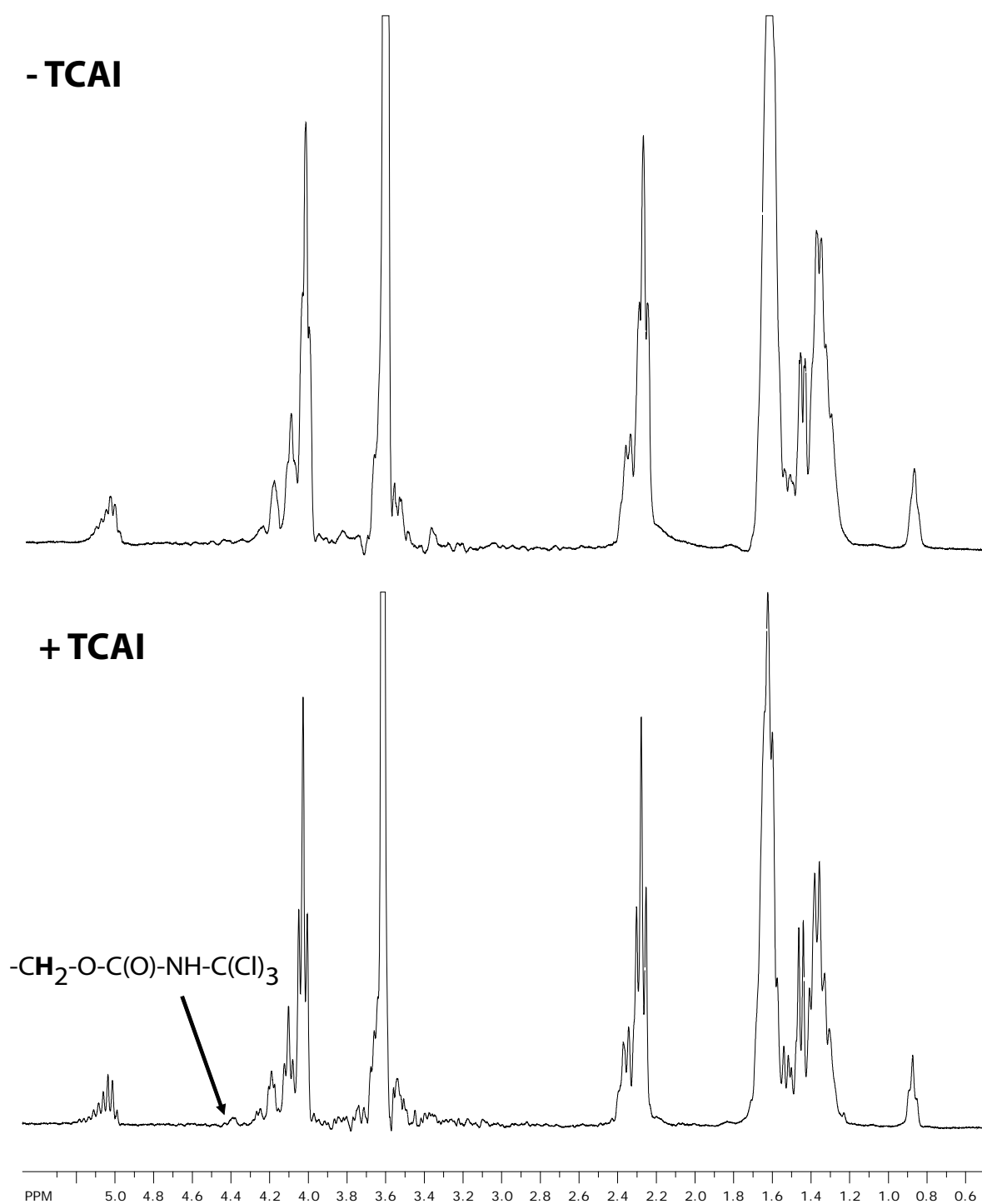


Figure A.6: Turbidity curves of DM0 and DM2 and their physical mixture DM0/DM2 = 20/80 in phosphate buffer at 2 mg/ml.



**Figure A.7:**  $^1\text{H}$  NMR spectra of polymers in the residual gels ( $t = 60$  days) of DM0/DM2 (20/80) at 25 wt% in phosphate buffer before and after addition of an excess of TCAI. No quantifiable peaks were observed at 4.2–4.6 ppm in the  $^1\text{H}$  NMR spectra of degradation samples, indicating gel degradation by dissolution and not by chemical polymer degradation.



## CHAPTER 3

# Effect of polymer composition on rheological and degradation properties of temperature-responsive gelling systems composed of acyl-capped **PCLA-PEG-PCLA**

Audrey Petit<sup>1,2</sup>, Benno Müller<sup>1</sup>, Ronald Meijboom<sup>1</sup>, Peter Bruin<sup>1</sup>, Frank van de Manakker<sup>1</sup>, Marjan Versluijs-Helder<sup>3</sup>, Leo GJ de Leede<sup>1</sup>, Albert Doornbos<sup>4</sup>, Mariana Landin<sup>5</sup>, Wim E Hennink<sup>2</sup> and Tina Vermonden<sup>2</sup>

<sup>1</sup> InGell Labs BV, Groningen, The Netherlands.

<sup>2</sup> Department of Pharmaceutics, Utrecht Institute for Pharmaceutical Sciences, Utrecht University, Utrecht, The Netherlands.

<sup>3</sup> Department of Inorganic Chemistry and Catalysis, Debye Institute for Nanomaterials Science, Utrecht University, Utrecht, The Netherlands.

<sup>4</sup> Innocore Technology BV, Groningen, The Netherlands

<sup>5</sup> Departamento de Farmacia y Tecnología Farmacéutica, Facultad de Farmacia, Universidad de Santiago, Santiago de Compostela, Spain



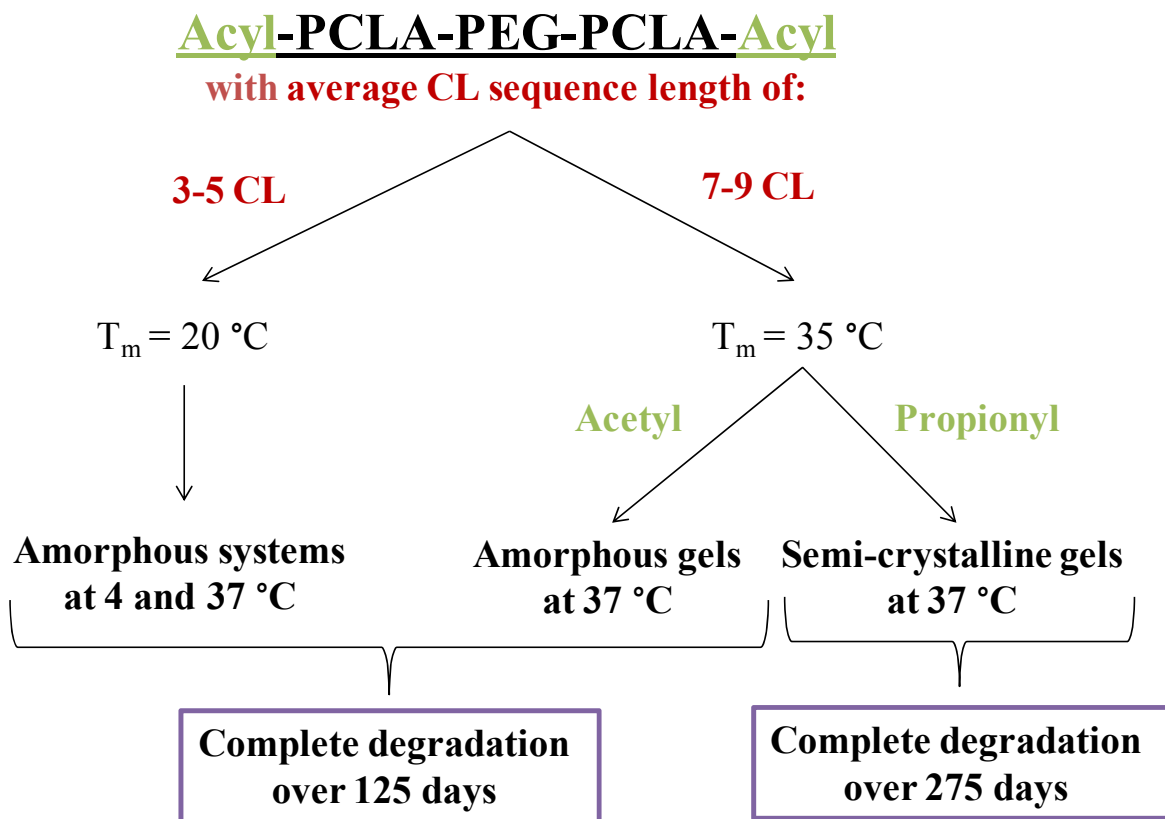
## **Abstract**

In this study, the ability to modulate the rheological and degradation properties of temperature-responsive gelling systems composed of acyl-capped poly( $\epsilon$ -caprolactone-*co*-lactide)-*b*-poly(ethylene glycol)-*b*-poly( $\epsilon$ -caprolactone-*co*-lactide) (PCLA-PEG-PCLA) triblock copolymers was investigated.

Eight polymers with varying molecular weights of PCLA, caproyl/lactoyl ratios (CL/LA) and capped with either acetyl- or propionyl-groups were synthesized by ring opening polymerization of L-lactide and  $\epsilon$ -caprolactone in toluene using PEG as initiator and tin (II) 2-ethylhexanoate as catalyst, and subsequently reacted in solution with an excess of acyl chloride to yield fully acyl-capped PCLA-PEG-PCLA. The microstructure of the polymers was determined by  $^1\text{H}$  NMR and the thermal properties and crystallinity of the polymers in dry state and in 25 wt% aqueous systems were studied by DSC and X-ray diffraction. Rheological and degradation/dissolution properties of aqueous systems composed of the polymers in 25 wt% aqueous systems were studied.

$^1\text{H}$  NMR analysis revealed that the monomer sequence in the PCLA blocks was not fully random resulting in relatively long CL sequences, even though transesterification was demonstrated by the enrichment with lactoyl units and the presence of PEG-OH end groups. Except the most hydrophilic polymer composed of acetyl-capped PCLA<sub>1400</sub>-PEG<sub>1500</sub>-PCLA<sub>1400</sub> having a CL/LA molar ratio of 2.5, the polymers of 25 wt% in buffer were sols below room temperature and transformed into gels between room temperature and 37 °C, which makes them suitable as temperature-responsive gelling systems for drug delivery. Over a period of weeks at 37 °C, the systems containing polymers with long CL sequences (~8 CL) and propionyl end-groups became semi-crystalline as shown by X-ray diffraction analysis. Degradation of the gels by dissolution at 37 °C took 100-150 days for the amorphous gels and 250-300 days for the semi-crystalline gels.

In conclusion, this study shows that changes in the polymer composition allow an easy but significant modulation of rheological and degradation properties.





## 1. Introduction

Aqueous systems containing copolymers composed of poly(lactide-*co*-glycolide) (PLGA) and poly(ethylene glycol) (PEG) can form temperature-responsive gelling systems [1-3], which have been evaluated in clinical trials for applications in oncology, particularly as matrices for the sustained release of paclitaxel [4-7]. Similar systems, composed of ABA triblock copolymers with PEG as B block and poly( $\epsilon$ -caprolactone-*co*-lactide) (PCLA) as A blocks, are also of interest since they have longer degradation times than PLGA-PEG-PLGA-based systems [8,9]. To mention, degradation times of over six months were shown for polymers based on PEG<sub>1500</sub> and PCLA [8], while PLGA/PEG copolymers typically degrade in one to two months [5,10,11].

Furthermore, Kang et al. [12] showed that the PCL block of methoxyPEG-*b*-PCLA diblock copolymers can form crystalline domains that affect the degradation kinetics of the systems in water. Indeed, it is known that crystalline domains are less rapidly degraded than amorphous domains due to limited hydration [13]. The crystalline structure of PCLA depends not only on the monomer ratio [12] but also on the monomer sequence, i.e. its microstructure [14]. The microstructure of aliphatic copolyesters is tailored by the polymerization conditions and extensive efforts have been made to understand and modulate it [14-16]. Ring opening of the lactones using a suitable initiator (e.g., a compound with a (primary) alcohol (such as PEG) and a catalyst (e.g., stannous octoate) involves cleavage of their acyl-oxygen bond followed by propagation and transesterification reactions [17]. The reaction parameters that influence transesterification reactions are temperature, reaction time, the type and concentration of catalyst, and the nature of the lactone [16-21]. In the case of copolymerization of lactide with  $\epsilon$ -caprolactone, the reactivity of lactide is considerably higher than that of caprolactone. Consequently, in the first step of copolymerization, lactide is preferentially polymerized and thereafter, transesterification takes place due to the attack of an active caproyl centre on the polylactide blocks resulting in randomization of the structure [14,22-26].

Besides the type of aliphatic copolyester and its microstructure that allow modulation of the degradation/dissolution kinetics of aqueous polyester-PEG-polyester-based systems, also modification of the terminal hydroxyl end-

groups of the polyester blocks has been applied to modulate the rheological as well as degradation/dissolution properties [25,27,28]. We showed previously [25] that the fraction of hexanoyl-capped PCLA-PEG-PCLA in aqueous blends with uncapped PCLA-PEG-PCLA allows control of the sol-to-gel transition temperature as well as of the viscoelasticity of the systems at 37 °C. It was also shown that temperature-responsive gelling systems composed of these blends degrade *in vitro* in ~3-4 months by dissolution and not by polymer hydrolysis [29-33]. However, these systems showed phase separation at temperatures above 20 °C, which makes them difficult to handle.

To prepare systems with improved properties, such as: (i) ease of administration (higher sol-to-gel transition temperature), (ii) none or slower phase-separation (i.e. higher gel-to-precipitate transition temperature) and (iii) controllable dissolution rate, structure-function relationships have to be established. It has been shown that the composition, the molecular weight and type of end groups of the PEG/polyester copolymers forming *in situ* gelling systems are important variables to take into consideration [8,10-12,25,27,28,34,35].

In this study, we synthesized eight structurally related polymers with varying compositions and investigated thoroughly the microstructure of the PCLA blocks. Also, we studied how these changes allow modulation of rheological and degradation properties of aqueous systems composed of acyl-capped PCLA-PEG-PCLA.

## 2. Experiments and protocols

### 2.1. Materials

L-lactide was obtained from Purac Biochem, The Netherlands. All other chemicals were obtained from Aldrich and used as received.

### 2.2. Experimental Design

Eight polymer compositions with three independent variables:  $M_n$  (number average molecular weight) of PCLA block (1400 vs. 1700 g/mol), caproyl/lactoyl (CL/LA) molar ratio (2.5/1 vs. 5.7/1 mol/mol) and type of end-group (acetyl or propionyl) were selected. We further refer to specific polymers as, for instance, PEG(PCLA<sub>1700</sub>CL<sub>5.7</sub>Prop)<sub>2</sub> being a polymer with

$M_{n,PCLA} = 1700$  g/mol per PCLA block, high CL content (CL/LA = 5.7/1, i.e. 90 wt% CL) and propionyl end-groups. The polymer series used in this study were composed of nine polymer batches: eight polymers with different compositions and one polymer composition, namely PEG(PCLA<sub>1700</sub>CL<sub>2.5</sub>Acet)<sub>2</sub>, was synthesized in duplicate to evaluate the reproducibility of the synthetic procedure (Table 1).

**Table 1:** Composition of the polymers synthesized in this study.

<i>Abbreviation</i>	$M_{n,PCLA}$ [g/mol]	$CL/LA$ [mol/mol]	<i>Acyl end-group</i>
PEG(PCLA <sub>1400</sub> CL <sub>2.5</sub> Acet) <sub>2</sub>	1400	2.5/1	acetyl-
PEG(PCLA <sub>1700</sub> CL <sub>2.5</sub> Acet) <sub>2</sub> *	1700		
PEG(PCLA <sub>1400</sub> CL <sub>5.7</sub> Acet) <sub>2</sub>	1400	5.7/1	acetyl-
PEG(PCLA <sub>1700</sub> CL <sub>5.7</sub> Acet) <sub>2</sub>	1700		
PEG(PCLA <sub>1400</sub> CL <sub>2.5</sub> Prop) <sub>2</sub>	1400	2.5/1	propionyl-
PEG(PCLA <sub>1700</sub> CL <sub>2.5</sub> Prop) <sub>2</sub>	1700		
PEG(PCLA <sub>1400</sub> CL <sub>5.7</sub> Prop) <sub>2</sub>	1400	5.7/1	propionyl-
PEG(PCLA <sub>1700</sub> CL <sub>5.7</sub> Prop) <sub>2</sub>	1700		

\* polymer synthesized in duplicate

### *2.3. Synthesis of acyl-capped PCLA-PEG-PCLA*

The synthesis of acyl-capped PCLA-PEG-PCLA was performed essentially as previously described [25]. Briefly, in a three-neck round-bottom flask equipped with a Dean Stark trap and a condenser, PEG<sub>1500</sub> (10-50 g), L-lactide (1-22 g),  $\epsilon$ -caprolactone (10-90 g) and toluene (30-150 ml) were introduced and, while stirring, heated to reflux ( $\sim 140$  °C; i.e. the boiling point of toluene is 111 °C but that of the mixture is  $\sim 140$  °C) under nitrogen atmosphere. Table A.1 gives the amount of PEG<sub>1500</sub> and monomers used for the synthesis of each of the nine different polymer batches. The solutions were azeotropically dried by distilling off toluene/water ( $\sim 50$  vol% of the initial volume). Next, the solutions were cooled to  $\sim 90$  °C and

tin(II) 2-ethylhexanoate (5 mmol per mol PEG<sub>1500</sub>) was added. Ring-opening polymerization was carried out at 110-120 °C overnight under nitrogen atmosphere. The solutions were cooled to room temperature and dichloromethane (20-100 ml) and triethylamine (3 mol per mol PEG<sub>1500</sub>) were added. The solutions were then cooled to 0 °C in an ice bath, and while stirring, an excess of acyl chloride (acetyl or propionyl chloride, ratio acyl/PEG = 4 mol/mol) was added drop wise and acylation was allowed to proceed for three hours. Dichloromethane was removed under vacuum at 60-65 °C. Next, ethyl acetate (20-100 ml) was added and triethylamine hydrochloride salts were removed by filtration. The polymers were precipitated by addition of a 1:1 mixture of hexane and diethyl ether (20-90 ml). Upon storage at -20 °C, the polymers separated as waxy solids from which non-solvents containing unreacted monomers and excess of acyl chloride could be decanted easily. The precipitated polymers were dried in vacuo and obtained in yield of at least 85 %.

#### 2.4. Synthesis of diacetyl-PEG

PEG<sub>1500</sub> (10 g, 6.7 mmol) and 4.5 ml (45 mmol) triethylamine were dissolved in 25 ml dry dichloromethane. The stirred solution was cooled in an ice bath and subsequently 2.1 ml acetyl chloride (27 mmol, ratio acyl/PEG = 4 mol/mol) was added slowly. The reaction was allowed to proceed for 3 hours at room temperature. The solvent was removed under vacuum and the obtained yellowish residue was dissolved in ~100 ml ethyl acetate and subsequently filtered. Hexane was added to precipitate the acetyl-capped PEG, which was subsequently dried in vacuo. The yield was 9 g.

#### 2.5. <sup>1</sup>H NMR and GPC analysis

<sup>1</sup>H NMR analysis of the polymers dissolved in CDCl<sub>3</sub> was performed using a Varian Oxford, operating at 300 MHz. <sup>1</sup>H NMR spectra were referenced to the signal of chloroform at 7.26 ppm. The characteristic peaks of the PCLA-PEG-PCLA backbone were identified as previously described [25].

Acetyl-end group: 2.14-2.12 ppm (*I*<sub>2.13</sub>, CH<sub>3</sub>-CO-O-CH(CH<sub>3</sub>-)); 2.03-2.05 ppm (*I*<sub>2.04</sub>, CH<sub>3</sub>-CO-O-(CH<sub>2</sub>)<sub>5</sub>-) [27,36-39], and 2.10-2.08 ppm (*I*<sub>2.09</sub>, CH<sub>3</sub>-CO-O-(CH<sub>2</sub>)<sub>2</sub>-O-) as shown in Figure A.1 in the appendices.

Propionyl-end group: 1.18 ppm ( $I_{1.2}$ ,  $\text{CH}_3\text{-CH}_2\text{-CO-O-}$ ); 2.4 ppm ( $\text{CH}_3\text{-CH}_2\text{-CO-O-}$ ) [27,36].

Since the peaks belonging to  $-\text{CO}(\text{CH}_2)_4\text{-CH}_2\text{-OH}$  of terminal CL and  $-\text{O-CH}_2\text{-CH}_2\text{-OH}$  of unreacted PEG overlap with the peak belonging to  $-\text{C-O-CH}_2\text{-CH}_2\text{-O-C-}$  of PEG at 3.85-3.25 ppm, the shift reagent trichloroacetylisocyanate (TCAI) was used to react with free hydroxyl end-groups to form  $-\text{O-C(O)-NH-C(Cl)}_3$  urethane-containing moieties [25]. The protons belonging to  $-\text{CH}_2\text{-O-C(O)-NH-C(Cl)}_3$  of CL, PEG and LA have chemical shifts around 1 ppm higher than that of protons before reaction with TCAI (4.6, 4.4 and 5.2 ppm, respectively) [25,40]. After addition of an excess of TCAI, the composition of the polymers was established from the integral of signals belonging to methine protons of LA ( $I_{5.1}$ ), methylene protons of PEG ( $I_{3.6}$  at 3.72-3.55 ppm), methylene protons of CL ( $I_{2.4} + I_{2.3}$ ), and methyl protons of end groups ( $I_{2.13}+I_{2.09}+I_{2.04}$  and  $I_{1.2}$  for acetyl and propionyl, respectively). The equation used to calculate the composition of the synthesized block copolymers is given in the appendices (Equation A.1 to A.12).

The  $M_n$  and polydispersity index (PDI) of the polymers were determined by GPC as previously described [25].

### *2.6. Differential scanning calorimetry (DSC) analysis of the polymers*

The thermal properties of acyl-capped PCLA-PEG-PCLA were determined by DSC (TA Instruments DSC Q2000 apparatus). Samples of ~10 mg were introduced into aluminum pans, which were subsequently sealed and heated from room temperature to 60 °C with a rate of 5 °C/min under nitrogen flow (50 ml/min). Next, the samples were cooled to -90 °C with the same rate, followed by a second heating cycle with the same rate to 60 °C. Using the second heat run, the glass transition temperature ( $T_g$ ) was set as the midpoint of heat capacity change, the temperature range of the melting ( $T_m$ ) was defined as the temperature range of the endothermic area and the melting enthalpy ( $\Delta H$ ) as its integration.

### *2.7. Preparation of aqueous systems containing 25 wt% polymer*

1.5 ml phosphate buffer pH 7.4 (44 mM  $\text{Na}_2\text{HPO}_4$ , 9 mM  $\text{NaH}_2\text{PO}_4$ , 72 mM  $\text{NaCl}$ , 0.02 wt%  $\text{NaN}_3$ ) was added to 500 mg of polymers in screw-

capped vials of 1-cm diameter to yield systems with 25 wt% solid content. The vials were closed and heated for 15 min at 50 °C, subsequently vortexed and then incubated at 4 °C for 48 hours to yield homogeneous dispersions.

### 2.8. X-ray diffraction (XRD)

X-ray diffraction patterns of the dry polymers as well as of 25 wt% aqueous systems after storage at 4 and 37 °C were recorded at room temperature. The samples were temporarily taken out of storage and measured within 2 hours. X-ray diffraction analysis was performed using a Bruker-AXS D8 Advance Powder X-ray diffractometer, in Bragg-Brentano mode, equipped with automatic divergence slit and a PSD Vântec-1 detector. The radiation used was Cobalt  $K\alpha_{1,2}$ ,  $\lambda = 1.79026 \text{ \AA}$ , operated at 30 kV, 45 mA. The X-ray diffraction patterns were recorded at a sample-to-detector distance of 435 mm. Separate patterns of blank samples were also recorded to allow subtraction of air- and capillary wall-scattering.

### 2.9. Vial tilting and rheological characterization

Vial tilting was used to visually establish the sol and gel state of systems of 25 wt% polymer in phosphate buffer. Vial tilting was performed at 4 °C, room temperature (20-22 °C) and at 37 °C after 30 min incubation. Immobility for 10 min, with vials upside down, was used to discriminate between mobile sols and immobile gels [25].

Rheological characteristics of systems of 25 wt% polymer in phosphate buffer were determined by oscillatory temperature sweep experiments using a TA AR-G2 rheometer equipped with a Peltier plate (1 ° steel cone, 20 mm diameter with solvent trap) at 1 % strain and 1 Hz frequency. The solvent trap of the Peltier plate was filled with water to prevent dehydration of the samples during the measurement. Samples (70  $\mu\text{l}$ ,  $\sim 4 \text{ °C}$ ) were introduced between the plates of the rheometer (pre-cooled to 4 °C), and were heated from 4 to 50 °C under oscillatory force with a heating rate of 1 °C/min.

### 2.10. Degradation properties

The degradation properties of the systems of 25 wt% polymer in phosphate buffer at 37 °C were investigated. Sols (300  $\mu\text{l}$ ) at 4 °C were transferred via a syringe into glass vials (8.2  $\times$  40 mm). Next, the vials were

closed and placed at 37 °C to allow gel formation, and after 30 min, 700  $\mu$ l phosphate buffer pre-heated to 37 °C was added. At predetermined time points, the buffer was removed, the weight of remaining gels was measured and fresh buffer was added. Also, samples were freeze-dried for further analysis (dry weight determination, GPC and  $^1\text{H}$  NMR analysis before and after addition of an excess of TCAI) [25]. Dry weight was determined by weighing residual gels after freeze drying.

### 3. Results and discussion

#### 3.1. Synthesis and characterization of acyl-capped PCLA-PEG-PCLA

PCLA-PEG<sub>1500</sub>-PCLA triblock copolymers were synthesized by ring opening polymerization of L-lactide and  $\epsilon$ -caprolactone in solution with PEG<sub>1500</sub>-diol as macroinitiator and tin(II) 2-ethylhexanoate as catalyst. Subsequently, acylation of the hydroxyl end-groups using an excess of acetyl or propionyl chloride resulted in the formation of acetyl- or propionyl-capped PCLA-PEG-PCLA, respectively with a yield of ~85 %. Representative  $^1\text{H}$  NMR spectra of PEG(PCLA<sub>1400</sub>CL<sub>2.5</sub>Acet)<sub>2</sub> and PEG(PCLA<sub>1700</sub>CL<sub>5.7</sub>Prop)<sub>2</sub> are given in Figure 1.

To get more insight into the microstructure of the PCLA polymers,  $^1\text{H}$  NMR spectra were analyzed in detail and Figure 2 shows the obtained information regarding the composition of the polymers, i.e. CL/LA molar ratio (Figure 2, #1), degree of end-group modification (Figure 2, #2), the monomer (CL or LA) adjacent to PEG (Figure 2, #3), the monomer (CL or LA) adjacent to the acyl groups (Figure 2, #4) and the randomness of the PCLA blocks (Figure 2, #5). As an example, the information related to PEG(PCLA<sub>1700</sub>CL<sub>2.5</sub>Acet)<sub>2</sub>, which was synthesized twice, is reported here in detail.

#### #1: CL/LA molar ratio of PEG(PCLA<sub>1700</sub>CL<sub>2.5</sub>Acet)<sub>2</sub>

The peaks at 5.25-4.95 and 2.50-2.10 ppm, corresponding to the methine protons of LA and the methylene protons of CL respectively, were used to calculate the molar ratio of CL to LA (Equation A.7). The molar ratio CL/LA was  $2.2 \pm 0.1$  mol/mol ( $n = 2$ ), which is 12 % lower than the CL/LA feed of 2.5. Assuming that the more reactive L-lactide fully reacted during

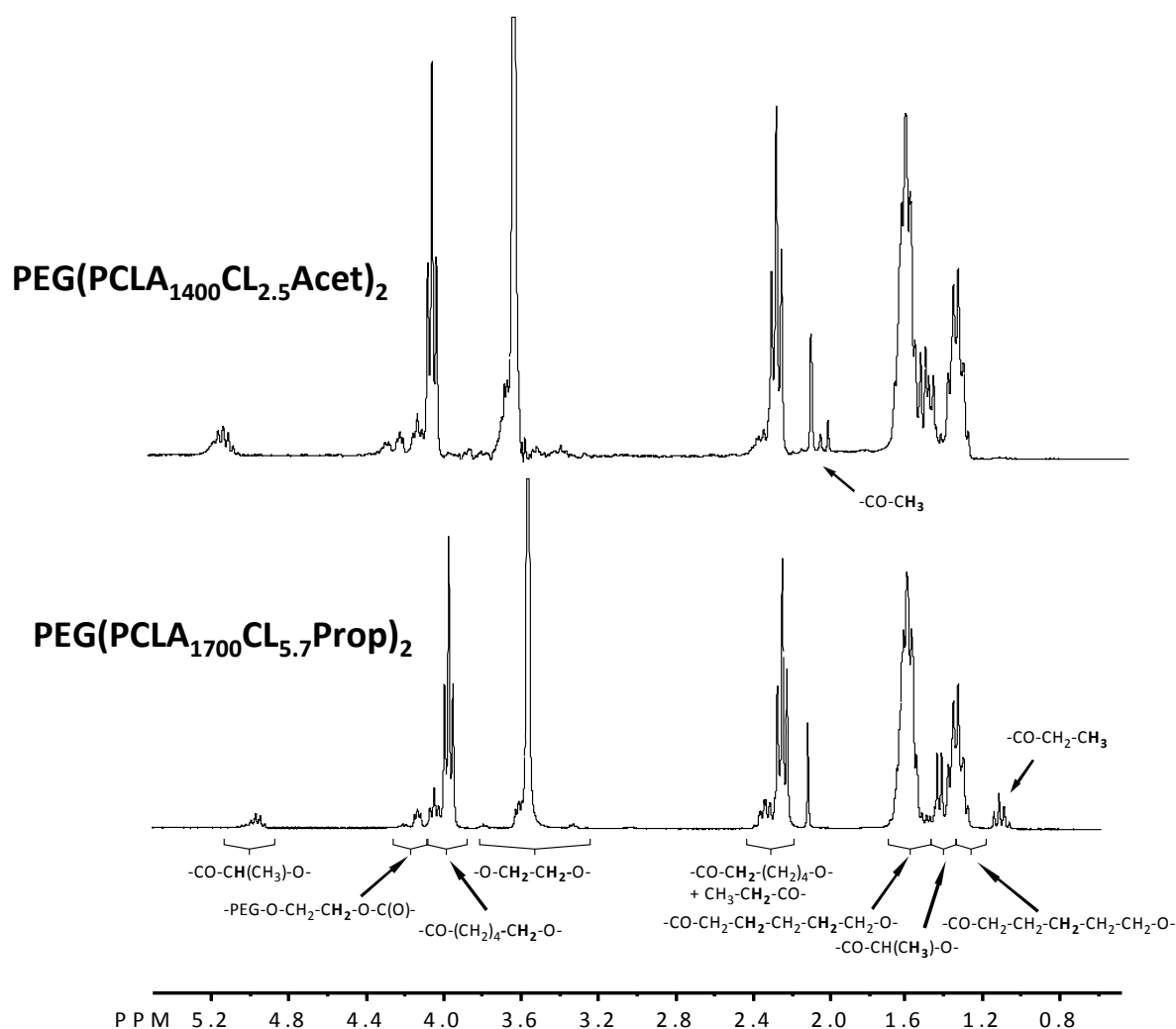


**Figure 1:** <sup>1</sup>H NMR spectra of PEG(PCLA<sub>1400</sub>CL<sub>2.5</sub>Acet)<sub>2</sub> and PEG(PCLA<sub>1700</sub>CL<sub>5.7</sub>Prop)<sub>2</sub> in CDCl<sub>3</sub>. PEG(PCLA<sub>1400</sub>CL<sub>2.5</sub>Acet)<sub>2</sub> ( $M_{n,PCLA} = 1400$  g/mol per block, CL/LA = 2./1 mol/mol (i.e 80 wt% CL), acetyl-end groups) and PEG(PCLA<sub>1700</sub>CL<sub>5.7</sub>Prop)<sub>2</sub> ( $M_{n,PCLA} = 1700$  g/mol per block, CL/LA = 5.7/1 mol/mol (i.e. 90 wt% CL), propionyl-end groups).

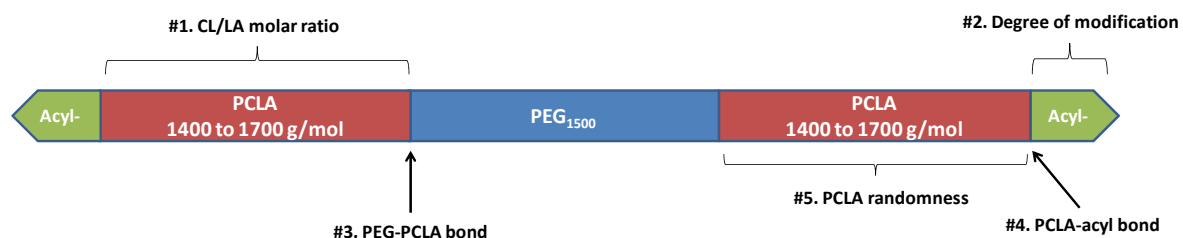


**Figure 2:** Composition and microstructure of the copolymers.



ring opening polymerization, a molar ratio CL/LA means that 88 % of  $\epsilon$ -caprolactone has reacted, which is in line with the yield of  $\sim 85$  %. The  $M_n$  of the PCLA blocks, calculated from the  $^1\text{H}$  NMR analysis (Equation A.8), was  $1600 \pm 100$  g/mol ( $n = 2$ ), which is slightly lower than the calculated  $M_n$  of 1700 g/mol, but in line with the incomplete polymerization of  $\epsilon$ -caprolactone (see discussion above). GPC analysis (calibration with PEG standards) showed that the  $M_n$  was  $5100 \pm 400$  g/mol ( $n = 2$ ), which is close to the value determined by  $^1\text{H}$  NMR ( $4700 \pm 200$  g/mol).

#2: Degree of modification of PEG(PCLA<sub>1700</sub>CL<sub>2.5</sub>Acet)<sub>2</sub>

The degree of acylation as determined by  $^1\text{H}$  NMR (Equation A.11) was above  $93 \pm 8\%$ , which is in line with previously reported data for polymers acylated under similar experimental conditions [25].

#3: Monomer adjacent to PEG of PEG(PCLA<sub>1700</sub>CL<sub>2.5</sub>Acet)<sub>2</sub>

The molar ratio -CL-PEG/-LA-PEG bonds calculated from the integrals of the -CL-O-CH<sub>2</sub>-CH<sub>2</sub>-O- peak at 4.23-4.15 ppm and -LA-O-CH<sub>2</sub>-CH<sub>2</sub>-O- peak at 4.35-4.23 ppm, was  $1.6 \pm 0.1$ , whereas a ratio of 2.2 was expected. Thus, there is a slight enrichment in LA of the PEG-PCLA bonds, meaning that PEG-OH preferentially reacted with L-lactide during the ring opening polymerization, likely due to the higher reactivity of lactide compared to  $\epsilon$ -caprolactone, as reported previously [21].

#4: Monomer adjacent to the acyl groups of PEG(PCLA<sub>1700</sub>CL<sub>2.5</sub>Acet)<sub>2</sub>

The methylene protons of propionyl-groups displayed quadruplets at 2.4 ppm, which overlap with the methylene protons of CL linked to LA, whereas the methyl protons of the propionyl groups showed triplets at 1.18 ppm [27,36]. On the other hand, the methyl protons of acetyl end-groups showed distinct peaks with different chemical shifts depending on the monomer (CL or LA) to which they are attached. Namely, the methyl protons of acetyl end-groups are found at 2.14-2.12 ppm for CH<sub>3</sub>-CO-LA- [27,36-38], 2.03-2.05 for CH<sub>3</sub>-CO-CL- [39] as well as at 2.08-2.10 ppm for CH<sub>3</sub>-CO-O-PEG- (originating from the reaction of PEG-OH and acetyl chloride) (Figure A.1 shows these different peaks and their assignments). To

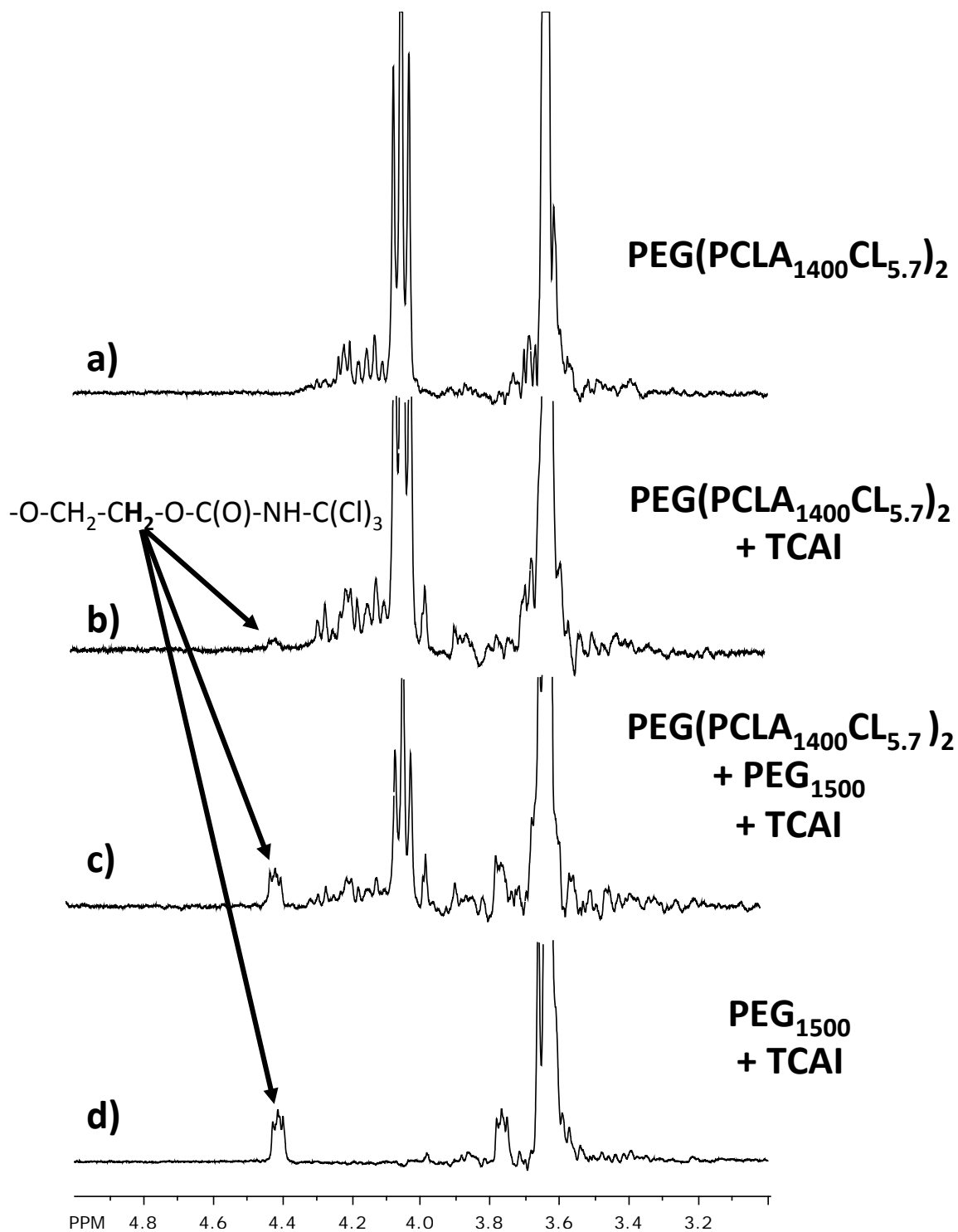


**Figure 3:**  $^1\text{H}$  NMR spectra of uncapped  $\text{PEG}(\text{PCLA}_{1400}\text{CL}_{5.7})_2$  before (a) and after (b) addition of trichloroacetylisocyanate (TCAI) as well as that of uncapped polymers spiked with  $\text{PEG}_{1500}$  (c) and that of  $\text{PEG}_{1500}$  (d) after addition of TCAI. The solvent was  $\text{CDCl}_3$ .

confirm the presence of PEG-OH groups, TCAI was added as shift reagent to react with free -OH groups present after polymerization but before acylation. Figure 3 shows that the  $^1\text{H}$  NMR spectrum of uncapped PEG(PCLA<sub>1400</sub>CL<sub>5.7</sub>)<sub>2</sub> reacted with TCAI had a peak with a chemical shift at 4.40 ppm, which is ascribed to PEG hydroxyl end-groups reacted with TCAI [25,40] and indeed demonstrates the presence of a small amount of PEG-OH end-groups in the synthesized polymers. The integrals of the three singlet peaks of the methyl protons of acetyl-end groups of PEG(PCLA<sub>1700</sub>CL<sub>2.5</sub>Acet)<sub>2</sub> show that the percentage of acetyl-LA ( $I_{2.13}$ ), acetyl-PEG ( $I_{2.09}$ ) and acetyl-CL ( $I_{2.04}$ ) moieties was  $71\pm 14$ ,  $5\pm 2$  and  $24\pm 12$  mol%, respectively. In the polymerization feed, 11.6 mol  $\epsilon$ -caprolactone and 2.3 mol L-lactide per PEG hydroxyl end group was present. Statistically, the number of free PEG hydroxyl groups at the end of the ring opening polymerization is about  $7\cdot 10^{-3}$  % (see Equation A.13 in the appendices), which is far less than the 5 % observed. Moreover, as mentioned above,  $^1\text{H}$  NMR analysis showed that there was a significant enrichment of PCLA chain ends with LA (71 mol% whereas 31 mol% is expected based on the CL/LA molar ratio of 2.2), which could originate from the lower reactivity of LA-OH groups compared to CL-OH for transesterification [14,23,24].

Ring opening polymerization of cyclic lactones with metal alkoxides, like tin(II) 2-ethylhexanoate, initiated by a compound with an alcohol functionality, occurs by activation of the hydroxyl group and a subsequent coordination-insertion mechanism that allows growing of the polymer chains by oxygen-acyl cleavage of cyclic lactones [14-16,41]. The active hydroxyl groups of growing polymer chains are known to be able to attack, besides the cyclic lactones, also ester bonds of a formed polymer chain (transesterification), which randomizes the copolymer chain microstructure [22,24,42,43]. Figure 4 shows that cleavage of PCLA chains by transesterification can occur in the polyester chain but also at the PEG-polyester bond. In the case of PEG(PCLA<sub>1700</sub>CL<sub>2.5</sub>Acet)<sub>2</sub>, the percentages of LA-ester, PEG-ester (2 per mol PEG) and CL-ester bonds based on molar ratio of LA, PEG and CL are 29, 6, and 65 mol%, respectively. The presence of the  $\sim 5$  mol% of PEG-OH thus matches with the calculated probability that such a bond is formed.

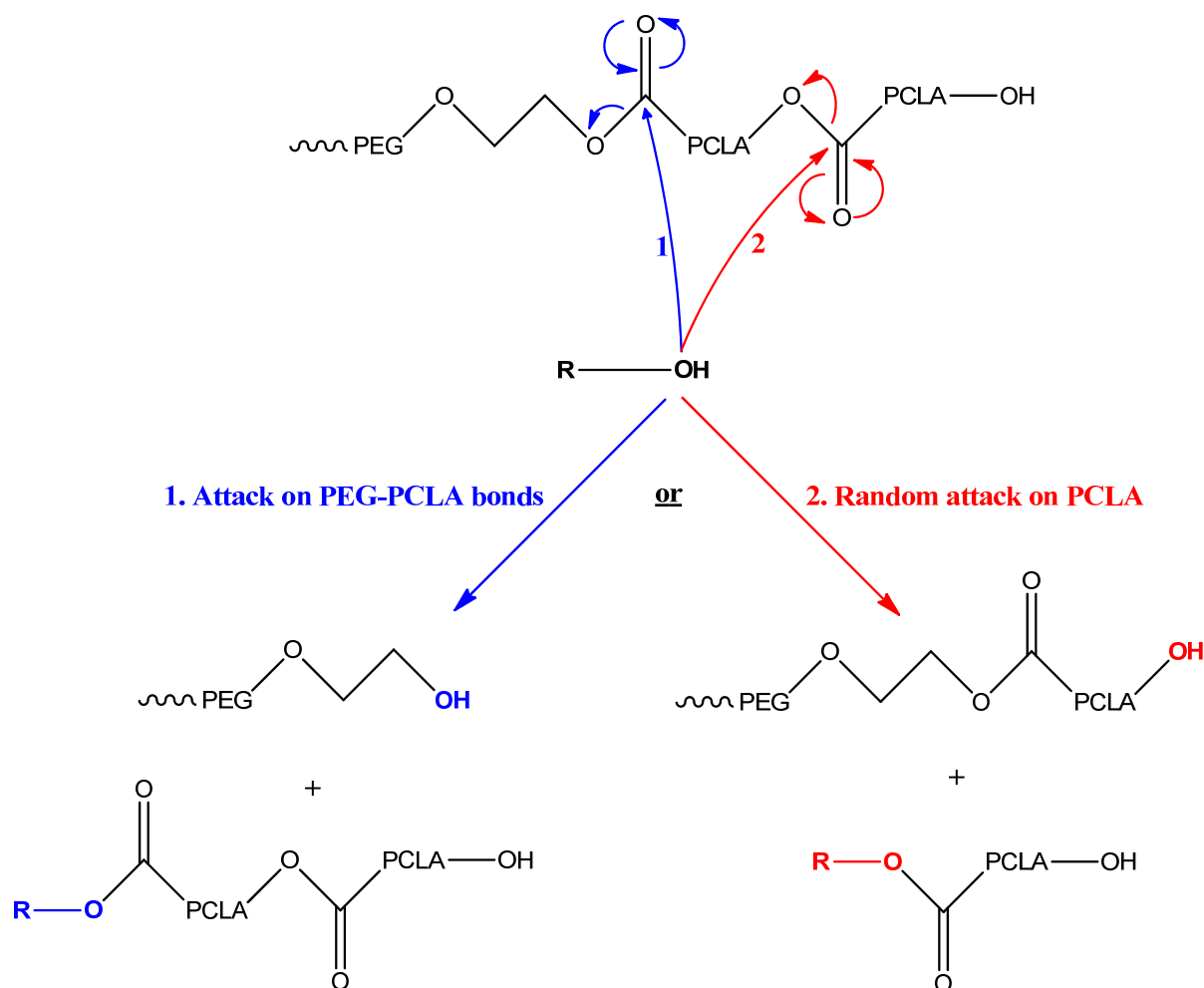


**Figure 4:** Schematic representation of transesterification reactions explaining the presence of PEG hydroxyl groups in PCLA/PEG copolymers.

#### #5: Randomness of the PCLA blocks of PEG(PCLA<sub>1700</sub>CL<sub>2.5</sub>Acet)<sub>2</sub>

The randomness of PCLA blocks was calculated from the integration of the  $\omega$ -methylene protons of CL linked to CL,  $I_{CL-CL}$  at 2.20-2.35 ppm, and to LA,  $I_{LA-CL}$  at 2.50-2.35 ppm, respectively [21,26,44,45]. The length of the CL blocks was calculated as follows:  $L_{CL} = (I_{CL-CL} / I_{LA-CL}) + 1$  (Equation 1) and found to be  $4.9 \pm 0.5$  ( $n = 2$ ) for PEG(PCLA<sub>1700</sub>CL<sub>2.5</sub>Acet)<sub>2</sub>. Taking into account that each PCLA block is composed of  $11.1 \pm 0.5$  CL and  $5.0 \pm 0.1$  LA units, there are thus in average 2.3 CL sequences of  $\sim 4.9$  CL per PCLA block separated by LA sequences, which indicates a rather blocky structure of PCLA, as we also observed in our previous study [25]. Thus, although transesterification took place during polymerization, as confirmed by the

**Table 2:** Characteristics of acyl-capped PCLA-PEG1500-PCLA triblock copolymers used in this study.

<i>Characteristic</i>	<i>Acyl-PCLA-PEG-PCLA-Acyl</i>							
	<i>PCLA<sub>1,400</sub></i>	<i>PCLA<sub>1,700</sub></i>	<i>PCLA<sub>1,400</sub></i>	<i>PCLA<sub>1,700</sub></i>	<i>PCLA<sub>1,400</sub></i>	<i>PCLA<sub>1,700</sub></i>	<i>PCLA<sub>1,400</sub></i>	<i>PCLA<sub>1,400</sub></i>
<i>M<sub>n,PCLA</sub> per block [g/mol]<sup>a)</sup></i>	1400	1600±100	1300	1600	1300	1400	1400	1700
<i>CL/LA ratio (k) [mol/mol]<sup>b)</sup></i>	2.2/1	2.2/1±0.1	4.3/1	4.2/1	2.6/1	2.2/1	4.5/1	4.3/1
<i>average CL-sequence length<sup>c)</sup></i>	8.2	4.9±0.5	8.8	8.4	3.9	4.0	8.0	7.4
<i>DM [%]<sup>d)</sup></i>	106	93±8	107	93	96	103	102	91
<i>M<sub>n,NMR</sub> [g/mol]<sup>e)</sup></i>	4300	4800±200	4200	4700	4100	4200	4200	4800
<i>M<sub>n,GPC</sub> [g/mol]<sup>f)</sup></i>	3400	5100±400	4200	4900	4400	5100	4600	5000
<i>PDI<sup>g)</sup></i>	1.5	1.4±0.1	1.4	1.4	1.4	1.4	1.4	1.4

\* polymer synthesized in duplicate (results depicted as mean±standard deviation)

<sup>a)</sup> number molecular weight PCLA determined by <sup>1</sup>H NMR (Equation A.8)

<sup>b)</sup> molar ratio of CL to LA in PCLA determined by <sup>1</sup>H NMR (Equation A.7)

<sup>c)</sup> determined by <sup>1</sup>H NMR (Equation A.13)

<sup>d)</sup> degree of modification represents the percentage of end groups per triblock copolymer determined by <sup>1</sup>H NMR (Equation A.11)

<sup>e)</sup> number average molecular weight determined by <sup>1</sup>H NMR (Equation A.12)

<sup>f)</sup> number average molecular weight determined by GPC, relative to PEG standards

<sup>g)</sup> polydispersity determined by GPC

presence of PEG hydroxyl groups and the enrichment of the end chains with LA units, we hypothesized that the PCLA blocks were not fully random because of the higher reactivity of CL hydroxyl groups (primary alcohol) than LA hydroxyl group (secondary alcohol) to attack ester bonds [14,22-24,26,46,47]. The consequences of the different reactivity of CL and LA on the randomness of PCLA and the incomplete randomness of PCLA even after transesterification is in line with literature [14,23-26], but has not been explained yet in terms of differential alcohol reactivity.

An overview of the characteristics of PEG(PCLA<sub>1700</sub>CL<sub>2.5</sub>Acet)<sub>2</sub> as well as that of the seven other polymers of this study as determined by <sup>1</sup>H NMR and GPC is given in Table 2. Six of the seven other polymers showed characteristics in line with those reported for PEG(PCLA<sub>1700</sub>CL<sub>2.5</sub>Acet)<sub>2</sub>. Only PEG(PCLA<sub>1400</sub>CL<sub>2.5</sub>Acet)<sub>2</sub> showed CL sequences of 8.2 CL whereas the expected length was 3-5 CL as observed for the polymers synthesized with an identical feed molar ratio CL/LA of 2.5. Thus PEG(PCLA<sub>1400</sub>CL<sub>2.5</sub>Acet)<sub>2</sub> had a more blocky structure than the other polymers likely because of a difference in the batch size (20 g vs. 30-160 g for the other batches) that might have resulted in an inhomogenous temperature distribution in the polymer solution during synthesis.

### 3.2. Thermal properties of the polymers determined by DSC

The thermal properties of PEG<sub>1500</sub> and the synthesized acyl-capped PCLA-PEG-PCLA polymers were investigated using DSC (Figure A.2). The thermograms of the polymers showed a single T<sub>g</sub> around -60 °C, which can be ascribed to the T<sub>g</sub> of the PEG block or the PCLA blocks, or that of their physical mixtures [45,48].

Figure A.2 and Figure 5 show that the three polymers with CL sequence lengths of ~4 had a melting endotherm in the range of 0-20 °C, whereas the other five polymers with CL sequences of ~8 (i.e. the PEG(PCLA<sub>1x00</sub>CL<sub>5.7</sub>Acet)<sub>2</sub>, PEG(PCLA<sub>1x00</sub>CL<sub>5.7</sub>Prop)<sub>2</sub> and PEG(PCLA<sub>1400</sub>CL<sub>2.5</sub>Acet)<sub>2</sub>) showed broader and higher melting endotherms (0-40 °C), which can be attributed to the melting of PCL crystals [49,50] in line with the X-ray diffraction patterns (see Figure A.3). It is thus noteworthy that PEG(PCLA<sub>1400</sub>CL<sub>2.5</sub>Acet)<sub>2</sub>, which has long CL sequences of ~8 CL units behaves like the other polymers with similar sequence length but higher

CL/LA ratio rather than like the polymers with shorter CL sequence length but similar CL/LA ratio.

Both PEG(PCLA<sub>1700</sub>CL<sub>2.5</sub>Acet)<sub>2</sub> batches showed a crystallization exotherm between -30 and -45 °C of 20-25 J/g in the second heat cycle, whereas the other seven polymers showed a crystallization exotherm in the cooling cycle. The differences in crystallization behaviour can be attributed to slow crystallisation as both PEG(PCLA<sub>1700</sub>CL<sub>2.5</sub>Acet)<sub>2</sub> batches also showed the lowest melting enthalphy ( $\Delta H = \sim 37 \pm 2$  J/g) of the polymer series.

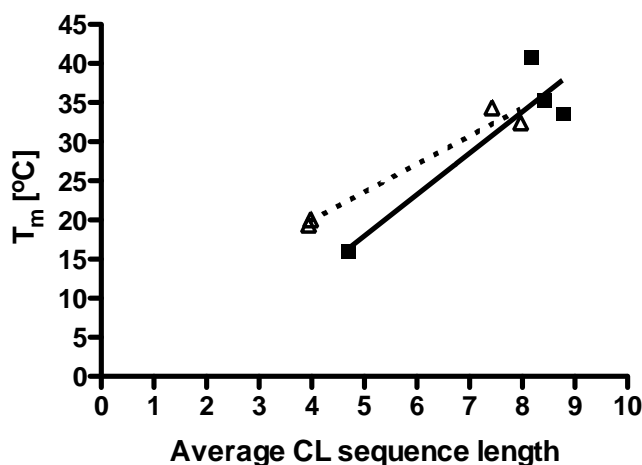


**Figure 5:** Melting temperature of end-capped PCLA-PEG-PCLA polymers determined by DSC (second heating) as a function of the average CL sequence lengths (as determined by <sup>1</sup>H NMR). Squares and triangles represent the acetyl- and propionyl-capped polymers, respectively.

Figure 6 shows that the melting enthalpy ( $\Delta H$ ) increased with the CL sequence length, in line with the effect on  $T_m$  (Figure 5). This figure also shows that  $\Delta H$  increased with the length of the end groups likely because acetyl groups to some extent inhibit formation of PCL crystals.

Based on the  $\Delta H$  of 100 % crystalline poly( $\epsilon$ -caprolactone) ( $\Delta H^\circ$ ) and the CL weight fraction of the polyester block,  $F_{CL}$ , in the polymers, the degree of crystallinity,  $\chi$ , of the CL-rich blocks can be calculated using Equation 2.

$$\chi = \frac{\Delta H}{\Delta H^\circ \times F_{CL}} \quad (\text{Equation 2})$$

The most commonly used value of 100 % crystalline poly( $\epsilon$ -caprolactone) is  $\Delta H^\circ = 139$  J/g, as reported by Crescenzi and co-workers [51]. Using this value, the crystallinity  $\chi$  of the PCLA blocks of PEG(PCLA<sub>1700</sub>CL<sub>2.5</sub>Acet)<sub>2</sub>,

was  $0.5 \pm 0.1$  ( $n = 2$ ) and the extent of crystallinity of the other polymers was between 0.5 and 0.9. Figure 7 shows that  $\chi$  increased with the CL sequence length and was dependent on the nature of the end group. In particular, propionyl groups increased CL crystallization, again in line with the effect observed on  $T_m$  and  $\Delta H$ .

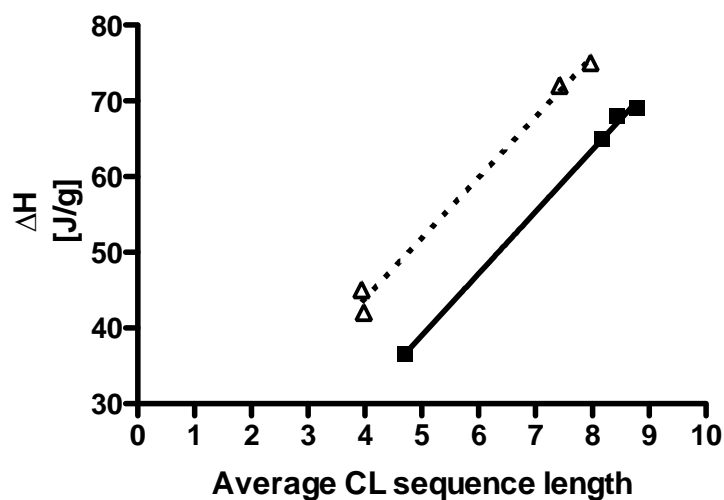


**Figure 6:** Melting enthalpy ( $\Delta H$ ) of end-capped PCLA-PEG-PCLA polymers determined by DSC (second heating) as a function of the average CL sequence lengths. Squares and triangles represent the acetyl- and propionyl-capped polymers, respectively.

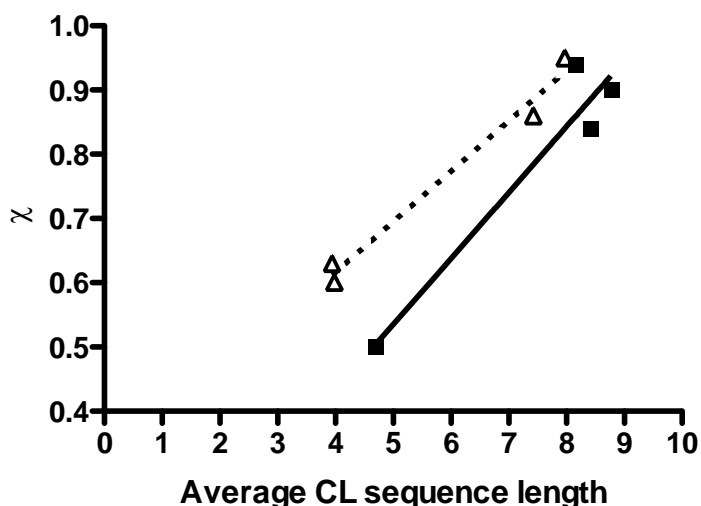


**Figure 7:** Crystallinity,  $\chi$  (calculated using Equation 2) of the PCLA blocks (capped with acetyl (squares) or propionyl end-groups (triangles)) as determined by DSC as a function of the average CL sequence length.



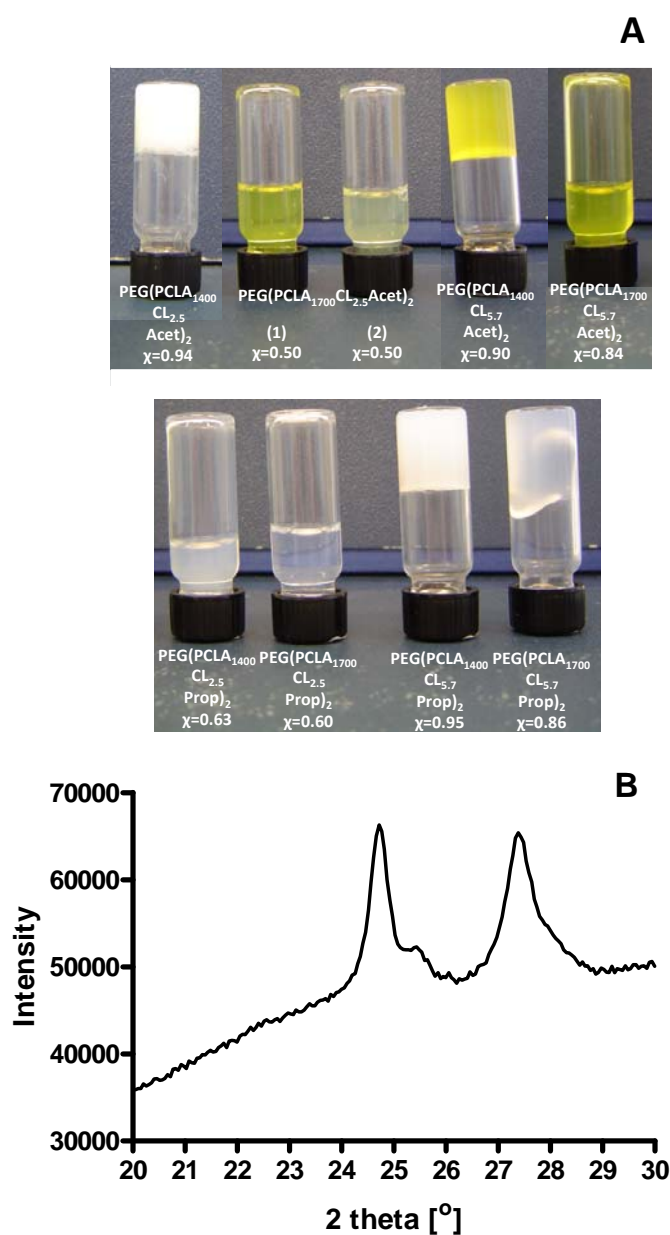


**Figure 8:** Behaviour of the systems during storage. 8A shows photographs of systems of 25 wt% acyl-capped PCLA-PEG-PCLA after one month storage at 4 °C and their respective crystallinity,  $\chi$  as determined by Equation 2. 8B shows the X-ray diffraction patterns of PEG(PCLA<sub>1400</sub>CL<sub>2.5</sub>Acet)<sub>2</sub> systems of 25 wt% in buffer after one month at 4 °C.

### 3.3. Crystallinity in the dry and wet state determined by X-ray diffraction

X-ray diffraction patterns of the acyl-capped PCLA-PEG-PCLA polymers with short CL sequences (~4 CL units) recorded at room temperature (Figure A.3) showed that the polymers were amorphous. On the other hand,

polymers with average CL sequence lengths of  $\sim 8$  showed diffraction peaks at  $2\theta$  of 24.8 and 27.2  $^\circ$ , which are ascribed to CL crystals [50].

Figure 8A shows photographs of the systems of the acyl-capped PCLA-PEG-PCLA triblock copolymers of 25 wt% in buffer, after one month storage at 4  $^\circ\text{C}$ . The samples, initially sols, were after storage:

- Opaque gels: PEG(PCLA<sub>1400</sub>CL<sub>2.5</sub>Acet)<sub>2</sub>, PEG(PCLA<sub>1400</sub>CL<sub>5.7</sub>Acet)<sub>2</sub>, PEG(PCLA<sub>1400</sub>CL<sub>5.7</sub>Prop)<sub>2</sub>, i.e. the three polymers with  $\chi > 0.90$ . Figure 8B shows that the X-ray diffraction pattern of 25 wt% systems of PEG(PCLA<sub>1400</sub>CL<sub>2.5</sub>Acet)<sub>2</sub> (the more blocky polymer) after one month storage at 4  $^\circ\text{C}$ . The diffraction pattern clearly shows two diffraction peaks at 24.8 and 27.2  $^\circ$ , which confirms the presence of CL crystals and thus that the immobility of the systems upon storage can be ascribed to crystallization of the CL-rich domains as also observed in a study of Kang et al [12].
- Sols: the other six polymers with  $\chi < 0.7$ .

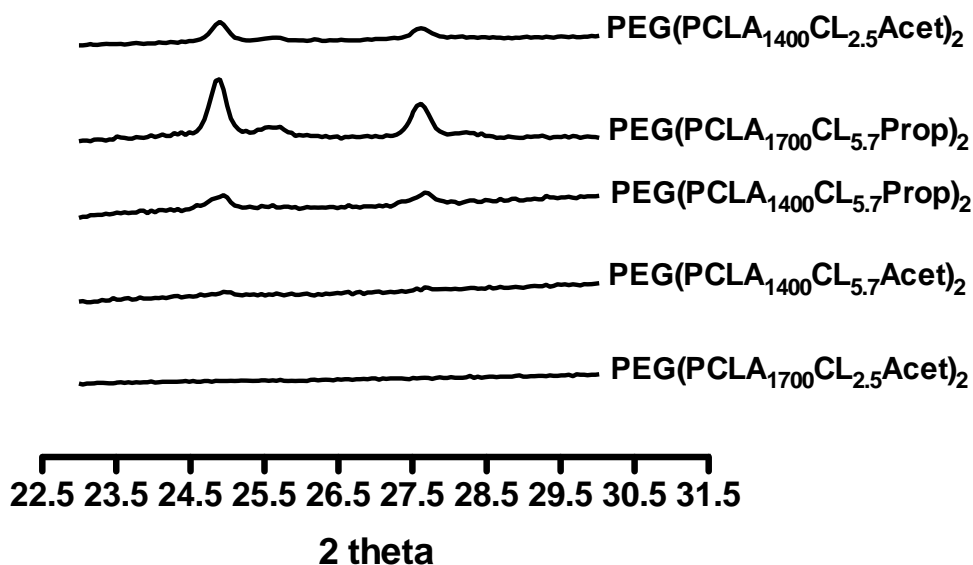


**Figure 9:** X-ray diffraction patterns of gels of 25 wt% in buffer pH 7.4 after 1-month storage at 37  $^\circ\text{C}$ .

The presence of crystallinity in aqueous systems after 2 days and 1 month incubation at 37  $^\circ\text{C}$  was investigated using X-ray diffraction. No crystallinity was observed after 2 days (results not shown), but Figure 9 shows that after

1 month at 37 °C, CL crystals were detected in the gels composed of the polymers with the highest melting temperature ( $>35$  °C, Figure 5). Thus, the high crystallinity and relatively high melting temperature of the polymers with relatively long CL sequences ( $\sim 8$  CL) lead to crystallization of the gels at 37 °C, which is in agreement with observations on CL-rich methoxyPEG-*b*-PCLA systems [12]. The gels containing acyl-capped PCLA-PEG-PCLA with average CL sequence length of  $\sim 5$  did not show crystallinity after 1 month at 37 °C, in line with the lower crystallinity of their CL-rich domains (see Figure 5, 6 and 7).

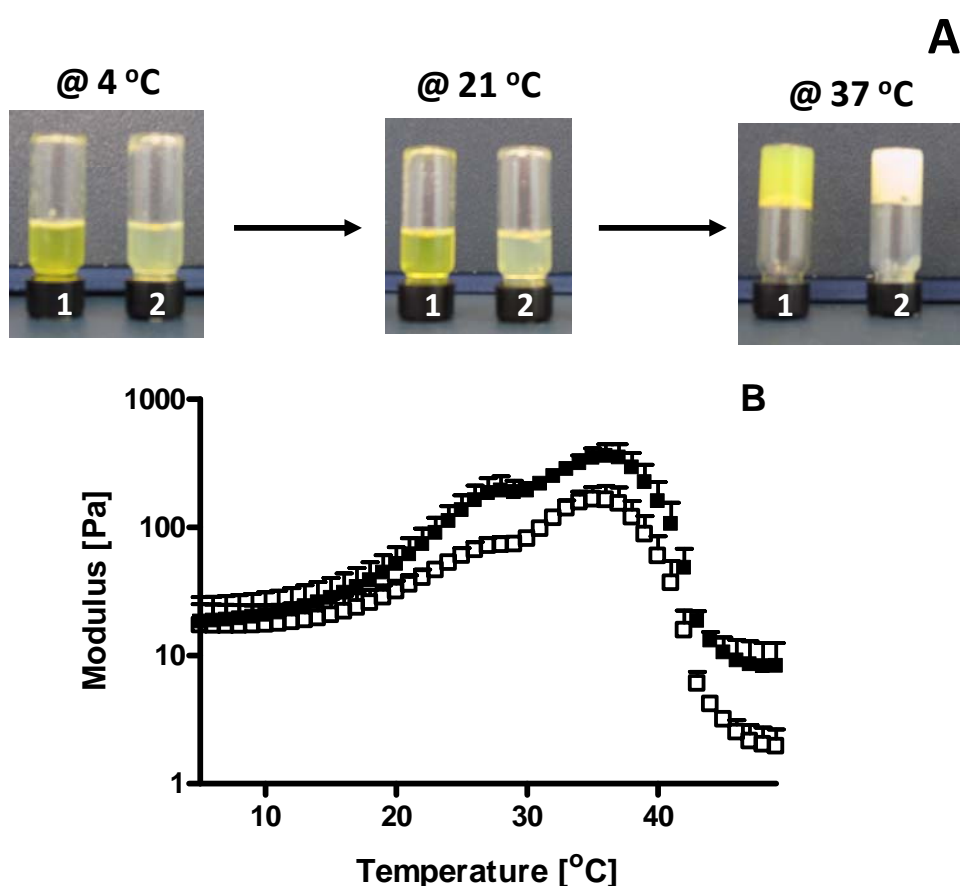


**Figure 10:** Behaviour of aqueous suspensions (25 wt%) containing PEG(PCLA<sub>1700</sub>CL<sub>2.5</sub>Acet)<sub>2</sub> at different temperatures. 10A shows photographs of samples made with both PEG(PCLA<sub>1700</sub>CL<sub>2.5</sub>Acet)<sub>2</sub> batches (vial 1, 2) after 30 min at 4, at  $\sim 22$  and 37 °C. 10B shows rheological temperature sweep measurements averaged for both PEG(PCLA<sub>1700</sub>CL<sub>2.5</sub>Acet)<sub>2</sub> batches. The closed and open symbols represent G' and G'', respectively. Error bars represent standard deviations.

3.4. *Rheological properties of aqueous systems of the acyl-capped polymers*  
 Figure 10 shows the rheogram of PEG(PCLA<sub>1700</sub>CL<sub>2.5</sub>Acet)<sub>2</sub> of 25 wt% in buffer. For all polymers (except PEG(PCLA<sub>1400</sub>CL<sub>2.5</sub>Acet)<sub>2</sub>), the samples were mobile sols at room temperature ( $G'' > G'$ ) and immobile gels ( $G' > G''$ ) at 37 °C after 30 minutes. The system (PEG(PCLA<sub>1400</sub>CL<sub>2.5</sub>Acet)<sub>2</sub>) was a sol up to 50 °C, most likely, because this polymer is too hydrophilic (lowest PCLA/PEG and CL/LA ratio, and shortest end group) to form a gel.

The storage modulus of samples prepared from both PEG(PCLA<sub>1700</sub>CL<sub>2.5</sub>Acet)<sub>2</sub> batches (Figure 10B) increased with temperature from ~20 Pa at 5 °C to ~360 Pa at 36 °C. Above 36 °C, both  $G'$  and  $G''$  slightly decreased, which can likely be ascribed to an artefact in the measurements because of phase-separation and subsequent loss of contact between the plates of the rheometer and the gels. An increase in moduli with temperature was observed for all polymers (see Figure A.5) even for PEG(PCLA<sub>1400</sub>CL<sub>2.5</sub>Acet)<sub>2</sub> (i.e. the most hydrophilic polymer with blocky structure), which surprisingly did not form an immobile gel using the vial tilting test. The different gelling behaviour of this system is likely related to the hydrophilicity and/or more blocky structure of the PCLA blocks and higher crystallinity compared to that of the other polymer systems.

No significant effect of the composition of the polymers on  $G'$  was observed at 4 °C, whereas significant effects were observed at temperatures

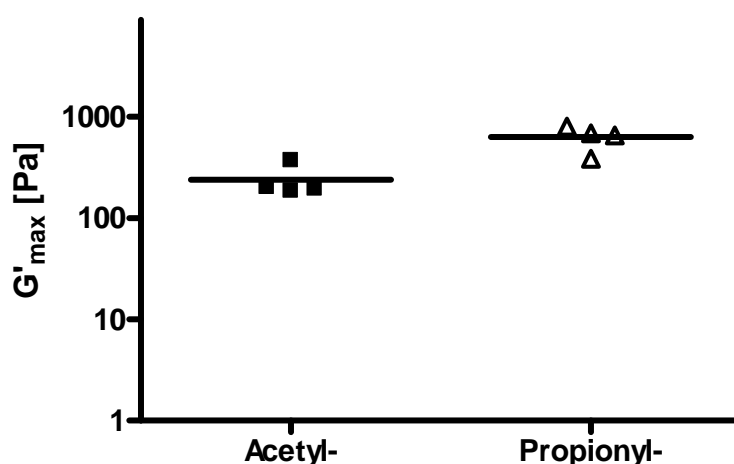


**Figure 11:** Maximum storage modulus ( $G'_{\max}$ ) of 25% gels as a function of the nature of the end group.

close to 37 °C at which  $G'$  reached its maximum. Figure 11 shows that the propionyl-capped polymers have a higher  $G'_{\max}$  ( $600\pm 200$  Pa) than the acetyl-ones ( $200\pm 100$  Pa). The effect of the type of end groups on  $G'_{\max}$  is in line with the study of Yu and co-workers [27] and likely originates from the fact that increasing hydrophobicity of the end groups strengthens the hydrophobic interactions between the polymer chains, and thus stronger gels with propionyl-capped polymers were formed than with acetyl-capped ones. It should be mentioned that crystallinity does not contribute to the strength of the gels, because it was demonstrated (see Paragraph 3.3) that the formation of CL crystals takes some time.

### *3.5. Degradation of gels based on the acyl-capped triblock copolymers*

The degradation of the acyl-capped PCLA-PEG-PCLA triblock copolymer gels (at a fixed initial solid content of 25 wt%) was investigated at 37 °C in phosphate buffer (pH 7.4). Systems composed of  $\text{PEG}(\text{PCLA}_{1400}\text{CL}_{2.5}\text{Acet})_2$  did not form gels at 37 °C and were therefore excluded from the degradation experiments. The wet and dry weight degradation profiles of the seven other gels are shown in Figure A.6. Figure 12 shows the degradation profiles of three representative examples.

For  $\text{PEG}(\text{PCLA}_{1700}\text{CL}_{2.5}\text{Acet})_2$  (Figure 12A, insert), both wet and dry weight remained constant during the first 5 days of incubation, and thereafter the wet weight of the gels increased, i.e. the gels swelled whereas the dry weight did not change. For  $\text{PEG}(\text{PCLA}_{1700}\text{CL}_{5.7}\text{Acet})_2$  (Figure 12B, insert), the swelling of the gel started immediately upon incubation. For  $\text{PEG}(\text{PCLA}_{1700}\text{CL}_{5.7}\text{Prop})_2$  (Figure 12C, insert), the gels first contracted during day 1 due to phase separation into a polymer-rich and polymer-poor phase and they started to swell after 15-20 days. Higher tendency to phase separate of the gels composed of propionyl-capped polymers can be ascribed to hydrophobicity of the propionyl end-groups that strengthens the hydrophobic interactions between polymer chains [27].

The time to reach the maximum swelling was dependent on the polymer composition and was, for example, 30, 50 and ~100-150 days for gels composed of  $\text{PEG}(\text{PCLA}_{1700}\text{CL}_{2.5}\text{Acet})_2$ ,  $\text{PEG}(\text{PCLA}_{1700}\text{CL}_{5.7}\text{Acet})_2$  and  $\text{PEG}(\text{PCLA}_{1700}\text{CL}_{5.7}\text{Prop})_2$ , respectively (see Figure 12 and A.6). The swelling phase was followed by a drop in wet weight until complete degradation in

90±5, 160 and 280 days for gels composed of PEG(PCLA<sub>1700</sub>CL<sub>2.5</sub>Acet)<sub>2</sub>, PEG(PCLA<sub>1700</sub>CL<sub>5.7</sub>Acet)<sub>2</sub> and PEG(PCLA<sub>1700</sub>CL<sub>5.7</sub>Prop)<sub>2</sub>, respectively.

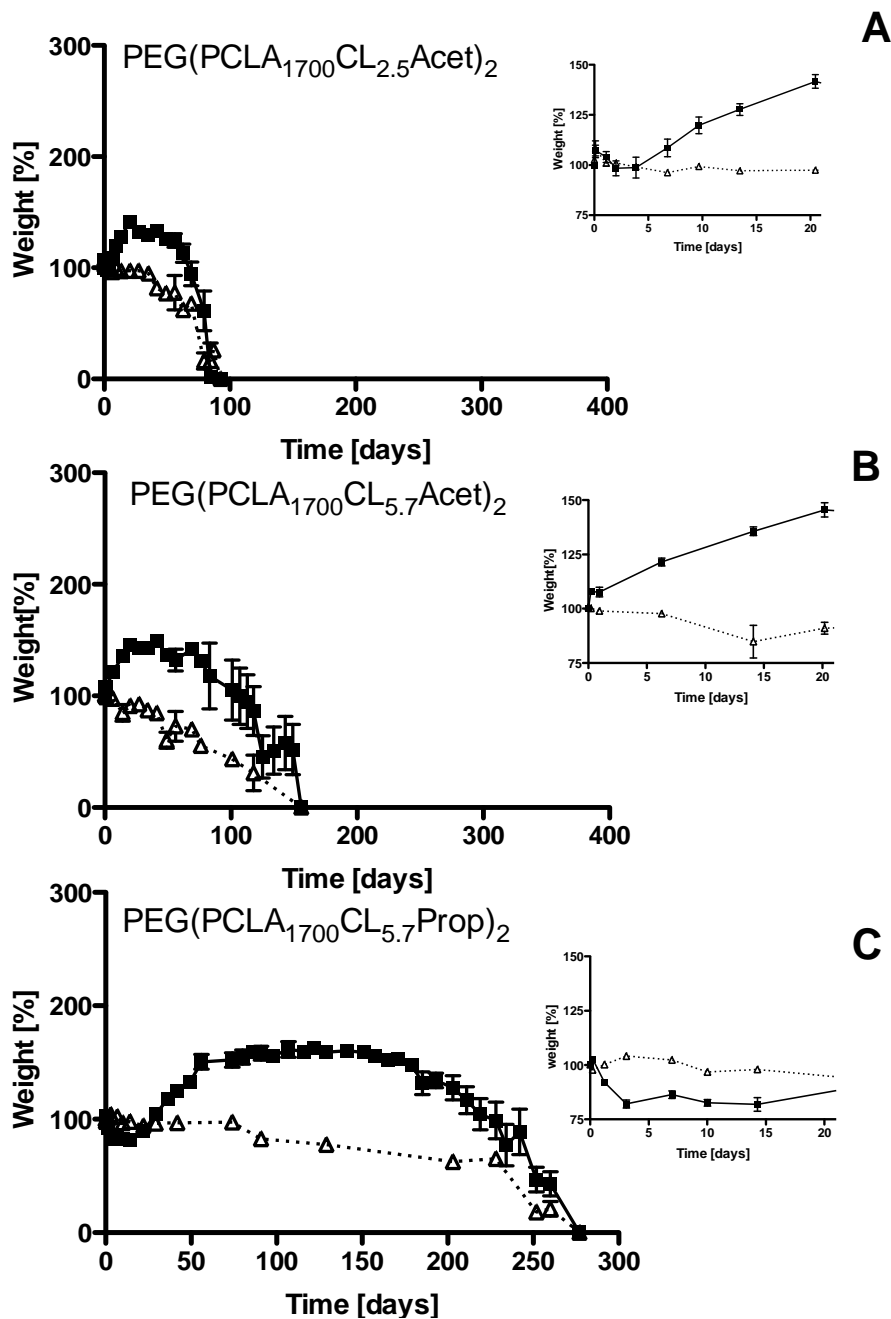


**Figure 12:** Degradation of gels (25 wt% in buffer) with the closed squares and open triangles for the wet and dry weight, respectively. The inserts show the degradation profile for the first 20 days. 11A shows the degradation profile of PEG(PCLA<sub>1700</sub>CL<sub>2.5</sub>Acet)<sub>2</sub> (average values of two batches). 11B shows the profile of PEG(PCLA<sub>1700</sub>CL<sub>5.7</sub>Acet)<sub>2</sub>. 11C shows the profile of PEG(PCLA<sub>1700</sub>CL<sub>5.7</sub>Prop)<sub>2</sub>. Experiments were performed at 37 °C in phosphate buffer (pH 7.4). Error bars represent standard error of the mean (n = 3).

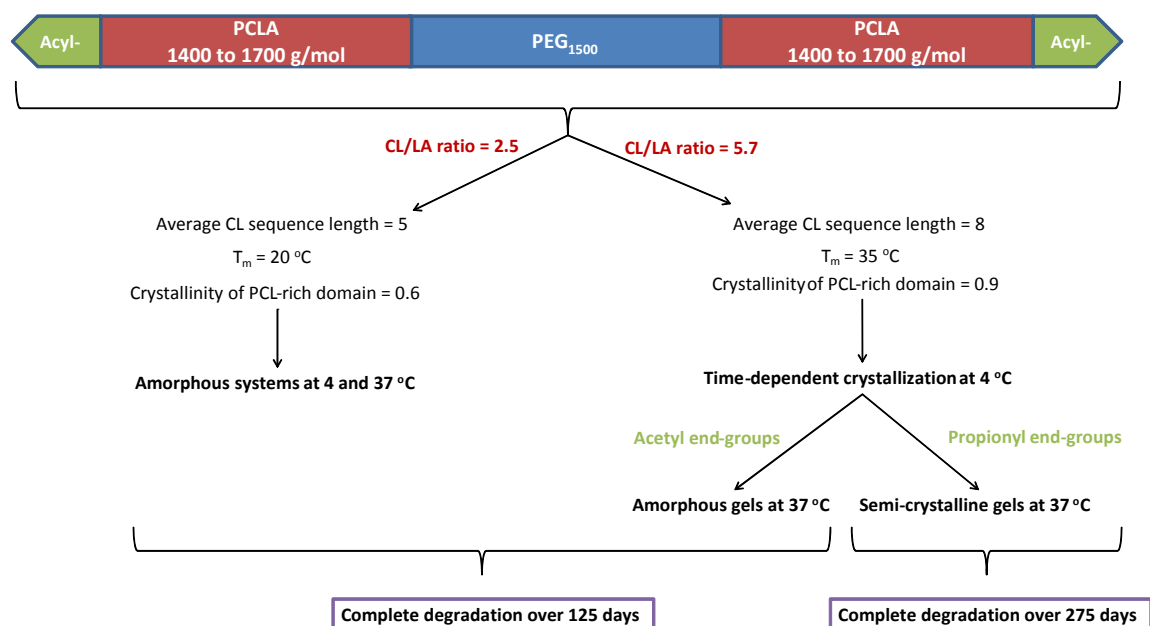


**Figure 13:** Overview of degradation time of the gels of 25 wt% in phosphate buffer at 37 °C as a function of their composition and tendency to crystallize.

As the gels swelled, their dry weight started to decrease progressively in time with a substantial drop in the last ~25-50 days depending on the composition. PEG(PCLA<sub>1700</sub>CL<sub>5.7</sub>Acet)<sub>2</sub> is the only polymer that showed a near-to-linear decrease of dry weight in time (Figure 12B), which might be an important feature for the controlled release of drugs from this gel driven by polymer dissolution.

An overview of the degradation characteristics of the gels as well as the properties of the polymers they contain as determined by DSC and X-ray diffraction is given in Table 3. Figure 13 shows an overview of the main factors that influence the degradation time of the gels. The degradation time increased with CL crystallinity of the gels at 37 °C, which is in line with literature on amorphous and semi-crystalline polyester systems [13]. In particular, both gels containing propionyl-capped polymers that showed crystallization upon storage at 37 °C (Figure 9) showed degradation time of ~275 days, whereas the other gels that did not show crystallinity at 37 °C (and thus were fully amorphous) degraded in 100 to 150 days.

**Table 3:** Properties of acyl-capped PCLA-PEG<sub>1500</sub>-PCLA triblock copolymers used in this study as determined by DSC, X-ray diffraction and during the degradation experiments of the gels made of them.

Characteristic	Acyl-PCLA-PEG-PCLA-Acyl									
	PCLA <sub>1400</sub>	PCLA <sub>1700</sub>	PCLA <sub>1400</sub>	PCLA <sub>1700</sub>	PCLA <sub>1400</sub>	PCLA <sub>1700</sub>	PCLA <sub>1400</sub>	PCLA <sub>1700</sub>	PCLA <sub>1400</sub>	PCLA <sub>1400</sub>
	<i>CL<sub>2.5</sub></i>	<i>CL<sub>2.5</sub></i>	<i>CL<sub>5.7</sub></i>	<i>CL<sub>5.7</sub></i>	<i>CL<sub>2.5</sub></i>	<i>CL<sub>2.5</sub></i>	<i>CL<sub>2.5</sub></i>	<i>CL<sub>5.7</sub></i>	<i>CL<sub>5.7</sub></i>	<i>CL<sub>5.7</sub></i>
	<i>Acet</i>	<i>Acet*</i>	<i>Acet</i>	<i>Acet</i>	<i>Acet</i>	<i>Prop</i>	<i>Prop</i>	<i>Prop</i>	<i>Prop</i>	<i>Prop</i>
Average CL-sequence length <sup>a)</sup>	8.2	4.9±0.5	8.8	8.4	3.9	4.0	8.0	7.4		
T <sub>m</sub> [°C] <sup>b)</sup>	41	15±3	34	35	19	20	32	34		
ΔH [J/g] <sup>c)</sup>	69	37±1	65	68	45	42	75	72		
χ <sup>d)</sup>	0.9	0.5±0.1	0.9	0.8	0.6	0.6	1.0	0.8		
Degradation time [days]	Not applicable	100±10	110	150	120	110	290	290		

\* polymer synthesized in duplicate (results depicted as mean±standard deviation)

<sup>a)</sup> determined by <sup>1</sup>H NMR (Equation A.13)

<sup>b)</sup> melting temperature determined by DSC analysis (Figure 5)

<sup>c)</sup> melting enthalpy determined by DSC (Figure 6)

<sup>d)</sup> crystallinity of the PCLA blocks determined by DSC (Figure 7)



Figure A.7 shows the time-dependent  $M_n$  and composition (GPC and  $^1\text{H}$  NMR analysis) of  $\text{PEG}(\text{PCLA}_{1700}\text{CL}_{5.7}\text{Prop})_2$ . GPC analysis showed that  $M_n$  was constant in time demonstrating that no chain hydrolysis occurred.  $^1\text{H}$  NMR analysis however showed enrichment in CL content, which is ascribed to a preferential leaching of CL-poor triblock copolymers from the gels. Therefore, degradation of the acyl-capped PCLA-PEG-PCLA gels is driven by polymer dissolution as also observed for systems containing hexanoyl-capped polymers [25], and not due to chemical hydrolysis of ester bonds. Both the high CL content of the polymers [12,52] and the end-capping [29-33] of PCLA-PEG-PCLA contribute to the observed lack of ester hydrolysis.

#### **4. Conclusions**

In this study, the physical properties of systems containing propionyl- or acetyl-capped PCLA-PEG-PCLA triblock copolymers in buffer (25 % solid content) were investigated. Except for the most hydrophilic polymer system, all systems showed a temperature-dependent sol-to-gel transition between 22 and 37 °C. Gel degradation of the systems proceeded by dissolution and occurred in 90 to 280 days. It was found that gels, in which crystallinity was detected at 37 °C had much longer degradation times. This study clearly shows that the CL sequence length is an important parameter that can be exploited to tailor the degradation time of *in situ* forming gels based on PCLA block copolymers. Systems containing acyl-capped PCLA-PEG-PCLA copolymers have the potential as injectable systems for the controlled release of drugs for therapies of a duration between a few months up to almost a year.

#### **Acknowledgements**

Mike de Leeuw and Dr. Theo Flipsen are gratefully acknowledged for their support and valuable discussions. Jan Wever (Polyvation BV) and Mies van Steenbergem are particularly thanked for their excellent technical support.

## References

- [1] Vermonden T, Censi R, Hennink WE. Hydrogels for protein delivery. *Chem Rev* 2012;5:2853-2888.
- [2] Ko DY, Shinde UP, Yeon B, Jeong, B. Recent progress of *in situ* formed gels for biomedical applications. *Prog Polym Sci* 2013;38:672-701.
- [3] Bonacucina G, Cespi M, Mencarelli G, Giorgioni G, Palmieri GF. Thermosensitive self-assembling block copolymers as drug delivery systems. *Polymers* 2011;3:779-811.
- [4] Elstad NL, Fowers KD. OncoGel® (ReGel®/paclitaxel) - clinical applications for a novel paclitaxel delivery system. *Adv Drug Deliv Rev* 2009;10:785-794.
- [5] Zentner GM, Rathi R, Shih C, McRea JC, Seo M, Oh H, et al. Biodegradable block copolymers for delivery of proteins and water-insoluble drugs. *J Control Release* 2001;1-3:203-215.
- [6] Jeong B, Bae YH, Lee D.S, Kim SW. Biodegradable block copolymers as injectable drug-delivery systems. *Nature* 1997;6645:860-862.
- [7] He C, Kim SW, Lee DS. *In situ* gelling stimuli-sensitive block copolymer hydrogels for drug delivery. *J Control Release* 2008;3:189-207.
- [8] Bramfeldt H, Sarazin P, Vermette P. Characterization, degradation, and mechanical strength of poly(D,L-lactide-*co*- $\epsilon$ -caprolactone)-poly(ethylene glycol)-poly(D,L-lactide-*co*- $\epsilon$ -caprolactone). *J Biomed Mater Res A* 2007;2:503-511.
- [9] Zhang Z, Ni J, Chen L, Yu L, Xu J, Ding J. Biodegradable and thermoreversible PCLA-PEG-PCLA hydrogel as a barrier for prevention of post-operative adhesion. *Biomaterials* 2011;21:4725-4736.
- [10] Yu L, Zhang Z, Zhang H, Ding J. Mixing a sol and a precipitate of block copolymers with different block ratios leads to an injectable hydrogel. *Biomacromolecules* 2009;6:1547-1553.
- [11] Yu L, Zhang Z, Zhang H, Ding J. Biodegradability and biocompatibility of thermoreversible hydrogels formed from mixing a sol and a precipitate of block copolymers in water. *Biomacromolecules* 2010;8:2169-2178.
- [12] Kang YM, Lee SH, Lee JY, Son JS, Kim BS, Lee B, et al. A biodegradable, injectable gel system based on mPEG-*b*-(PCL-*ran*-PLLA) diblock copolymers with an adjustable therapeutic window. *Biomaterials* 2010;9:2453-2460.

- [13] Li S, Dobrzynski P, Kasperczyk J, Bero M, Braud C, Vert M. Structure-property relationships of copolymers obtained by ring-opening polymerization of glycolide and  $\epsilon$ -caprolactone. Part 2. Influence of composition and chain microstructure on the hydrolytic degradation. *Biomacromolecules* 2005;1:489-497.
- [14] Dobrzynski P, Li S, Kasperczyk J, Bero M, Gasc F, Vert M. Structure-property relationships of copolymers obtained by ring-opening polymerization of glycolide and  $\epsilon$ -caprolactone. Part 1. Synthesis and characterization. *Biomacromolecules* 2005;1:483-488.
- [15] Albertsson AC, Varma IK. Recent developments in ring opening polymerization of lactones for biomedical applications. *Biomacromolecules* 2003;4:1466-1486.
- [16] Yu L, Zhang Z, Ding J. Influence of LA and GA sequence in the PLGA block on the properties of thermogelling PLGA-PEG-PLGA block copolymers. *Biomacromolecules* 2011;4:1290-1297.
- [17] Kricheldorf HR, Berl M, Scharnagl N. Poly(lactones). 9. Polymerization mechanism of metal alkoxide initiated polymerizations of lactide and various lactones. *Macromolecules* 1988;21:286-293.
- [18] Jacobs C, Dubois P, Jerome R, Teyssie P. Macromolecular engineering of polylactones and polylactides. 5. Synthesis and characterization of diblock copolymers based on poly- $\epsilon$ -caprolactone and poly(L,L or D,L)lactide by aluminum alkoxides. *Macromolecules* 1991;24:3027-3034.
- [19] Darensbourg DJ, Karroonnirun O. Ring-opening polymerization of L-lactide and  $\epsilon$ -caprolactone utilizing biocompatible zinc catalysts. Random copolymerization of L-lactide and  $\epsilon$ -caprolactone. *Macromolecules* 2010;43: 8880-8886.
- [20] Vanhoorne P, Dubois P, Jerome R, Teyssie P. Macromolecular engineering of polylactones and polylactides. 7. Structural analysis of copolyesters of  $\epsilon$ -caprolactone and L- or D,L-lactide initiated by triisopropoxyaluminum. *Macromolecules* 1992;25:37-44.
- [21] Kricheldorf HR, Bornhorst K, Hachmann-Thiessen H. Bismuth(III) n-hexanoate and tin(II) 2-ethylhexanoate initiated copolymerizations of  $\epsilon$ -caprolactone and L-lactide. *Macromolecules* 2005;38:5017-5024.
- [22] Bero M, Kasperczyk J. Coordination polymerization of lactides. 5. Influence of lactide structure on the transesterification processes in the copolymerization with  $\epsilon$ -caprolactone. *Macromol Chem Phys* 1996, 10, 3251-3258.

- [23] Stevels WM, Bernard A, van de Witte P, Dijkstra PJ, Feijen J. Block copolymers of poly(L-lactide) and poly( $\epsilon$ -caprolactone) or poly(ethylene glycol) prepared by reactive extrusion. *J Appl Polym Sci* 1996;62:1295-1301.
- [24] in't Veld PJA, Velner EM, van de Witte P, Hamhuis J, Dijkstra PJ, Feijen, J. Melt block copolymerization of  $\epsilon$ -caprolactone and L-lactide. *J Polym Sci A Polym Chem* 1997;35:219-226.
- [25] Petit A, Müller B, Bruin P, Meijboom R, Piest M, Kroon-Batenburg LMJ, et al. Modulating rheological and degradation properties of temperature-responsive gelling systems composed of blends of PCLA-PEG-PCLA triblock copolymers and their fully hexanoyl-capped derivatives. *Acta Biomater* 2012;8:4260-4267.
- [26] Grijpma DW, Pennings AJ. Polymerization temperature effects on the properties of L-lactide and  $\epsilon$ -caprolactone copolymers. *Polym Bull* 1991;25:335-341.
- [27] Yu L, Chang G, Zhang H, Ding J. Temperature-induced spontaneous sol-gel transitions of poly(D,L-lactic acid-*co*-glycolic acid)-*b*-poly(ethylene glycol)-*b*-poly(D,L-lactic acid-*co*-glycolic acid) triblock copolymers and their end-capped derivatives in water. *J Polym Sci A Polym Chem* 2007;45:1122-1133.
- [28] Jo S, Kim J, Kim SW. Reverse thermal gelation of aliphatically modified biodegradable triblock copolymers. *Macromol Biosci* 2006;6:923-928.
- [29] Shim WS, Kim J, Park H, Kim K, Chan Kwon I, Lee DS. Biodegradability and biocompatibility of a pH- and thermo-sensitive hydrogel formed from a sulfonamide-modified poly( $\epsilon$ -caprolactone-*co*-lactide)-poly(ethylene glycol)-poly( $\epsilon$ -caprolactone-*co*-lactide) block copolymer. *Biomaterials* 2006;27:5178-5185.
- [30] Carstens MG, van Nostrum CF, Verrijck R, de Leede LGJ, Crommelin DJA, Hennink WE. A mechanistic study on the chemical and enzymatic degradation of PEG-oligo( $\epsilon$ -caprolactone) micelles. *J Pharm Sci* 2008;97:506-518.
- [31] van Nostrum CF, Veldhuis TFJ, Bos GW, Hennink WE. Hydrolytic degradation of oligo(lactic acid): a kinetic and mechanistic study. *Polymer* 2004;45:6779-6787.
- [32] Geng Y, Discher D. Hydrolytic degradation of poly(ethylene oxide)-*block*-polycaprolactone worm micelles. *J Am Chem Soc* 2005;127:12780-12781.
- [33] Pitt CG, Zhong-wei G. Modification of the rates of chain cleavage of poly( $\epsilon$ -caprolactone) and related polyesters in the solid state. *J Control Release* 1987;4:283-292.

- [34] Shim MS, Lee HT, Shim WS, Park I, Lee H, Chang T, et al. Poly(D,L-lactic acid-*co*-glycolic acid)-*b*-poly(ethylene glycol)-*b*-poly (D,L-lactic acid-*co*-glycolic acid) triblock copolymer and thermoreversible phase transition in water. *J Biomed Mater Res* 2002;61:188-196.
- [35] Lee DS, Shim MS, Kim SW, Lee H, Park I, Chang T. Novel thermoreversible gelation of biodegradable PLGA-*block*-PEO-*block*-PLGA triblock copolymers in aqueous solution. *Macromol Rapid Commun* 2001;22:587-592.
- [36] Yu L, Zhang H, Ding J. A subtle end-group effect on macroscopic physical gelation of triblock copolymer aqueous solutions. *Angew Chem Int Ed Engl* 2006;45:2232-2235.
- [37] Fan Y, Nishida H, Shirai Y, Endo T. Thermal stability of poly (L-lactide): influence of end protection by acetyl group. *Polym Degrad Stab* 2004;84:143-149.
- [38] McNeill IC, Leiper HA. Degradation studies of some polyesters and polycarbonates. 1. Polylactide: general features of the degradation under programmed heating conditions. *Polym Degrad Stab* 1985;11:267-285.
- [39] Abe H, Takahashi N, Kim KJ, Mochizuki M, Doi Y. Effects of residual zinc compounds and chain-end structure on thermal degradation of poly( $\epsilon$ -caprolactone). *Biomacromolecules* 2004;5:1480-1488.
- [40] Vos R, Goethals E. End group analysis of commercial poly(ethylene glycol) monomethyl ether's. *Polym Bull* 1986;15:547-549.
- [41] Zhang X, MacDonald DA, Goosen MFA, McAuley KB. Mechanism of lactide polymerization in the presence of stannous octoate: the effect of hydroxyl and carboxylic acid substances. *J Polym Sci A Polym Chem* 1994;32:2965-2970.
- [42] Kasperczyk, J. Microstructural analysis of poly[(L,L-lactide)-*co*-(glycolide)] by  $^1\text{H}$  and  $^{13}\text{C}$  NMR spectroscopy. *Polymer* 1996;37:201-203.
- [43] de Jong SJ, van Dijk-Wolthuis WNE, Kettenes-van den Bosch JJ, Schuyl PJW, Hennink WE. Monodisperse enantiomeric lactic acid oligomers: preparation, characterization, and stereocomplex formation. *Macromolecules* 1998;31:6397-6402.
- [44] Loontjens CAM, Vermonden T, Leemhuis M, van Steenberg MJ, van Nostrum CF, Hennink WE. Synthesis and characterization of random and triblock copolymers of  $\epsilon$ -caprolactone and (benzylated)hydroxymethyl glycolide. *Macromolecules* 2007;40:7208-7216.

- [45] Hao J, Keller T, Cai K, Klemm E, Bossert J, Jandt KD. The effect of D,L-lactidyl/ $\epsilon$ -caproyl weight ratio and chemical microstructure on surface properties of biodegradable poly (D,L-lactide)-*co*-poly( $\epsilon$ -caprolactone) random copolymers. *Adv Eng Mater* 2008;10:B23-B32.
- [46] Smith, M. B.; March, J. 9. Effects of structure and medium on reactivity. In *March's advanced organic chemistry: reactions, mechanisms, and structure*, 6th Ed; Wiley-Interscience, 2007; p 395
- [47] Carey, F. A.; Sundberg, R. J. Structural effects on stability and reactivity In *Advanced Organic Chemistry*, 5th Ed; Springer, 2007; p 253.
- [48] van de Velde K, Kiekens P. Biopolymers: overview of several properties and consequences on their applications. *Polym Test* 2002;21:433-442.
- [49] Goonoo N, Bhaw-Luximon A, Bowlin G, Jhurry D. Diblock poly(ester)-poly(ester-ether) copolymers: I. Synthesis, thermal properties, and degradation kinetics. *Ind Eng Chem Res* 2012;51:12031-12040.
- [50] Sosnik A, Cohn D. Poly(ethylene glycol)-poly( $\epsilon$ -caprolactone) block oligomers as injectable materials. *Polymer* 2003;44:7033-7042.
- [51] Crescenzi V, Manzini G, Calzolari G, Borri C. Thermodynamics of fusion of poly- $\beta$ -propiolactone and poly- $\epsilon$ -caprolactone. comparative analysis of the melting of aliphatic polylactone and polyester chains. *Eur Polym J* 1972;8:449-463.
- [52] Lin G, Cosimbescu L, Karin NJ, Gutowskab A, Tarasevich BJ. Injectable and thermogelling hydrogels of PCL-*g*-PEG: mechanisms, rheological and enzymatic degradation properties. *J Mater Chem B* 2013;1:1249-1255.

## Appendices

### Equation

**Equation A.1:** Theoretical number of methylene protons in PEG<sub>1500</sub> per mole,  $I_{PEG}$

$$I_{PEG} = 4 \times \left( \frac{M_{PEG}}{M_{EG}} \right) = 136 \quad \text{with } M_{PEG} = 1500 \text{ g/mol and } M_{EG} = 44 \text{ g/mol.}$$

**Equation A.2:** Number of methylene protons in PEG at 3.72-3.55 ppm,  $I_{3.6}$

This value was determined by adding an excess of TCAI to PEG<sub>1500</sub>. The formation of  $\text{Cl}_3\text{C-NH-C(O)-(O-CH}_2\text{-CH}_2)_n\text{-O-C(O)-NH-CCl}_3$  led to the formation of a new peak at 4.40ppm ( $I_{4.4}$ , 4H,  $\text{Cl}_3\text{C-NH-C(O)-O-CH}_2\text{-CH}_2\text{-O-}$ ) [40].

$I_{3.6} = 122$  for  $I_{4.4} = 4$ . This value is in agreement with the expected value of  $136 - 4 = 132$  H (as determined in Equation A.1.).

**Equation A.3:** Number of CL-CL bonds per mol PEG

$$n_{CL-CL} = \frac{I_{2.2}}{2} \quad \text{for normalized } I_{3.6} = 122.$$

**Equation A.4:** Number of CL-LA bonds per mol PEG

$$n_{CL-LA} = \frac{I_{2.3}}{2} - \frac{I_{1.2}}{6} \quad \text{for normalized } I_{3.6} = 122.$$

**Equation A.5:** Number of CL per polymer chain

$$n_{CL} = n_{CL-CL} + n_{CL-LA}.$$

**Equation A.6:** Number of LA per polymer chain

$$n_{LA} = I_{5.1} \quad \text{for normalized } I_{3.6} = 122.$$

**Equation A.7:** Molar ratio CL/LA

$$k = \frac{n_{CL}}{n_{LA}}.$$

**Equation A.8:** Number average molecular weight of PCLA

$$M_{n,PCLA} = n_{CL} \times 114 + n_{LA} \times 72.$$

**Equation A.9:** Weight CL content

$$CL(\text{wt}\%) = 100 \times \left[ \frac{(n_{CL} \times 114)}{M_{n,PCLA}} \right].$$

**Equation A.10:** Weight ratio PCLA/PEG

$$PCLA/PEG = M_{n,PCLA} / M_{PEG}$$

**Equation A.11:** Degree of Modification

$$DM(mol) = \frac{I_{CH_3-}}{3} \quad \text{for normalized } I_{3.6} = 122 \quad \text{with } I_{CH_3-} = I_{1.3} \quad \text{and} \\ I_{CH_3-} = I_{2.13} + I_{2.09} + I_{2.04} \quad \text{for the propionyl- and acetyl-capped polymers, respectively.}$$

**Equation A.12:** Number average molecular weight

$$M_{n,NMR} = M_{PEG} + M_{n,PCLA} + (x \times DM) \quad \text{with } x = 43 \quad \text{and } 57 \text{ g/mol for acetyl- and} \\ \text{propionyl-capped polymers, respectively.}$$

**Equation A.13:** Probability for the presence of unreacted PEG at the end of the synthesis of PEG(PCLA<sub>1700</sub>CL<sub>2.5</sub>Acet)<sub>2</sub>

Statistically, the probability of each monomer to be or not be attached to PEG is 50/50, hence the number of free PEG hydroxyl groups at the end of the ring opening polymerization is  $0.5^{(11.6+2.3)} = 7 \cdot 10^{-3} \%$  for a feed molar ratio of CL/PEG and lactide/PEG of 11.6 and 2.3, respectively.



**Figure**

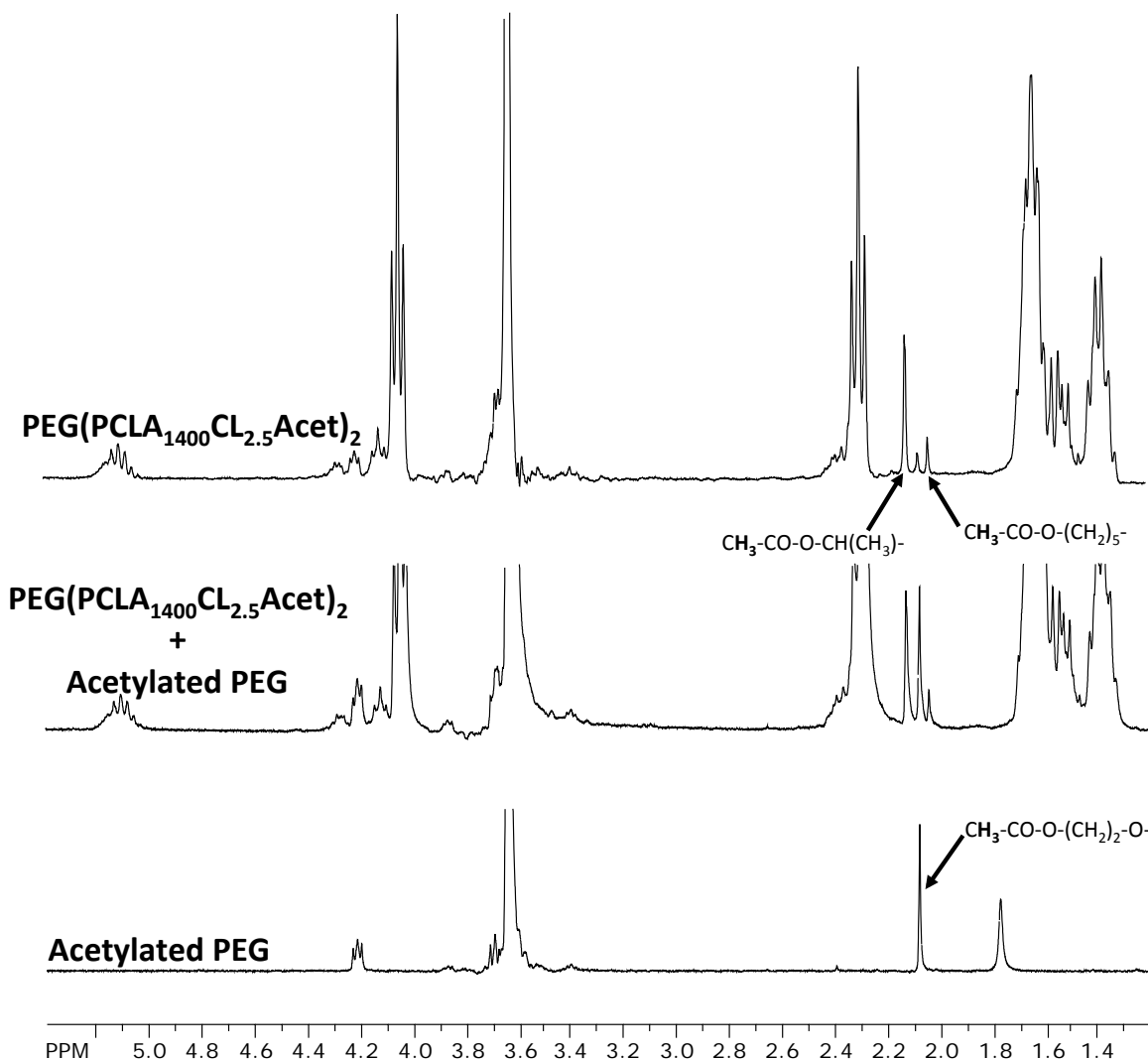


**Figure A.1:** <sup>1</sup>H NMR spectra of PEG(PCLA<sub>1400</sub>CL<sub>2.5</sub>Acet)<sub>2</sub> and acetylated PEG<sub>1500</sub> as well as their 1:1 mixture. The methyl protons of CH<sub>3</sub>-CO-O-C(H<sub>2</sub>)<sub>2</sub>-O- of acetylated PEG have a chemical shift at 2.10-2.08 ppm. The methyl protons of the acetyl groups of PCLA<sub>2x1400</sub>CL<sub>2.5</sub>Acet have chemical shifts at 2.14-2.12 and 2.03-2.05, corresponding to CH<sub>3</sub>-CO-O-CH(CH<sub>3</sub>)- and CH<sub>3</sub>-CO-O-(CH<sub>2</sub>)<sub>5</sub>-, respectively as well as a chemical shift at 2.10-2.08 ppm. The spectrum of the mixture acetylated PEG<sub>1500</sub>/PEG(PCLA<sub>1400</sub>CL<sub>2.5</sub>Acet)<sub>2</sub> shows different ratios of the three peaks between 2.14 and 2.03 ppm, which clearly demonstrates that the chemical shift at 2.10-2.08 corresponds to CH<sub>3</sub>-CO-O-C(H<sub>2</sub>)<sub>2</sub>-O-. Hence, acetylated PCLA-PEG diblock copolymers are present in PEG(PCLA<sub>1400</sub>CL<sub>2.5</sub>Acet)<sub>2</sub>, which is likely to originate from the formation of diblocks due to transesterification.

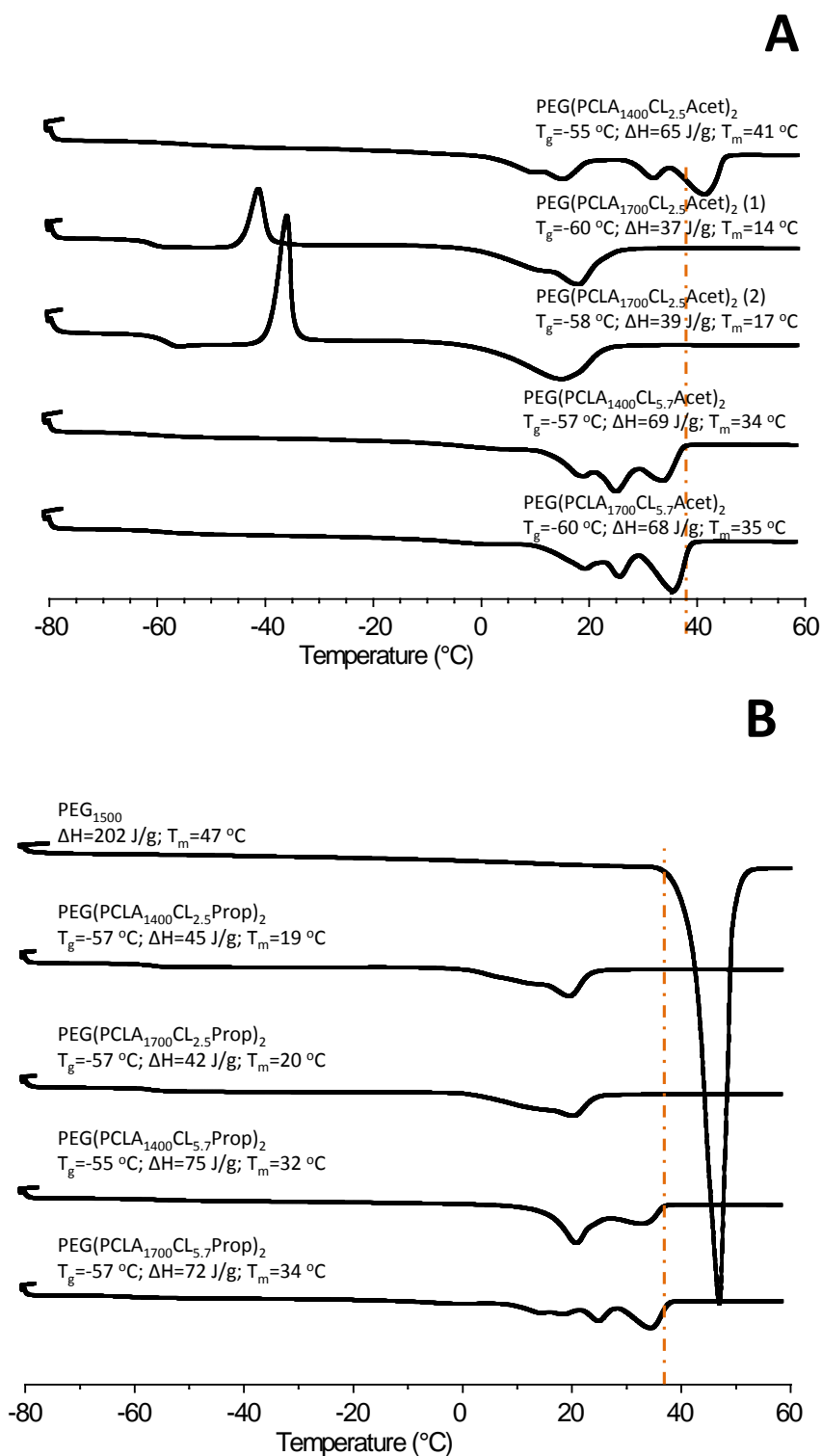


**Figure A.2:** DSC thermograms (second heating) of the acyl-capped triblock copolymers. A.2A shows the patterns for the acetyl-capped triblock copolymers. A.2B shows the patterns for PEG<sub>1500</sub> and the propionyl-capped triblock copolymers.

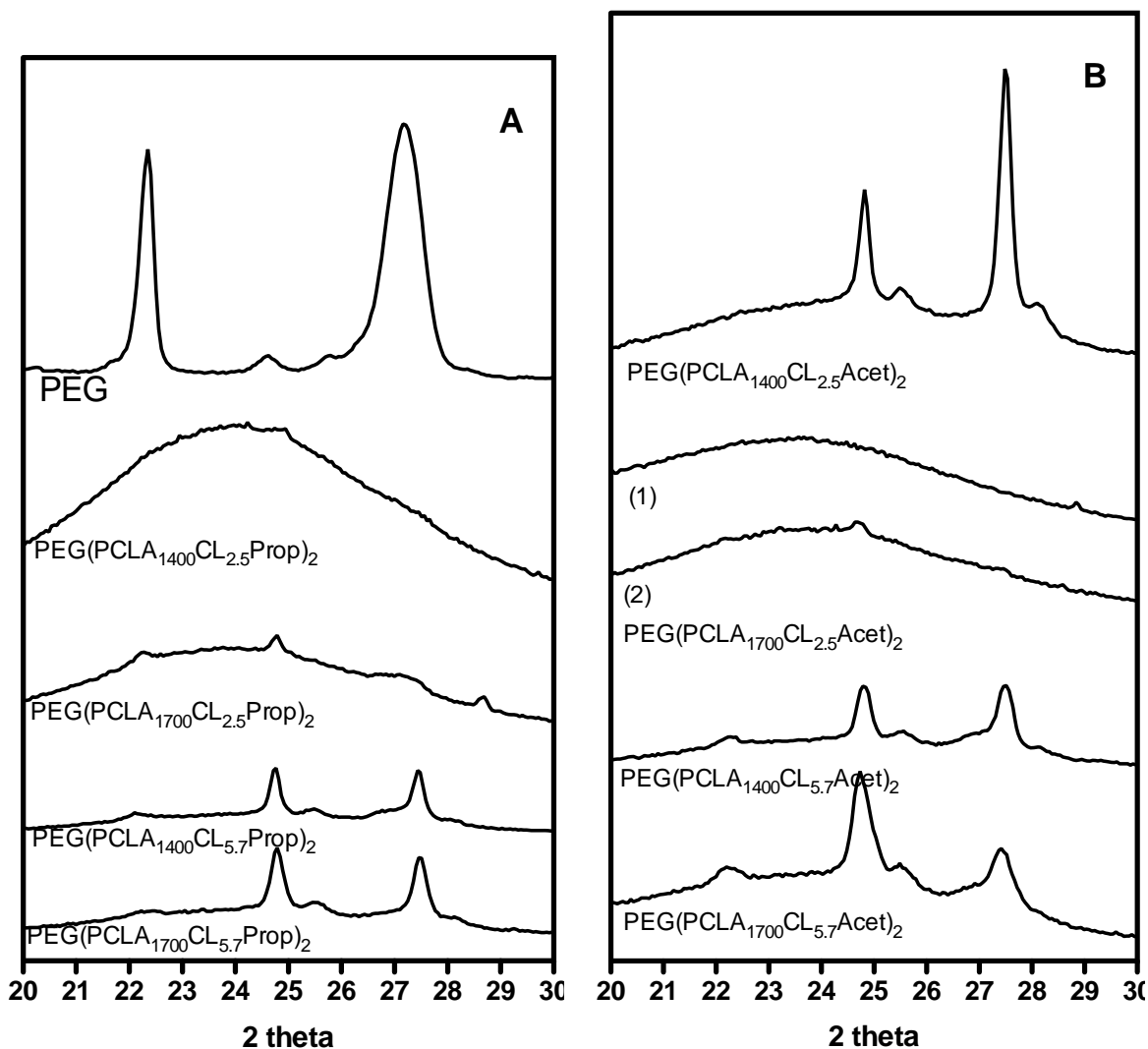


**Figure A.3:** X-ray diffraction patterns. A.3A shows the patterns for PEG<sub>1500</sub> and the propionyl-capped triblock copolymers. A.3B shows the patterns for the acetyl-capped triblock copolymers. It should be stressed that in Figure A.3, the thermal history of the polymers was not removed as in the case of the DSC measurements depicted in Figure A.2.

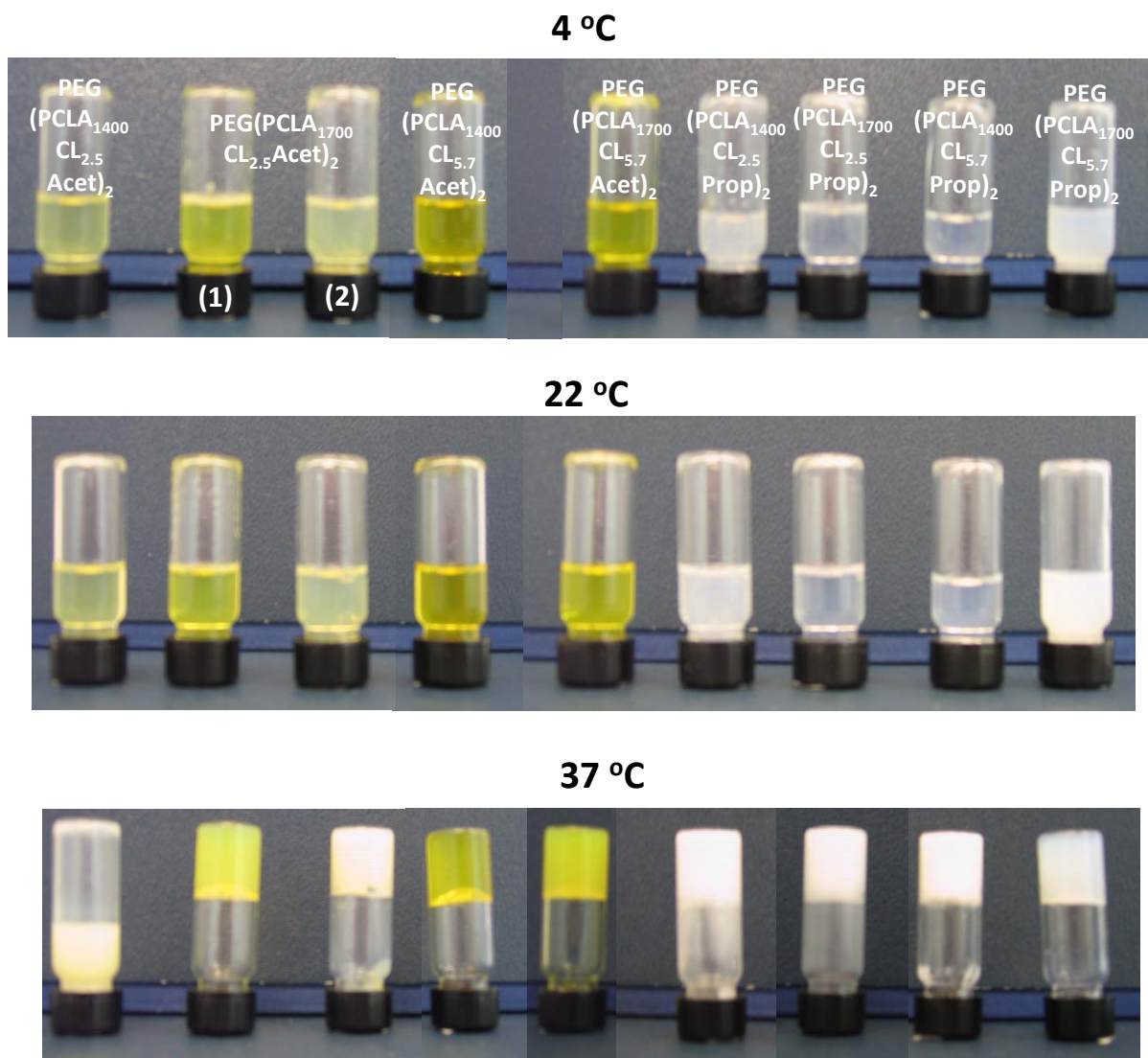


**Figure A.4:** Photographs of samples made of the polymers at 25 wt% solid content after 30 min at 4, at ~22 and 37 °C. It is noteworthy that the propionyl-capped polymer solutions were colourless whereas the acetyl-capped polymer solutions were yellow.

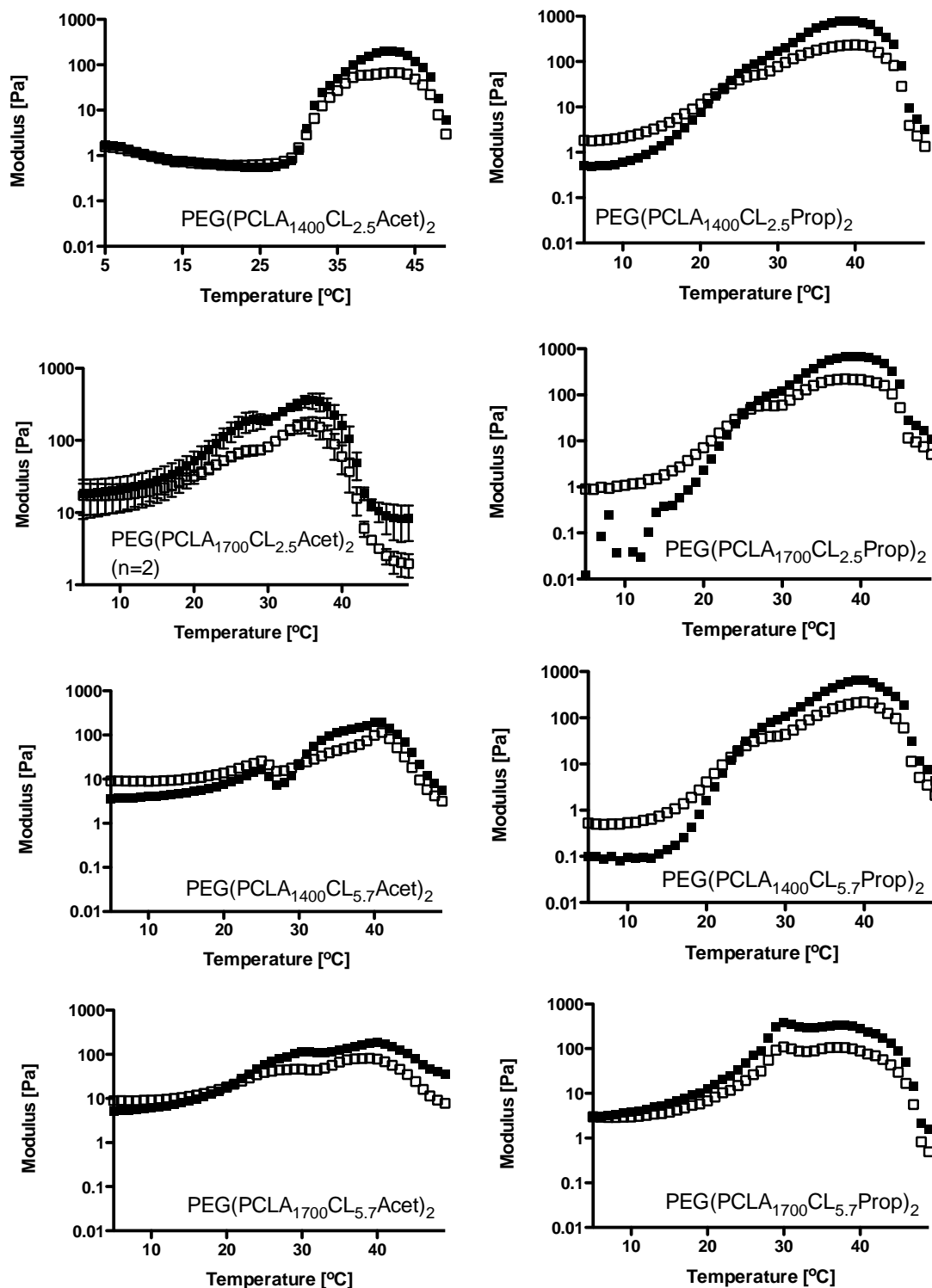
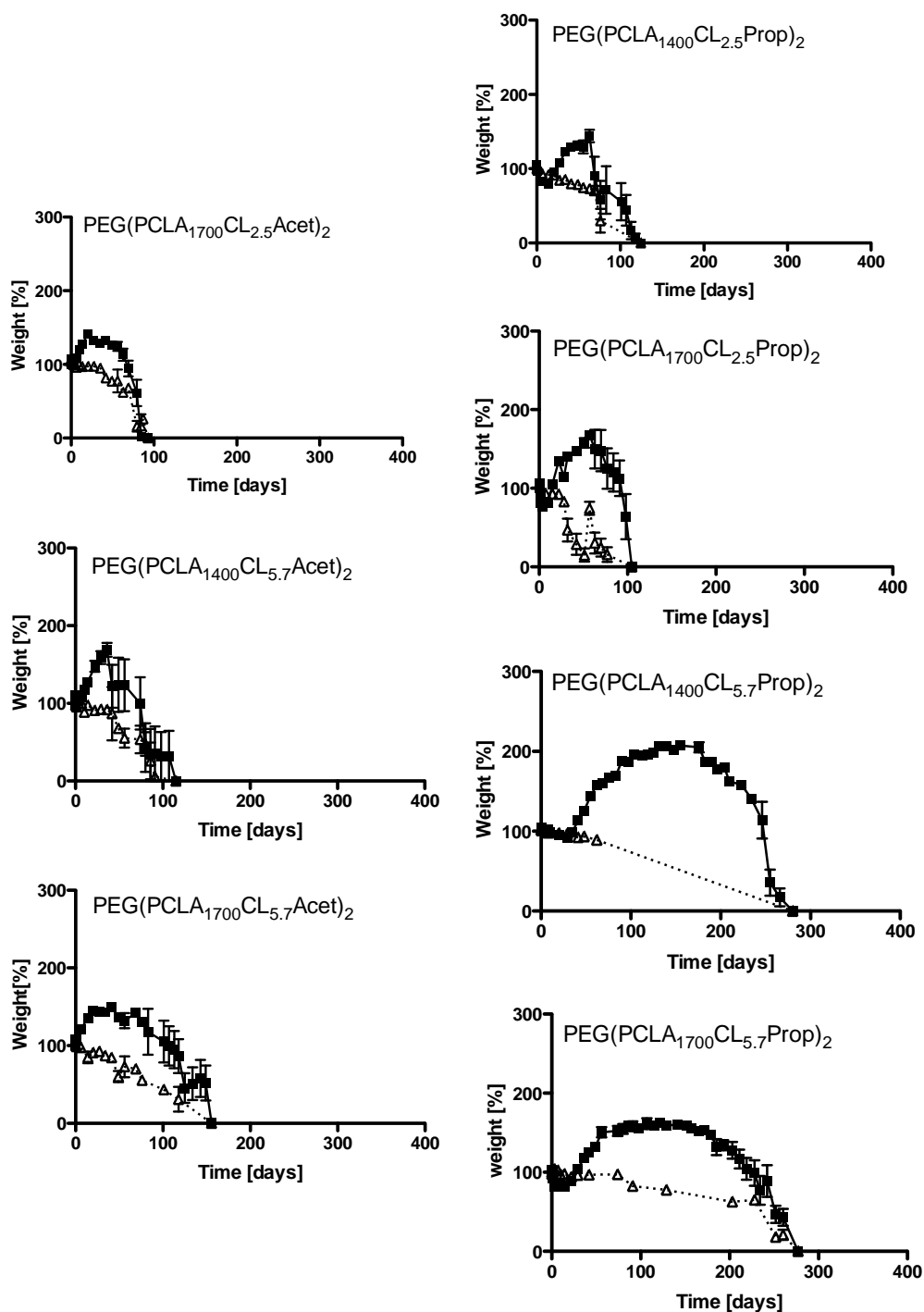
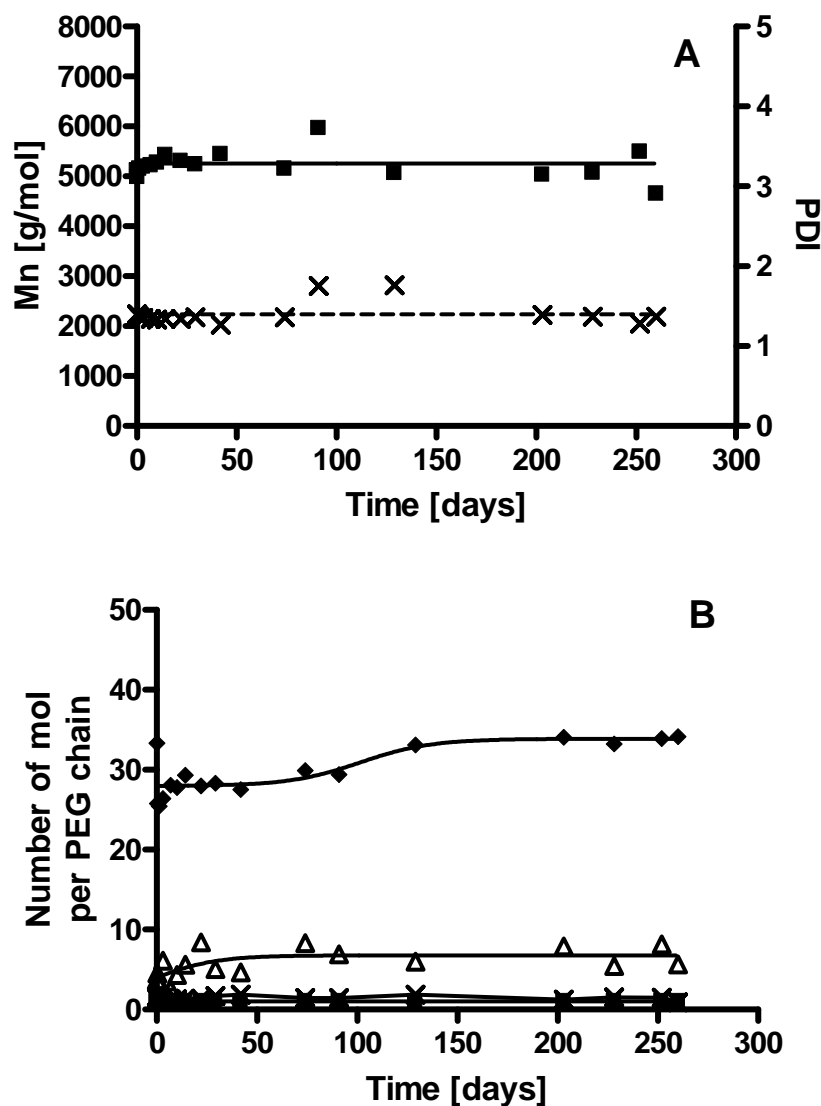


Figure A.5: Temperature sweep of samples at 25 wt% acyl-capped triblock copolymers with the closed and open symbols representing  $G'$  and  $G''$ , respectively.



**Figure A.6:** Degradation of gels (25 wt% in buffer) composed of acyl-capped triblock copolymers. Squares and triangles represent wet weight and dry weight, respectively. Experiments were performed at 37 °C in phosphate buffer (pH 7.4). Error bars represent standard error of the mean ( $n = 3$ ).



**Figure A.7:** Analysis of residual gels of PEG(PCLA<sub>1700</sub>CL<sub>5.7</sub>Prop)<sub>2</sub> in time. A.7A shows the  $M_n$  (squares) and PDI or  $M_w/M_n$  ratio (crosses) as determined by GPC. A.7B shows the composition of the residual polymers with CL (diamonds), LA (triangles), end group (crosses) and PEG (squares) as determined by  $^1\text{H}$  NMR data after addition of an excess TCAI.

**Table A.1.** Amount of PEG, monomers and acyl chloride used to synthesize the acyl-capped PCLA-PEG-PCLA copolymers.

Polymer	Acyl-PCLA-PEG-PCLA-Acyl									
	<i>PCLA</i> <sub>1400</sub>	<i>PCLA</i> <sub>1700</sub>	<i>PCLA</i> <sub>1400</sub>	<i>PCLA</i> <sub>1700</sub>	<i>PCLA</i> <sub>1400</sub>	<i>PCLA</i> <sub>1700</sub>	<i>PCLA</i> <sub>1400</sub>	<i>PCLA</i> <sub>1700</sub>	<i>PCLA</i> <sub>1400</sub>	<i>PCLA</i> <sub>1700</sub>
	<i>CL</i> <sub>2.5</sub> <i>Acet</i>	<i>CL</i> <sub>2.5</sub> <i>Acet</i> *	<i>CL</i> <sub>5.7</sub> <i>Acet</i>	<i>CL</i> <sub>5.7</sub> <i>Acet</i>	<i>CL</i> <sub>2.5</sub> <i>Prop</i>	<i>CL</i> <sub>2.5</sub> <i>Prop</i>	<i>CL</i> <sub>5.7</sub> <i>Prop</i>	<i>CL</i> <sub>5.7</sub> <i>Prop</i>	<i>CL</i> <sub>5.7</sub> <i>Prop</i>	<i>CL</i> <sub>5.7</sub> <i>Prop</i>
	(1)	(2)								
	<i>PCLA</i> [g/mol] <sup>a)</sup>	1400	1700	1400	1700	1400	1700	1400	1700	1700
	Aimed <i>CL/LA</i> <sup>b)</sup>	2.5	2.5	5.7	5.7	2.5	2.5	5.7	5.7	5.7
	Acyl		acetyl-				propionyl-			
	PEG [g]	10.0	50.0	50.0	10.1	25.0	25.0	10.0	10.1	10.0
	CL [g]	14.4	88.0	88.0	16.3	49.5	36.0	17.6	16.4	19.8
Feed	Lactide [g]	3.6	22.0	22.0	1.8	5.5	9.0	4.4	1.8	2.2
	Acyl chloride [g]	2.0	10.0	10.0	2.0	5.0	6.2	2.5	2.3	2.5

<sup>a)</sup> Aimed PCLA/PEG: the weight ratio of PCLA to PEG

<sup>b)</sup> Aimed CL content: the weight of CL in PCLA

**Table**





## CHAPTER 4

# *In situ* forming acyl-capped PCLA-PEG-PCLA triblock copolymer-based hydrogels

Marian J. Sandker<sup>1\*</sup>, Audrey Petit<sup>2,3\*</sup>, Everaldo M Redout<sup>4</sup>, Michiel Siebelt<sup>1</sup>, Benno Müller<sup>2</sup>, Peter Bruin<sup>2</sup>, Ronald Meyboom<sup>2</sup>, Tina Vermonden<sup>3</sup>, Wim E Hennink<sup>4</sup> and Harrie Weinans<sup>1,5,6,7</sup>

<sup>1</sup> Department of Orthopaedics, Erasmus Medical Centre, Rotterdam, The Netherlands

<sup>2</sup> InGell Labs BV, Groningen, The Netherlands

<sup>3</sup> Department of Pharmaceutics, Utrecht Institute for Pharmaceutical Sciences, Utrecht, The Netherlands

<sup>4</sup> Department of Equine Sciences, Faculty of Veterinary Sciences, Utrecht University, The Netherlands

<sup>5</sup> Department of Orthopaedics, UMC Utrecht, The Netherlands

<sup>6</sup> Department of Rheumatology, UMC Utrecht, The Netherlands

<sup>7</sup> Department of Biomechanical Engineering, TU Delft, The Netherlands

\* *Authors with equal contribution*

Chapter 4

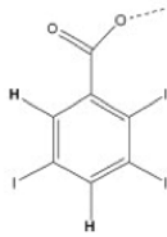
Radiopaque gel

### **Abstract**

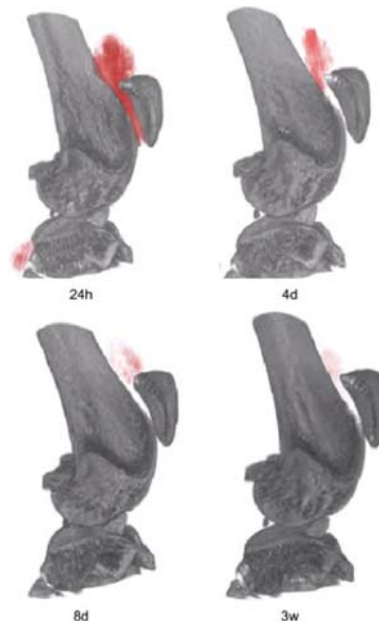
Sustained intra-articular drug delivery opens up new opportunities for targeted treatment of osteoarthritis. In this study, we investigated the *in vitro* and *in vivo* properties and performance of a newly developed hydrogel based on acyl-capped PCLA-PEG-PCLA specifically designed for intra-articular use. The hydrogel formulation consisted of a blend of polymers either capped with acetyl, or with triiodobenzoyl (TIB) moieties. TIB was added to visualize the gel using  $\mu$ CT, enabling longitudinal quantification of its degradation. Blends containing a TIB-capped polymer degraded *in vitro* (37 °C, pH 7.4) through dissolution over a period of ~20 weeks, and degraded slightly faster (~12 weeks) after subcutaneous injection in rats. This *in vivo* acceleration was likely due to active (enzymatic) degradation, shown by changes in polymer composition and molecular weight as well as the presence of macrophages. After intra-articular administration in rats, the visualized gel gradually lost signal intensity over the course of 4 weeks. Good cytocompatibility of an acetyl-capped polymer-based hydrogel was proven *in vitro* on erythrocytes and chondrocytes. Moreover, intra-articular biocompatibility was demonstrated using  $\mu$ CT-imaging and histology, since both techniques showed no changes in cartilage quality and/or quantity.

Longitudinal visualization of acyl-capped PCLA-PEG-PLCA systems *in vivo*

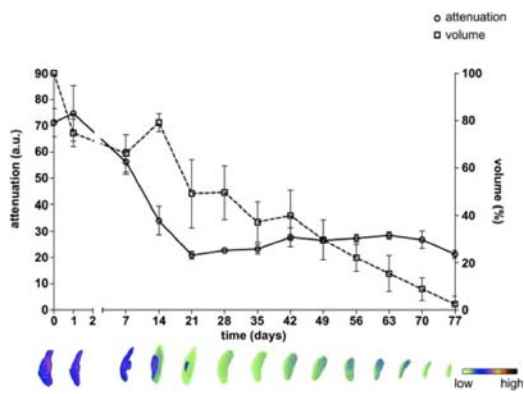
Radiopaque iodine-based end group:



after intra-articular administration



after subcutaneous administration



## 1. Introduction

Osteoarthritis (OA) is a common joint disease that affects approximately 30 % of the elderly population [1]. Current treatment is mainly based on pain prevention through orally administered drugs, like often non-steroidal anti-inflammatory drugs [2], since disease modifying drugs (DMOADs) are not (yet) available. The development and application of DMOADs are hindered by the fact that it is difficult to obtain sufficient intra-articular (i.a.) concentrations, while high systemic exposure of some putative drugs leads to unwanted side-effects [2,3]. The best local therapies for OA so far are i.a. injections (of hyaluronic acid or corticosteroids), thereby circumventing the problem of sub-therapeutic local drug concentrations. However, i.a. injections also provide limited effects, due to the rapid i.a. drug turnover leading to a fast decline of the local drug concentrations to therapeutically inactive levels. For example, i.a. administration of Kenalog<sup>®</sup> (triamcinolone acetonide suspension) allows for local delivery [4], but only for a limited period of one week [4,5,6]. Therefore, often multiple i.a. injections are given [7], leading to the risk of cartilage and joint damage and/or infections [2,5,7,8].

Ideally, a single i.a. injection of a local drug delivery system (DDS) for OA would provide sustained drug concentrations in a joint in a controlled way for at least one month. Suitable DDSs are easy to inject, show high encapsulation efficiency with low burst release, tunable release kinetics, and full recovery of the loaded drug. Ideal systems release a drug of interest for weeks while maintaining a therapeutically effective concentration at the target site. DDSs developed for i.a. use have, up to now, been mainly based on liposomes or polymeric nano/microparticles [9,10]. Liposomes for local i.a. treatment (and other non-vascular routes) usually show a short drug release duration, which is hardly adjustable [11] although biological stability of liposomes can be improved by surface PEGylation [12,13]. On the other hand, microparticle-based systems show a more controllable and sustained release [11,14]. The main drawback of both liposome- and microparticle-based systems is their costly and non-straightforward manufacturing mainly because up-scaling is challenging [11,15,16].

Alternatively, an *in situ* forming depot containing highly concentrated solutions (400 mg/ml) of the hydrophobic drug celecoxib in poly(ethylene glycol) 400 (PEG<sub>400</sub>) has recently been developed [17]. Upon i.a. injection,

PEG<sub>400</sub> is diluted and celecoxib precipitates/crystallizes, allowing a sustained release by slow dissolution (~10 days). This shows the potential i.a. use of *in situ* forming depots, but modulating release rates and durations using this system are not possible [18]. Temperature-responsive gelling systems (composed of ABA triblock copolymers with a PEG middle block flanked by polyester blocks of diverse compositions, dispersed in aqueous medium) do meet desirable DDS properties including high encapsulation efficiency, low burst and good drug recovery. They can be injected as a solution and transform into a gel after injection [19-24]. Moreover, terminal hydroxyl-end group modification of the polyester-PEG-polyester triblock copolymers enables further modulation of rheological and degradation/dissolution properties of aqueous and temperature-responsive gelling systems [25,26]. Indeed, we previously showed that the rheological properties of aqueous systems containing acyl-capped poly( $\epsilon$ -caprolactone-*co*-lactide)-*b*-poly(ethylene glycol)-*b*-poly( $\epsilon$ -caprolactone-*co*-lactide) (PCLA-PEG-PCLA) are easy to modulate [27].

Getting more insight into the *in vivo* behaviour of DDSs is a crucial step towards clinical applications for treatment in a joint. In that respect, it is pivotal to determine whether a DDS forms a depot that is retained at the injection site and to investigate its degradation kinetics. Fluorescent particles [28,29] and dye-loaded microparticles [28] are examples of visible DDSs used previously. For both systems, the initial distribution of the particles after administration can be visualized, however due to diffusion and release of the dyes from the DDSs, biodegradation kinetics cannot be investigated. To circumvent this problem, dyes have been covalently bound to polymeric particles [30]. This method facilitates visualization, but only through *ex vivo* sectioning, hence lacking longitudinal follow-up possibilities of particle quantification and spatiotemporal distribution. Non-invasive *in vivo* imaging of DDSs can be achieved by, for instance, computed tomography (CT) using iodine-containing moieties that confer a degree of X-ray opacity [31,32]. Indeed, others have shown that different systems, for instance polymethacrylate-based microparticles [33] and hydrogels [34], containing covalently bound 2-(2',3',5'-triiodobenzoyl) moieties (TIB) are suitable for *in vivo* visualization.

In the current study, we investigated the potential of biodegradable,

temperature-responsive gelling systems made of an aqueous acyl-capped PCLA-PEG-PCLA triblock copolymer dispersion for *in vivo* use, and in particular i.a. application. Primarily, we assessed the real time degradation kinetics of the gel both *in vitro* and *in vivo* (subcutaneous (s.c.) and i.a.) in a non-invasive manner. For this, we modified the hydroxyl end groups of PCLA-PEG-PCLA with 2-(2',3',5'-triiodobenzoyl) moieties (TIB) to obtain radiopaque gels suitable for long-term *in vivo* visualization using  $\mu$ CT. Secondly, the cytocompatibility and i.a. biocompatibility of the gels were tested.

## 2. Experiments and protocols

### 2.1. Materials

L-lactide was obtained from Purac Biochem, The Netherlands. Hexabrix 320<sup>®</sup>, a clinical iodine-based contrast agent, was obtained from Guerget, The Netherlands. All other chemicals were obtained from Aldrich and used as received.

### 2.2. Synthesis of TIB chloride

2-(2',3',5'-triiodobenzoyl) (TIB) chloride was synthesized as described previously [35]. Briefly, 2,3,5-triiodobenzoic acid (10.5 g, 21 mmol) was dissolved in dichloromethane (100 ml), followed by the addition of a catalytic amount of dimethylformamide (10 mg, 0.14 mmol) [35]. An excess of oxalyl chloride (10 ml; 79 mmol,  $-\text{COCl}/-\text{COOH} = 8 \text{ mol/mol}$ ) was added drop wise and the mixture was stirred for two days at room temperature. Volatiles were evaporated under reduced pressure and the remainder was stripped with toluene three times to yield 9.3 g (85 %) of TIB chloride. Characterization of TIB chloride dissolved in  $\text{CDCl}_3$  was done with  $^1\text{H}$  NMR using a Varian Oxford, operating at 300 MHz.  $^1\text{H}$  NMR spectra were referenced to the signal of chloroform at 7.26 ppm.

### 2.3. Synthesis of acetyl-capped and TIB-capped polymers

The acetyl-capped and TIB-capped PCLA-PEG-PCLA triblock copolymers (namely  $\text{PCLA}_{2 \times 1700}\text{CL}_{2.5}\text{Acet}$ ,  $\text{PCLA}_{2 \times 1700}\text{CL}_{2.5}\text{TIB}$  and  $\text{PCLA}_{2 \times 750}\text{CL}_{5.7}\text{TIB}$ ) used in this study were essentially synthesized and characterized as described previously [27]. In short, L-lactide and

$\epsilon$ -caprolactone dissolved in toluene were polymerized with PEG<sub>1500</sub>-diol as a macroinitiator in the presence of tin(II) 2-ethylhexanoate as a catalyst. The exact amounts used in the synthesis are summarized in Table 1. For PCLA<sub>2×1700</sub>CL<sub>2.5</sub> and PCLA<sub>2×750</sub>CL<sub>5.7</sub>, a caproyl/lactoyl (CL/LA) molar ratio of 2.5/1 and 5.7/1 mol/mol, respectively were used. Subsequently, acylation of the hydroxyl end-groups using an excess of acetyl chloride or TIB chloride (ratio chloride/OH groups = 4 mol/mol) resulted in the formation of acetyl-capped and TIB-capped PCLA-PEG-PCLA respectively, with a yield of 85 %.

TIB-end group: 8.40-7.60 ppm ( $I_{8.0}$ , m, 2H, Ar H) [36-38].

Acetyl-end group: 2.14-2.12 ppm ( $I_{2.13}$ , CH<sub>3</sub>-CO-O-CH(CH<sub>3</sub>)-); 2.03-2.05 ppm ( $I_{2.04}$ , CH<sub>3</sub>-CO-O-(CH<sub>2</sub>)<sub>5</sub>-) [26,39-42] and 2.10-2.08 ppm ( $I_{2.09}$ , CH<sub>3</sub>-CO-O-C(H<sub>2</sub>)<sub>2</sub>-O-) as shown in Figure A.1.

The composition of acyl-capped PCLA-PEG-PCLA was established from integral of signals belonging to methine protons of LA subdivided in four quadruplets ( $I_{5.1}$  at 5.25-4.95 ppm), methylene protons of PEG ( $I_{3.6}$  at 3.72-3.55 ppm), methylene protons of CL subdivided in two triplets ( $I_{2.4} + I_{2.3}$  at 2.50-2.20 ppm). The degree of modification was calculated from the ratio between protons of the end groups and methylene protons of PEG ( $I_{3.6}$  at 3.72-3.55 ppm).

#### 2.4. Gel permeation chromatography (GPC) analysis

Molecular weight ( $M_n$ ) of the synthesized polymers was determined by GPC as described previously [25]. The characteristics of PCLA<sub>2×1700</sub>CL<sub>2.5</sub>Acet, PCLA<sub>2×1700</sub>CL<sub>2.5</sub>TIB and PCLA<sub>2×750</sub>CL<sub>5.7</sub>TIB are given in Table 1.

#### 2.5. Preparation of blends

PCLA<sub>2×1700</sub>CL<sub>2.5</sub>Acet and PCLA<sub>2×1700</sub>CL<sub>2.5</sub>TIB or PCLA<sub>2×750</sub>CL<sub>5.7</sub>TIB were separately dissolved in 15 ml ethyl acetate at a concentration of 500 mg/ml. The solutions were mixed to achieve specific ratios and the obtained mixtures were transferred to 11-cm Petri dishes. The solvent was removed under nitrogen flow for 48 hours (gas chromatography analysis indicated a residual ethyl acetate content <0.5%).



**Table 1:** Characteristics of acetyl-capped and TIB-capped PCLA-PEG-PCLA triblock copolymers.

<i>Polymer</i>	<i>Acetyl-capped</i> <i>PCLA<sub>1700</sub>-PEG<sub>1500</sub>-</i> <i>PCLA<sub>1700</sub></i>	<i>TIB-capped</i> <i>PCLA<sub>1700</sub>-PEG<sub>1500</sub>-</i> <i>PCLA<sub>1700</sub></i>	<i>TIB-capped</i> <i>PCLA<sub>750</sub>-PEG<sub>1500</sub>-</i> <i>PCLA<sub>750</sub></i>
<i>Abbreviation</i>	<i>PCLA<sub>2×1700</sub>CL<sub>2.5</sub>Acet</i>	<i>PCLA<sub>2×1700</sub>CL<sub>2.5</sub>TIB</i>	<i>PCLA<sub>2×750</sub>CL<sub>5.7</sub>TIB</i>
PEG feed [g]	50	50	50
ε-caprolactone feed [g]	88	88	45
Lactide feed [g]	10	10	5
Acetyl chloride feed [g]	10	0	0
TIB chloride feed [g]	0	9.3	9.3
Aimed M <sub>n,PCLA</sub> [g/mol]	4900	4900	3200
PCLA/PEG <sup>a)</sup>	2.1/1	2.1/1	1.1/1
CL/LA [mol/mol] <sup>b)</sup>	4.9/1	5.7/1	4.4/1
DM [%] <sup>c)</sup>	93	90	90
M <sub>n</sub> [g/mol] <sup>d)</sup>	4700	3100	3400
PDI <sup>e)</sup>	1.4	1.2	1.3

<sup>a)</sup> weight ratio of PCLA to PEG determined by <sup>1</sup>H NMR

<sup>b)</sup> weight ratio of ε-caprolactone to L-lactide determined by <sup>1</sup>H NMR

<sup>c)</sup> degree of modification represents the number of end groups per triblock copolymer determined by <sup>1</sup>H NMR

<sup>d)</sup> determined by GPC

<sup>e)</sup> determined by GPC

### 2.6. Preparation of the aqueous dispersions

21 ml phosphate buffer (44 mM Na<sub>2</sub>HPO<sub>4</sub>, 9 mM NaH<sub>2</sub>PO<sub>4</sub>, 72 mM NaCl, pH 7.4) was added to 7 g PCLA<sub>2×1700</sub>CL<sub>2.5</sub>Acet, PCLA<sub>2×1700</sub>CL<sub>2.5</sub>Acet/PCLA<sub>2×1700</sub>CL<sub>2.5</sub>TIB or PCLA<sub>2×1700</sub>CL<sub>2.5</sub>Acet/PCLA<sub>2×750</sub>CL<sub>5.7</sub>TIB blend in 50-ml centrifuge tubes to yield systems with 25 wt% solid content. Samples were heated for 15 min at 50 °C and vortexed thoroughly. Next, the samples were stored at 4 °C for 48 h to allow formation of homogeneous systems.

### 2.7. Rheological characterization

Oscillatory stress was applied to the PCLA<sub>2×1700</sub>CL<sub>2.5</sub>Acet/PCLA<sub>2×750</sub>CL<sub>5.7</sub>TIB system (25 wt% in buffer) from 10 to 400 Pa with 10 points per decade using a TA AR-G2 rheometer equipped with a Peltier plate (1 ° steel cone, 20 mm diameter with solvent trap). The run duration was 2 min and the time between runs was <30 s. Rheological analysis of 70 µl samples of PCLA<sub>2×1700</sub>CL<sub>2.5</sub>Acet/PCLA<sub>2×750</sub>CL<sub>5.7</sub>TIB systems (25 wt% in phosphate buffer) was done by dynamic mechanical analyzer (DMA, TA Instruments). A static force sweep of 5 N/min, starting at 0.1 N, was applied on a sample-loaded syringe (2 ml).

### 2.8. In vitro degradation behaviour

PCLA<sub>2×1700</sub>CL<sub>2.5</sub>Acet/PCLA<sub>2×750</sub>CL<sub>5.7</sub>TIB (25/75 w/w) systems of 25 wt% solid content were used to study degradation properties of gels under physiological conditions (37 °C, pH 7.4). Samples (300 µl) cooled to 4 °C were transferred via a syringe into glass vials (8.2 × 40 mm). The closed vials were placed at 37 °C to induce a sol-to-gel transition. After 30 min, 700 µl phosphate buffer was added. At different time points, the buffer was removed, the weight of residual gels was measured, and fresh buffer was added. In addition, samples were freeze-dried for further analysis (dry weight and analysis by GPC and <sup>1</sup>H NMR).

### 2.9. In vitro cytocompatibility of PCLA<sub>2×1700</sub>CL<sub>2.5</sub>Acet

Cytocompatibility tests of the PCLA<sub>2×1700</sub>CL<sub>2.5</sub>Acet gel (25 wt% in phosphate buffer) were performed on primary equine chondrocytes. Full thickness cartilage was harvested from metacarpophalangeal joints from four horses and digested in 0.15 % collagenase type II in DMEM (10 % FBS,

100 U/ml penicillin, 100 U/ml streptomycin, 25 mM Hepes) overnight. Then, the digest was filtered through a 100- $\mu$ m cell strainer, and centrifuged (10 min, 1500 rpm, 4 °C). The supernatant was aspirated and the pellet resuspended in PBS and centrifuged (10 min, 1500 rpm, 4 °C); this step was repeated twice. Subsequently, PBS was aspirated and cells were resuspended in DMEM/F12 supplemented with 5 % FBS, 100 U/ml penicillin, 100 U/ml streptomycin, 0.5 % Fungizone, 0.085 mM vitamine C, 1 % glutamax and cultured (37 °C, 5 % CO<sub>2</sub>). Cytocompatibility of the gel was assessed by AlamarBlue (Invitrogen) assay. Cells were seeded in 96-well plates at 10<sup>4</sup> cells per well in 100  $\mu$ l DMEM/F12 containing aforementioned supplements and incubated (37 °C, 5 % CO<sub>2</sub>) for 24 hours. Then 100  $\mu$ l of PCLA<sub>2 $\times$ 1700</sub>CL<sub>2.5</sub>Acet, Pluronic<sup>®</sup> F-127 (a non-ionic copolymer frequently used for cell culture; positive control) or SDS (sodium dodecyl sulphate, negative control) were dissolved in DMEM/F12 (1 % ITS, 100 U/ml penicillin, 100 U/ml streptomycin, 0.5 % Fungizone, 0.085 mM vitamine C, 1 % glutamax and 5 mg/ml BSA) at concentrations ranging from 0.001 to 2.0 mg/ml. After 24 hours incubation, DMEM/F12 was replaced by 100  $\mu$ l fresh medium containing AlamarBlue (1:10) followed by 24 hours incubation at 37 °C and the absorbance was measured at 570 nm. Cytocompatibility is expressed as relative viability; cells cultured in blank DMEM/F12 medium served as a control, which was set at 100 %.

Hemolytic activity of PCLA<sub>2 $\times$ 1700</sub>CL<sub>2.5</sub>Acet and its dissolving buffer (44 mM Na<sub>2</sub>HPO<sub>4</sub>, 9 mM NaH<sub>2</sub>PO<sub>4</sub>, 72 mM NaCl) was measured. PBS solution containing 1 % Triton X-100 was used as a positive, and PBS as a negative control. Equine erythrocytes were isolated from fresh citrate treated blood, washed with PBS by four centrifugation cycles (10 min, 1000 rpm, 4 °C). The erythrocyte pellet was diluted 10-fold in 150 mM NaCl. Next, 50  $\mu$ l of 25 wt% polymer or buffer were added to a 450- $\mu$ l erythrocyte suspension, and incubated at 4 or 37 °C for 1 hour under constant shaking. Eppendorfs were centrifuged (5 min, 2000 rpm) and 60  $\mu$ l supernatant was transferred into a flat bottom 96-well plate. Hemoglobin content was obtained by measuring absorbance at 540 nm.

### *2.10. In vivo experiments*

Sixteen 16-week-old (400–450 g) male Wistar rats (Charles River

Netherlands, Maastricht, The Netherlands) were housed in the animal facility of the Erasmus Medical Center, with a 12-h light–dark regimen, at 21 °C. Animals were fed with standard food pellets and water *ad libitum*. The animal ethic committee of the Erasmus Medical Center, Rotterdam, The Netherlands, approved all conducted procedures.

Group 1: *in vivo* retention and degradation of PCLA<sub>2×1700</sub>CL<sub>2.5</sub>Acet/PCLA<sub>2×750</sub>CL<sub>5.7</sub>TIB (25/75) blends (25 wt% in buffer) was assessed in a first group of six rats. Four rats received a s.c. injection of 100 μl PCLA<sub>2×1700</sub>CL<sub>2.5</sub>Acet/PCLA<sub>2×750</sub>CL<sub>5.7</sub>TIB (25 wt% solid content) each; the other two rats received an injection of 50 μl in the knee joint. The gels were scanned regularly to visualize degradation longitudinally. All rats received two additional s.c. injections of 100 μl PCLA<sub>2×1700</sub>CL<sub>2.5</sub>Acet/PCLA<sub>2×750</sub>CL<sub>5.7</sub>TIB, which were explanted at predetermined time points, dried and analyzed by GPC and <sup>1</sup>H NMR.

Group 2: In a second group of rats (n = 10), *in vivo* biocompatibility was assessed. Each rat received an injection at t = 0 of 50 μl aqueous dispersion of PCLA<sub>2×1700</sub>CL<sub>2.5</sub>Acet (25 wt% solid content) in the left knee and 50 μl of saline in the right knee (control). Of both knees, μCT scans were acquired before gel injection and at 6 and 12 weeks, to visualize potential cartilage degeneration (using a contrast agent). Simultaneously, each rat received a 500 μl 25 wt% PCLA<sub>2×1700</sub>CL<sub>2.5</sub>Acet s.c. injection (tibia region) in order to follow *in vivo* gelling properties and degradation kinetics. The total s.c. gel volume was measured at set time points using a skin fold meter.

### 2.11. μCT-imaging

In vitro: Vials containing PCLA<sub>2×1700</sub>CL<sub>2.5</sub>Acet/PCLA<sub>2×750</sub>CL<sub>5.7</sub>TIB or PCLA<sub>2×1700</sub>CL<sub>2.5</sub>Acet/PCLA<sub>2×1700</sub>CL<sub>2.5</sub>TIB were scanned *in vitro*. Scans were performed using the following scanner settings: isotropic voxelsize of 35 μm; 55 kV; 170 mA; 35 mm field of view; 0.5 mm Al filter; 0.8 rotation step over 198 °; frame averaging of 3.

Group 1: Scans were performed t = 0, 1 day, 4 days, 1 week and thereafter on a weekly basis until the PCLA<sub>2×1700</sub>CL<sub>2.5</sub>Acet/PCLA<sub>2×750</sub>CL<sub>5.7</sub>TIB blend was no longer visible. The following scan settings were used; isotropic voxelsize of 35 μm; 55 kV; 170 mA; field of view 35 mm; a 0.5 mm Al filter; 0.8 rotation step over 198 ° with a frame averaging of 3.

Group 2: cartilage quality (sulfated glycosaminoglycan (sGAG) content) and quantity (thickness) was measured with *in vivo*  $\mu$ CT arthrography. Therefore, knees were injected with a radiographic contrast (Hexabrix mixed with 10  $\mu$ g/ml Epinephrine) as described previously [43,44]. Influx of Hexabrix into the cartilage correlates inversely with sGAG content [45,46] to detect early changes in cartilage quality using *in vivo*  $\mu$ CT arthrography [43,44]. After injecting Hexabrix, rats were placed in a custom-made scanner bed fixing the hind limb in extended position. Scans were performed using the following scanner settings: isotropic voxelsize of 35  $\mu$ m; 55 kV; 170 mA; 35 mm field of view; 0.5 mm Al filter; 0.8 rotation step over 198 °; frame averaging of 2.

### *2.12. $\mu$ CT data analysis*

Raw  $\mu$ CT images were converted into 3D reconstructions using the reconstruction software nRecon version 1.5 (SkyScan). With 3D Calc software, segmentation into binary images [47] took place creating a mask overlaying bone and Hexabrix in the original gray value images of Group 2 (ImageJ; NIH, <http://imagej.nih.gov/ij/index.html>) [43]. Subsequently, regions of interest (ROI's) were drawn around the patellar cartilage (40 slices) for which attenuation and thickness were calculated. In the datasets of Group 1 (gel degradation) as well as the *in vitro* degradation images, ROI's were drawn directly around the visible gels in the reconstructed images. Subsequently, segmentation took place between gel and surrounding tissue and attenuation and volume of the gels were calculated.

### *2.13. Histology*

Following the last scan, the rats of Group 2 (n = 10) were sacrificed and the knee joints were fixed with formalin, decalcified and embedded in paraffin. Next, 6- $\mu$ m sections were prepared sagittally at 300- $\mu$ m intervals and stained with Safranin-O. Patellar, tibial (lateral/medial) and trochlear cartilage were scored using a modified Mankin scoring system (0, normal cartilage; 1, slight reduction; 2, moderate reduction; 3, severe reduction; 4, no dye noted) [48] for GAG-staining and a modified Pritzker score for structure composition (0, surface intact; 1, surface discontinuity; 2, vertical fissures; 3, erosion; 4, denudation; 5, deformation) [49]. Both scores were multiplied by

number representing the affected area (1: <10 %; 2: 10–25 %; 3: 25–40 %; 4: >40 %). Final score is expressed as a percentage of the maximal score (GAG-depletion: 16; structural score: 20). Then, the average of all regions per knee was calculated, resulting in total knee joint scores ranging from 0 % (not affected) to 100 % (severe OA in >40 % of the joint).

At the same time, also the site of the PCL<sub>A<sub>2</sub>×1700</sub>CL<sub>2.5</sub>Acet depot including the surrounding tissue was resected en-bloc, fixed in 4 % paraformaldehyde (48 h at 4 °C), embedded in paraffin and sectioned at 6 μm. These sections were dewaxed and pre-treated with heat mediated antigen retrieval (Dako S1699, Glostrup, Denmark) at 90 °C for 20 min. Subsequently, sections were incubated with CD68 (1:100, Acris, Herford, Germany) for 60 min and visualized with PO link and label kit (Biogenex, Fremont, CA, USA), followed by a DAB (3,3'-diaminobenzidine) substrate. Sections were dried overnight and mounted with Vectamount (Vector Laboratories, Burlingame, CA, USA).

#### 2.14. Statistical analysis

Differences in μCT-data and histological scoring between the gel-injected and saline-injected knees were analyzed using type-1, two-tailed, paired t-tests. *In vitro* biocompatibility data were analyzed using one-way ANOVA with Bonferroni correction for multiple testing. All data are presented as mean ± SD, p-values <0.05 were considered significant.

### 3. Results and discussion

#### 3.1. Synthesis and characterization of the copolymers

<sup>1</sup>H NMR analysis showed the presence of characteristic peaks of PCL<sub>A<sub>2</sub>×750</sub>CL<sub>5.7</sub>TIB for methine protons of LA, methylene protons of PEG and methylene protons of CL at 5.25–4.95, 3.65–3.55 and 2.50–2.10 respectively (Figure A.1 in the appendices) [25,27]. A CL content of 87 wt% CL (CL/LA = 2.1 mol/mol) was found by <sup>1</sup>H NMR, which is slightly lower than the feed (90 wt%), a finding in accordance with previous data [27]. The extent of acylation (calculated by comparison of the integral of the aromatic peaks of TIB groups to the methylene peak of PEG) was 1.8, indicating 90 % TIB capping. The M<sub>n</sub> of PCL<sub>A<sub>2</sub>×750</sub>CL<sub>5.7</sub>TIB and PCL<sub>A<sub>2</sub>×1700</sub>CL<sub>2.5</sub>TIB (determined by <sup>1</sup>H NMR) was respectively 3400 g/mol and 3100 g/mol and

the  $M_n$  determined by GPC relative to PEG standards showed equal values (see Table 1).

### *3.2. Selecting a blend suitable for longitudinal in vivo gel visualization*

PCLA<sub>2×1700</sub>CL<sub>2.5</sub>TIB was synthesized, but appeared to be too hydrophobic and consequently did not form a homogeneous suspension in buffer. In order to obtain homogeneity, it was mixed with PCLA<sub>2×1700</sub>CL<sub>2.5</sub>Acet at different PCLA<sub>2×1700</sub>CL<sub>2.5</sub>Acet/PCLA<sub>2×1700</sub>CL<sub>2.5</sub>TIB ratios (25/75 w/w, 50/50 w/w and 75/25 w/w; all 25 wt% solid content).  $\mu$ CT scanning (Table 2) revealed that of these three different blends, only the 75/25 PCLA<sub>2×1700</sub>CL<sub>2.5</sub>Acet/PCLA<sub>2×1700</sub>CL<sub>2.5</sub>TIB blend formed a homogeneous suspension. The acetyl-/TIB-capped polymer ratio slightly influenced attenuation (higher TIB-ratios led to a higher attenuation). Based on the minor differences in attenuation combined with the formation of a heterogeneous blend, the 75/25 PCLA<sub>2×1700</sub>CL<sub>2.5</sub>Acet/PCLA<sub>2×1700</sub>CL<sub>2.5</sub>TIB blend was injected i.a. However, the  $\mu$ CT scan revealed that radiopacity of this blend was too low for longitudinal *in vivo* visualization. In order to be able to inject a homogeneous blend and follow it by  $\mu$ CT over time, a blend with a higher wt% of TIB was used, which was obtained by TIB capping of a triblock copolymer with the same PEG molecular weight but with a shorter PCLA chains (PCLA<sub>2×750</sub>CL<sub>5.7</sub>TIB). This polymer was blended with PCLA<sub>2×1700</sub>CL<sub>2.5</sub>Acet and all PCLA<sub>2×1700</sub>CL<sub>2.5</sub>Acet/PCLA<sub>2×750</sub>CL<sub>5.7</sub>TIB blends (25/75, 50/50, 75/25) were homogenous. Importantly, the attenuation greatly increased as compared to the blends containing PCLA<sub>2×1700</sub>CL<sub>2.5</sub>TIB. Based on the good attenuation and homogeneity, the blend containing the highest TIB content (75 %) was injected i.a. and was indeed well visible. This blend is therefore suitable for longitudinal  $\mu$ CT visualization and all following experiments were consequently performed using this blend.

### *3.3. Rheological properties of 25 wt% blend (25/75)*

The PCLA<sub>2×1700</sub>CL<sub>2.5</sub>Acet/PCLA<sub>2×750</sub>CL<sub>5.7</sub>TIB (25/75) blend of 25 wt% in buffer was a gel at temperatures below 10–15 °C and rapidly phase-separated at higher temperatures (as seen on the  $\mu$ CT images). This behavior is different from the behavior of PCLA<sub>2×1700</sub>CL<sub>2.5</sub>Acet only of 25 wt% in buffer and is likely due to the hydrophobicity of the TIB moieties as also observed

for hexanoyl-capped PCLA-PEG-PCLA [27]. However, the cold PCLA<sub>2×1700</sub>CL<sub>2.5</sub>Acet/PCLA<sub>2×750</sub>CL<sub>5.7</sub>TIB gel could be manually injected through a 27 G needle (normally used for i.a. injection into a rat knee) and DMA analysis confirmed that a force of 5.8 N was required to expel the gel from the syringe, which is slightly higher than the force required to expel air or PCLA<sub>2×1700</sub>CL<sub>2.5</sub>Acet dispersion (~4 °C) from the syringe (1.5 and 1.8 N, respectively).

**Table 2:**  $\mu$ CT analysis of *in vitro* scanned blends with different polymer compositions (PCLA<sub>2×1700</sub>CL<sub>2.5</sub>TIB vs PCLA<sub>2×750</sub>CL<sub>5.7</sub>TIB) and acetyl-/TIB-capped ratios.

<i>Polymer blend</i> ( <i>Acetyl-/TIB-capped ratio</i> )	Attenuation (a.u.)	Homogeneity <sup>a)</sup>	Intra-articular visibility <sup>b)</sup>
PCLA <sub>2×1700</sub> CL <sub>2.5</sub> Acet/ PCLA <sub>2×1700</sub> CL <sub>2.5</sub> TIB (75/25)	25.0	+	too low
PCLA <sub>2×1700</sub> CL <sub>2.5</sub> Acet/ PCLA <sub>2×1700</sub> CL <sub>2.5</sub> TIB (50/50)	30.4	+/-	n.t.
PCLA <sub>2×1700</sub> CL <sub>2.5</sub> Acet/ PCLA <sub>2×1700</sub> CL <sub>2.5</sub> TIB (25/75)	35.8	-	n.t.
PCLA <sub>2×1700</sub> CL <sub>2.5</sub> Acet/ PCLA <sub>2×750</sub> CL <sub>5.7</sub> TIB (75/25)	39.3	+	n.t.
PCLA <sub>2×1700</sub> CL <sub>2.5</sub> Acet/ PCLA <sub>2×750</sub> CL <sub>5.7</sub> TIB (50/50)	58.3	+	n.t.
PCLA <sub>2×1700</sub> CL <sub>2.5</sub> Acet/ PCLA <sub>2×750</sub> CL <sub>5.7</sub> TIB (25/75)	60.5	+	Good

a.u.: arbitrary unit.

a) -: Heterogeneous; +/-: slight heterogeneous areas; + homogenous.

b) not tested.

To get more insight into the rheological properties of 25/75 PCLA<sub>2×1700</sub>CL<sub>2.5</sub>Acet/PCLA<sub>2×750</sub>CL<sub>5.7</sub>TIB (25 wt% in buffer), oscillatory stress experiments were performed (Figure 1). At 4 °C, the gel had a storage



modulus ( $G'$ ) of 350 Pa and a  $\tan \delta$  ( $G''/G'$ ) of 0.6 at an oscillatory stress below 200 Pa. However, at an oscillatory stress of around 250 Pa, the gel started to loosen and its  $G'$  decreased to  $<30$  Pa with an increase in  $\tan \delta$  to 5. After releasing and subsequently applying the same oscillatory stress, the exact same  $G'$  and  $\tan \delta$  patterns were found during subsequent stress applications. These findings indicate thixotropic behaviour of the gel and explain its injectability through a thin 27 G needle. Thixotropic behaviour of aqueous polyester/PEG temperature-responsive systems has not been reported yet, but is very similar to what was reported for thixotropic systems based on charged hydrogel microspheres [50]. In the sol state, the polyester/PEG copolymers form micelles with a hydrophobic polyester core and a hydrated PEG shell [22,26,39]. The flow in thixotropic systems is likely due to weakening/loosing interactions that exist between the particles.

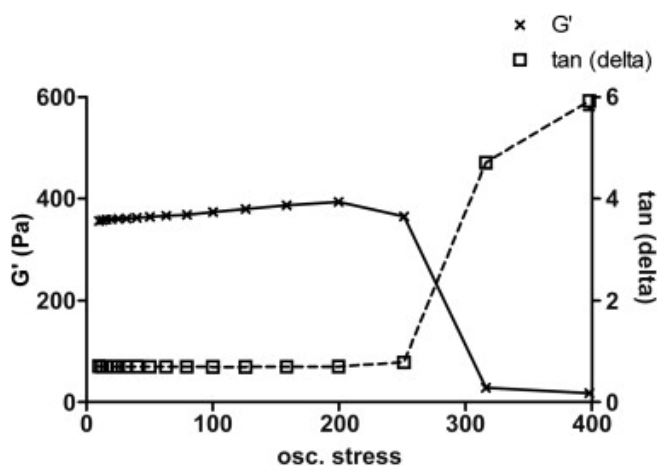


**Figure 1:** Stress sweeps of 25 wt% sample containing PCLA<sub>2×1700</sub>CL<sub>2.2</sub>Acet/PCLA<sub>2×750</sub>CL<sub>5.7</sub>TIB (25/75) at 4 °C. Three consecutive measurements ( $<30$  s between measurements) were performed at 1 Hz.

### 3.4. *In vitro* degradation behaviour of the 25 wt% blend (25/75)

Upon incubation of PCLA<sub>2×1700</sub>CL<sub>2.5</sub>Acet/PCLA<sub>2×750</sub>CL<sub>5.7</sub>TIB blend of 25 wt% in PBS buffer (pH 7.4, 37 °C), a 20 wt% decrease in wet weight was observed during the first 2 hours, which was not accompanied by loss in dry weight. Most likely, phase-separation of the gel into a polymer-rich and polymer poor phase occurred without degradation and/or dissolution of the triblock copolymers. During the next 30-40 days of incubation, a linear decrease in wet weight from 80 to 50 wt% was observed, accompanied by a

10 % decrease in dry weight. Thereafter, wet and dry weight stabilized at 50 % and 90 %, respectively, until day 80. Then, both wet and dry weight dropped substantially at a constant rate until complete degradation at 130-140 days (Figure 2). These findings are very similar to the *in vitro* degradation previously reported for acyl-capped PCLA-PEG-PCLA blends [27].

The drop in volume could be depicted accurately using  $\mu$ CT. Also, the changes in dry weight correlated well with the attenuation values acquired using  $\mu$ CT; samples containing 90-100 % of the initial dry weight showed an attenuation of  $60.7 \pm 3.5$  whereas for samples containing  $< 50$  % of the initial dry weight, this value dropped to  $36.6 \pm 2.2$ . These findings prove that  $\mu$ CT is indeed a useful surrogate for longitudinal follow-up of gel degradation kinetics.

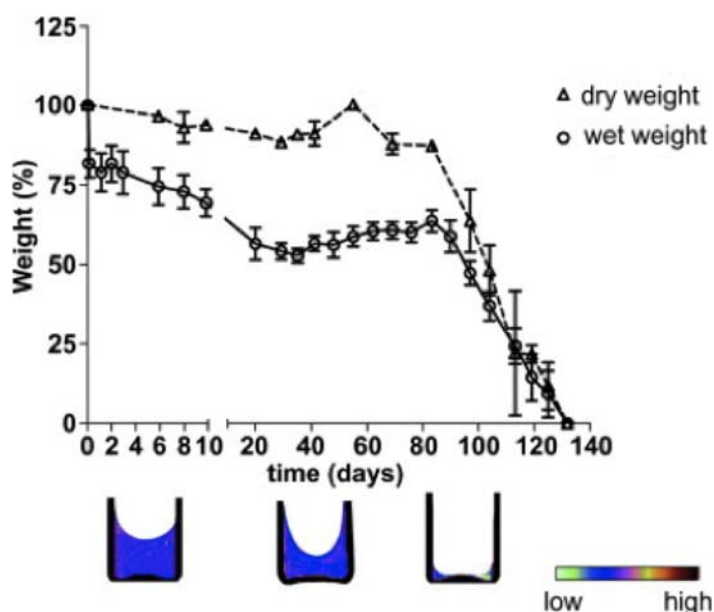


**Figure 2:** *In vitro* degradation of gels composed of PCLA<sub>2×1700</sub>CL<sub>2.2</sub>Acet/PCLA<sub>2×750</sub>CL<sub>5.7</sub>TIB blends (25 wt% in buffer) presented as loss [%] of wet (n = 6) and dry weight (n = 2) over time. Experiments were performed in phosphate buffer at 37 °C. Under the graph, representative  $\mu$ CT images are depicted for the corresponding time points on the x-axis, showing a decline in volume and attenuation (see color scheme) during degradation.

The  $M_n$  of the residual polymer mixture of PCLA<sub>2×1700</sub>CL<sub>2.5</sub>Acet/PCLA<sub>2×750</sub>CL<sub>5.7</sub>TIB gels (GPC analysis) as well as the copolymer composition (<sup>1</sup>H NMR analysis) remained constant during the entire duration of *in vitro*

degradation (data not shown). This demonstrates that degradation of the gel took place through polymer dissolution and not by chemical polymer degradation, which is in line with our previous data on other acyl-capped PCLA-PEG-PCLA systems [27].

### *3.5. Subcutaneous degradation of the 25 wt% blend (25/75 Acet/TIB)*

Upon s.c. injection of 25 wt% PCLA<sub>2×1700</sub>CL<sub>2.5</sub>Acet, a depot was formed immediately that could be palpated easily. Total gel volume remained stable for 2 weeks, after which the volume started to decrease and complete degradation was observed in a range of 4-12 weeks. Although these data give a good indication of *in vivo* gelation and degradation kinetics, this method lacks accuracy on quantification and no distinction could be made between gel volume and possible fibrous tissue present at the injection site. Also, no longitudinal details about the type of degradation (e.g., surface or bulk erosion, loss in wet or dry weight) could be obtained using this method. In order to facilitate reliable and accurate longitudinal *in vivo* degradation data, the PCLA<sub>2×1700</sub>CL<sub>2.5</sub>Acet/PCLA<sub>2×750</sub>CL<sub>5.7</sub>TIB blend was used for the rest of the degradation experiments. PCLA<sub>2×1700</sub>CL<sub>2.5</sub>Acet/PCLA<sub>2×750</sub>CL<sub>5.7</sub>TIB showed a 25 % drop in volume within the first day after s.c. injection, while attenuation (proportional to the total amount of TIB-polymer present in the gel) remained stable during this phase (Figure 3). This is in line with our *in vitro* observations of early phase separation in a polymer-rich and a polymer-poor phase (Figure 2). Subsequently, a decline in attenuation was observed between day 1 and day 21, while the volume of the gel hardly changed during this period (which is quite similar to the findings on s.c. degradation of PCLA<sub>2×1700</sub>CL<sub>2.5</sub>Acet where no volume changes were found during the first 2 weeks). This indicates that the polymers dissolved while wet volume was maintained. Subsequently, attenuation stabilized at a value of 20 while the gel volume decreased slowly, indicating a gradual gel degradation with equal degradation rates for wet and dry weight. The s.c. gel degradation followed a pattern with regions of high attenuation in the center surrounded by lower attenuation in the peripheral regions. This indicates that degradation occurs mainly at the surface while the polymer within the center of the depot remained unchanged, a phenomenon that has been shown before for other biomaterials implanted in animals [51,52,53].

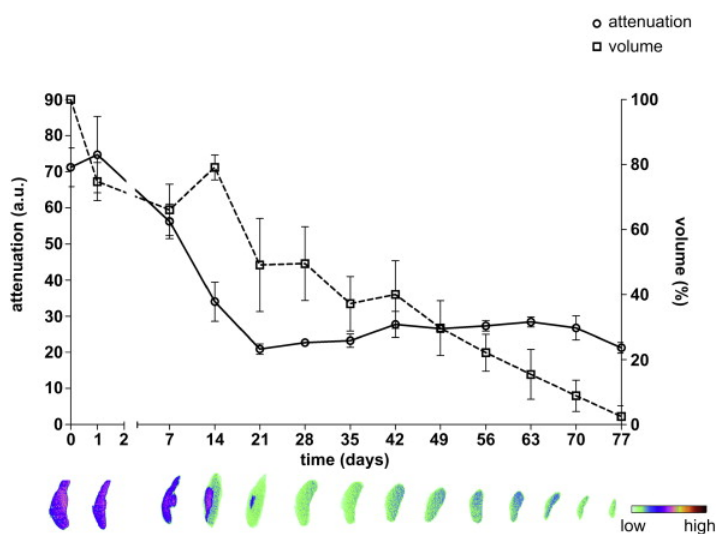


**Figure 3:** Volume [%] and attenuation [arbitrary unit] changes over time following s.c. injection of 25% PCLA<sub>2×1700</sub>CL<sub>2.5</sub>Acet/PCLA<sub>2×750</sub>CL<sub>5.7</sub>TIB blend (n = 4). For each time point, representative CT-images of the s.c. depots are depicted under the graph, with the color representing the attenuation of the gel.

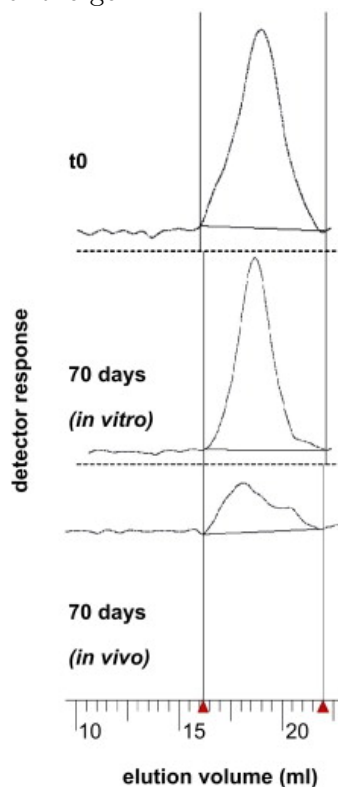


**Figure 4:** GPC chromatograms of the PCLA<sub>2×1700</sub>CL<sub>2.5</sub>Acet/PCLA<sub>2×750</sub>CL<sub>5.7</sub>TIB depots in time *in vitro* and *in vivo*. No changes were observed during the *in vitro* degradation, while *in vivo* a broadening of the polymer peak occurred which indicates shorter chain lengths thus (active) polymer degradation.

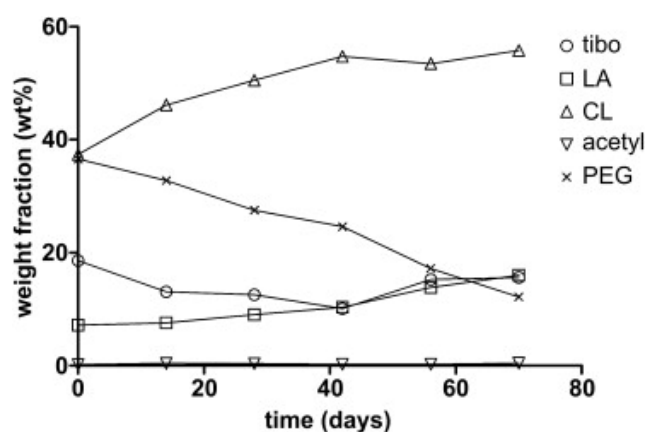


**Figure 5:** *In vivo* degradation of 25 wt% PCLA<sub>2</sub>×<sub>1700</sub>CL<sub>2.5</sub>Acet/PCLA<sub>2</sub>×<sub>750</sub>CL<sub>5.7</sub>TIB gels (25/75) after s.c. injection in time. The graph shows the weight fraction of CL, LA, TIB and acetyl, PEG, determined by <sup>1</sup>H NMR.

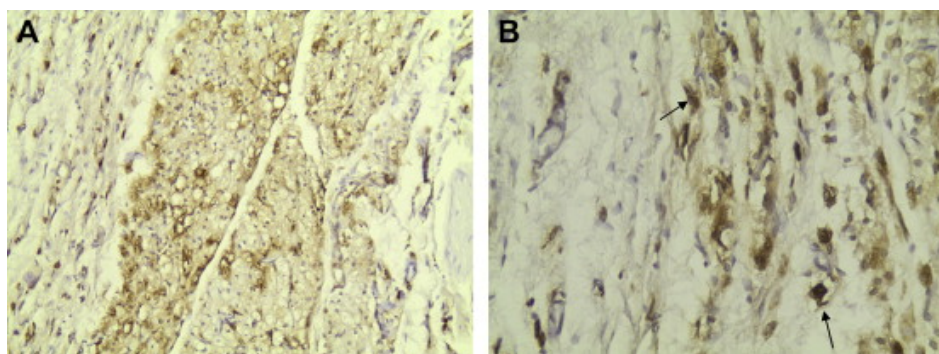


**Figure 6:** Representative images of immunohistochemistry CD68 staining of the excised subcutaneous depot at  $t = 12$  weeks. 6A shows macrophage infiltration (deep brown staining), surrounded by fibrous tissue at the site of the depot, indicating active degradation of the gel *in vivo* (magnification 10×). 6B shows the same image in a higher magnification (20×); the dark arrows indicate macrophages.

GPC analysis showed that during *in vivo* gel degradation the peak of the polymer broadened towards longer retention times, hence shorter  $M_n$ 's, accompanied with an increase in PDI (Figure 4). This indicates the formation of polymer entities with shorter chain lengths, which is not in line with the findings for *in vitro* degradation. In addition, the composition of residual polymer determined by <sup>1</sup>H NMR significantly changed in time (Figure 5). The CL content increased from 37 wt% at day 0 to 56 wt% at day 75, and the LA weight fraction increased during the same time frame from 7 to 16 wt%. On the other hand, the PEG weight fraction decreased from 37 wt%

(day 0) to 12 wt% (day 75). These changes in composition are likely due to chain scission preferentially at the PEG-PCLA bonds and dissolution of PEG-rich chains [54], as also observed previously for structurally related gels [27]. This indicates that, opposed to *in vitro*, the *in vivo* degradation did not only take place by dissolution, but also by another (active) degradation mechanism [54-57]. Others have previously shown that macrophages secrete enzymes including lipase, known for catalyzing PCL and PLLA degradation [51,52]. Immunohistochemistry on the excised s.c. PCLA<sub>2×1700</sub>CL<sub>2.5</sub>Acet depots indeed showed positive CD68 staining, indicating macrophage infiltration (Figure 6). It is therefore very likely that enzyme-catalyzed degradation also played a significant role in the *in vivo* (active) degradation of our PCLA/PEG-based gels. TIB-content remained more or less stable over the course of degradation, proving that the attenuation changes observed by  $\mu$ CT were in fact due to gel degradation and not chain cleavage of the TIB-capped polymer.

### 3.6. I.a. injection of the 25 wt% blend (25/75 Acet/TIB)

Directly after i.a. injection of PCLA<sub>2×1700</sub>CL<sub>2.5</sub>Acet/PCLA<sub>2×750</sub>CL<sub>5.7</sub>TIB, the gel volume distributed to the supra-patellar pouch (Figure 7). After 8 days, 50 % of the initial injected volume was still present within this pouch and 25 % remained at day 14. At 3 weeks, traces of the depot were still visible but the signal was too weak for proper quantification and 4 weeks post-injection no gel could be detected. It is very important for a DDS that is specifically designed for i.a. application to stay within the injected joint for a period of time long enough to release the incorporated drug in a timescale where it can be effective for joint repair and/or pain relief. Although the PCLA<sub>2×1700</sub>CL<sub>2.5</sub>Acet/PCLA<sub>2×750</sub>CL<sub>5.7</sub>TIB blend could indeed be traced for a period of 3 weeks within the knee joint, complete degradation was much faster compared to s.c. application (~12 weeks). Multiple factors might contribute to this large difference. Most importantly, the geometry and size of the gel in the knee cavity are quite different from the confined s.c. environment. The injected i.a. volume is smaller and also, due to dispersion and mechanical loading in the joint the geometry is quite different with higher surface/volume ratio compared to s.c. application, leading to faster degradation. In addition the mechanical stress in the weight bearing joint

may even create smaller sequestered gel particles that subsequently become phagocytosed by macrophages. In case these particles become smaller than 5  $\mu\text{m}$  and stay detached from the larger gel-depot-mass, they could leave the joint with the normal physiological (daily) efflux of synovial fluid directly through gaps within the fenestrated synovial tissue [58]. While the results that were found for the i.a. injected  $\text{PCLA}_{2 \times 1700}\text{CL}_{2.5}\text{Acet}/\text{PCLA}_{2 \times 750}\text{CL}_{5.7}\text{TIB}$  blend are very promising and rendered good longitudinal visualization, quantification was more difficult. Firstly, i.a. dispersion of the gel makes volume and attenuation values less reliable compared to the s.c. depot. Secondly, differentiation between the  $\text{PCLA}_{2 \times 1700}\text{CL}_{2.5}\text{Acet}/\text{PCLA}_{2 \times 750}\text{CL}_{5.7}\text{TIB}$  blend and structures within the joint is hindered due to

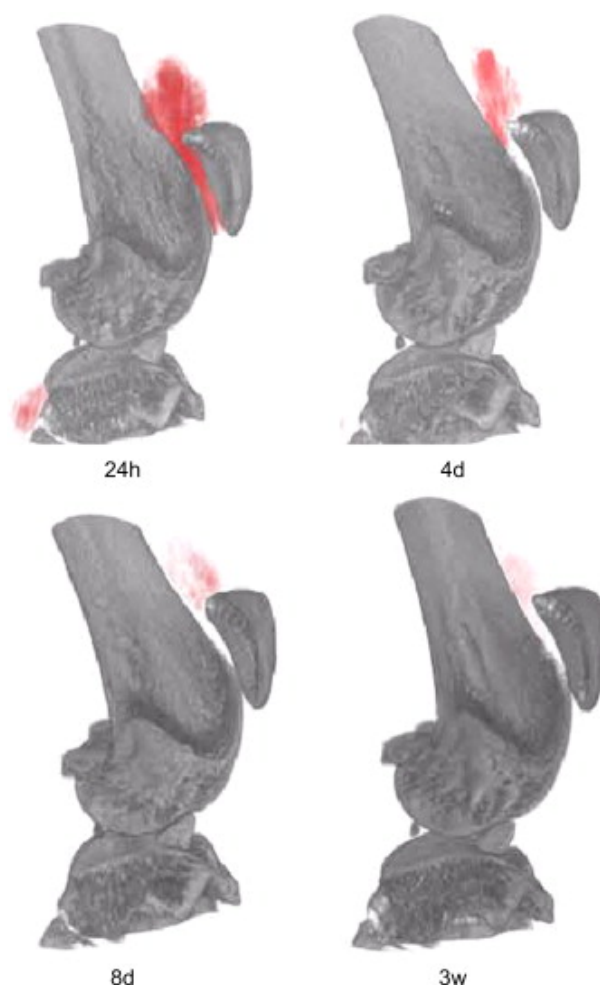


**Figure 7:** Reconstructed 3D  $\mu\text{CT}$  images of i.a. injected  $\text{PCLA}_{2 \times 1700}\text{CL}_{2.5}\text{Acet}/\text{PCLA}_{2 \times 750}\text{CL}_{5.7}\text{TIB}$ . The gel (red) was contained i.a. while slowly degrading over time. At the 4-week scan, the gel was no longer visible.

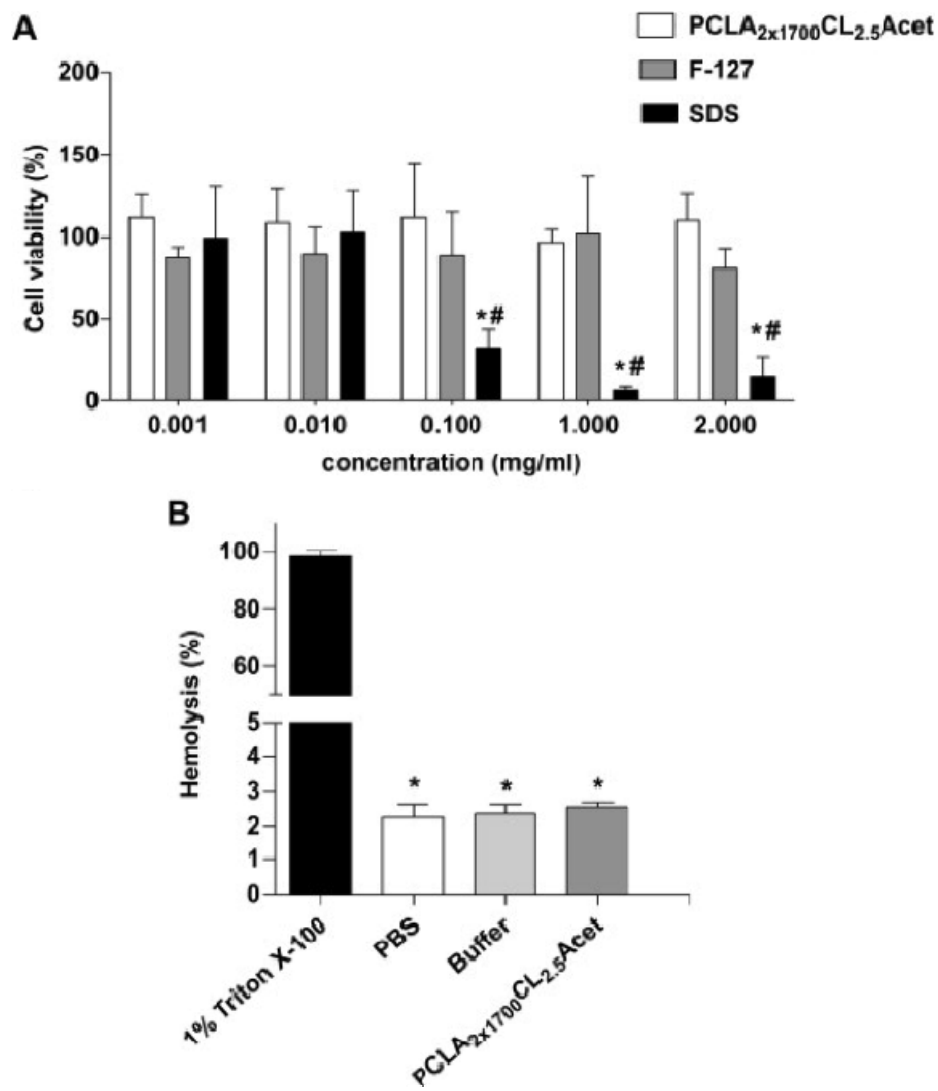


**Figure 8:** *In vitro* PCLA<sub>2x1700</sub>CL<sub>2.5</sub>Acet biocompatibility. 8A shows the viability of primary equine chondrocytes after addition of PCLA<sub>2x1700</sub>CL<sub>2.5</sub>Acet compared to positive control (F-127) and negative control (SDS) detected by AlamarBlue assay. Primary equine chondrocytes cultured with culture medium only served as a control and were set as 100% viability (n = 4). Values are depicted as mean±SD, \*  $p < 0.05$  vs. PCLA<sub>2x1700</sub>CL<sub>2.5</sub>Acet, #  $p < 0.05$  vs. F-127. 8B shows the hemolytic activity of PCLA<sub>2x1700</sub>CL<sub>2.5</sub>Acet (gel) and its buffer. PBS was set as a negative control while 1% Triton X-100 was set as a positive control (n = 3). \*  $p < 0.05$  vs. 1 % Triton X-100.

similar attenuations most likely leading to an underestimation of the amount of gel at later time points. Despite this, the i.a. degradation data clearly show that our gel has the capacity to remain within the joint for a period of time that, to our knowledge, has not been shown before for any other gelling systems [11].



### 3.7. *In vitro* cytocompatibility of $PCLA_{2 \times 1700}CL_{2.5}Acet$

In terms of cytocompatibility and *in vivo* biocompatibility, we are interested in the purest form of the gel ( $PCLA_{2 \times 1700}CL_{2.5}Acet$ ) since this is the formulation that would eventually be used for i.a. treatment and is representative for the acyl-capped PCLA-PEG-PCLA family. Also, the TIB-group might have an (negative) effect on cytocompatibility and/or i.a.

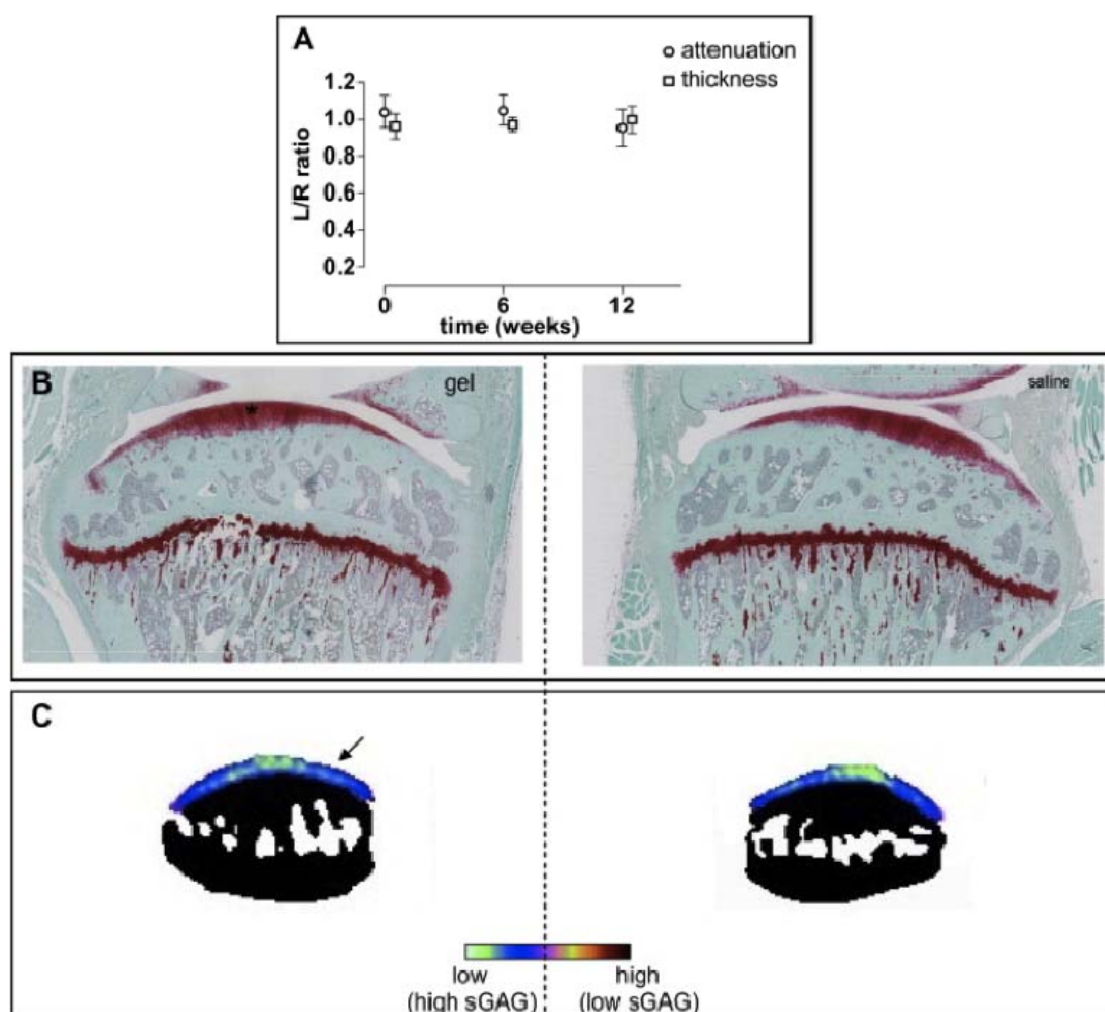


**Figure 9:** Tolerability of the gels after intra-articular administration. 9A shows a graph representing left (gel)-to-right (saline) ratio of patellar cartilage attenuation and thickness at 3 time points ( $n = 10$ ). 9B shows representative histological images of the tibia plateau (\* indicating the cartilage). 9C shows  $\mu$ CT images (patella) of 25 wt%  $PCLA_{2 \times 1700}CL_{2.5}Acet$ -injected (left images) and saline-injected (right images) knees 12 weeks after injection (arrow indicating the cartilage); no changes in cartilage thickness and attenuation occurred (see color scheme; a low attenuation represents high sGAGs thus good cartilage quality).

biocompatibility. Therefore, primary equine chondrocytes were incubated with PCLA<sub>2×1700</sub>CL<sub>2.5</sub>Acet (up to 2 mg/ml). The viability of the cells was not affected when compared to medium only or F-127 (negative control). Also, no differences in hemolytic activity were observed for erythrocytes incubated with PCLA<sub>2×1700</sub>CL<sub>2.5</sub>Acet (in buffer) or its buffer alone at body temperature (37 °C). The results on viability and hemolytic activity prove good cytocompatibility of the gel (Figure 8). Previously, similar results were found for uncapped polymers [59] and our findings demonstrate that cytocompatibility of the polymers was not jeopardized by capping acetyl groups.

### 3.8. I.a. biocompatibility of PCLA<sub>2×1700</sub>CL<sub>2.5</sub>Acet

Left knees were injected with 25 wt% PCLA<sub>2×1700</sub>CL<sub>2.5</sub>Acet; right knees received a saline injection and served as a control (n = 10, minus n = 1 due to incomplete Hexabrix influx). No toxic responses such as joint redness/swelling or changed locomotion occurred during the entire 12-weeks follow-up period in neither gel injected nor control knees. At 0, 6 and 12 weeks post-injection the patellar cartilage did not show any significant thickness nor attenuation differences with the contralateral control side (Figure 9A). Histology of the joint samples after 12 weeks (n = 10) confirmed these findings (Figure 9B); GAG-depletion score for the gel injected knees was 13±7 % vs. 10±3 % for the control knees and no structural changes were seen (0 %). These findings show that the PCLA<sub>2×1700</sub>CL<sub>2.5</sub>Acet gel is safe for i.a. use.

## 4. Conclusion

Acyl-capped PCLA-PEG-PCLA polymers form a hydrogel depot that degrades gradually both s.c. and i.a. *In vivo* degradation of the gel depot differed from *in vitro* degradation and was driven both by dissociation and active degradation by macrophages. The desirable degradation kinetics combined with the excellent i.a. biocompatibility makes these gels suitable for i.a. drug delivery.

## Acknowledgments

Mike de Leeuw, Dr. Theo Flipsen and Dr. Leo G.J. de Leede from InGell

Labs are gratefully acknowledged for their support and valuable discussion. This research was partly supported by a grant of the ministry of Economic Affairs, The Netherlands (BMM/TerM P2.02).

## References

- [1] Odding E, Valkenburg HA, Stam HJ, Hofman A. Determinants of locomotor disability in people aged 55 years and over: the Rotterdam study. *Eur J Epidemiol* 2001;17:1033-1041.
- [2] Recommendations for the medical management of osteoarthritis of the hip and knee: 2000 update. American College of Rheumatology subcommittee on osteoarthritis guidelines. *Arthritis Rheum* 2000;43:1905-1915.
- [3] Roth SH, Anderson S. The NSAID dilemma: managing osteoarthritis in high-risk patients. *Phys Sportsmed* 2011;39:62-74.
- [4] Bahadir C, Onal B, Dayan VY, Gurer N. Comparison of therapeutic effects of sodium hyaluronate and corticosteroid injections on trapeziometacarpal joint osteoarthritis. *Clin Rheumatol* 2009;28:529-533.
- [5] Hunter DJ. In the clinic. Osteoarthritis. *Ann Intern med* 2007;147:ITC8-1-ITC8-16.
- [6] Ayral X. Injections in the treatment of osteoarthritis. *Best Pract Res Clin Rheumatol* 2001;15:609-626.
- [7] Bellamy N, Campbell J, Robinson V, Gee T, Bourne R, Wells G. Intra-articular corticosteroid for treatment of osteoarthritis of the knee. *Cochrane Database Syst Rev* 2006:CD005328.
- [8] Charalambous CP, Tryfonidis M, Sadiq S, Hirst P, Paul A. Septic arthritis following intra-articular steroid injection of the knee - a survey of current practice regarding antiseptic technique used during intra-articular steroid injection of the knee. *Clin Rheumatol* 2003;22 :386-390.
- [9] Gerwin N, Hops C, Lucke A. Intra-articular drug delivery in osteoarthritis. *Adv Drug Deliv Rev* 2006;58:226-242.
- [10] Edwards SH. Intra-articular drug delivery: the challenge to extend drug residence time within the joint. *Vet J* 2011;190:15-21.
- [11] Larsen C, Ostergaard J, Larsen SW, Jensen H, Jacobsen S, Lindegaard C, et al. Intra-articular depot formulation principles: role in the management of postoperative pain and arthritic disorders. *J Pharm Sci* 2008;97:4622-4654.
- [12] Woodle MC. Surface-modified liposomes: assessment and characterization for increased stability and prolonged blood circulation. *Chem Phys Lipids* 1993;64:249-262.
- [13] Immordino ML, Brusa P, Arpicco S, Stella B, Dosio F, Cattel L. Preparation,

- characterization, cytotoxicity and pharmacokinetics of liposomes containing docetaxel. *J Control Release* 2003;91:417-429.
- [14] Thakkar H, Sharma RK, Mishra AK, Chuttani K, Murthy RS. Celecoxib incorporated chitosan microspheres: *in vitro* and *in vivo* evaluation. *J Drug Target* 2004;12:549-557.
- [15] Shi Y, Li LC. Current advances in sustained-release systems for parenteral drug delivery. *Expert Opin Drug Deliv* 2005;2:1039-1058.
- [16] Sharma A, Sharma US. Liposomes in drug delivery: progress and limitations. *Int J Pharm* 1997;154:123-140.
- [17] Larsen SW, Frost AB, Ostergaard J, Thomsen MH, Jacobsen S, Skonberg C, et al. *In vitro* and *in vivo* characteristics of celecoxib *in situ* formed suspensions for intra-articular administration. *J Pharm Sci* 2011;100:4330-4337.
- [18] Chen ZP, Liu W, Liu D, Xiao YY, Chen HX, Chen J, et al. Development of brucine-loaded microsphere/thermally responsive hydrogel combination system for intra-articular administration. *J Control Release* 2012;162:628-635.
- [19] van Tomme SR, Storm G, Hennink WE. *In situ* gelling hydrogels for pharmaceutical and biomedical applications. *Int J Pharm* 2008;355:1-18.
- [20] Vermonden T, Censi R, Hennink WE. Hydrogels for protein delivery. *Chem Rev* 2012;112:2853-2888.
- [21] Jeong B, Kibbey MR, Birnbaum JC, Won YY, Gutowska A. Thermogelling biodegradable polymers with hydrophilic backbones: PEG-*g*-PLGA. *Macromolecules* 2000;33:8317-8322.
- [22] Yu L, Ding JD. Injectable hydrogels as unique biomedical materials. *Chem Soc Rev* 2008;37:1473-1481.
- [23] Ko DY, Shinde UP, Yeon B, Jeong B. Recent progress of *in situ* formed gels for biomedical applications. *Prog Polym Sci* 2013;38:672-701.
- [24] Bonacucina G, Cespi M, Mencarelli G, Giorgioni G, Palmieri GP. Thermosensitive self-assembling block copolymers as drug delivery systems. *Polymers* 2011;3:779-811.
- [25] Jo S, Kim J, Kim SW. Reverse thermal gelation of aliphatically modified biodegradable triblock copolymers. *Macromol Biosci* 2006;6:923-928.
- [26] Yu L, Chang G, Zhang H, Ding J. Temperature-induced spontaneous sol-gel transitions of poly(D,L-lactic acid-*co*-glycolic acid)-*b*-poly(ethylene glycol)-*b*-poly(D,L-lactic acid-*co*-glycolic acid) triblock copolymers and their end-capped derivatives in

- water. *J Polym Sci A Polym Chem* 2007;45:1122-1133.
- [27] Petit A, Muller B, Bruin P, Meyboom R, Piest M, Kroon-Batenburg LM, et al. Modulating rheological and degradation properties of temperature-responsive gelling systems composed of blends of PCLA-PEG-PCLA triblock copolymers and their fully hexanoyl-capped derivatives. *Acta Biomater* 2012;8:4260-4267.
- [28] Butoescu N, Seemayer CA, Palmer G, Guerne PA, Gabay C, Doelker E, et al. Magnetically retainable microparticles for drug delivery to the joint: efficacy studies in an antigen-induced arthritis model in mice. *Arthritis Res Ther* 2009;11:R72.
- [29] Mountziaris PM, Sing DC, Mikos AG, Kramer PR. Intra-articular microparticles for drug delivery to the TMJ. *J Dent Res* 2010;89:1039-1044.
- [30] Horisawa E, Kubota K, Tuboi I, Sato K, Yamamoto H, Takeuchi H, et al. Size-dependency of DL-lactide/glycolide copolymer particulates for intra-articular delivery system on phagocytosis in rat synovium. *Pharm Res* 2002;19:132-139.
- [31] Mottu F, Rufenacht DA, Doelker E. Radiopaque polymeric materials for medical applications. Current aspects of biomaterial research. *Invest Radiol* 1999;34:323-335.
- [32] Zaharia C, Zecheru T, Moreau MF, Pascaretti-Grizon F, Mabilleanu G, Marculescu B, et al. Chemical structure of methylmethacrylate-2-[2',3',5'-triiodobenzoyl]oxoethyl methacrylate copolymer, radio-opacity, *in vitro* and *in vivo* biocompatibility. *Acta Biomater* 2008;4:1762-1769.
- [33] Emans PJ, Saralidze K, Knetsch ML, Gijbels MJ, Kuijter R, Koole LH. Development of new injectable bulking agents: biocompatibility of radiopaque polymeric microspheres studied in a mouse model. *J Biomed Mater Res A* 2005;73:430-436.
- [34] Okamura M, Uehara H, Yamanobe T, Komoto T, Hosoi S, Kumazaki T. Synthesis and properties of radiopaque polymer hydrogels: polyion complexes of copolymers of acrylamide derivatives having triiodophenyl and carboxyl groups and p-styrene sulfonate and polyallylamine. *J Mol Struct* 2000;554:35-45.
- [35] Li JJ. Name reactions: a collection of detailed reaction mechanisms (3rd Ed.) Springer, New York (2006).
- [36] Benzina A, Krufft MA, van der Veen FH, Bar FH, Blezer R, Lindhout T et al. A versatile three-iodine molecular building block leading to new radiopaque polymeric biomaterials. *J Biomed Mater Res* 1996;32:459-466.
- [37] Mottu F, Rufenacht DA, Laurent A, Doelker E. Iodine-containing cellulose mixed esters as radiopaque polymers for direct embolization of cerebral aneurysms and arteriovenous malformations. *Biomaterials* 2002;23:121-131.

- [38] Saralidze K, Aldenhoff YBJ, Knetsch MLW, Koole LH. Injectable polymeric microspheres with X-ray visibility. Preparation, properties, and potential utility as new traceable bulking agents. *Biomacromolecules* 2003;4:793-798.
- [39] Yu L, Zhang H, Ding J. A subtle end-group effect on macroscopic physical gelation of triblock copolymer aqueous solutions. *Angew Chem Int Ed Engl* 2006;45:2232–2235.
- [40] Fan Y, Nishida H, Shirai Y, Endo T. Thermal stability of poly (L-lactide); influence of end protection by acetyl group. *Polym Degrad Stab* 2004;84:143-149.
- [41] Abe H, Takahashi N, Kim KJ, Mochizuki M, Doi Y. Effects of residual zinc compounds and chain-end structure on thermal degradation of poly( $\epsilon$ -caprolactone). *Biomacromolecules* 2004;5:1480-1488.
- [42] McNeill IC, Leiper HA. Degradation studies of some polyesters and polycarbonates. 1. Polylactide - general features of the degradation under programmed heating conditions. *Polym Degrad Stab* 1985;11:267-285.
- [43] Siebelt M, Waarsing JH, Kops N, Piscaer TM, Verhaar JAN, Oei EHG et al. Quantifying osteoarthritic cartilage changes accurately using *in vivo* microCT arthrography in three etiologically distinct rat models. *J Orthop Res* 2011;29:1788-1794.
- [44] Piscaer TM, Waarsing JH, Kops N, Pavljasevic P, Verhaar JAN, van Osch GJVM, et al. *In vivo* imaging of cartilage degeneration using microCT-arthrography. *Osteoarthr Cartil* 2008;16:1011-1017.
- [45] Silvast TS, Jurvelin JS, Aula AS, Lammi MJ, Toyras J. Contrast agent-enhanced computed tomography of articular cartilage: association with tissue composition and properties. *Acta Radiol* 2009;50:78-85.
- [46] Silvast TS, Jurvelin JS, Lammi MJ, Toyras J. pQCT study on diffusion and equilibrium distribution of iodinated anionic contrast agent in human articular cartilage - associations to matrix composition and integrity. *Osteoarthr Cartil* 2009;17:26-32.
- [47] Waarsing JH, Day JS, Weinans H. An improved segmentation method for *in vivo* microCT Imaging. *J Bone Miner Res* 2004;19:1640-1650.
- [48] Mankin HJ, Dorfman H, Lippiello L, Zarins A. Biochemical and metabolic abnormalities in articular cartilage from osteo-arthritic human hips. II. Correlation of morphology with biochemical and metabolic data. *J Bone Joint Surg Am* 1971;53:523-537.
- [49] Pritzker KPH, Gay S, Jimenez SA, Ostergaard K, Pelletier JP, Revell PA, et al.

- Osteoarthritis cartilage histopathology: grading and staging. *Osteoarthr Cartil* 2006;14:13-29.
- [50] van Tomme SR, van Nostrum CF, Dijkstra M, de Smedt SC, Hennink WE. Effect of particle size and charge on the network properties of microsphere-based hydrogels. *Eur J Pharm Biopharm* 2008;70:522-530.
- [51] Seyednejad H, Gawlitta D, Kuiper RV, de Bruin A, van Nostrum CF, Vermonden T, et al. *In vivo* biocompatibility and biodegradation of 3D-printed porous scaffolds based on a hydroxyl-functionalized poly( $\epsilon$ -caprolactone). *Biomaterials* 2012;33:4309-4318.
- [52] Zeng J, Chen XS, Liang QZ, Xu XL, Jing XB. Enzymatic degradation of poly(L-lactide) and poly ( $\epsilon$ -caprolactone) electrospun fibers. *Macromol Biosci* 2004;4:1118-1125.
- [53] Gan Z, Yu D, Zhong Z, Liang Q, Jing X. Enzymatic degradation of poly ( $\epsilon$ -caprolactone)/poly(DL-lactide) blends in phosphate buffer solution. *Polymer* 1999;40:2859-2862.
- [54] Buwalda SJ, Dijkstra PJ, Calucci L, Forte C, Feijen J. Influence of amide versus ester linkages on the properties of eight-armed PEG-PLA star block copolymer hydrogels. *Biomacromolecules* 2010;11:224-232.
- [55] Yu L, Zhang Z, Zhang H, Ding J. Biodegradability and biocompatibility of thermoreversible hydrogels formed from mixing a sol and a precipitate of block copolymers in water. *Biomacromolecules* 2010;11:2169-2178.
- [56] Bramfeldt H, Sarazin P, Vermette P. Characterization, degradation, and mechanical strength of poly(D,L-lactide-*co*- $\epsilon$ -caprolactone)-poly(ethylene glycol)-poly(D,L-lactide-*co*- $\epsilon$ -caprolactone). *J Biomed Mater Res A* 2007;83:503-511.
- [57] Jeong B, Bae YH, Kim SW. *In situ* gelation of PEG-PLGA-PEG triblock copolymer aqueous solutions and degradation thereof. *J Biomed Mater Res* 2000;50:171-177.
- [58] Knight AD, Levick JR. The influence of blood pressure on trans-synovial flow in the rabbit. *J Physiol* 1984; 349:27-42.
- [59] Zhang ZNJ, Chen L, Yu L, Xu J, Ding J. Biodegradable and thermoreversible PCLA-PEG-PCLA hydrogel as a barrier for prevention of post-operative adhesion. *Biomaterials* 2011;32:4725-4736.



## Appendices

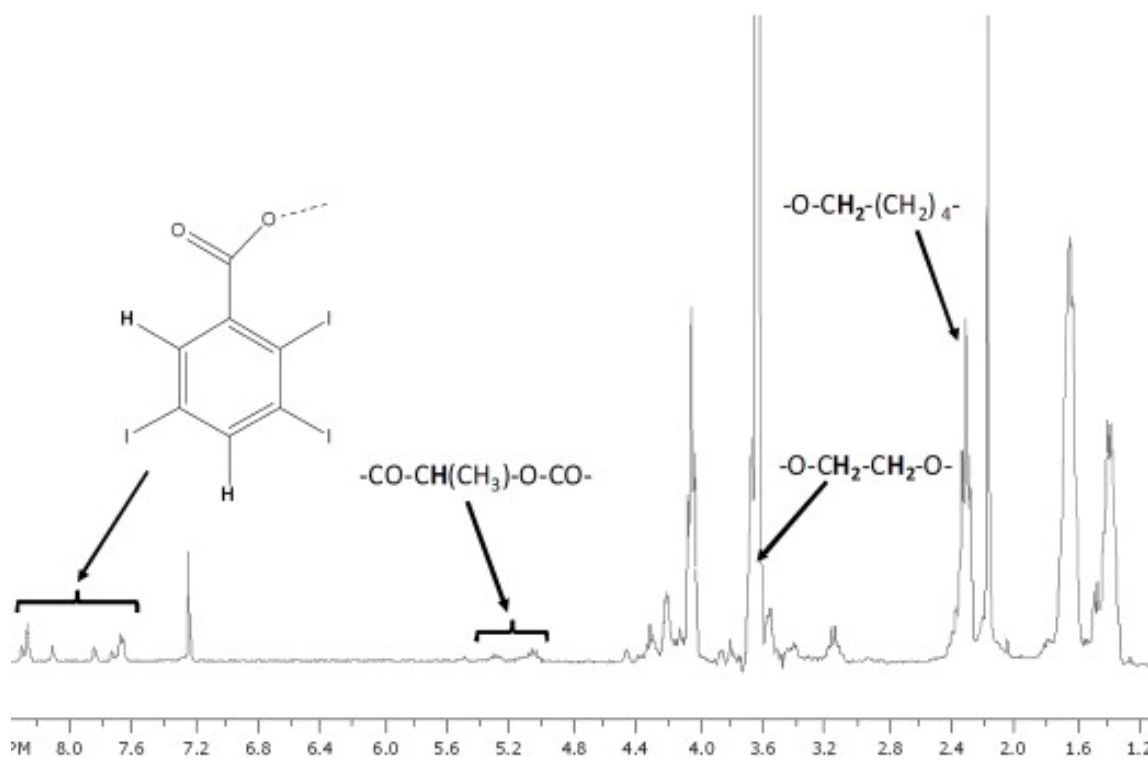


**Figure A.1:** <sup>1</sup>H NMR spectra of TIB-capped PCLA-PEG-PCLA in CDCl<sub>3</sub>. The characteristic peaks at 5.25–4.95, 3.65–3.55, 2.50–2.10 and 8.40–7.60 ppm correspond to methine protons of LA, methylene protons of PEG, methylene protons of CL [25], and aromatic protons of TIB-end groups [36,37,38], respectively.

Chapter 4

Radiopaque gel



## CHAPTER 5

# Celecoxib-loaded acetyl-capped PCLA- PEG-PCLA thermogels: *in vitro* and *in vivo* release behaviour and intra-articular biocompatibility

Audrey Petit<sup>1,2\*</sup>, Marjan J Sandker<sup>3\*</sup>, Benno Müller<sup>1</sup>, Ronald Meyboom<sup>1</sup>, Paul van Midwoud<sup>1</sup>, Everaldo M Redout<sup>4</sup>, Chris H van de Lest<sup>4</sup>, Sytze J Buwalda<sup>2</sup>, Leo GJ de Leede<sup>1</sup>, Tina Vermonden<sup>2</sup>, Robbert Jan Kok<sup>2</sup>, Harrie Weinans<sup>5,6</sup> and Wim E Hennink<sup>2</sup>

<sup>1</sup> InGell Labs BV, Groningen, The Netherlands

<sup>2</sup> Department of Pharmaceutics, Utrecht Institute for Pharmaceutical Sciences, Utrecht University, Utrecht, The Netherlands

<sup>3</sup> Department of Orthopaedics, Erasmus Medical Center, Rotterdam, The Netherlands

<sup>4</sup> Department of Equine Sciences, Faculty of Veterinary Medicine, Utrecht University, Utrecht, The Netherlands

<sup>5</sup> Department of Orthopaedics and Department of Rheumatology, UMC Utrecht, Utrecht, The Netherlands

<sup>6</sup> Department of Biomechanical Engineering, TU Delft, Delft, The Netherlands

\* *Authors with equal contribution*

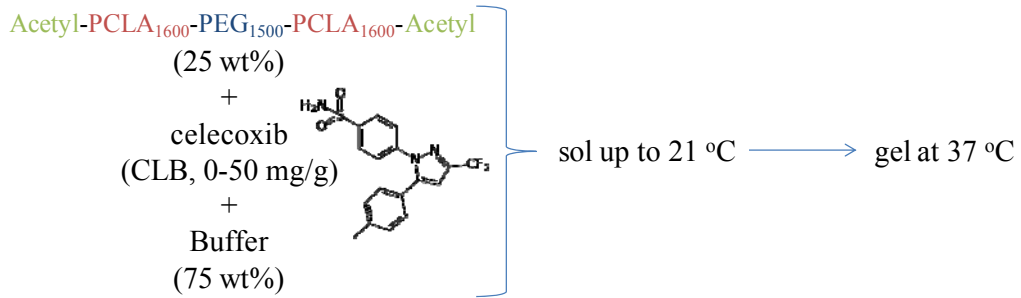
Submitted

Chapter 5

**IVIVC in rats**

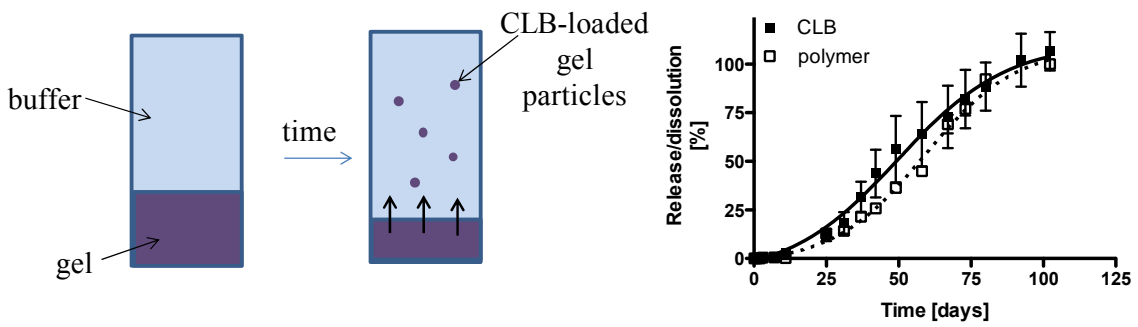
### **Abstract**

In this study, we investigated the *in vitro* and *in vivo* properties and performance of a celecoxib-loaded hydrogel based on a fully acetyl-capped PCLA-PEG-PCLA triblock copolymer. Blends of different compositions of celecoxib, a drug used for pain management in osteoarthritis, and the acetyl-capped PCLA-PEG-PCLA triblock copolymer were mixed with buffer to yield temperature-responsive gelling systems. These systems containing up to 50 mg celecoxib per gram polymer, were sols at room temperature and converted into immobile gels at 37 °C. *In vitro*, release of celecoxib started after a ~10 days lag phase followed by a sustained release of ~90 days. Celecoxib release was proven to be mediated by polymer dissolution from the gels. *In vivo* (subcutaneous injection in rats) experiments showed an initial celecoxib release of ~30 % during the first 3 days followed by a sustained release of celecoxib for 4-8 weeks. The absence of a lag phase and the faster release seen *in vivo* were likely due to the enhanced celecoxib solubility in biological fluids and active degradation of the gel by macrophages. Finally, intra-articular biocompatibility of the 50 mg/g celecoxib-loaded gel was demonstrated using  $\mu$ CT-scanning, where no cartilage or bone changes were observed following injection into the knee joints of healthy rats. In conclusion, this study shows that celecoxib-loaded acetyl-capped PCLA-PEG-PCLA hydrogels form a safe drug delivery platform for sustained intra-articular release.



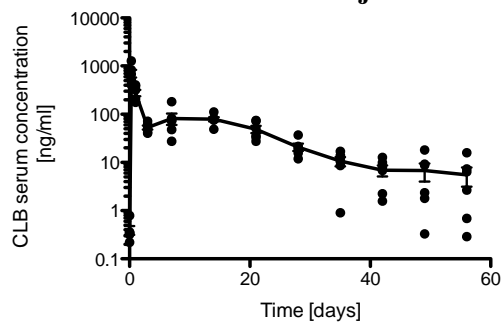
**In vitro at 37 °C**

*In vitro* release mediated by polymer dissolution due to physical interactions between CLB and PCLA



**In vivo**

after subcutaneous injection



## 1. Introduction

Celecoxib (Figure 1) is a non-steroidal anti-inflammatory drug (NSAID) and a selective inhibitor of cyclo-oxygenase-2 (COX-2), approved as Celebrex® for the pain management of, amongst others, rheumatic diseases and osteoarthritis [1]. Some authors even consider celecoxib to have anti-catabolic and/or even anabolic potential on cartilage, however, there is quite some conflicting data and further research is needed regarding this topic [2-4]. Celecoxib has a very low aqueous solubility ( $<1 \mu\text{g/ml}$ ) with a large apparent volume of distribution ( $>\sim 1 \text{ l/kg}$ ) due to its high plasma protein binding ( $\sim 97 \%$ ) [5]. Concerns have risen about the systemic toxicity of celecoxib, mainly on myocardial muscles [6], and consequently there is a need for formulations reducing its toxicity. One way to reach this goal is to develop formulations, which are able to locally release drugs for a prolonged period. These drug delivery systems (DDSs) ideally lead to therapeutically effective local concentrations while plasma concentrations remain below toxic level. Moreover, not only the exposure is targeted and localized, but also patient compliance is greatly improved compared to daily oral administration.

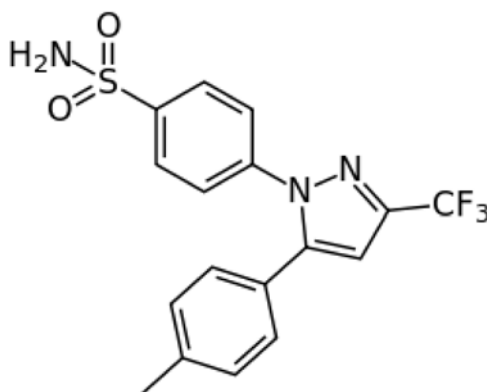


**Figure 1:** Chemical structure of celecoxib, a NSAID COX-2 inhibitor.

Other desired DDS properties are ease of injection, high encapsulation efficiency (preferably 100 %), and a low burst release to prevent high drug concentrations (and consequently possible toxic side effects) shortly after administration. In addition, the ideal DDS should have tunable release kinetics and show full recovery of the loaded drug. Injectable DDSs developed for the controlled release of celecoxib have been based up to now

mainly on micro/nano-particles composed of poly(lactide-*co*-glycolide) (PLGA) [7-12]. These systems show some limitations in encapsulation efficiency (as low as 50 %), burst release (up to 60 %), and recovery rates (down to 25 %), which all together hinder their clinical applicability [7-12]. Recently, highly concentrated solutions of celecoxib in PEG<sub>400</sub> (400 mg/ml) were used as *in situ* forming depots after injection in equine joint cavities [13]. Upon injection, PEG<sub>400</sub> is diluted in the synovial fluid of the joints and celecoxib subsequently precipitates/crystallizes. Its release is achieved by slow dissolution of the celecoxib precipitates/crystals, which is however difficult to predict and control and the crystals may harm the cartilage.

Temperature-responsive aqueous formulations of ABA triblock copolymers composed of PEG as middle block flanked by polyester blocks of diverse compositions, are systems that fulfil the aforementioned desired DDS properties [14-23]. Importantly, these gels offer the possibility of complete encapsulation of hydrophobic drugs with release kinetics that can be modulated [24-26]. Systems based on PLGA-PEG-PLGA loaded with paclitaxel were clinically evaluated up to Phase IIa in oncology for targeted delivery to the tumor via intralesional injection or placement into the tumor cavity [27]. Drug release from these systems is mediated by a combination of diffusion and chemical polymer degradation, which takes around six weeks (both *in vitro* and *in vivo*) [24-26]. For some applications, however, longer release times are required. To slow down hydrolysis and thereby increase the degradation time, PLGA blocks have been replaced by poly( $\epsilon$ -caprolactone-*co*-lactide) (PCLA) blocks. Indeed, gels based on PCLA-PEG-PCLA (depending on the ratio of caproyl units (CL) to lactoyl units (LA)) are more stable compared to PLGA-based gels. For instance, systems with PCLA blocks containing 70 mol% CL showed a complete degradation time of approximately six months [28,29]. Moreover, modification of the terminal hydroxyl groups of these triblock copolymers allowed modulation of mechanical properties and provided extended degradation time of temperature-responsive gelling systems made of these copolymers [15,16,19,30].

In this study, we investigated the feasibility of acetyl-capped PCLA-PEG-PCLA triblock copolymer-based temperature-responsive gelling systems as an intra-articular drug delivery system for celecoxib. We characterized the



systems (*in vitro* release and gel degradation), examined *in vivo* release kinetics of a subcutaneous injected formulation and the biocompatibility of the same formulation after intra-articular injection.

## **2. Experiments and protocols**

### *2.1. Materials*

Celecoxib was obtained from LC Laboratories, USA. TNF $\alpha$  was obtained from Ebioscience, Austria. Hexabrix 320<sup>®</sup>, a clinical iodine-based contrast agent, was obtained from Guerget, The Netherlands. All other chemicals were obtained from Aldrich and used as received.

### *2.2 Synthesis of acetyl-capped PCLA-PEG-PCLA*

The acetyl-capped PCLA-PEG-PCLA triblock copolymer used in this study was synthesized and characterized as described previously [16]. In short, in a three-neck round-bottom flask equipped with a Dean Stark trap and a condenser, PEG<sub>1500</sub> (50 g), L-lactide (22 g),  $\epsilon$ -caprolactone (88 g) and toluene (150 ml) were introduced and, while stirring, heated to reflux ( $\sim 140$  °C; i.e. the boiling point of toluene is 111 °C but that of the mixture is  $\sim 140$  °C) under nitrogen atmosphere. The solution was azeotropically dried by distilling off toluene/water ( $\sim 50$  vol% of the initial volume). Next, the solution was cooled to  $\sim 90$  °C and tin(II) 2-ethylhexanoate (5 mmol per mol PEG<sub>1500</sub>) was added. Ring-opening polymerization was carried out at 110-120 °C overnight under a nitrogen atmosphere. The solution was cooled to room temperature and dichloromethane (100 ml) and triethylamine (6 mol per mol PEG<sub>1500</sub>) were added. Then, the solution was cooled to 0 °C in an ice bath, and while stirring, an excess of acetyl chloride (10 g, ratio acetyl chloride/PEG = 4 mol/mol) was added drop wise and acylation was allowed to proceed for three hours. Next, dichloromethane was removed under vacuum at 60-65 °C, ethyl acetate (100 ml) was subsequently added and triethylamine hydrochloride salts were removed by filtration. The polymer was precipitated by adding a 1:1 mixture of hexane and diethyl ether (290 ml). Upon storage at -20 °C, the polymer separated as a waxy solid from which non-solvents containing unreacted monomers and the excess of acyl chloride could be decanted easily. The precipitated polymer was dried in

vacuo and obtained in yield of 85 %. The polymer was characterized by  $^1\text{H}$  NMR and GPC as previously described [15].

### 2.3. Miscibility of celecoxib in PEG<sub>1500</sub> and in PCLA-PEG-PCLA

Celecoxib, PEG<sub>1500</sub> and PCLA-PEG-PCLA were separately dissolved in ethyl acetate (300, 150 and 300 mg/ml, respectively). The solutions were mixed to prepare celecoxib/PEG<sub>1500</sub> mixtures with weight ratios between 10/90 and 80/20 w/w as well as celecoxib/PCLA-PEG-PCLA mixtures with weight ratios between 5/95 and 70/30 w/w. The solutions (1-10 ml) were transferred into 6-cm Petri dishes. Next, the solvent was removed under nitrogen flow for 48 hours. The thermal properties of the mixtures were analyzed by DSC (see paragraph 2.5).

### 2.4. Solubility of celecoxib in polymer/buffer systems

100 mg of celecoxib/PEG<sub>1500</sub> (10/90 w/w) mixture was added to 750  $\mu\text{l}$  phosphate buffer pH 7.4 (44 mM Na<sub>2</sub>HPO<sub>4</sub>, 9 mM NaH<sub>2</sub>PO<sub>4</sub>, 72 mM NaCl, 0.02 wt% NaN<sub>3</sub>). Similarly, 260 to 830 mg of celecoxib/PCLA-PEG-PCLA mixtures 10/90 to 80/20 were added to 750  $\mu\text{l}$  phosphate buffer to yield celecoxib-loaded aqueous PCLA-PEG-PCLA of 25 wt% gel formulations. Samples were vortexed for 1 min and then incubated at 4 °C for 48 hours. To check for possible presence of celecoxib crystals, the samples were investigated under a microscope (Nikon Eclipse TE2000U) and analyzed by X-ray diffractometry as described previously [16].

Celecoxib/PEG<sub>1500</sub>/buffer mixtures were further filtered with standard GPC/HPLC syringe filters (0.45  $\mu\text{m}$ ), and the amount of celecoxib in the transparent filtrates was measured by UPLC (see Paragraph 2.8).

### 2.5. Differential Scanning Calorimetry (DSC) analysis

The thermal properties of celecoxib and the polymers (PEG<sub>1500</sub> and PCLA-PEG-PCLA) as well as those of the celecoxib/polymer mixtures were determined by DSC (TA Instruments DSC Q2000 apparatus). Samples of ~10 mg in closed aluminum pans were heated under nitrogen flow at a rate of 50 ml/min from room temperature to 170 °C and kept at this temperature for 5 min. Next, the samples were cooled to -80 °C with a rate of 10 °C/min, followed by a second heating cycle at the same rate to 170 °C. Using the

second heat run, the glass transition temperature ( $T_g$ ) was set as the midpoint of heat capacity change and the melting enthalpy ( $\Delta H$ ) as the integration of the endothermic area.

### *2.6. Gelling properties of celecoxib-loaded PCLA-PEG-PCLA systems*

Vial tilting to visually characterize sol and gel state of celecoxib-loaded PCLA-PEG-PCLA 25 wt% systems was performed at 4 °C, room temperature and at 37 °C after 30 min of incubation. Immobility of the systems for 10 min with the vial upside down was used to discriminate between mobile sols and immobile gels [16,18].

Rheological characteristics of the systems were monitored by oscillatory temperature sweep experiments using a TA AR-G2 rheometer equipped with a Peltier plate (1 ° steel cone, 20 mm diameter with solvent trap) at 1 % strain and a frequency of 1 Hz. The solvent trap of the Peltier plate was filled with water to prevent dehydration of the samples during measurement. A 70  $\mu$ l sample (cooled to 4 °C) was introduced between the rheometer plates (pre-cooled to 4 °C), and subsequently heated from 4 to 50 °C under oscillatory force with a heating rate of 1 °C/min.

### *2.7. Degradation and release behaviour of celecoxib-loaded gels*

The *in vitro* degradation and release behaviour of unloaded and loaded (0.125, 1.25 and 50 mg celecoxib per g gel) PCLA-PEG-PCLA 25 wt% gel was investigated in phosphate buffer pH 7.4 (same composition as described in section 2.4) with 0.2 wt% Tween® 80. Tween® 80 (sorbitan oleate ester,  $M = 1310$  g/mol) is a surfactant with a critical micelle concentration (CMC) of 0.02 mM, i.e. 0.0026 wt% [31], which increases the solubility of celecoxib [12,32]. Celecoxib solubility in phosphate buffer pH 7.4 with Tween® 80 was investigated. Therefore, an excess of celecoxib (~10 mg) was added to 1 ml of phosphate with 0.1 to 2.0 wt% Tween® 80 (i.e. above its CMC), which was incubated for 24 hours at room temperature and after centrifugation for 5 min at 3500 rpm, celecoxib concentrations in the supernatant were determined by UPLC (see Paragraph 2.8).

For the *in vitro* degradation and release, 6 g of dry celecoxib/PCLA-PEG-PCLA mixture was added to 21 ml phosphate buffer pH 7.4. Samples were heated for 15 min at ~50 °C (i.e. above the melting temperature of the

polymer in dry state), subsequently vortexed (1 min) and then incubated at 4 °C for 48 hours to allow formation of homogeneous dispersions. Subsequently, 300 µl sample cooled to 4 °C was transferred into glass vials (8.2 × 40 mm) using a syringe. The vials were incubated at 37 °C to allow gel formation, 30 min later 700 µl phosphate, with or without 0.2 wt% Tween® 80 was added. At predetermined time points, the buffer was removed, the weight of the remaining gels was measured and fresh buffer containing Tween® 80 was added. In addition, gel samples were freeze-dried and analyzed for their dry weight and for the  $M_n$  of the polymer by GPC as described previously [16]. The buffer samples that were taken during the release experiments were observed under a microscope (Nikon Eclipse TE2000U) and celecoxib concentrations were determined by UPLC (see Paragraph 2.8).

### *2.8. Determination of celecoxib concentration in release samples*

The celecoxib concentration in the different release samples was determined by UPLC using a Waters UPLC system equipped with a Waters column (BEH C18 1.7 µm, size: 2.1 x 100 nm). Celecoxib was dissolved in DMSO at 5 mg/ml. This celecoxib solution was diluted 10 times with DMSO and subsequently with buffer containing Tween® 80 to prepare celecoxib standards used for calibration (final celecoxib concentration ranged from 0.5 to 100 µg/ml). Two eluents containing 0.1 vol% trifluoroacetic acid (TFA) were used: 95/5 vol/vol acetonitrile/water (Eluent A) and 45/45/10 vol/vol/vol methanol/acetonitrile/water (Eluent B), the elution rate was 0.08 ml/min, and the column temperature was 50 °C. A gradient was run from 100 % Eluent A to 100 % Eluent B in 2 minutes and kept at 100 % B for 10 min before returning to 100 % Eluent A. Detection was performed with a UV detector at 254 nm and the injection volume was 10 µl. The retention time of celecoxib was 10.5 min with a total run time of 16 min. The autosampler temperature was 20 °C. The release samples were analyzed undiluted and after a 4× dilution with acetonitrile (ACN) to dissolve gel particles, if present.

### 2.9. *In vivo celecoxib release study*

The Animal Ethic Committee of the Erasmus Medical Center, Rotterdam, The Netherlands, approved all conducted procedures (Agreement number EMC2255(116-11-02)). Six 14-week-old (400-450 g) male Wistar rats (Charles River Nederland, Maastricht, The Netherlands) were housed in the animal facility of the Erasmus Medical Center, with a 12-h light-dark regimen, at 21 °C. Animals were fed standard food pellets and water *ad libitum*. Experiments started after an acclimatization period of 2 weeks. To investigate the *in vivo* celecoxib release kinetics from the gel, six rats were injected subcutaneously in the neck region with 500 µl aseptically prepared PCLA-PEG-PCLA 20 wt% gel loaded with 50 mg/g celecoxib. Experiments (see Figure A.1 in the appendices) showed that there is no difference in *in vitro* release kinetics between the 20 and 25 wt %. The 20 wt% formulation had the right viscosity for injection (the viscosity of the 25 % formulation was too high) and was therefore selected for investigation of the *in vivo* performance. At predetermined time points between 0 and 100 days, blood samples (500 µl) were taken from the lateral tail vein using Vacutainer SST™ II Advance (BD Plymouth) tubes that contain Silica (clot activator). After spinning down the cells (3500 rpm, 10 min), 100 µl of serum was taken and extracted with ethyl acetate [33]. Briefly, 100 µl serum was mixed with 100 µl internal standard (200 ng paracoxib in 5 % BSA). Then, 200 µl 0.1 M Na acetate buffer (pH 5.0) was added, followed by ethyl acetate (1 ml) and the samples were vortexed for 10 min. Then, samples were centrifuged at 11,000 rpm for 10 min and stored at -80 °C for at least 30 minutes. The upper ethyl acetate phases were transferred into HPLC glass vials and evaporated under nitrogen atmosphere. After evaporation, the samples were dissolved in 100 µl of methanol:acetate buffer (3:1 vol:vol) of which 5 µl was injected onto a Kinetex® C<sub>18</sub> (30 × 3.0 mm, particle size of 2.6 µm) analytical column (Phenomenex, Utrecht, The Netherlands). Separation was performed at a flow rate of 500 µl/min, with a total runtime of 3 minutes. The mobile phases consisted of acetonitrile:water (1:1 vol:vol) (A), and acetonitrile:methanol (1:1 vol:vol) (B). Samples were separated using the following gradient A/B vol/vol: 0-0.6 minutes, 100/0; 0.6-0.7 minutes, 100/0 to 30/70 0.7-1.6 minutes, 30/70 to 0/100; 1.6-2.4 minutes, 0/100; 2.4-2.7 minutes, 0/100 to 100/0; 2.7-3.0 minutes, 100/0 at a column temperature of

40 °C. The column effluent was introduced by an atmospheric pressure chemical ionization (APCI) interface (Sciex, Toronto, USA) into a API3000 mass spectrometer. For maximal sensitivity and for linearity of the response, the mass spectrometer was operated in multiple-reaction monitoring (MRM) mode at unit mass resolution. Peaks were identified by comparison of retention time and mass spectra of standards. For each component two ion transitions were monitored, celecoxib: 380.3 → 316.3 and 380.3 → 276.3 (collision energy: -50 V, both), and paracoxib: 369.3 → 250.2 and 369.3 → 234.2 (collision energy: -30 V, both). The following MS parameters were used: nebulizer gas: 10 psi; curtain gas: 10 psi; ion current: -2 µA; source temperature: 500 °C; gas flow 1: 30 psi; gas flow 2: 20 psi; decluster potential: -70 V and entrance potential: -10 V. Data were analyzed with Analyst software version 1.4.2 (Applied Biosystems, Nieuwerkerk a/d IJssel, The Netherlands). Celecoxib peak areas were corrected for the paracoxib recovery, and concentrations were calculated using a celecoxib reference line ranging from 0.5 ng to 1000 ng/ml. The reference line was linear in this range ( $r=0.9997$ ). Further calculations on the pharmacokinetics were done using the freeware PK solver [34]. AUC was calculated using the “linear trapezoidal method”.

#### *2.10. Intra-articular biocompatibility of celecoxib-loaded 25 wt% gels*

Five 14-week-old (400-450 g) male Wistar rats (Charles River Nederland, Maastricht, The Netherlands) were housed in the animal facility of the Erasmus Medical Centre, with a 12-hour light-dark regimen, at 21 °C. The animals (kept under the same conditions as described in 2.9) were used to investigate intra-articular biocompatibility of celecoxib-loaded temperature-responsive gels composed of PCLA-PEG-PCLA of 25 wt% polymer in phosphate buffer (without  $\text{NaN}_3$ ) loaded with 50 mg celecoxib per gram gel. Gels were prepared aseptically and 50 µl (cooled to 4 °C) was injected directly into the knee joint through the patellar tendon using Luer-lock® syringes mounted with 27G needles. After injection, the knee was flexed and extended a couple of times to distribute the gel within the knee. Contralateral knees were injected with saline to serve as negative control.

12 weeks post injection, the animals were euthanized and both knee joints were harvested for equilibrium partitioning of a contrast agent using µCT

(EPIC- $\mu$ CT) analysis, a method that has a strong correlation with cartilage sulphated-glycosaminoglycan (sGAG) content, which is a direct measurement for cartilage quality [35,36]. All samples were incubated in a 40 % Hexabrix solution (diluted with PBS) for 24 hours at room temperature [37]. EPIC- $\mu$ CT was performed on a Skyscan 1076 *in vivo*  $\mu$ CT scanner (Skyscan, Kontich, Belgium), using previously described scan settings [36]. In all EPIC- $\mu$ CT datasets, X-ray attenuation (arbitrary gray values inversely related to sGAG content) and thickness were calculated for cartilage of the medial and lateral tibial plateau [37]. Using Skyscan analysis software, all datasets were segmented using a fixed attenuation threshold between air (30) and subchondral bone (120). In all segmented  $\mu$ CT datasets, regions of interest (150 slices) were drawn around the cartilage of the medial and lateral plateau of the tibia separately and for these regions, cartilage attenuation and thickness ( $\mu$ m) were calculated. As a positive control, osteoarthritic knee joints from a previous article in rats of the same age, sex and species as the animals in our current study were used [36]. In short, a strenuous running protocol was combined with 3 unilateral papain injections, leading to cartilage damage. The abovementioned protocols for EPIC- $\mu$ CT scanning as well as data analysis were used.

### *2.12. Statistical analysis*

Differences in  $\mu$ CT-data between the gel-injected and saline-injected knees were analyzed using type-1, two-tailed, paired t-tests. Comparing both the celecoxib loaded gel-injected knees to the osteoarthritis induced knees (PRO) and the saline-injected knees to the OA induced knees (PRO), type-1, two-tailed, unpaired t-tests were performed. Distribution normality for both analysis was  $>0.05$  (Shapiro-Wilk). All data are presented as mean $\pm$ SD,  $p$ -values  $<0.05$  were considered significant.

## **3. Results and discussion**

### *3.1 $^1H$ NMR and GPC analysis of acetyl-capped PCLA-PEG<sub>1500</sub>-PCLA*

The acetyl-capped PCLA-PEG<sub>1500</sub>-PCLA copolymer used in this study was synthesized by ring opening solution polymerization of a mixture of L-lactide and  $\epsilon$ -caprolactone using PEG<sub>1500</sub> as initiator and tin(II) 2-ethylhexanoate as catalyst, followed by capping of the terminal hydroxyl

with acetyl groups by reaction with an excess of acetyl chloride as previously described [15]. It was aimed to synthesize a fully acetylated polymer with two PCLA blocks of 1700 g/mol and with a CL/LA molar ratio of 2.5.  $^1\text{H}$  NMR analysis and GPC analysis showed that the polymer had two PCLA blocks of 1600 g/mol with a molar CL/LA ratio of 2.2, hence slightly below the feed value as previously reported [15]. The degree of acylation was almost quantitative. The characteristics of the synthesized triblock copolymer are summarized in Table 1.

**Table 1:** Characteristics of the acetyl-capped PCLA-PEG-PCLA triblock copolymer used in this study.

<i>Polymer</i>	<i>Acetyl-capped PCLA-PEG<sub>1500</sub>-PCLA</i>
$M_{n,\text{PCLA}}$ [g/mol] <sup>a)</sup>	1600
CL/LA ratio [mol/mol] <sup>b)</sup>	2.2/1
Average CL-sequence length	4.9
Degree of acylation [%] <sup>c)</sup>	93
$M_{n,\text{NMR}}$ [g/mol] <sup>d)</sup>	4800
$M_{n,\text{GPC}}$ [g/mol] <sup>e)</sup>	5100
PDI <sup>f)</sup>	1.38

<sup>a)</sup> molecular weight of each PCLA block determined by  $^1\text{H}$  NMR

<sup>b)</sup> molar ratio of CL to LA in PCLA determined by  $^1\text{H}$  NMR

<sup>c)</sup> determined by  $^1\text{H}$  NMR

<sup>d)</sup> number average molecular weight determined by  $^1\text{H}$  NMR

<sup>e)</sup> number average molecular weight determined by GPC, relative to PEG standards

<sup>f)</sup> polydispersity determined by GPC

### 3.2. Miscibility of celecoxib with PEG and acetyl-capped copolymer

The miscibility of celecoxib with PEG<sub>1500</sub> and acetyl-capped PCLA-PEG-PCLA triblock copolymer was investigated by DSC analysis (Figure A.2 in the appendices). The thermogram of PEG<sub>1500</sub> showed no  $T_g$  and a melting endotherm at  $\sim 50$  °C ( $\Delta H = 156$  J/g), which is in accordance with literature



[38]. The thermogram of celecoxib showed no  $T_g$  and a melting endotherm at 165 °C ( $\Delta H = 102$  J/g), also in accordance with literature [39,40]. The thermogram of the celecoxib/PEG<sub>1500</sub> mixture (10/90 w/w) showed a melting endotherm at ~50 °C ( $\Delta H=138$  J/g), which can be ascribed to melting of PEG. Similarly, the thermograms of celecoxib/PEG<sub>1500</sub> mixtures (30/70 and 40/60 w/w) showed melting enthalpies of the PEG endotherm at ~50 °C ( $\Delta H$  of 77 and 2 J/g, respectively) whereas no melting endotherm of celecoxib was observed. However the thermograms showed a  $T_g$  at -47 and -33 °C, respectively, which likely can be ascribed to miscibility of celecoxib and PEG (Fox equation, see below). Hence celecoxib/PEG<sub>1500</sub> mixtures with weight ratios 10/90, 30/70 and 40/60 have an amorphous celecoxib/PEG<sub>1500</sub> phase and crystalline PEG<sub>1500</sub> domains. Upon further increase in celecoxib weight ratio, the thermograms of the celecoxib/PEG<sub>1500</sub> mixtures (50/50 and 80/20 w/w) showed a further increase of the  $T_g$  (-23 and 25 °C, respectively) and no melting endotherm of PEG and celecoxib. Hence, these mixtures were composed of an amorphous celecoxib/PEG<sub>1500</sub> phase only. Table 2 summarizes the thermal properties of celecoxib/PEG<sub>1500</sub> mixtures.

**Table 2:** Thermal properties of celecoxib/PEG<sub>1500</sub> mixtures as determined by DSC.

<i>Celecoxib</i> [wt%]	<i>PEG<sub>1500</sub></i> [wt%]	$T_g$ [°C]	$T_m$ [°C]	$\Delta H$ [J/g]
0	100	not detectable	~50*	156
10	90	not detectable	~50*	138
30	70	-47	~50*	77
40	60	-33	~50*	2
50	50	-23	not detectable	not detectable
80	20	25	not detectable	not detectable
100	0	not detectable	165 <sup>#</sup>	102 <sup>#</sup>

\* melting due to PEG

<sup>#</sup> melting due to celecoxib

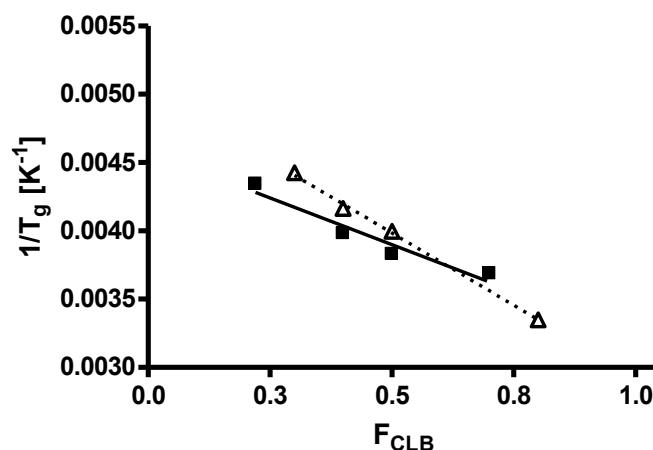


**Figure 2:** Reciprocal  $T_g$  of celecoxib/PCLA-PEG-PCLA (squares) and celecoxib/PEG<sub>1500</sub> (triangles) mixtures as a function of celecoxib weight fraction ( $F_{\text{celecoxib}}$ ).

**Table 3:** Thermal properties of celecoxib/PCLA-PEG-PCLA mixtures as determined by DSC.

Celecoxib [wt%]	PCLA-PEG-PCLA [wt%]	$T_g$ [°C]	$T_m$ [°C]	$\Delta H$ [J/g]
-	100	-58	0-25*	38
5	95	-55	-10-20*	33
17	83	-47	10-20*	13
22	78	-43	not detectable	-
40	60	-22	not detectable	-
50	50	-12	not detectable	-
70	30	-2	not detectable	-
100	0	-	165 <sup>#</sup>	102

\* melting due to PCLA-PEG-PCLA

<sup>#</sup> melting due to celecoxib

Figure 2 shows that the reciprocal  $T_g$  of celecoxib/PEG<sub>1500</sub> mixtures linearly decreases with increasing celecoxib weight fraction ( $F_{\text{Celecoxib}}$ ), which

indicates that the  $T_g$  of these mixtures follows the Fox Equation (Equation 1 [41]) in which  $F_{CLB}$  and  $F_{Polymer}$  are the weight fraction of celecoxib and PEG<sub>1500</sub>, respectively.

$$\frac{1}{T_g} = \frac{F_{CLB}}{T_{g_{CLB}}} + \frac{F_{Polymer}}{T_{g_{Polymer}}} \quad \text{(Equation 1)}$$

Extrapolation of the weight fraction of celecoxib to 100 % and 0 (100 % PEG<sub>1500</sub>) gives a calculated  $T_g$  for celecoxib and PEG<sub>1500</sub> of 70 and -70 °C respectively, which is only slightly deviating of the reported  $T_g$  of celecoxib and PEG (51 °C [40] and -60 °C [38], respectively). The results therefore confirm that celecoxib and PEG<sub>1500</sub> are miscible, which is in line with the reported miscibility of celecoxib with PEG<sub>6000</sub> [39] and PEG<sub>400</sub> [13,42]. Evidence of the miscibility of drugs structurally related to celecoxib (i.e. drugs containing -SO<sub>2</sub>N- moieties) and PEG has been discussed elsewhere [39,42-45] and, FTIR analysis showed the occurrence of intermolecular interactions and hydrogen bonding but also non-polar interactions between PEG and the studied drugs.

The thermograms of PCLA-PEG-PCLA and its mixtures with celecoxib are shown in Figure A.3. The thermogram of PCLA-PEG-PCLA showed a  $T_g$  at -58 °C, which can be ascribed to the  $T_g$  of the PCLA domains [16,18-20] and a crystallization exotherm at around -40 °C (38 J/g), as well as a melting endotherm at 10-40 °C ( $\Delta H = 40$  J/g), which can be ascribed to melting of PEG as we showed previously that this polymer do not show crystallinity of the CL-rich domains because the CL sequence length are too short, i.e. less than 5 CL units [16,18-20]. With increasing celecoxib content, the thermograms of celecoxib/PCLA-PEG-PCLA mixtures (5/95 and 17/83 w/w) showed an increasing  $T_g$  (-55 and -47 °C, respectively), a crystallization exotherm at higher temperature and of lower enthalpy (-30 °C ( $\Delta H = 25$  J/g) and 0 °C ( $\Delta H = 1$  J/g), respectively), which is likely attributed to miscibility of celecoxib and PCLA-PEG-PCLA. In line herewith, these thermograms also showed a melting endotherm at ~10-40 °C and of decreasing melting enthalpy ( $\Delta H = 33$  and 13 J/g, respectively). Hence these systems have amorphous celecoxib/PCLA/PEG domains and PEG crystals. Upon further increase of the celecoxib weight fraction, the thermograms of celecoxib/PCLA-PEG-PCLA mixtures (22/78, 40/60, 50/50 and 70/30) showed a further increase in  $T_g$  (-43 to -2 °C, respectively), and no

crystallization/melting endotherm. This shows that these systems consist of one amorphous celecoxib/PCLA/PEG phase. Table 3 summarizes the thermal properties of celecoxib/PCLA-PEG-PCLA mixtures.

As can be seen in Figure 2, the reciprocal  $T_g$  of celecoxib/PCLA-PEG-PCLA mixtures linearly decreases with increasing celecoxib weight fraction (Fox Equation [41], see Equation 1) confirming that celecoxib and PCLA-PEG-PCLA are miscible. Extrapolation of the weight fraction of celecoxib to 100 % and 0 (100 % PCLA-PEG-PCLA) gives a calculated  $T_g$  for celecoxib and PCLA-PEG-PCLA of 49 and -56 °C respectively, which is in good agreement with the reported  $T_g$  of celecoxib (51 °C [40]) and of PCLA-PEG-PCLA (-58 °C, Table 3). The presence of favorable interactions between celecoxib and PCLA-PEG-PCLA is in line with the miscibility of celecoxib with PLGA [7,9,10] and might be ascribed to hydrogen bonding between the N-H groups of celecoxib and the carbonyl C=O groups of polymers as described for celecoxib/PLGA and celecoxib/polyvinylpyrrolidone systems [46]. Because of favorable interactions of celecoxib with both PEG and PCLA, celecoxib is soluble to more than 70 wt% in the acetyl capped PCLA-PEG-PCLA.

### 3.3. Phase behaviour of aqueous celecoxib-loaded systems

Visualization by light microscopy and X-ray diffraction analysis were performed on aqueous systems (25 wt% PCLA-PEG-PCLA in buffer) with celecoxib/PCLA-PEG-PCLA ratios between 0/100 to 50/50 w/w. In systems of celecoxib/PCLA-PEG-PCLA ratios from 0/100 to 17/83, no crystals were detected, but above a concentration of 70 mg/g celecoxib, needle-shaped crystals ( $\sim 500 \times 1 \mu\text{m}$ ) were observed and identified as celecoxib crystals by X-ray analysis (see Figure A.4 in the appendices). Although celecoxib is molecularly dispersed in celecoxib/PCLA-PEG-PCLA mixtures (with celecoxib loading from 22 wt% to 70%, Table 3 and Figure A.2), it (partly) crystallizes upon addition of buffer. The solubility of celecoxib in PEG<sub>1500</sub>/buffer mixtures (10/90 w/w, corresponding to the same PEG content as in PCLA-PEG-PCLA 25 wt% systems) was only  $\sim 35 \mu\text{g/g}$ , meaning that, because celecoxib is highly soluble in PCLA-PEG-PCLA 25 wt% systems ( $\sim 50 \text{ mg/g}$ ), celecoxib is solubilized in the hydrophobic PCLA domains of the gel. The high solubility of celecoxib in aqueous PCLA-

PEG-PCLA 25 wt% systems (~50 mg/g) is in line with the reported good solubility (5-15 mg/g gel) of other hydrophobic drugs such as paclitaxel [24], cyclosporine A [24], docetaxel [26] and indomethacin [25] in other structurally-related temperature-responsive gelling systems based on PLGA-PEG-PLGA.

### 3.4. Gelling properties of celecoxib-loaded 25 wt% systems

Photographs of aqueous PCLA-PEG-PCLA 25 wt% systems with a celecoxib load of 1.25 mg per g formulation are shown in Figure 3A. At 4 °C and room temperature, the samples were sols, whereas they formed immobile opaque gels at 37 °C, similar to samples without celecoxib. This sol-to-gel conversion between 21 and 37 °C occurred in all tested celecoxib-loaded PCLA-PEG-PCLA 25 wt% systems containing up to 50 mg/g celecoxib.

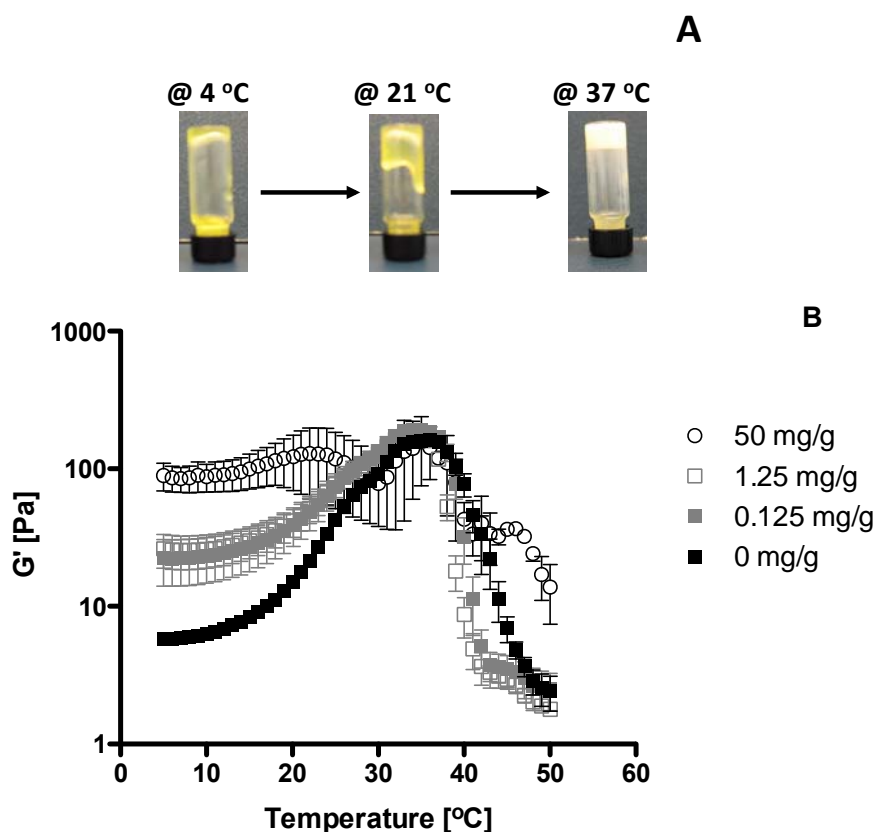


**Figure 3:** Phase behaviour and rheological properties of celecoxib-loaded PCLA-PEG-PCLA systems of 25 wt% in phosphate buffer. 3A shows photographs of systems containing 1.25 mg celecoxib per gram PCLA-PEG-PCLA formulation at 4, 21 and 37 °C. 3B shows the temperature-dependent storage modulus  $G'$  of systems containing different celecoxib loadings ( $n = 3$ ). Error bars represent the standard deviation of the mean.

Figure 3B shows the temperature-dependent storage modulus ( $G'$ ) of PCLA-PEG-PCLA 25 wt% systems with different celecoxib loadings (up to 50 mg/g containing fully dissolved celecoxib, see Paragraph 3.3). The  $G'$  of the unloaded systems was below 10 Pa at 4 °C, and increased to 100 Pa at 40 °C. Above 40 °C, a drop in  $G'$  was observed which is likely caused by phase separation of the systems and loss of contact between the gel phase and the plate of the rheometer. The  $G'$  of systems loaded with 1.25 to 50 mg/g celecoxib at 4 °C increased with increasing celecoxib loading from ~10 to 100 Pa, but these values were independent of the celecoxib loading at temperatures above 25 °C. Despite the observed increase of  $G'$  with increasing celecoxib loading (up to 50 mg/g), no significant effect on the sol-to-gel transition temperature of the systems was detected. The effect of drug loading on rheological properties of temperature-responsive systems has been described in literature before, but the underlying mechanism for the observed effects is not yet fully understood [26,47,48]. However, it was shown that a lowering of the sol-to-gel transition temperature of the systems, measured by rheological measurements or vial tilting, was observed with increasing drug loading as reported for systems made of PLGA-PEG-PLGA loaded with docetaxel [26], PEGylated-camptothecin [47] as well as that of paclitaxel in systems composed of sulfamethazine-capped PCLA-PEG-PCLA copolymers [48].

### 3.5. *In vitro* release and degradation of celecoxib-loaded 25 wt% gels

Degradation and release behaviour of PCLA-PEG-PCLA 25 wt% gels with or without celecoxib (1.25 mg/g) was investigated at 37 °C in phosphate buffer (pH 7.4) in the absence and presence of Tween® 80 (to ensure sink conditions for celecoxib; solubility of celecoxib in buffer without Tween® 80 was <1 µg/ml while addition of 0.2% Tween® 80 increased it to 500 µg/ml). Degradation of gels without celecoxib and with 1.25 mg celecoxib per gram loaded gels in the presence of Tween® 80 as well as that of 1.25 mg/g celecoxib loaded gels in the absence of Tween® 80 started after a lag time of ~10 days in a sustained manner over ~100 days (Figure A.5A in the appendices). Hence, no difference in gel degradation behaviour in the presence and absence Tween® 80 was observed. The  $M_n$  of the polymer of the

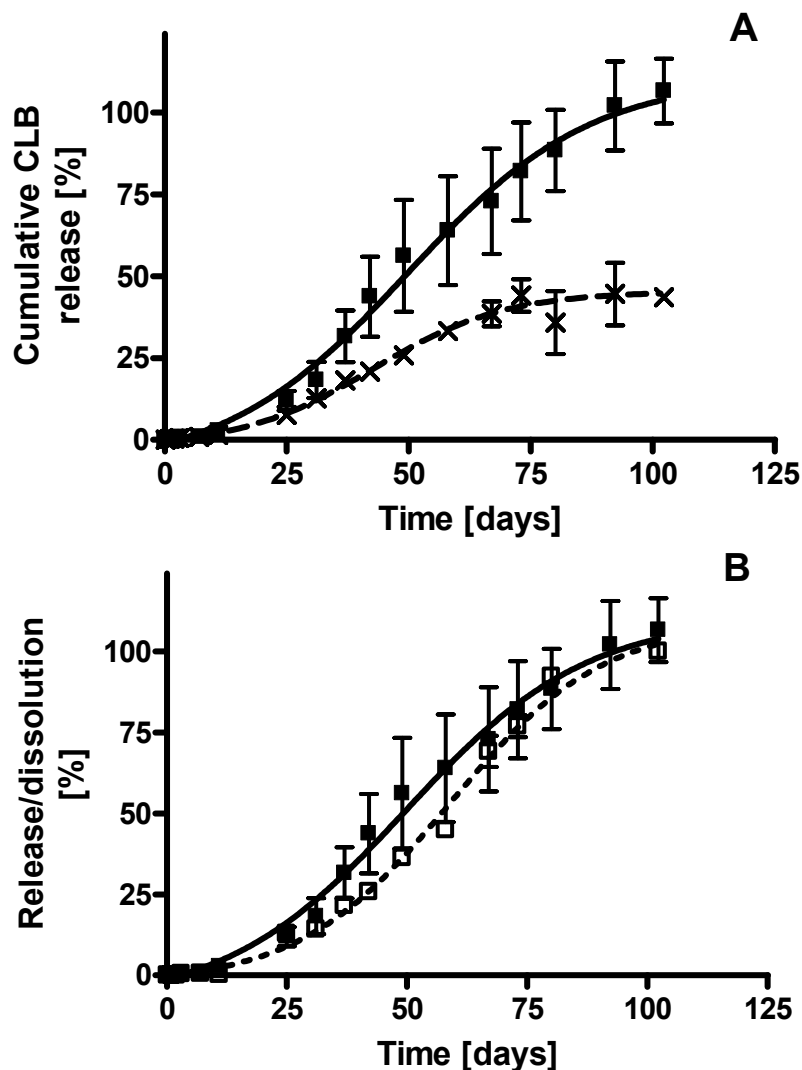


**Figure 4:** Release and degradation behaviour ( $n = 6$ ) of PCLA-PEG-PCLA 25 wt% gels loaded with 1.25 mg celecoxib per g gel at 37 °C in the presence of Tween® 80 (0.2 wt%). 4A shows celecoxib release before (crosses) and after (closed squares) dilution of the release samples with acetonitrile. 4B shows celecoxib release (closed symbols) and polymer dissolution (open symbols).

residual gels did not change in time (Figure A.4B in the appendices). This shows that the *in vitro* degradation of the gels loaded with 1.25 mg/g celecoxib was not affected by the celecoxib load and occurred via polymer dissolution, in line with previous data [16]. Hence, Tween® 80 is not required to solubilize celecoxib (and respect sink condition) during the *in vitro* release experiments. Previously, we reported [15] that the gels in phosphate buffer

first swelled (lag time in dissolution) to reach <20 wt% polymer content and thereafter start to dissolve. However, no swelling was observed in phosphate buffer containing Tween. This makes the lag time in dissolution difficult to explain and warrants further research, but is likely linked to disentanglement of the polymer chains.

The release of celecoxib started after the lag time of ~10 days (Figure 4A), after which a sustained release was maintained until day 75, where it reached a plateau at 40 % of the loaded amount. The chromatograms of the samples showed an injection peak with high absorption at 254 nm, which is hypothesized as a peak corresponding to micelles/gel particles loaded with celecoxib. Full recovery of celecoxib was achieved only after dilution of the release samples with ACN, which likely led to the disassembly of the celecoxib-loaded micelles present in the samples. This might be linked to the fact that gels made of triblock copolymers release (flower-like) micelles loaded with drug as reported previously [49].

In line with the release of celecoxib-loaded micelles, the release of celecoxib followed the polymer dissolution (Figure 4B), demonstrating that celecoxib release was mediated by polymer dissolution as earlier reported for other temperature-responsive gelling systems based on amphiphilic copolymers, loaded with hydrophobic drugs like paclitaxel [24,49,50] and indomethacin [51]. The observed release lag phase might be due to the high solubility of celecoxib in the gels (50 mg/g) compared to its solubility in Tween® (~50 µg/ml).

### *3.6. Effect of the celecoxib loading on its release from 25 wt% gels*

The release of celecoxib from PCLA-PEG-PCLA 25 wt% gels with different celecoxib loadings in the presence of Tween® 80 is shown in Figure 5A. Independent of the drug loading, the release started after a lag phase of ~10 days, after which the drug was released in a sustained manner to reach 100 % release at day 75-100, depending on the drug loading. Dissolution time of the gels increased from 75 days for gels loaded with 0.125 mg/g to 100 days for gels loaded with 1.25 mg/g and 50 mg/g (Figure 5B). This observation suggests that celecoxib affects gel stability, which can be ascribed to the hydrophobicity of the celecoxib and its interactions with PCLA-PEG-PCLA, thereby influencing the mechanical integrity of the gel (Figure 3).



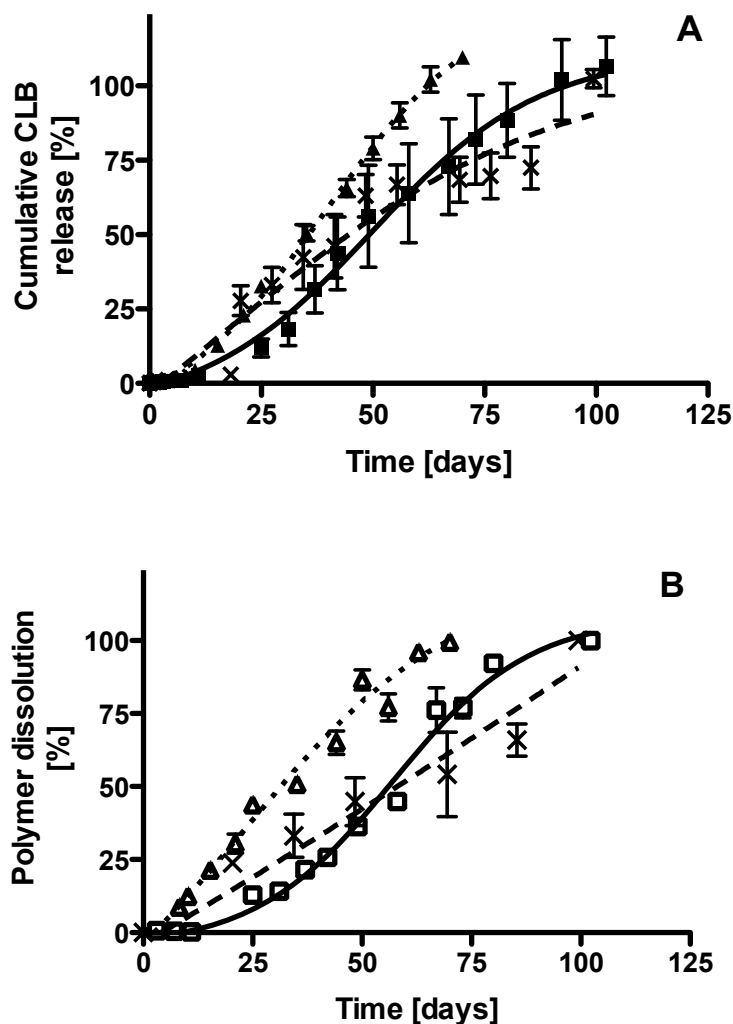


**Figure 5:** Release and degradation behaviour ( $n = 6$ ) of PCLA-PEG-PCLA 25 wt% gels loaded with 0.125 (triangles), 1.25 mg/g (squares) and 50 mg/g (crosses) at 37 °C. 5A shows celecoxib release after dilution of the release samples with acetonitrile. 5B shows polymer dissolution in the presence of Tween® 80 (0.2 wt%).

The effect of loading on the release of drugs from temperature-responsive systems has been reported in other studies and is controversial [24,48,51,52]. No effect of drug loading on the release of paclitaxel from PLGA-PEG-PLGA systems (loading up to 20 mg/g) was reported [24] as well as from sulfamethazine-capped PCLA-PEG-PCLA hydrogels (loading up to 10 mg/g) [48]. However, PLGA-PEG-PLGA systems showed longer release periods with increasing drug loading of docetaxel [26] and bee venom peptide (up to

8 mg/g) [51]. Finally, faster release of salmon calcitonin was observed from PEG-PLGA-PEG gels with increasing loading (loading up to 5 mg/g) [52].

### 3.8 *In vivo* pharmacokinetics (PK) data of gels with 50 mg/g celecoxib

The designed gel is aimed for local release of celecoxib in the knee while minimizing the systemic exposure. However, the small total volume of synovial fluid in rat knees (<50  $\mu$ l) does not allowed for synovial fluid sampling after intra-articular administration in order to monitor local PK. Therefore, the serum levels acquired from rats with subcutaneous administration of the gel with the highest celecoxib loading (50 mg/g) were utilized to gather insight in the *in vivo* duration and kinetics of celecoxib release from the gel. Figure 6 shows the serum concentration of celecoxib in time after subcutaneous injection of 500  $\mu$ l 20 % PCL-PEG-PCL containing 50 mg/g celecoxib, with a  $C_{max}$  of  $705 \pm 322$  ng/ml after 8 hours. After 24 hours, celecoxib concentrations dropped to  $278 \pm 103$  ng/ml and from day 3, a continuous and sustained drug release was observed with average serum concentrations between 5-80 ng/ml for a period of 4-8 weeks after injection. Four out of the six animals still showed measurable celecoxib serum concentrations at the end of the experiment (8 weeks). Total area under the curve (AUC) was  $2565 \pm 396$  ng $\times$ d/ml with the initial peak in the first day accounting for 17 % and the peak of the first 3 days for 30 % of the total release, meaning that ~70-80% of the dose was released in a sustained mode over 4-8 weeks.

*In vivo*, no lag time of celecoxib release from the gel was observed, in contrast to what was observed *in vitro*, where the lag time was linked to a lag time in gel dissolution (see Figure 4). In our previously conducted experiment using unloaded gel (500  $\mu$ l) of similar composition, the same difference was observed with the absence of an *in vivo* lag time, while *in vitro* this was present [17]. Another observation is the significantly faster *in vivo* release compared to *in vitro* for both the previously conducted experiments [17] and the celecoxib-loaded gels of the current study. Non-linearity of level A *in vitro/in vivo* correlations (IVIVCs) was addressed by Dunne and coworkers [53] and is likely explained by the complex phenomena that govern release and absorption *in vivo* compared to *in vitro* models. The absence of an *in vivo* lag phase might be due to the enhanced celecoxib solubility in

biological fluids likely caused by the relatively high protein binding of celecoxib [1,54,55]. Differences in gel degradation kinetics were shown to be influenced by the *in vivo* presence of macrophages as well as differences in gel depot geometry with a larger surface area and therefore multi-directional diffusion of the gels *in vivo* [17,56,57].

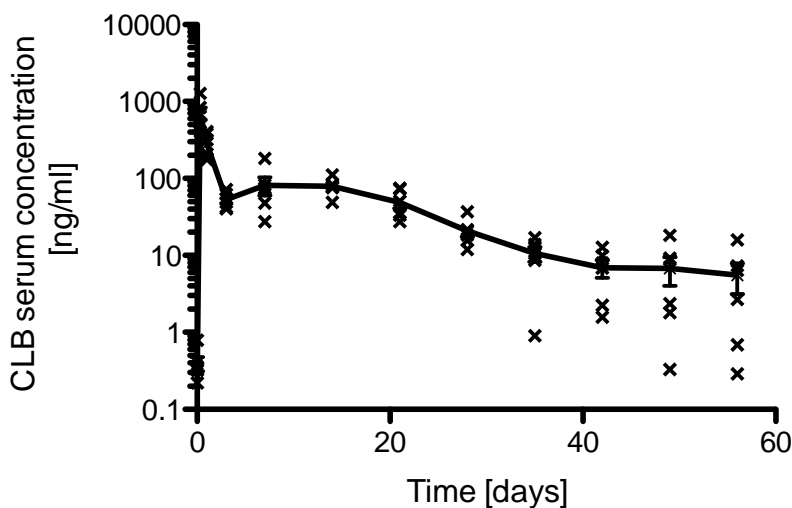


**Figure 6:** *In vivo* release of celecoxib from 20 wt% gels with 50 mg celecoxib per g gel. The serum concentrations of celecoxib after injection of 500  $\mu$ l subcutaneously in rats are shown. Each dot represents the individual measurements; error bars represents standard error of the mean ( $n = 6$ ).

### 3.9. Intra-articular biocompatibility of 25 wt% gels with 50 mg/g celecoxib

In a previous study, we have shown good intra-articular biocompatibility of unloaded PCLA-PEG-PCLA 25 wt% gels [17]. Now, we want to show that loading these gels with the highest amount of celecoxib does not jeopardize this biocompatibility. This formulation is representative for the lower celecoxib/PCLA-PEG-PCLA ratios as well, and by showing the combination of highest amount of polymer (25 wt%) with the highest celecoxib loading (50 mg/g) does not harm the injected joint, we can conclude that the other formulations would also be safe. Healthy knees ( $n = 5$ ) of 16-week old Wistar rats were injected with 50  $\mu$ l gel of high polymer content (25 wt%) containing 50 mg/g celecoxib, while the contralateral knees of these rats served as control (50  $\mu$ l saline injection). During the entire follow-up period, no clinical signs of a toxic response, such as joint redness/swelling or changed

locomotion occurred. The EPIC- $\mu$ CT (Figure 7) of these five rats showed significantly ( $p = 0.025$ ) thicker cartilage in the lateral compartment of celecoxib-loaded gel injected knees compared to saline ( $230 \pm 13$  vs.  $205 \pm 12$   $\mu\text{m}$ ), with no difference in attenuation ( $70.7 \pm 1.5$  vs.  $71.2 \pm 1.1$ ). Medially, the celecoxib-loaded gel injected knees showed significantly ( $p = 0.033$ ) higher attenuation values, indicating a lower amount of sGAGs, compared to saline injected knees ( $69.3 \pm 1.3$  vs.  $65.6 \pm 2.5$ ) while no significant difference in thickness was present ( $276 \pm 17$  vs.  $301 \pm 17$   $\mu\text{m}$ ).

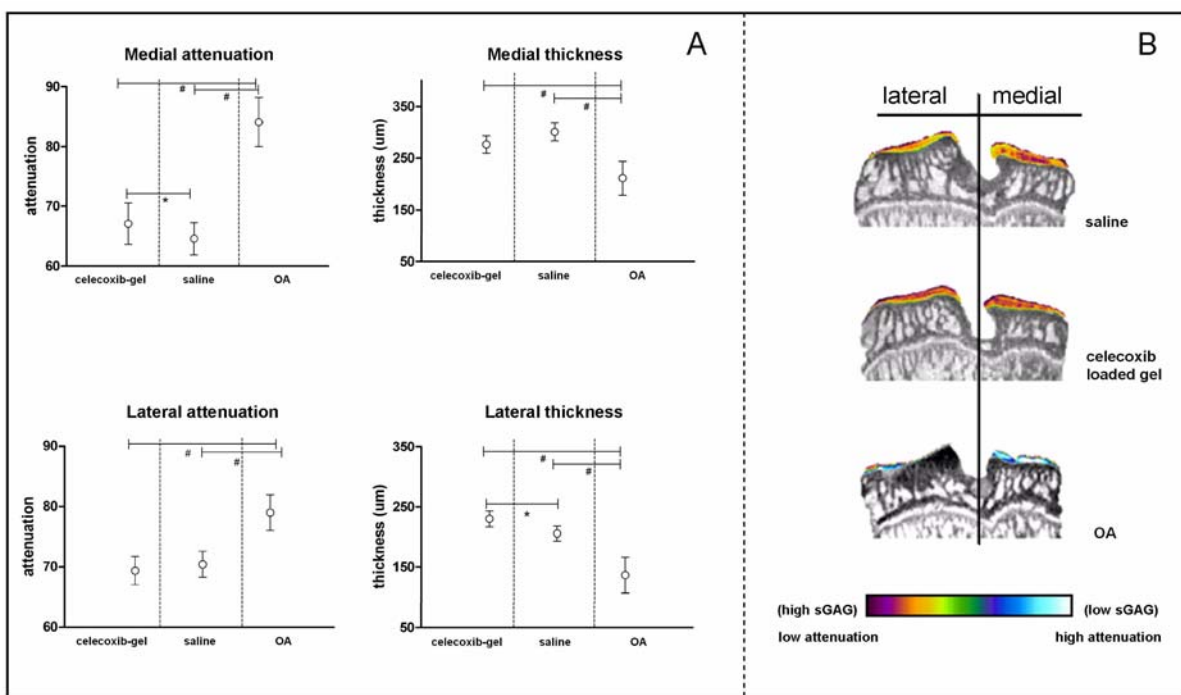


**Figure 7:** Intra-articular biocompatibility of celecoxib-loaded gel (50 mg/g; 50  $\mu\text{l}$ ). 7A shows the thickness and attenuation of both the medial and lateral tibial plateau of the different groups (celecoxib-gel ( $n = 5$ ), saline injected ( $n = 5$ ), OA ( $n = 9$ )) measured by EPIC- $\mu$ CT 12 weeks after intra-articular injection of either celecoxib-loaded gel, saline or papain (OA). \* significant difference ( $p < 0.05$ ) between celecoxib-loaded gel and saline injection (paired t-test); # significant difference ( $p < 0.05$ ) between saline or celecoxib loaded gel injection and OA model (unpaired t-test). 7B shows representative EPIC- $\mu$ CT images of the three different groups.

All values of healthy knees injected with either saline or celecoxib-loaded gel remained within the range of what is normally seen in healthy cartilage

[36]. It should be noticed that due to the high sensitivity of EPIC-  $\mu$ CT very subtle differences in cartilage quality and quantity that would have remained unnoticed when using less quantitative techniques like histology, are picked up.

To better understand the clinical relevance of our values, we compared them to what was found earlier for knees in which osteoarthritis was induced [36]. These osteoarthritic knees indeed showed significantly ( $p < 0.01$ ) worse attenuation and cartilage thickness values for both compartments, with (respectively medial and lateral) attenuation values of  $84.1 \pm 4.1$  and  $79.0 \pm 3.0$  and cartilage thickness of  $211 \pm 33$  and  $137 \pm 29$   $\mu\text{m}$ .

Since bone changes are also a feature of osteoarthritis [58], scans were inspected for bone changes in terms of osteophyte formation. Neither in the saline injected knees, nor the knees injected with celecoxib-loaded gel these changes occurred.

The findings on both cartilage and bone show that celecoxib-loaded PCLA-PEG-PCLA 25 wt% gel is safe for intra-articular use. A next step will be to apply these celecoxib-loaded gels in an osteoarthritis model in order to achieve positive treatment effects in these joints.

#### **4. Conclusions**

Acetyl-capped PCLA-PEG-PCLA based gels show good potential as a drug delivery system for the sustained and local release of celecoxib with desirable release kinetics (*in vitro* as well as *in vivo*) intra-articular biocompatibility. Therefore, this drug delivery system has great potential in the field of orthopedics, especially for the local treatment of osteoarthritis.

#### **Acknowledgements**

Mike de Leeuw and Dr. Theo Flipsen are gratefully acknowledged for their support and valuable discussions. Jan Wever (Polyvation) is thanked for carrying out the GPC measurements. This work is part of the BMM/Term program (Project P2.02) and the Dutch Ministry of Economic Affairs is thanked for the financial support.

## References

- [1] Davies NM, McLachlan AJ, Day RO, Williams KM. Clinical pharmacokinetics and pharmacodynamics of celecoxib: a selective cyclo-oxygenase-2 inhibitor. *Clin Pharmacokinet* 2000;38:225-242.
- [2] Zweers MC, de Boer TN, van Roon J, Bijlsma JW, Lafeber FP, Mastbergen SC. Celecoxib: considerations regarding its potential disease-modifying properties in osteoarthritis. *Arthritis Res Ther* 2011;13:239.
- [3] Tsutsumi R, Ito H, Hiramitsu T, Nishitani K, Akiyoshi M, Kitaori T, et al. Celecoxib inhibits production of MMP and NO via down-regulation of NF-kappaB and JNK in a PGE2 independent manner in human articular chondrocytes. *Rheumatol Int* 2008;28:727-736.
- [4] Mastbergen SC, Bijlsma JW, Lafeber FP. Selective COX-2 inhibition is favorable to human early and late-stage osteoarthritic cartilage: a human *in vitro* study. *Osteoarthritis Cartilage* 2005;13:519-526.
- [5] Paulson SK, Kaprak TA, Gresk CJ, Fast DM, Baratta MT, Burton EG, et al. Plasma protein binding of celecoxib in mice, rat, rabbit, dog and human. *Biopharm Drug Dispos* 1999;20:293-299.
- [6] Gong L, Thorn CF, Bertagnolli MM, Grosser T, Altman RB, Klein TE. Celecoxib pathways: pharmacokinetics and pharmacodynamics. *Pharmacogenet Genomics* 2012;22:310-318.
- [7] Zvonar A, Kristl J, Kerč J, Grabnar PA. High celecoxib-loaded nanoparticles prepared by a vibrating nozzle device. *J Microencapsul* 2009;26:748-759.
- [8] Amrite AC, Ayalasomayajula SP, Cheruvu NPS, Kompella UB. Single periocular injection of celecoxib-PLGA microparticles inhibits diabetes-induced elevations in retinal PGE<sub>2</sub>, VEGF, and vascular leakage. *Invest Ophthalmol Vis Sci* 2006;47:1149-1160.
- [9] McCarron PA, Donnelly RF, Marouf W. Celecoxib-loaded poly(D,L-lactide-co-glycolide) nanoparticles prepared using a novel and controllable combination of diffusion and emulsification steps as part of the salting-out procedure. *J Microencapsul* 2006;23:480-498.

- [10] Bohr A, Kristensen J, Stride E, Dyas M, Edirisinghe M. Preparation of microspheres containing low solubility drug compound by electrohydrodynamic spraying. *Int J Pharm* 2011;412:59-67.
- [11] Ayalasonmayajula SP, Kompella UB. Subconjunctivally administered celecoxib-PLGA microparticles sustain retinal drug levels and alleviate diabetes-induced oxidative stress in a rat model. *Eur J Pharmacol* 2005;511:191-198.
- [12] Homar M, Ubrich N, Ghazouani FE, Kristl J, Kerč J, Maincent P. Influence of polymers on the bioavailability of microencapsulated celecoxib. *J Microencapsul* 2007;24:621-633.
- [13] Larsen SW, Frost AB, Østergaard J, Thomsen MH, Jacobsen S, Skonberg C, et al. *In vitro* and *in vivo* characteristics of celecoxib *in situ* formed suspensions for intra-articular administration. *J Pharm Sci* 2011;100:4330-4337.
- [14] van Tomme SR, Storm G, Hennink WE. *In situ* gelling hydrogels for pharmaceutical and biomedical applications. *Int J Pharm* 2008;355:1-18.
- [15] Petit A, Müller B, Meijboom R, Bruin P, van de Manakker F, Versluijs-Helder M, et al. Effect of polymer composition on rheological and degradation properties of temperature-responsive gelling systems composed of acyl-capped PCLA-PEG-PCLA. *Biomacromolecules* 2013;14:3172-3182.
- [16] Petit A, Müller B, Bruin P, Meijboom R, Piest M, Kroon-Batenburg LMJ, et al. Modulating the rheological and degradation properties of hydrogels composed of blends of PCLA-PEG-PCLA triblock copolymers and their fully hexanoyl-capped derivatives. *Acta Biomater* 2012;8:4260-4267.
- [17] Sandker MJ, Petit A, Redout EM, Siebelt M, Müller B, Bruin P, et al. *In situ* forming acyl-capped PCLA-PEG-PCLA triblock copolymer based hydrogels. *Biomaterials* 2013;34:8002-8011.
- [18] Lee DS, Shim MS, Kim SW, Lee H, Park I, Chang T. Novel thermoreversible gelation of biodegradable PLGA-*block*-PEO-*block*-PLGA triblock copolymers in aqueous solution. *Macromol Rapid Commun* 2001;22:587-592.
- [19] Jo S, Kim J, Kim SW. Reverse thermal gelation of aliphatically modified biodegradable triblock copolymers. *Macromol Biosci* 2006;6:923-928.
- [20] Vermonden T, Censi R, Hennink WE. Hydrogels for protein delivery. *Chem Rev* 2012;112:2853-2888.

- [21] Ko DY, Shinde UP, Yeon B, Jeong B. Recent progress of in situ formed gels for biomedical applications. *Prog Polym Sci* 2013 0;38:672-701.
- [22] Bonacucina G, Cespi M, Mencarelli G, Giorgioni G, Palmieri GF. Thermosensitive self-assembling block copolymers as drug delivery systems. *Polymers* 2011;3:779-811.
- [23] Bae KH, Wang L, Kurisaw M. Injectable biodegradable hydrogels: progress and challenges. *J Mater Chem B* 2013;1:5371-5388.
- [24] Zentner GM, Rathi R, Shih C, McRea JC, Seo M, Oh H, et al. Biodegradable block copolymers for delivery of proteins and water-insoluble drugs. *J Control Release* 2001;72:203-215.
- [25] Qiao M, Chen D, Ma X, Liu Y. Injectable biodegradable temperature-responsive PLGA-PEG-PLGA copolymers: synthesis and effect of copolymer composition on the drug release from the copolymer-based hydrogels. *Int J Pharm* 2005;294:103-112.
- [26] Gao Y, Ren F, Ding B, Sun N, Liu X, Ding X, et al. A thermo-sensitive PLGA-PEG-PLGA hydrogel for sustained release of docetaxel. *J Drug Target* 2011;19:516-527.
- [27] Elstad NL, Fowers KD. OncoGel® (ReGel®/paclitaxel) - clinical applications for a novel paclitaxel delivery system. *Adv Drug Deliv Rev* 2009;61:785-794.
- [28] Bramfeldt H, Sarazin P, Vermette P. Characterization, degradation, and mechanical strength of poly(D,L-lactide-*co*- $\epsilon$ -caprolactone)-poly(ethylene glycol)-poly(D,L-lactide-*co*- $\epsilon$ -caprolactone). *J Biomed Mater Res A* 2007;83A:503-511.
- [29] Zhang Z, Ni J, Chen L, Yu L, Xu J, Ding J. Biodegradable and thermoreversible PCLA-PEG-PCLA hydrogel as a barrier for prevention of post-operative adhesion. *Biomaterials* 2011 7;32:4725-4736.
- [30] Yu L, Zhang H, Ding J. A subtle end-group effect on macroscopic physical gelation of triblock copolymer aqueous solutions. *Angew Chem Int Ed Engl* 2006;45:2232-2235.
- [31] Patist A, Bhagwat S, Penfield K, Aikens P, Shah D. On the measurement of critical micelle concentrations of pure and technical-grade nonionic surfactants. *J Surfactants Deterg* 2000;3:53-58.
- [32] Bozdağ-Pehlivan S, Subaşı B, Vural I, Unlü N, Capan Y. Evaluation of drug-excipient interaction in the formulation of celecoxib tablets. *Acta Pol Pharm* 2011;68:423-433.

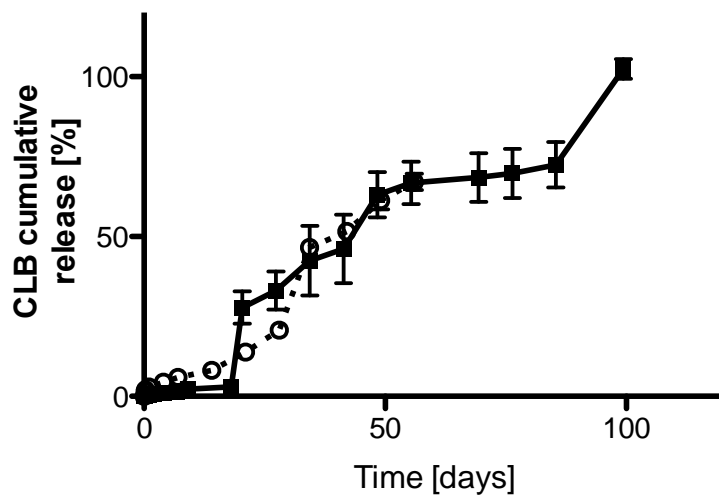


- [33] Gika HG, Theodoridou A, Michopoulos F, Theodoridis G, Diza E, Settas L, et al. Determination of two COX-2 inhibitors in serum and synovial fluid of patients with inflammatory arthritis by ultra performance liquid chromatography–inductively coupled plasma mass spectroscopy and quadrupole time-of-flight mass spectrometry. *J Pharm Biomed Anal* 2009;49:579-586.
- [34] Zhang Y, Huo M, Zhou J, Xie S. PKSolver: an add-in program for pharmacokinetic and pharmacodynamic data analysis in Microsoft Excel. *Comput Methods Programs Biomed* 2010;99:306-314.
- [35] Palmer AW, Guldberg RE, Levenston ME. Analysis of cartilage matrix fixed charge density and three-dimensional morphology via contrast-enhanced microcomputed tomography. *Proc Natl Acad Sci U S A* 2006;103:19255-19260.
- [36] Siebelt M. Increased physical activity severely induces osteoarthritic changes in knee joints with sulphate-glycosaminoglycan depleted cartilage. *Arthritis Res Ther* 2014;16(1):R32.
- [37] Silvast TS, Jurvelin JS, Lammi MJ, Töyräs J. pQCT study on diffusion and equilibrium distribution of iodinated anionic contrast agent in human articular cartilage - associations to matrix composition and integrity. *Osteoarthritis Cartilage* 2009 1;17:26-32.
- [38] Schneider HA, Di Marzio EA. The glass temperature of polymer blends: comparison of both the free volume and the entropy predictions with data. *Polymer* 1992;33:3453-3461.
- [39] Fouad EA, El-Badry M, Mahrous GM, Alanazi FK, Neau SH, Alsarra IA. The use of spray-drying to enhance celecoxib solubility. *Drug Dev Ind Pharm* 2011;37:1463-1472.
- [40] Chawla G, Gupta P, Thilagavathi R, Chakraborti AK, Bansal AK. Characterization of solid-state forms of celecoxib. *Eur J Pharm Sci* 2003;20:305-317.
- [41] Fox TG. Influence of diluent and of copolymer composition. *Polymer* 1956;1:123.
- [42] Seedher N BS. Solubility enhancement of COX-2 inhibitors using various solvent systems. *AAPS PharmSciTech* 2003;4:E33.
- [43] Vijaya Kumar SG, Mishra DN. Preparation, characterization and *in vitro* dissolution studies of solid dispersion of meloxicam with PEG 6000. *Yakugaku Zasshi* 2006;126:657-664.

- [44] Biswal S, Sahoo J, Murthy PN, Giradkar RP, Avari JG. Enhancement of dissolution rate of gliclazide using solid dispersions with polyethylene glycol 6000. *AAPS PharmSciTech* 2008;9:563-570.
- [45] Liu C, Liu C, Desai KG. Enhancement of dissolution rate of valdecoxib using solid dispersions with polyethylene glycol 4000. *Drug Dev. Ind. Pharm* 2005;31:1-10.
- [46] Gupta P, Thilagavathi R, Chakraborti AK, Bansal AK. Role of molecular interaction in stability of Celecoxib-PVP amorphous systems. *Mol Pharm* 2005;2:384-391.
- [47] Yu L, Chang GT, Zhang H, Ding JD. Injectable block copolymer hydrogels for sustained release of a PEGylated drug. *Int J Pharm* 2008;348:95-106.
- [48] Shim WS, Kim J, Kim K, Kim Y, Park R, Kim I, et al. pH- and temperature-sensitive, injectable, biodegradable block copolymer hydrogels as carriers for paclitaxel. *Int J Pharm* 2007;331(1):11-18.
- [49] de Graaf AJ, Azevedo Próspero dos Santos II, Pieters EH, Rijkers DT, van Nostrum CF, Vermonden T, et al. A micelle-shedding thermosensitive hydrogel as sustained release formulation. *J Control Release* 2012;162:582-590.
- [50] Wang W, Deng L, Liu S, Li X, Zhao X, Hu R, et al. Adjustable degradation and drug release of a thermosensitive hydrogel based on a pendant cyclic ether modified poly( $\epsilon$ -caprolactone) and poly(ethylene glycol) copolymer. *Acta Biomater* 2012;8:3963-3973.
- [51] Qiao M, Chen D, Hao T, Zhao X, Hu H, Ma X. Effect of bee venom peptide-copolymer interactions on thermosensitive hydrogel delivery systems. *Int J Pharm* 2007;345:116-124.
- [52] Yu T, Singh J. Thermosensitive drug delivery system of salmon calcitonin: *in vitro* release, *in vivo* absorption, bioactivity and therapeutic efficacies. *Pharm Res* 2010;27:272-284.
- [53] Dunne A, O'Hara T, Devane J. Level A *in vivo-in vitro* correlation: Nonlinear models and statistical methodology. *J Pharm Sci* 1997;86:1245-1249.
- [54] Guirguis MS, Sattari S, Jamali F. Pharmacokinetics of celecoxib in the presence and absence of interferon-induced acute inflammation in the rat: application of a novel HPLC assay. *J Pharm Sci* 2001;4:1-6.

- [55] Paulson SK, Vaughn MB, Jessen SM, Lawal Y, Gresk CJ, Yan B, et al. Pharmacokinetics of celecoxib after oral administration in dogs and humans: effect of food and site of absorption. *J Pharmacol Exp Ther* 2001;297:638-645.
- [56] Martinez M, Rathbone M, Burgess D, Huynh M. *In vitro* and *in vivo* considerations associated with parenteral sustained release products: a review based upon information presented and points expressed at the 2007 Controlled Release Society Annual Meeting. *J Control Release* 2008;129:79-87.
- [57] D'Aurizio E, Sozio P, Cerasa LS, Vacca M, Brunetti L, Orlando G, et al. Biodegradable microspheres loaded with an anti-Parkinson prodrug: an *in vivo* pharmacokinetic study. *Mol. Pharm* 2011;8:2408-2415.
- [58] van der Kraan PM, van den Berg WB. Osteophytes: relevance and biology. *Osteoarthritis Cartilage* 2007;15:237-244.

## Appendices

Figure

**Figure A.1:** Release ( $n = 3$ ) of PCLA-PEG-PCLA 25 wt% gels (closed squares) and 20 wt% gels (open circles) loaded with 50 mg celecoxib/g gel at 37 °C in the presence of Tween® 80 (0.2 wt%).

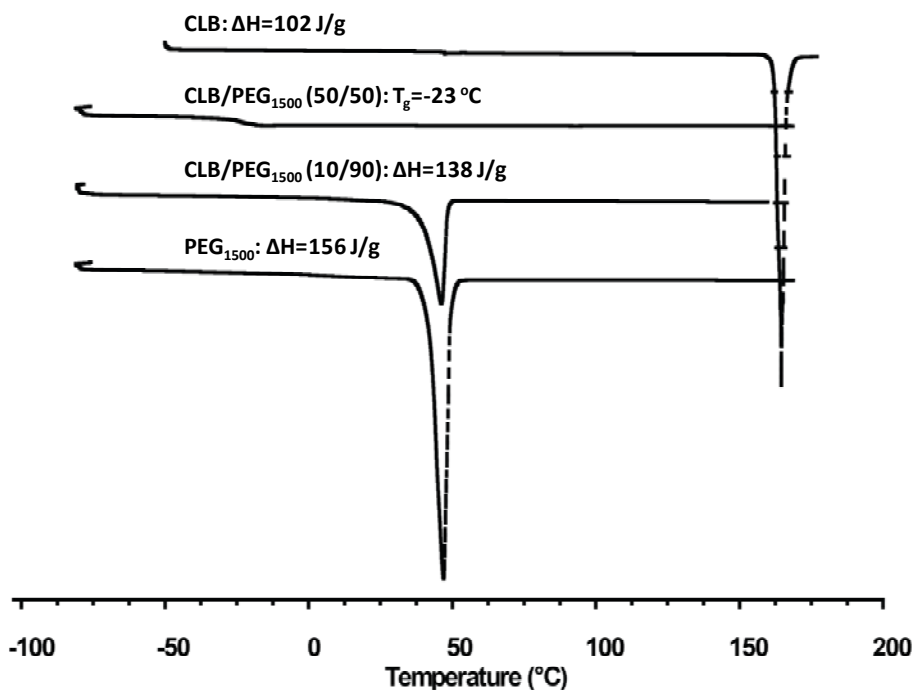


**Figure A.2:** DSC thermograms of PEG<sub>1500</sub>, celecoxib and their mixtures (second heating).

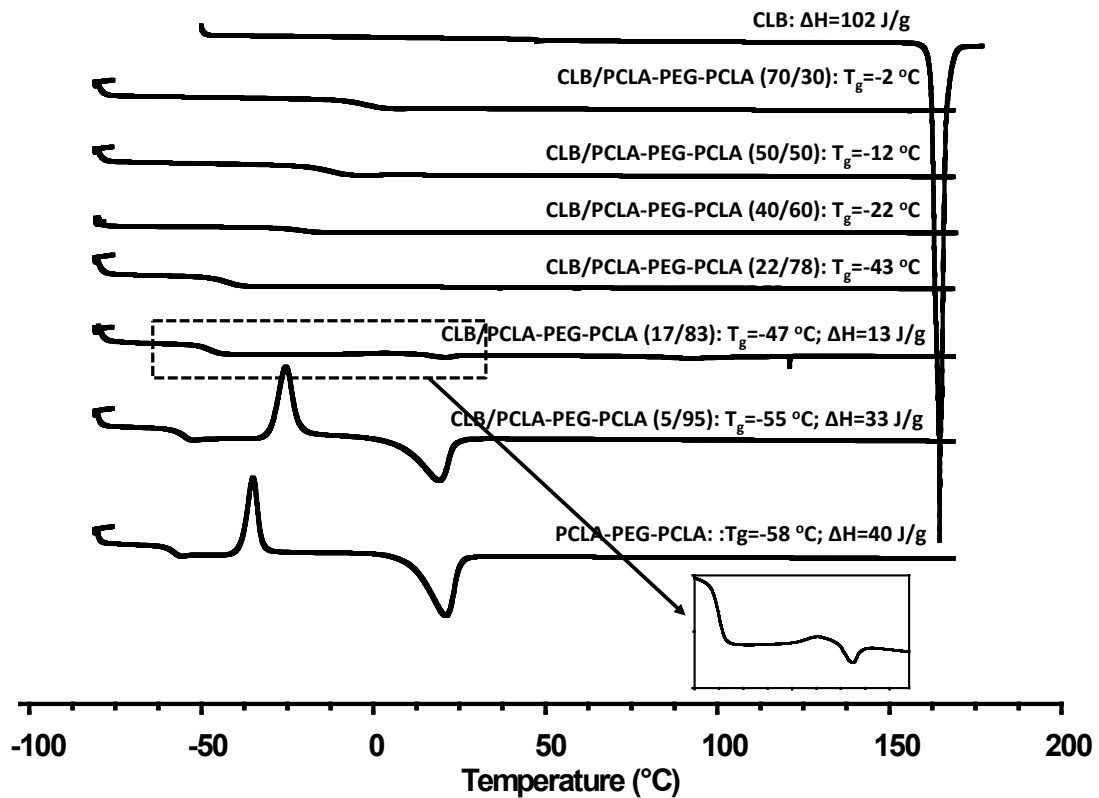


**Figure A.3:** DSC thermograms of acetyl-capped PCLA-PEG-PCLA, celecoxib and their mixtures (second heating). The insert shows the thermograms of celecoxib/PCLA-PEG-PCLA mixture (17/83 w/w) between -60 and 50 °C.

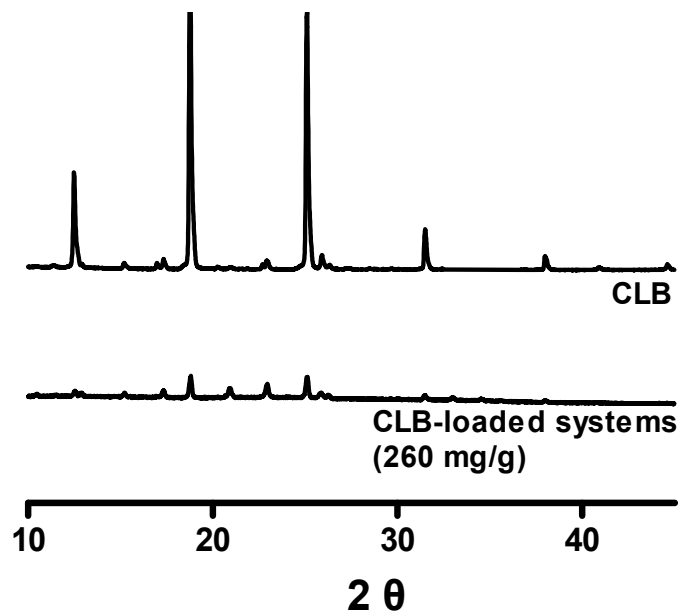


**Figure A.4:** X-ray diffraction pattern of celecoxib and a representative sample at 260 mg/g celecoxib containing celecoxib crystals.

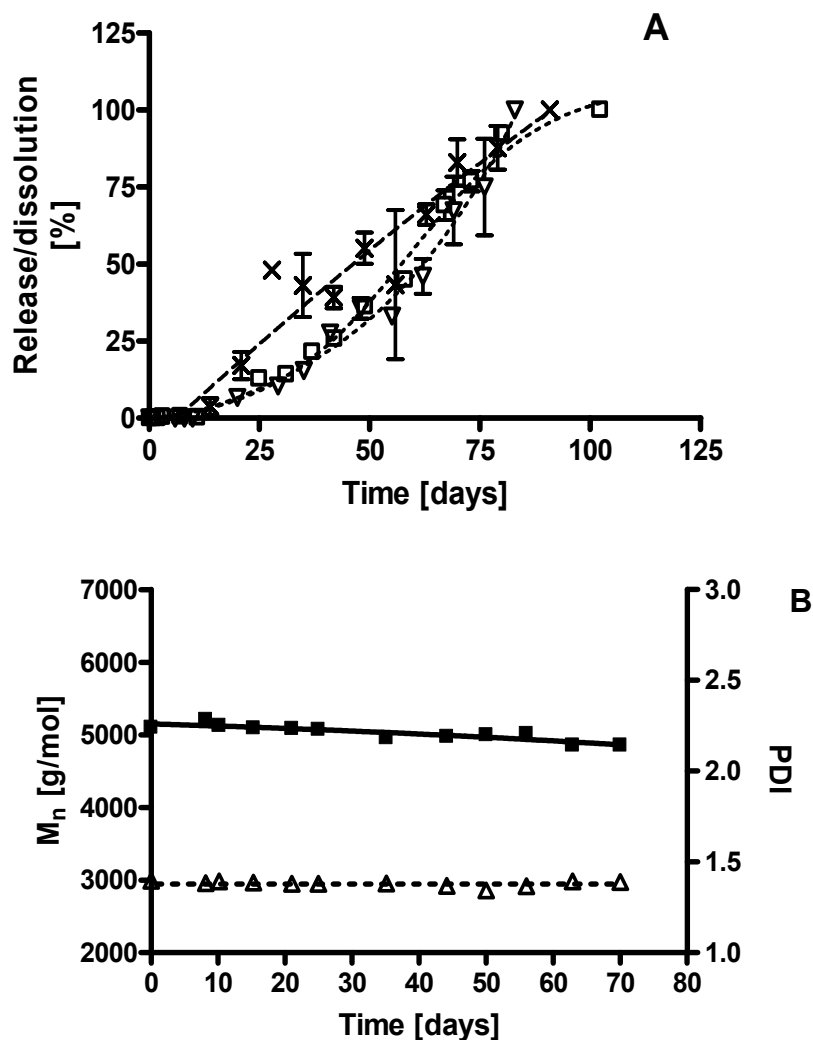


**Figure A.5:** Effect of Tween® 80 and celecoxib on the degradation of PCLA-PEG-PCLA gels. A.5A shows dissolution rate of the polymers from the gels without celecoxib (crosses) in the presence of Tween® 80 as well as that of gels with 1.25 mg/g celecoxib in the presence of Tween® 80 (squares) and in the absence of Tween® 80 (triangles). A.5B shows the  $M_n$  (squares) and PDI (triangles) of the polymers in the residual acetylated PCLA-PEG-PCLA gels loaded with 1.25 mg/g celecoxib in the presence of Tween® 80 as determined by GPC.



## CHAPTER 6

# Sustained intra-articular release of celecoxib from *in situ* forming gels made of acetyl-capped PCLA-PEG-PCLA triblock copolymers in horses

Everaldo M Redout<sup>1\*</sup>, Audrey Petit<sup>2,3\*</sup>, Chris H van de Lest<sup>1</sup>, Benno Müller<sup>2</sup>, Ronald Meyboom<sup>2</sup>, Paul van Midwoud<sup>2</sup>, Tina Vermonden<sup>3</sup>, Wim E Hennink<sup>3</sup> and P René van Weeren<sup>1</sup>

<sup>1</sup> Department of Equine Sciences, Faculty of Veterinary Medicine, Utrecht University, Utrecht, The Netherlands

<sup>2</sup> InGell Labs BV, Groningen, The Netherlands

<sup>3</sup> Department of Pharmaceutics, Utrecht Institute for Pharmaceutical Sciences, Utrecht University, Utrecht, The Netherlands

\* *Authors with equal contribution*

Chapter 6

PK in horses



### **Abstract**

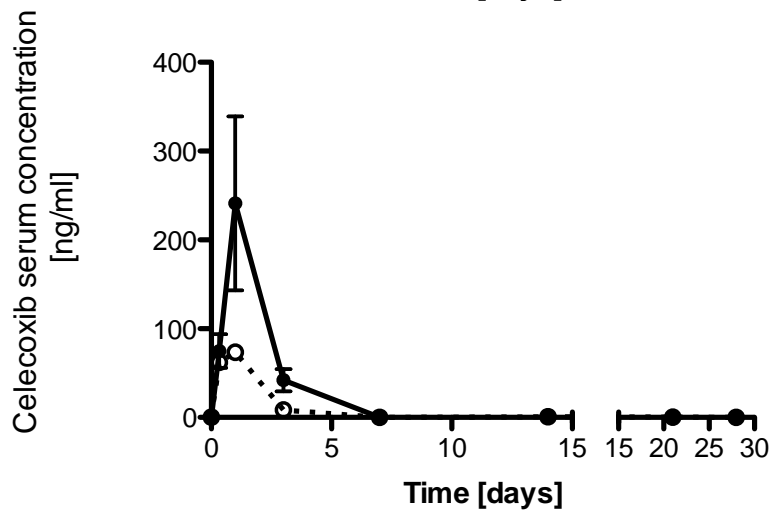
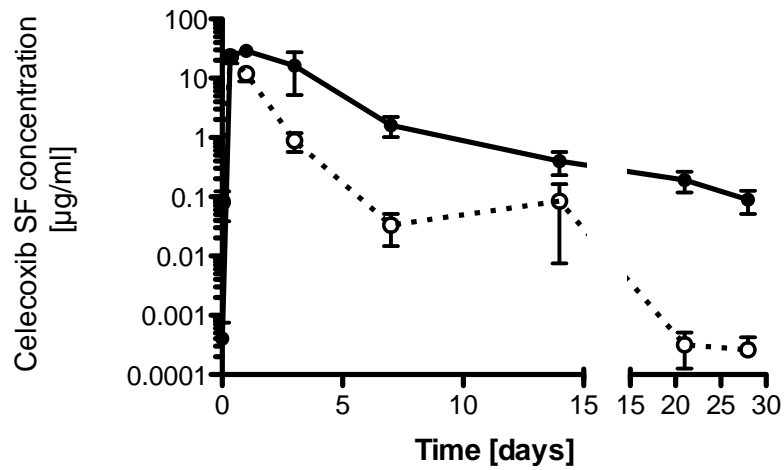
In this study, the intra-articular tolerability and suitability for local and sustained release of an *in situ* forming gel composed of an acetyl-capped poly( $\epsilon$ -caprolactone-*co*-lactide)-*b*-poly(ethylene glycol)-*b*-poly( $\epsilon$ -caprolactone-*co*-lactide) (PCLA-PEG-PCLA) copolymer loaded with celecoxib was investigated in horse joints.

The systems were loaded with two dosages of celecoxib, 50 mg/g ('low CLB gel') and 260 mg/g ('high CLB gel'). Subsequently, they were injected into the joints of five healthy horses. For 72 hours after intra-articular injection, they induced a transient inflammatory response, which was also observed after application of Hyonate®, a commercial formulation containing hyaluronic acid for the intra-articular treatment of synovitis in horses. However, only after administration of the 'high CLB gel' the horses showed signs of discomfort (lameness score:  $1.6 \pm 1.3$  on a 5-point scale) 1 day after injection, which completely disappeared 3 days after injection. Importantly, there was no indication of cartilage damage. Celecoxib  $C_{\max}$  in the joints was reached at 8 hours and 24 hours after administration of the 'low CLB gel' and 'high CLB gel', respectively. In the joints, concentrations of celecoxib were detected 4 weeks post administration. Celecoxib was also detected in plasma at concentrations of 150 ng/ml at day 3 post administration and thereafter its concentration dropped below the detection limit.

These results show that the systems were well tolerated after intra-articular administration and showed local and sustained release of celecoxib for 4 weeks with low and short systemic exposure to the drug, demonstrating that these injectable *in situ* forming hydrogels are promising vehicles for intra-articular drug delivery.

## Local and sustained release of celecoxib in equine joints

	<i>'Low CLB gel'</i>		<i>'High CLB gel'</i>	
	<i>Synovial fluid</i>	<i>Serum</i>	<i>Synovial fluid</i>	<i>Serum</i>
$t_{\max}$ [h]	8-24	8-24	8-72	8-24
$C_{\max}$ [ $\mu\text{g/ml}$ ]	23.6 $\pm$ 6.6	0.081 $\pm$ 0.072	36 $\pm$ 13	0.23 $\pm$ 0.22
AUC [ $\mu\text{g}\times\text{d/ml}$ ]	30.8 $\pm$ 8.9	0.18 $\pm$ 0.08	113 $\pm$ 85	0.38 $\pm$ 0.33



## 1. Introduction

Osteoarthritis (OA) is a major cause of disability in the elderly [1]. OA is, among others, characterized by progressive loss of cartilage in the joint, which disrupts its functional integrity, and is accompanied by chronic pain [2]. The current treatment options for OA are merely symptomatic, focusing on attenuation of inflammation and pain relief [3]. The most commonly used approach to treat inflammation and pain associated with OA is administration of non-steroidal anti-inflammatory drugs (NSAIDs) [4]. These drugs exert their effect by inhibiting cyclo-oxygenase (COX), a key enzyme involved in the conversion of arachidonic acid to prostaglandins, mediators of pain and inflammation. At present, three COX isoforms are known: COX-1, COX-2 and COX-3. The first-line drug for the treatment of OA is the COX-2 inhibitor celecoxib [5,6]. Although celecoxib induces fewer side effects than less specific NSAIDs (e.g., naproxen and ibuprofen), prolonged use and high dosages increase the risk for cardiovascular events [7]. Hence, local drug delivery might be suitable to avoid drug-related systemic side effects [8-14].

One of the strategies to reduce drug disposition to other organs than the target tissue is the use of drug-loaded *in situ* forming systems [15-17]. In particular, systems composed of ABA triblock copolymers (a PEG middle block flanked by polyester blocks of diverse compositions) meet the basic requirements for drug delivery systems (DDSs), e.g., encapsulation efficiency close to 100%, burst < 10%, sustained and controlled release for prolonged duration and complete drug recovery [16,18-21], while being easy to inject and having the capacity of forming gels at body temperature. Indeed, these systems have been shown to be suitable for loading and release of hydrophobic drugs [22-24]. A good example is the paclitaxel-loaded system based on poly(lactide-*co*-glycolide)-*b*-poly(ethylene glycol)-*b*-poly(lactide-*co*-glycolide) (PLGA-PEG-PLGA) [25]. The release of paclitaxel from this system is mediated by a combination of diffusion and chemical polymer degradation, which takes around six weeks *in vitro* as well as *in vivo* [22-24].

For some applications however, longer release times are required. Therefore, to slow down hydrolysis and increase the degradation time, the PLGA blocks have been replaced by poly( $\epsilon$ -caprolactone-*co*-lactide) (PCLA) blocks. Systems based on PCLA-PEG-PCLA are indeed stable for longer times depending on the ratio of caproyl units (CL) to lactoyl units (LA). For

instance, systems with PCLA blocks containing 70 mol% CL showed complete degradation in about six months [26,27]. Moreover, modification of the terminal hydroxyl groups of these triblock copolymers allows modulating the rheological and degradation properties of the *in situ* forming systems made of these copolymers [28,29]. These systems showed sustained release of celecoxib after subcutaneous injection and are well tolerated after intra-articular (i.a.) injection in rats [21,30].

The rat is an inappropriate animal model for frequent sampling of synovial fluid for local drug concentration determination. Therefore in the present study we used the horse, which is a much more suitable animal model to further investigate whether these systems are suitable for i.a. and sustained release of drugs. Also, horses have been shown to be a good translational animal model for OA, with treatment outcomes relevant for human OA [31-33]. Further, when developing new gels for i.a. administration, it is interesting to compare their tolerability with that of a registered hyaluronic acid gel (Hyonate®), clinically used for the treatment of horses suffering from lameness due to non-septic joint disease, which is usually accompanied by some form of synovitis [34]. Hyonate® is an aqueous solution of sodium hyaluronate, which due to polymer entanglements has high viscosity. Even though its efficacy is controversial, Hyonate® is used as a lubricant and has shock-absorbing as well as anti-inflammatory properties when injected into a joint. It is clinically used to replenish the hyaluronic acid concentration in the joint, which is known to be decreased in the synovial fluid of both human and equine OA patients [35-38].

In the present study, we investigated the tolerability of *in situ* forming systems composed of an acetyl-capped poly( $\epsilon$ -caprolactone-*co*-lactide)-*b*-poly(ethylene glycol)-*b*-poly( $\epsilon$ -caprolactone-*co*-lactide) (PCLA-PEG-PCLA) triblock copolymer for i.a. administration and performed a comparative study with Hyonate®. Also, we investigated the suitability of these systems to release locally celecoxib in a sustained and prolonged manner. We administered our systems in the joints of healthy horses.

## 2. Experiments and protocols

### 2.1. Materials

L-lactide was obtained from Purac Biochem, The Netherlands. Celecoxib was obtained from LC Laboratories, USA. Hyonate® was purchased from Bayer Animal Health. Sterile water for injection was purchased from B. Braun Medical. All other chemicals were obtained from Aldrich and used as received.

### 2.2. Synthesis of fully acetyl-capped PCLA-PEG-PCLA

The synthesis of acetylated PCLA-PEG-PCLA was performed essentially as previously described [28-30,39]. Briefly, in a three-neck round-bottom flask equipped with a Dean Stark trap and a condenser, 50 g PEG<sub>1500</sub> (1 mol eq.), 22 g L-lactide (4.6 mol eq.), 88 g  $\epsilon$ -caprolactone (23 mol eq.) and 600 ml toluene were introduced and, while stirring, heated to reflux under nitrogen atmosphere. The solution was azeotropically dried by distilling off toluene/water (~100 ml). Next, the solution was cooled to ~90 °C and 0.214 g tin(II) 2-ethylhexanoate (0.016 mol eq. relative to PEG hydroxyl groups) was added. Ring opening polymerization was performed at reflux for 16 hours (i.e. 110-120 °C, the boiling temperature of the solution of toluene, PEG, caprolactone and lactide) under nitrogen atmosphere. Subsequently, the solution was cooled to ~90 °C, followed by addition of 20 g triethylamine (6 mol eq.) and 11 g acetic anhydride (3.3 mol eq.). The reaction mixture was allowed to reflux for ~4 hours.

The solution was slowly dropped into 2 l of a 1:1 mixture of pentane and diethyl ether to precipitate the polymer. Upon storage at -20 °C, the polymer separated as waxy solid from which non-solvents containing unreacted monomers, unreacted acetic anhydride and formed acetic acid could be decanted easily. The precipitated polymer was dried in vacuo.

### 2.3. <sup>1</sup>H NMR analysis

<sup>1</sup>H NMR analysis of the polymers dissolved in CDCl<sub>3</sub> was performed using a Varian Oxford, operating at 300 MHz. <sup>1</sup>H NMR spectra were referenced to the signal of chloroform at 7.26 ppm.

PCLA-PEG-PCLA backbone: 5.25-4.95 (*I*<sub>5.1</sub>, 1H,-CO-CH(CH<sub>3</sub>)-O-); 4.35-4.23 (2H,-PEG-O-CH<sub>2</sub>-CH<sub>2</sub>-O-C(O)-CH(CH<sub>3</sub>)-O- + 1H,-CO-CH(CH<sub>3</sub>)-OH);

4.23-4.15 (2H, PEG-O-CH<sub>2</sub>-CH<sub>2</sub>-O-C(O)-(CH<sub>2</sub>)<sub>4</sub>-); 4.15-4.05 (2H, -CO(CH<sub>2</sub>)<sub>4</sub>-CH<sub>2</sub>-O-CO-CH(CH<sub>3</sub>)-O-); 4.05-3.95 (2H, -CO(CH<sub>2</sub>)<sub>4</sub>-CH<sub>2</sub>-O-C(O)-(CH<sub>2</sub>)<sub>4</sub>-); 3.85-3.25 (*I*<sub>3.6</sub>, 132H, -O-CH<sub>2</sub>-CH<sub>2</sub>-O- + 2H, CO(CH<sub>2</sub>)<sub>4</sub>-CH<sub>2</sub>-OH); 2.50-2.35 (*I*<sub>2.3</sub>, 2H, -O-CO-CH(CH<sub>3</sub>)-O-CO-CH<sub>2</sub>-(CH<sub>2</sub>)<sub>4</sub>); 2.35-2.20 (*I*<sub>2.2</sub>, 2H, -O-CO-CH<sub>2</sub>-(CH<sub>2</sub>)<sub>4</sub>-O-CO-CH<sub>2</sub>-(CH<sub>2</sub>)<sub>4</sub>); 1.80-1.55 (2H, -CO-CH<sub>2</sub>-CH<sub>2</sub>-CH<sub>2</sub>-CH<sub>2</sub>-O-); 1.58-1.44 (3H, -CO-CH(CH<sub>3</sub>)-O-); 1.45-1.25 (2H, -CO-CH<sub>2</sub>-CH<sub>2</sub>-CH<sub>2</sub>-CH<sub>2</sub>-CH<sub>2</sub>-) [28,30].

Acetyl-end group: 2.14-2.12 ppm (*I*<sub>2.13</sub>, CH<sub>3</sub>-CO-O-CH(CH<sub>3</sub>)-); 2.03-2.05 ppm (*I*<sub>2.04</sub>, CH<sub>3</sub>-CO-O-C(H<sub>2</sub>)<sub>5</sub>-) and 2.10-2.08 ppm (*I*<sub>2.09</sub>, CH<sub>3</sub>-CO-O-C(H<sub>2</sub>)<sub>2</sub>-O-) [28,30].

#### 2.4. Preparation of celecoxib-loaded PCLA-PEG-PCLA mixtures

Before preparing the systems, the glassware was depyrogenized at 260 °C for 2 hours. Use was made of the solubility of celecoxib (~300 mg/ml) and acetylated PCLA-PEG-PCLA triblock copolymers (>300 mg/ml) in ethyl acetate to prepare celecoxib/polymer solutions with celecoxib/polymer weight ratios between 14/86 and 54/46 w/w. The solutions were filtered with 0.2 μm PTFE filters, aseptically transferred into 6-cm Petri dishes and ethyl acetate was evaporated under nitrogen flow for 48 hours.

#### 2.5. Preparation of gels of the copolymer with and without celecoxib

Before preparing the systems, the glassware was depyrogenized at 260 °C for 2 hours. For the unloaded systems ('placebo'), 3.1 g of polymer was added to 6.9 g of phosphate buffer pH 7.4 (20 mM Na<sub>2</sub>HPO<sub>4</sub>, 5 mM NaH<sub>2</sub>PO<sub>4</sub>, 120 mM NaCl prepared using sterile water for injection). For the systems loaded with 50 ('low CLB gel') and 260 mg/g celecoxib ('high CLB gel'), 3.6 g and 5.7 g of celecoxib/polymer mixture (containing 3.1 g polymer mixed with 0.5 and 2.6 g celecoxib, respectively) was added to 6.4 and 4.3 g of the same buffer, respectively. Subsequently, the samples were autoclaved for 15 min at 120 °C. In addition, the effect of the autoclaving on the properties of 25 wt% unloaded system was measured by GPC and rheometry as previously described [28-30]. Also the pH of the mixture after autoclaving was measured.

After autoclaving, the samples were vortexed for 1 min and subsequently incubated at 4 °C for 48 hours to yield macroscopically homogeneous systems, i.e. a gel with fully dissolved celecoxib for the 'low CLB gel' and a

paste containing undissolved celecoxib for the ‘high CLB gel’. All handling steps were performed aseptically and resulted in samples containing low endotoxin (<0.1 EU/ml as assessed by a LAL test (PyroGene™, Lonza). To check for the presence of celecoxib crystals, samples were observed under a microscope (Nikon Eclipse TE2000U).

### *2.6. X-ray diffraction (XRD) analysis*

X-ray diffraction patterns were recorded for celecoxib, the acetylated PCLA-PEG-PCLA triblock copolymer, the celecoxib-loaded acetylated PCLA-PEG-PCLA block copolymers and the celecoxib-loaded acetylated PCLA-PEG-PCLA block copolymer gel (31 wt% in phosphate buffer pH 7.4, as described above) using a Bruker-AXS D8 Advance powder X-ray diffractometer, in Bragg-Brentano mode, equipped with automatic divergence slit and a PSD Vântec-1 detector. The radiation used was cobalt  $K\alpha_{1,2}$ ,  $\lambda = 1.79026 \text{ \AA}$ , operated at 30 kV, 45 mA. The patterns were recorded at a sample-to-detector distance of 435 mm. Separate blank patterns were also recorded to allow subtraction of air- and capillary wall-scattering.

### *2.7. In vivo experimental set up*

The study design was approved by the institutional Ethics Committee on the Care and Use of Experimental Animals in compliance with Dutch legislation on animal experimentation. 2 ml of unloaded gel formulation of acetylated PCLA-PEG-PCLA triblock copolymer (‘placebo’) was administered into the right middle carpal joint of five healthy geldings with clinically normal carpal and talocrural joints, as determined by radiographic evaluation. 2 ml Hyonate® was injected into the contra-lateral middle carpal joint. 2 ml of 50 mg/g celecoxib loaded gel formulation (‘low CLB gel’) was injected into the left talocrural joint, while 2 ml of 260 mg/g celecoxib loaded formulation (‘high CLB gel’) was injected into the right talocrural joint 4 weeks later to allow quantification of the systemic exposure to celecoxib for both gels separately.

### *2.8. Evaluation of clinical response to the treatment*

Lameness examinations (scored on a standardized 0 to 5 scale [31]) were conducted at 0, 8, 24, 72 hours and 1, 2, 3, 4 weeks (i.e. post injection of

Hyonate®, ‘placebo’ and ‘low CLB gel’). At 4 weeks, the right talocrural joint was injected with ‘high CLB gel’ and lameness examinations were performed again at the same timepoints (i.e. 0, 8, 24, 72 hours and 1, 2, 3, 4 weeks post injection). Horses were monitored throughout the study for signs of discomfort.

### *2.9. Collection of synovial fluid and plasma*

Synovial fluid of the treated joints and plasma samples were aspirated at 0, 8, 24, 72 hours and 1, 2, 3, 4 weeks after the first series of injections (Hyonate®, ‘placebo’ and ‘low CLB gel’) as well as 4 weeks later with the same schedule after injection of ‘high CLB gel’. A portion of the fluid was processed for white blood cell (WBC) count and total protein content. The remaining volume was centrifuged, and the supernatant was stored at -80 °C until celecoxib content determination. The serum samples were used for celecoxib content determination

### *2.10. Synovial fluid analysis*

The synovial fluid WBC and total protein concentrations were determined using a Coulter Counter® Z1 (Beckman Coulter, Inc.) and refractometer [31,40], respectively. Protein concentrations were measured using a validated method based on refractometry [31,40] that is used in the clinic. Synovial fluid samples were also evaluated for glycosaminoglycan (GAG) concentrations using a modified 1,9-dimethylmethylene blue dye-binding assay as previously described [41]. To check for possible damage to the collagen network of the cartilage, we also measured the concentration of the C2C epitope of collagen in synovial fluid, as previously reported [42].

### *2.11. Celecoxib concentrations in the synovial fluid and serum*

Celecoxib was extracted from the synovial fluid as well as from serum samples. Briefly, 100 µl synovial fluid or serum was used to which 100 µl internal standard (200 ng paracoxib (Dynastat, Pfizer) in 5 % BSA) was added. Then, 200 µl 0.1 M Na acetate buffer (pH 5) was added. Ethyl acetate (1 ml) was added and the samples were vortexed for 10 min. Then, the samples were centrifuged at 11,000 rpm for 10 min and stored at -80 °C for at least 30 min. The upper ethyl acetate phase was transferred into an HPLC



glass vial and the solvent was evaporated under nitrogen flow. The extraction was repeated on the remaining aqueous phase with 1 ml hexane and this fraction was added to the evaporated ethyl acetate fraction. After evaporation of hexane, the residues were dissolved in 100  $\mu$ l of a 3:1 vol:vol methanol:acetate buffer (0.1 M, pH 5), of which 10  $\mu$ l was injected onto a Kinetex® C<sub>18</sub> (150  $\times$  3.0 mm, particle size of 2.6  $\mu$ m) analytical column (Phenomenex, Utrecht, NL). Separation was performed at a flow rate of 250  $\mu$ l/min, with a total runtime of 13 minutes. The mobile phases consisted of acetonitrile:water (1:1 vol:vol) (A), and acetonitrile:methanol (1:1 vol:vol) (B). Samples were separated using the following gradient A/B vol/vol: 0–2 min, 100/0; 2–8.5 min 25/75 to 0/100; 8.5–11 min, 0/100; 11–12 min 0/100 to 100/0; 12–13 min 100/0. The column effluent was introduced by an atmospheric pressure chemical ionization (APCI) interface (Sciex, Toronto) into an API3000 mass spectrometer. For maximal sensitivity and for linearity of the response, the mass spectrometer was operated in multiple-reaction monitoring (MRM) mode at unit mass resolution. Peaks were identified by comparison of retention times and mass spectrum of celecoxib and paracoxib. For each component two ion transitions were monitored, celecoxib: 380.3 $\rightarrow$ 316.3 and 380.3 $\rightarrow$ 276.3 (collision energy: -50 V, both), and paracoxib (Dynastat, Pfizer): 369.3 $\rightarrow$ 250.2 and 369.3 $\rightarrow$ 234.2 (collision energy: -30 V, both). The following MS parameters were used: nebulizer gas: 10 psi; curtain gas: 10 psi; ion current: -2  $\mu$ A; source temperature: 500 °C; gas flow 1: 30 psi; gas flow 2: 20 psi; decluster potential: -70 V and entrance potential: -10 V. Data were analyzed with Analyst software version 1.4.2 (Applied Biosystems, The Netherlands). Celecoxib peak areas were corrected for the recovery of paracoxib, and concentrations were calculated using celecoxib standards with concentrations ranging from 5 pg to 20 ng/ml. The calibration curve was linear in this range ( $r=0.998$ ) and the average extraction efficiency was 68 %. Further calculations on the pharmacokinetics were done using the freeware PK solver [43]. AUC was calculated using the “linear trapezoidal method”.

### *2.12. Solubility of celecoxib in 10 % fetal bovine serum*

Celecoxib has a very low aqueous solubility (<1  $\mu$ g/ml) with a large apparent volume of distribution (>~1 l/kg) due to its high plasma protein binding (~97 %) [44]. As the protein content of equine synovial fluid is 1–2 g/dl

[41,42,45], we investigated the effect of plasma protein on the solubility of celecoxib in cell medium (DMEM 31965 + pen/strep) with 10 % fetal bovine serum (FBS, 30 g/dl [46]). Therefore, an excess of celecoxib (~100 mg) was added to 1 ml of cell medium with FBS, which was incubated for 24 hours at room temperature and after centrifugation for 5 min at 3500 rpm, the sample was filtered using a 0.2 µm filter. Subsequently, the proteins present in the sample were precipitated by adding 1 vol of acetonitrile. The celecoxib concentrations in the supernatant were determined by UPLC using a Waters UPLC system equipped with a Waters column (BEH C18 1.7 µm, size: 2.1 × 100 nm). Standards were prepared by dissolving celecoxib in DMSO at 5 mg/ml. This celecoxib solution was diluted 10 times with DMSO and subsequently with buffer containing Tween® 80 to prepare celecoxib standards used for calibration (final celecoxib concentration ranged from 0.5 to 100 µg/ml). Two eluents containing 0.1 vol% trifluoroacetic acid (TFA) were used: 95:5 vol:vol acetonitrile/water (Eluent A) and 45:45:10 vol:vol:vol methanol/acetonitrile/water (Eluent B); the elution rate was 0.08 ml/min, and the column temperature was 50 °C. A gradient was run from 100 % Eluent A to 100 % Eluent B in 2 minutes and kept at 100 % B for 10 min before returning to 100 % Eluent A. Detection was performed with a UV detector at 254 nm and the injection volume was 10 µl. The retention time of celecoxib was 10.5 min with a total run time of 16 min. The autosampler temperature was 20 °C.

### *2.13. Histological analysis of articular cartilage*

8 weeks after the start of the study, i.e. the administration of Hyonate®, ‘placebo’ and ‘low CLB gel’, and thus 4 weeks after the injection of ‘high CLB gel’, the animals were sacrificed. Full thickness cartilage was harvested from the injected joints and fixed in buffered formaldehyde 4 % solution (Klinipath, The Netherlands) and, after embedding in paraffin, sections (5 µm) were cut. The sections were deparaffinized and stained as previously described by Gawlitta et al [47].

### *2.14. Statistical analysis*

Synovial fluid data (WBC, total protein, GAG content, C2C epitope) were compared using two-way ANOVA for repeated measures (GraphPad Prism 5). Significance level was set at  $p \leq 0.05$ ; differences were further

analyzed using a Bonferroni post-hoc test. The data are presented as mean $\pm$ SEM.

### **3. Results and Discussion**

#### *3.1. Synthesis and characterization of fully acetylated PCLA-PEG-PCLA*

The synthesis of PCLA-PEG<sub>1500</sub>-PCLA was performed by ring opening polymerization of L-lactide and  $\epsilon$ -caprolactone in solution with PEG<sub>1500</sub>-diol as macroinitiator in the presence of tin(II) 2-ethylhexanoate as catalyst. Subsequently, acylation of hydroxyl-end groups using an excess of acetic anhydride resulted in the formation of acetyl-capped PCLA-PEG-PCLA with a yield of 81 %. The <sup>1</sup>H NMR spectrum of the polymer is given in Figure 1 and shows the characteristic peaks at 5.25-4.95, 3.65-3.55 and 2.50-2.10 ppm corresponding to the methine protons of LA, the methylene protons of PEG and the methylene protons of caproyl units [28-30]. Also, <sup>1</sup>H NMR analysis shows that the acetyl-capped triblock copolymers have peaks belonging to the methyl protons of acetyl-end groups at 2.14-2.03 ppm [28]. The composition of the polymers was determined according to Equation A.1 to A.13 as described previously [28-30]. The molar ratio of CL to LA (as defined in Equation A.7), *k*, was calculated from the <sup>1</sup>H NMR spectrum and found to be 2.7 mol/mol, in accordance with the CL/LA feed of 2.5 mol/mol. The average length of CL sequences was calculated according to Equation A.13 and found to be 4.3. This indicates an incomplete random distribution of the monomers in PCLA as previously reported for similar polymers [28-30]. The number molecular weight (*M<sub>n</sub>*) of the synthesized polymer as determined by <sup>1</sup>H NMR analysis (equation A.12) was 4500 g/mol, which is slightly below the *M<sub>n</sub>* of 4900 g/mol expected from the feed. The extent of acetylation, calculated by comparing the methyl peaks of end groups to the methylene peak of PEG measured by <sup>1</sup>H-NMR, was found to be ~100 % indicating that the polymer was fully capped with acetyl end-groups. Table 1 summarizes the characteristics of the polymer.

#### *3.2. Characteristics of celecoxib-loaded acetylated PCLA-PEG-PCLA gels*

Figure 2A shows a microscopic photograph of a 'high CLB gel' (a celecoxib-loaded gel made of acetylated PCLA-PEG-PCLA triblock copolymers in buffer containing celecoxib at 260 mg/g (i.e. 26 wt%) and

31 wt% polymer). Needle-shaped crystals ( $\sim 500 \times 1 \mu\text{m}$ ) were clearly visible which were neither present in the unloaded systems ('placebo') nor in the 50 mg/g celecoxib ('low CLB gel'), as reported previously for similar gels of 25 wt% polymer in buffer [21]. X-ray analysis convincingly showed that celecoxib crystals were present (Figure 2B). Thus, celecoxib up to 50 mg/g was fully dissolved in the gel, but present in the form of crystals at 260 mg/ml.

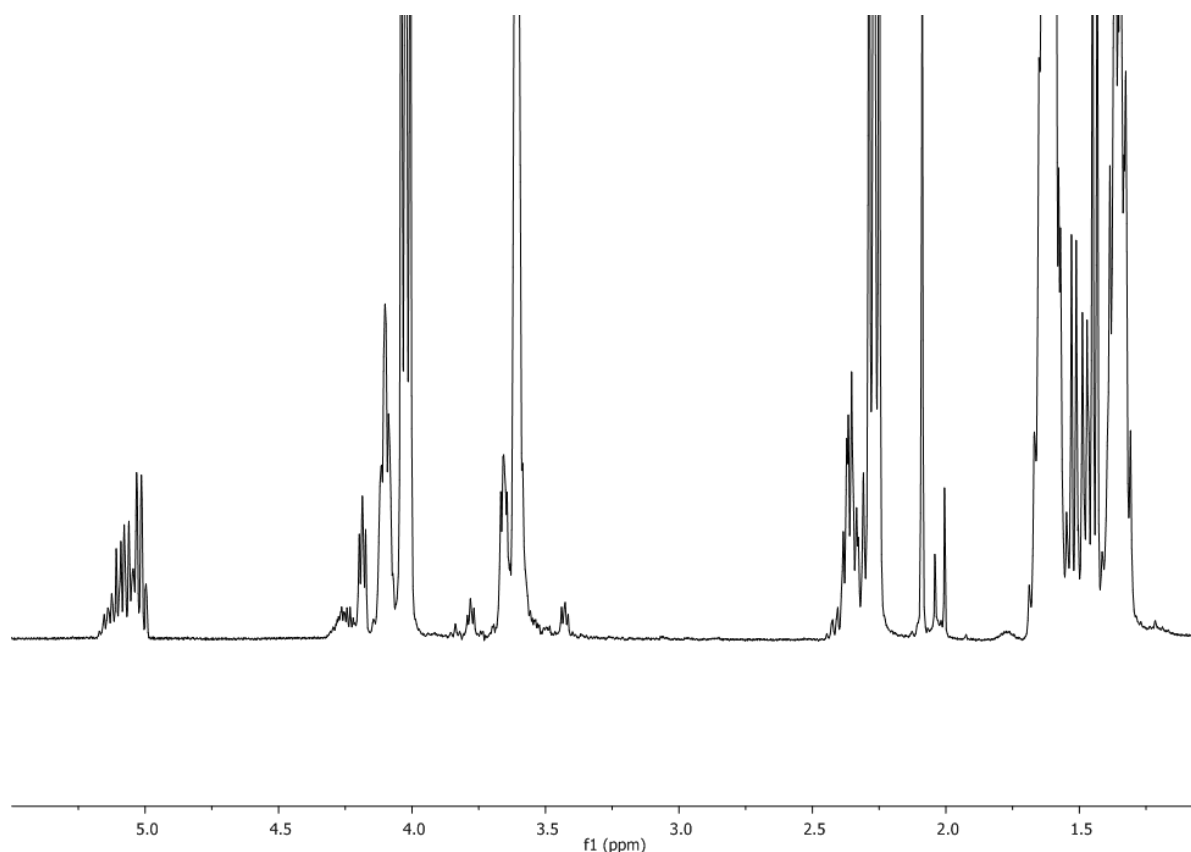


**Figure 1:**  $^1\text{H}$  NMR spectrum of acetyl-capped PCLA-PEG-PCLA in  $\text{CDCl}_3$ .

The formulation without celecoxib as well as that loaded with 50 mg celecoxib/g ('low CLB gel') were injectable sols at room temperature and gels at  $37^\circ\text{C}$ . However, 'high CLB gel' was a paste at room temperature and above, but could still be injected through an 18 G needle, which is the size mostly used to inject medications into horse joints.

**Table 1:** Characteristics of the acetyl-capped PCLA-PEG-PCLA triblock copolymer used in this study

<i>Polymer</i>	<i>Acetyl-PCLA-PEG-PCLA-Acetyl</i>
PEG feed [g]	50
$\epsilon$ -caprolactone feed [g]	88
L-lactide feed [g]	22
Acetic anhydride feed [g]	11.1
Aimed $M_n$ [g/mol]	4900
yield [%]	81
PCLA/PEG <sup>a)</sup>	1.9
CL/LA [mol/mol] <sup>b)</sup>	2.7
DM <sup>c)</sup>	~2
$M_n$ <sup>d)</sup> [g/mol]	4300

a) weight ratio of PCLA to PEG determined by <sup>1</sup>H NMR

b) weight ratio of  $\epsilon$ -caprolactone to L-lactide determined by <sup>1</sup>H NMR

c) degree of modification represents the number of end groups per triblock copolymer determined by <sup>1</sup>H NMR

d) number average molecular weight determined by <sup>1</sup>H NMR

**Table 2:** Effect of autoclaving on acetyl-capped PCLA-PEG-PCLA of 25 wt% in buffer as measured by <sup>1</sup>H NMR, GPC, oscillatory rheometry and pH.

<i>Treatment</i>	$M_{n,NMR}$ [g/mol]	<i>GPC</i>		$G'_{max}$ [Pa]	<i>pH</i>
		$M_n$ [g/mol]	<i>PDI</i>		
none	4600	4900	1.40	192	7.1
121 °C for 15 minutes	4600	5000	1.42	154	6.9

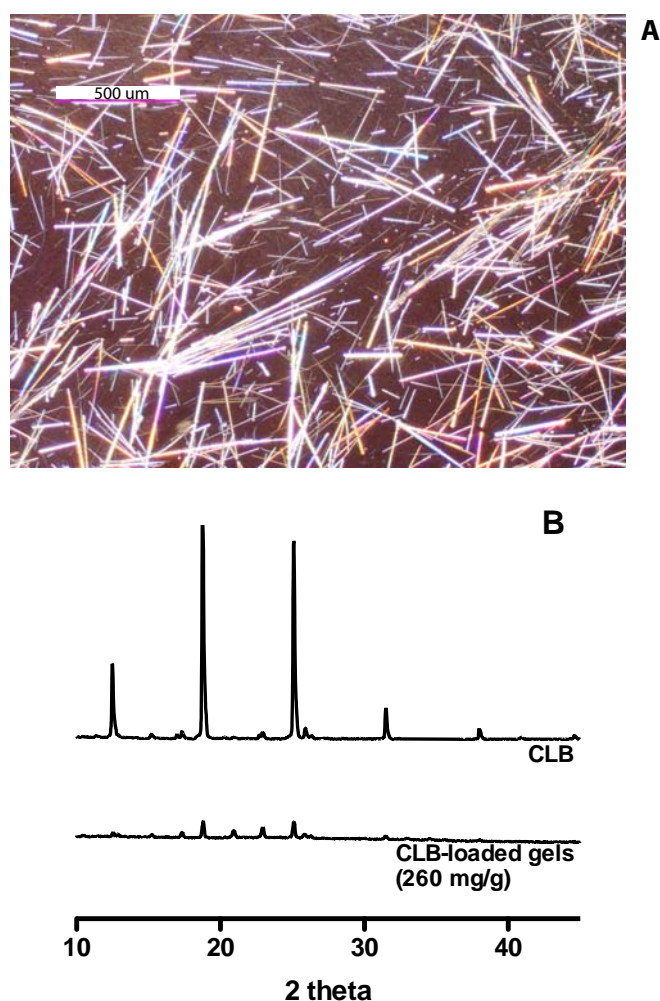


**Figure 2:** Samples of ‘high CLB gel’ (260 mg celecoxib per g gel). 2A shows a microphotograph (magnification = 10×). 2B shows the X-ray diffraction pattern of celecoxib and the gel.

Table 2 shows that no significant effects of the autoclaving of unloaded systems of 25 wt% in buffer compared to control were observed as measured by GPC and oscillatory rheology measurements, even though a slight decrease of ~40 Pa was observed for  $G'_{\max}$  (i.e. the maximum value of  $G'$  in the temperature range 4 to 50 °C). Table 2 shows a slight drop in pH from 7.1 to 6.9 after autoclaving, which might indicate formation of traces of acidic degradation products. Sterilization of polyester-based drug delivery systems by autoclaving have not been reported, likely because significant hydrolysis of the polymers will occur. We hypothesized that autoclaving of our systems with only minimal hydrolysis of the polyester chains is possible

because of the presence of end-capping groups, which slows down back biting reactions and thus in turn degradation [21,28-30].

### *3.3. Clinical response to intra-articular injection of the gels*

All horses were free of lameness prior to injection and none of the limbs injected with Hyonate®, ‘placebo’ or ‘low CLB gel’ showed signs of lameness throughout the study. However, four of the five horses, which received an injection of ‘high CLB gel’ in their left tarsus showed signs of lameness 24 hours post injection (average lameness score was  $1.6 \pm 1.3$  on a 5-point scale). The lameness was only temporary as at 72 hours post injection it had disappeared. These temporary adverse clinical symptoms can be ascribed to the acute inflammatory response to ‘high CLB gel’, likely triggered by the presence of needles of crystalline celecoxib (Figure 2A).

### *3.4. Synovial fluid analysis*

Figure 3 shows the WBC count, total protein count, GAG content and C2C content in synovial fluid prior and post injection of Hyonate®, ‘placebo’ and celecoxib-loaded gels. At 8 hours post injection, the synovial fluid from joints injected with Hyonate®, ‘low CLB gel’ or ‘high CLB gel’ all had an increased WBC count ( $>10 \times 10^9$  cells/l) compared to synovial fluid from joints injected with ‘placebo’. At 24 hours post injection, only WBC in joints treated with Hyonate and ‘high CLB gel’ remained significantly increased ( $\sim 30$  and  $\sim 20 \times 10^9$  cells/l, respectively). At 72 hours post injection, the WBC count of all injected joints returned to control levels ( $\sim 2 \times 10^9$  cells/l) and remained at this level until the end of the study (Figure 3A), indicating that the inflammatory response to the gels was transient and of a similar magnitude as after Hyonate® injection.

Concentrations of synovial fluid proteins are known to vary with the extent of joint inflammation [31,40,42]. At 8 hours post injection, the synovial fluid from joints injected with ‘placebo’ or ‘high CLB gel’ had an increased protein content ( $\sim 4$  g/dl) compared to synovial fluid from joints injected with Hyonate or ‘low CLB gel’ (1-2 g/dl). At 24 hours post injection, the synovial fluid from joints injected with ‘placebo’ or ‘high CLB gel’ had still an increased protein content of 4 g/dl, whereas the synovial

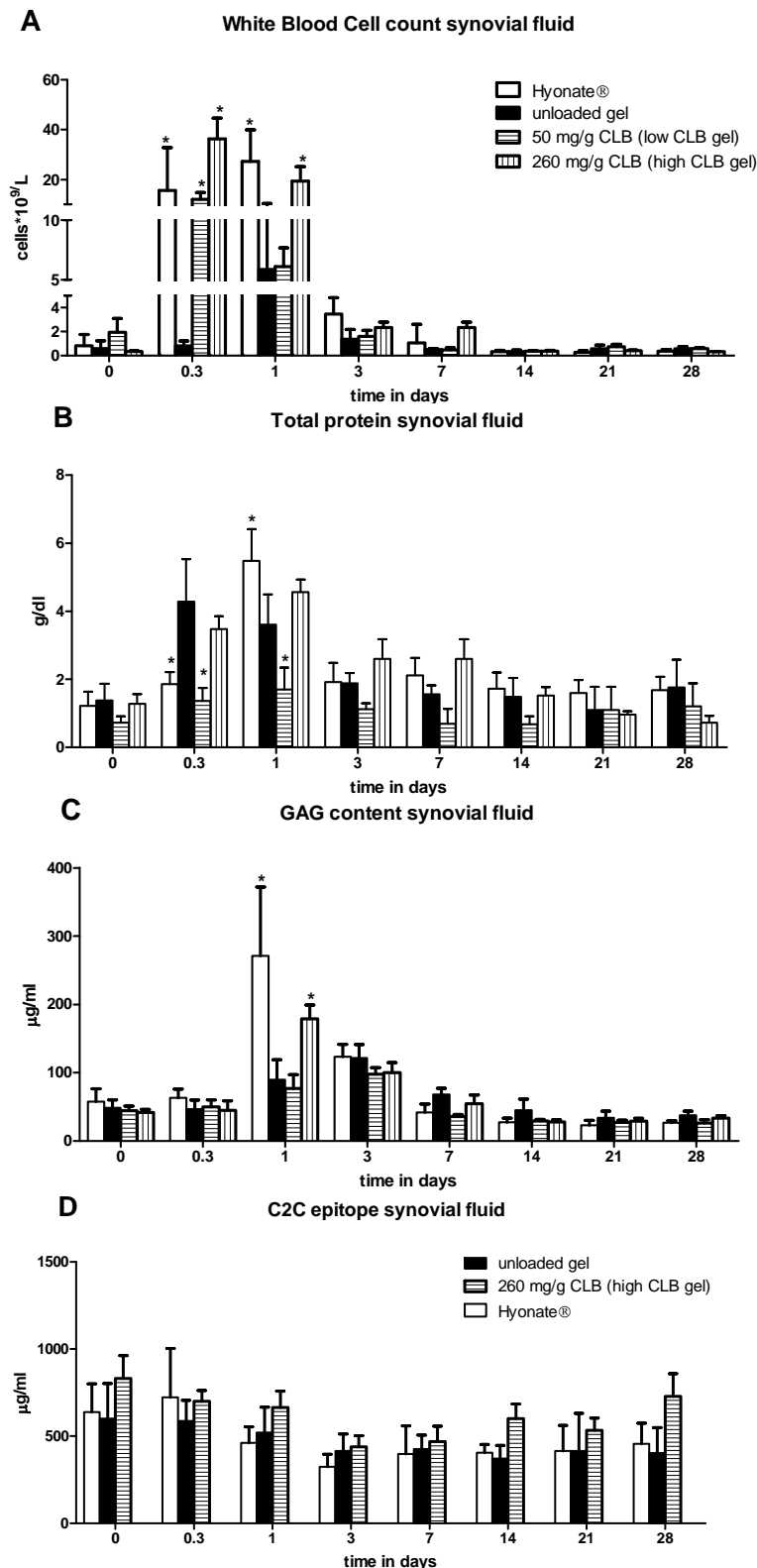


**Figure 3:** Synovial fluid analysis. 2A shows the white blood cell count. 2B shows the total protein levels. 2C shows the GAG content. 2D shows the C2C content. Values are depicted as mean $\pm$ SEM (n = 5); \*:  $p < 0.05$  vs. 'placebo'.



fluid from joints injected with ‘low CLB gel’ remained close to baseline, and that of Hyonate® had an increased protein content of 6 g/dl. Just like WBC, the total protein concentrations returned to control levels 72 hours post injection (Figure 3B), again indicating that the inflammatory response due to the injected gel was transient and in the same range as after Hyonate® injection.

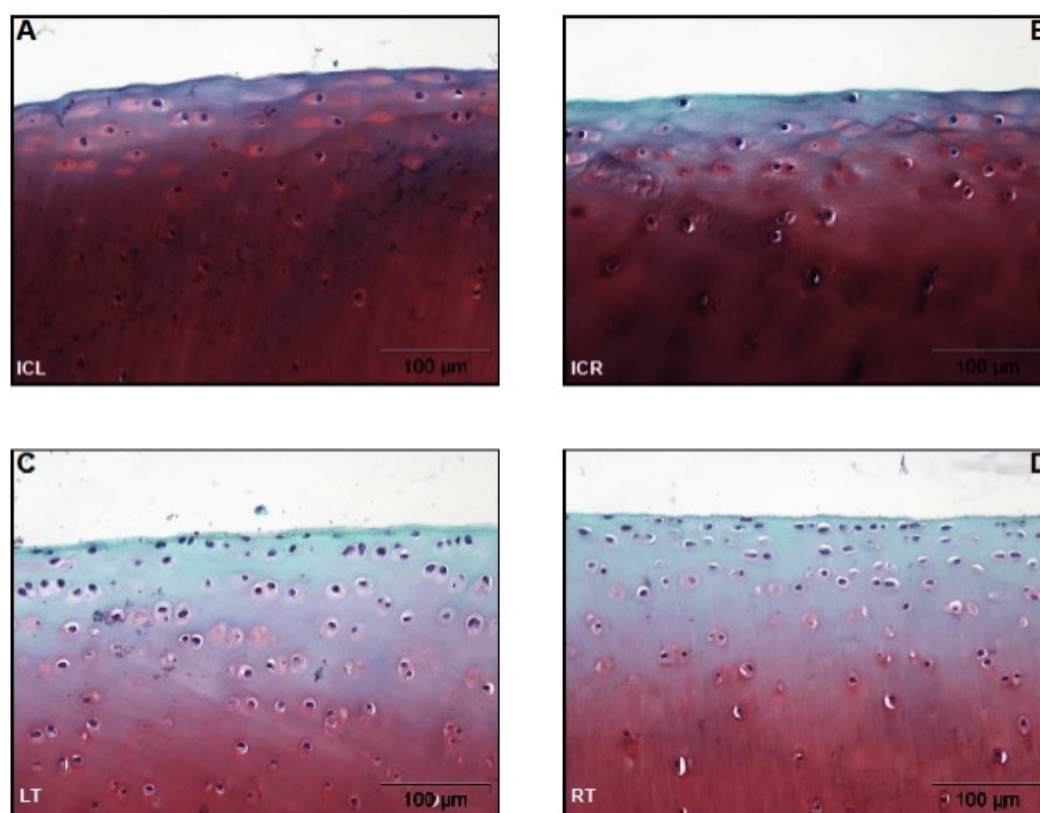


**Figure 4:** Representative histological sections of cartilage harvested from injected joints stained with Safranin O/ Fast green. 4A shows full thickness cartilage harvested from a joint injected with Hyonate® 8 weeks post injection. 4B shows full thickness cartilage harvested from a joint injected with ‘placebo’ 8 weeks post injection. 4C shows full thickness cartilage harvested from a joint injected with ‘high CLB gel’ 4 weeks post injection. 4D shows full thickness cartilage harvested from a joint injected with ‘low CLB gel’ 8 weeks post injection.

To determine whether the inflammatory response had a detrimental effect on the cartilage, the GAG content as well as the concentration of the C2C epitope of collagen in the synovial fluid samples was measured. Figure 3C shows the total GAG content in the synovial fluid samples. At 8 hours post

injection, the synovial fluid from all injected joints showed a GAG content in the range of the baseline level (50 µg/ml). At 24 hours post injection, the synovial fluid from joints injected with Hyonate® or 'high CLB gel' had an increased GAG content (271 and 197 µg/ml, respectively). Just like WBC and protein content, the GAG concentrations returned to control levels 72 hours post injection, again indicating that the inflammatory response due to the injected gel was transient and in the same range as after Hyonate® injection.

Figure 3D shows the concentration of the C2C epitope of collagen type II, a biomarker for cartilage damage [31,42]. There were no significant differences in level of C2C epitope of collagen between the Hyonate®, 'placebo' and the celecoxib-loaded gels indicating that the treatments did not have adverse effects on the collagen component of the cartilage.

To further confirm this finding, histological staining of cartilage harvested from the injected joints was performed. Figures 4A-D show representative histological sections of cartilage from the joints injected with Hyonate®, 'placebo' and the celecoxib-loaded gels. The surface of the cartilage was smooth, indicating that the treatments had not damaged the structural components of the cartilage. Moreover, the intact cartilage stained deeply reddish with safranin-O for glycosaminoglycans, which further demonstrates that no lasting cartilage damage occurred, as there were no differences between Hyonate®, 'placebo', 'low CLB gel' and 'high CLB gel'. Any GAG loss from the extracellular matrix of the cartilage, as may have occurred shortly after the injection given the temporary rise in synovial fluid GAG content, was hence repaired in the following period. It is known that in articular cartilage damage GAG loss is reversible, as long as the collagen network remains intact [48]. The fact that no increase occurred in C2C content demonstrates there was no significant damage to the collagen network in our study. Thus, the gels were well tolerated. Larsen et al. [49] reported the injection into equine carpal joints of 2 ml *in situ* forming depot composed of PEG<sub>400</sub> and celecoxib loaded at 290 mg celecoxib per g solution, which is similar to the dose of the 'high CLB gel' (2 ml of 260 mg celecoxib per g gel). They did however report the presence of granulomatous synovitis 10 days after i.a. injection of the PEG<sub>400</sub> solution of celecoxib, and the

synovial membrane being hyperaemic, which indicate tolerability issues of their system.

### *3.5. In vivo release of celecoxib from gels administered in the horse joints*

After administration of the 'low CLB gel' and 'high CLB gel', the celecoxib concentrations in synovial fluid as well as in plasma were measured over time. Figure 6 shows the celecoxib concentrations in synovial fluid. Celecoxib concentration in synovial fluid 8 hours after i.a. administration was 20-25 µg/ml and independent of the type of gel administered. For the 'low CLB gel', the  $C_{\max}$  of celecoxib in synovial fluid was reached at 8 hours (four animals) and 24 hours (one animal) post injection ( $23.6 \pm 6.6$  µg/ml). For the 'high CLB gel', the  $C_{\max}$  of celecoxib in synovial fluid was reached at 8 hours (three animals) and 72 hours (one animal) with a  $t_{\max}$  at 24 hours for one animal and was  $36 \pm 14$  µg/ml. The high values of the  $C_{\max}$  are in line with celecoxib solubility in 10 % FSB solution, which was found to be 10-20 µg/ml likely due to celecoxib solubilization by proteins. After  $t_{\max}$ , the celecoxib concentration in synovial fluid of the joints treated with 'low CLB gel' rapidly decreased in time reaching a concentration of  $0.034 \pm 0.041$  µg/ml 7 days post injection, whereas the celecoxib concentration in synovial fluid taken from the joints that received 'high CLB gel' decreased more slowly to reach  $1.6 \pm 1.4$  µg/ml at day 7 and finally dropped at day 28 below 0.1 µg/ml. The calculated AUC in synovial fluid was  $30.8 \pm 8.9$  and  $113 \pm 85$  µg×d/ml for the joints that received the 'low CLB gel' and 'high CLB gel', respectively. Thus, there is a factor 3-4 difference in the AUCs between the joints that received the 'low CLB gels' and 'high CLB gels', which is in the range of the factor ~5 difference in loading between the two administered gels (50 and 260 mg/g, respectively). Table 3 summarizes the pharmacokinetics values.

Figure 7 shows that serum celecoxib concentrations in horses that received the celecoxib-loaded gels were detected up to 72 hours. The  $C_{\max}$  of celecoxib in plasma was reached at 8 hours (one animal) and 24 hours (four animals) post injection ( $81 \pm 72$  and  $230 \pm 220$  ng/ml for 'low CLB gel' and 'high CLB gel', respectively). The plasma  $C_{\max}$  values were thus 150 and 330 times lower than in synovial fluid for 'low CLB gel' and 'high CLB gel', respectively. It is remarkable that the serum  $C_{\max}$  coincided with the maximum of the inflammatory response (Figure 3A-B), which indicates that celecoxib leaked

from the joint into the periphery most likely because of the increased vascular permeability due to the inflammatory response in the joints [50,51]. In line with the biochemical analysis of the synovial fluid (WBC, protein count) showing inflammation for 3-7 days, no celecoxib could be detected in plasma at 7 days. The AUC in serum was  $0.177 \pm 0.075$  and  $0.38 \pm 0.33 \mu\text{g} \times \text{d}/\text{ml}$  for horses that received ‘low CLB gel’ and ‘high CLB gel’, respectively. Thus, there is a factor 2-3 difference between the serum AUC of animals that received the ‘low CLB gels’ and ‘high CLB gels’, which is in line with that of synovial fluid.

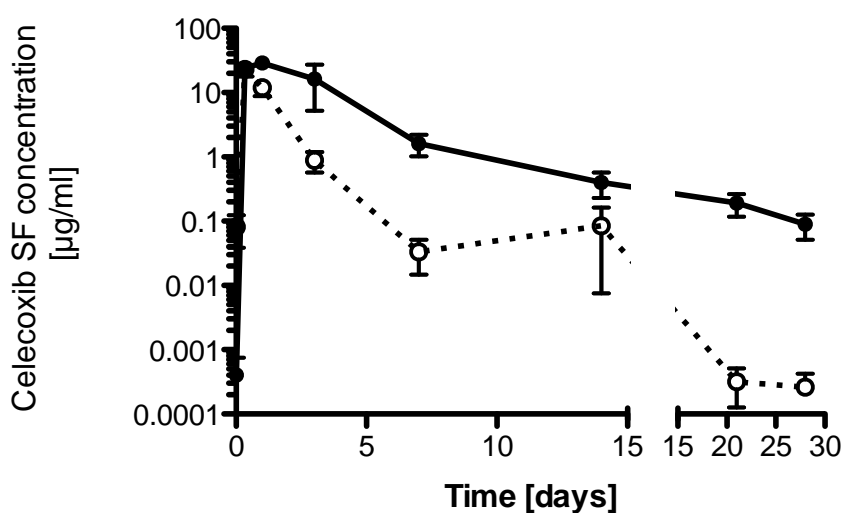


**Figure 6:** Celecoxib concentrations in synovial fluid after i.a. administration of ‘low CLB gel’ (open circles) and ‘high CLB gel’ (closed circles) loaded with 50 and 260 mg celecoxib per g gel, respectively.

In the earlier referred study by Larsen et al. [49], celecoxib was detected in serum samples for ten days after intra-articular administration of a formulation of celecoxib in PEG<sub>400</sub>, but they could not quantify these low concentrations (~1 ng/ml) and no data regarding celecoxib concentrations in synovial fluid were reported. Although we show a higher systemic exposure to celecoxib in the present study than reported by Larsen et al., we found a shorter systemic exposure time.

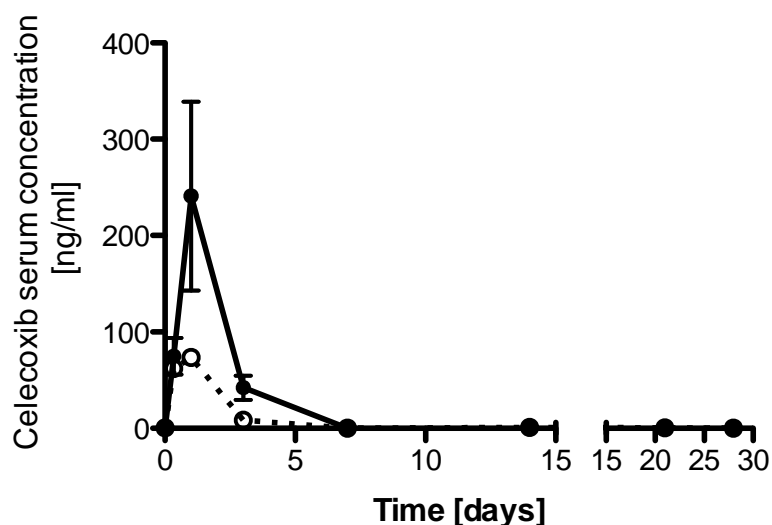


**Figure 7:** Celecoxib concentrations in serum after i.a. administration of ‘low CLB gel’ (open circles) and ‘high CLB gel’ (closed circles) loaded at 50 and 260 mg celecoxib per g gel, respectively.

**Table 3:** Pharmacokinetics parameters of celecoxib in synovial fluid and in serum as calculated by the PKsolver after injection of ‘low CLB gel’ and ‘high CLB gel’.

	<i>‘Low CLB gel’</i>		<i>‘High CLB gel’</i>	
	<i>Synovial fluid</i>	<i>Serum</i>	<i>Synovial fluid</i>	<i>Serum</i>
$t_{\max}$ [h]	8-24	8-24	8-72	8-24
$C_{\max}$ [ $\mu\text{g}/\text{ml}$ ]	23.6 $\pm$ 6.6	0.081 $\pm$ 0.072	36 $\pm$ 13	0.23 $\pm$ 0.22
AUC [ $\mu\text{g}\times\text{d}/\text{ml}$ ]	30.8 $\pm$ 8.9	0.18 $\pm$ 0.08	113 $\pm$ 85	0.38 $\pm$ 0.33

A study by Gika et al. [52] showed that in only six out of seventeen patients, treated with 200 mg celecoxib/day for 5 days orally, celecoxib could be detected in synovial fluid (0.33-0.79  $\mu\text{g}/\text{ml}$ ), while the plasma concentrations after oral administration (200 mg/day for 5 days) ranged from 350-1850 ng/ml. In the present study, 8 hours after administration of the celecoxib-loaded gels, a celecoxib concentration in the synovial fluid of 20-25  $\mu\text{g}/\text{ml}$  was reached (Figure 6), thus  $\sim$ 50 times higher than that after

oral administration [52]. Importantly, 24 hours after a single injection of the celecoxib-loaded gels, the peak serum concentration was 75-145 ng/ml (Figure 7), thus 5-25 times lower than that after oral administration [52]. Hence, by using *in situ* forming gels based on acetyl-capped PCLA-PEG-PCLA triblock copolymers loaded with celecoxib, we greatly improved the celecoxib concentrations in synovial fluid while drastically reducing the exposure to systemic concentrations of the drug. It can be assumed that, by reducing the systemic celecoxib concentrations through local delivery, the occurrence of side effects will also be reduced [53].

#### 4. Conclusions

This study demonstrates that gels based on acetyl-capped PCLA-PEG-PCLA triblock copolymer loaded with celecoxib have potential for successful local drug delivery for the treatment of osteoarthritis. It is shown that injection in the joints of horses results in high local celecoxib concentrations in the joint for a prolonged time, while significantly limiting systemic exposure. Histological and synovial fluid analyses showed that the gels had a good tolerability and did not result in damage of the cartilage. These gels are therefore attractive vehicles for local drug administration which generate high local doses without the risk of side effects associated with oral administration and have therefore potential for clinical applications.

#### Acknowledgments

Mike de Leeuw and Dr. Theo Flipsen are gratefully acknowledged for their support and valuable discussions. This work is part of the BMM/Term program (Project P2.02) and the Dutch Ministry of Economic Affairs is thanked for their financial support.

## References

- [1] Odding E, Valkenburg HA, Stam HJ, Hofman A. Determinants of locomotor disability in people aged 55 years and over: the Rotterdam Study. *Eur J Epidemiol* 2001;17:1033-1041.
- [2] Suri P, Morgenroth DC, Hunter DJ. Epidemiology of osteoarthritis and associated comorbidities. *P M R* 2012;4:S10-S19.
- [3] van Weeren PR, de Grauw JC. Pain in osteoarthritis. *Vet Clin North Am Equine Pract* 2010;26:619-642.
- [4] Roth SH, Anderson S. The NSAID dilemma: managing osteoarthritis in high-risk patients. *Phys Sportsmed* 2011;39:62.
- [5] Mastbergen SC, Bijlsma JW, Lafeber FP. Selective COX-2 inhibition is favorable to human early and late-stage osteoarthritic cartilage: a human *in vitro* study. *Osteoarthritis Cartilage* 2005;13:519-526.
- [6] Gong L, Thorn CF, Bertagnolli MM, Grosser T, Altman RB, Klein TE. Celecoxib pathways: pharmacokinetics and pharmacodynamics. *Pharmacogenet Genomics* 2012;22:310-318.
- [7] Brophy JM. Celecoxib and cardiovascular risks. *Expert Opin Drug Saf* 2005;4:1005-1015.
- [8] Edwards SHR. Intra-articular drug delivery: the challenge to extend drug residence time within the joint. *Vet J* 2011;190:15-21.
- [9] Jiang D, Zou J, Huang L, Shi Q, Zhu X, Wang G, et al. Efficacy of intra-articular injection of celecoxib in a rabbit model of osteoarthritis. *Int J Mol Sci* 2010;11:4106-4113.
- [10] Butoescu N, Jordan O, Doelker E. Intra-articular drug delivery systems for the treatment of rheumatic diseases: a review of the factors influencing their performance. *Eur J Pharm Biopharm* 2009;73:205-218.
- [11] Larsen C, Østergaard J, Larsen SW, Jensen H, Jacobsen S, Lindegaard C, et al. Intra-articular depot formulation principles: role in the management of postoperative pain and arthritic disorders. *J Pharm Sci* 2008;97:4622-4654.

- [12] Gerwin N, Hops C, Lucke A. Intra-articular drug delivery in osteoarthritis. *Adv Drug Deliv Rev* 2006;58:226-242.
- [13] Hameed F, Ihm J. Injectable medications for osteoarthritis. *PM R* 2012;4:S75-81.
- [14] Xavier A. Injections in the treatment of osteoarthritis. *Best Pract Res Clin Rheumat* 2001;15:609-626.
- [15] Chan A, Orme RP, Fricker RA, Roach P. Remote and local control of stimuli responsive materials for therapeutic applications. *Adv Drug Deliv Rev* 2013;65:497-514.
- [16] Ko DY, Shinde UP, Yeon B, Jeong B. Recent progress of *in situ* formed gels for biomedical applications. *Prog Polym Sci* 2013;38:672-701.
- [17] Wolinsky JB, Colson YL, Grinstaff MW. Local drug delivery strategies for cancer treatment: gels, nanoparticles, polymeric films, rods, and wafers. *J Control. Release* 2012;159:14-26.
- [18] Vermonden T, Censi R, Hennink WE. Hydrogels for protein delivery. *Chem Rev* 2012;112:2853-2888.
- [19] Bonacucina G, Cespi M, Mencarelli G, Giorgioni G, Palmieri GF. Thermosensitive self-assembling block copolymers as drug delivery systems. *Polymers* 2011;3:779-811.
- [20] van Tomme SR, Storm G, Hennink WE. *In situ* gelling hydrogels for pharmaceutical and biomedical applications. *Int J Pharm* 2008;355:1-18.
- [21] Petit A, Sandker M, Müller B, Meyboom R, van Midwoud P, Redout EM, et al. Celecoxib-loaded acetyl-capped PCLA-PEG-PCLA thermogels: *in vitro* and *in vivo* release behavior and intra-articular biocompatibility. Submitted
- [22] Zentner GM, Rathi R, Shih C, McRea JC, Seo M, Oh H, et al. Biodegradable block copolymers for delivery of proteins and water-insoluble drugs. *J Control Release* 2001;72:203-215.
- [23] Qiao M, Chen D, Ma X, Liu Y. Injectable biodegradable temperature-responsive PLGA-PEG-PLGA copolymers: synthesis and effect of copolymer composition on the drug release from the copolymer-based hydrogels. *Int J Pharm* 2005;294:103-112.



- [24] Gao Y, Ren F, Ding B, Sun N, Liu X, Ding X, et al. A thermo-sensitive PLGA-PEG-PLGA hydrogel for sustained release of docetaxel. *J Drug Target* 2011;19:516-527.
- [25] Elstad NL, Fowers KD. OncoGel® (ReGel®/paclitaxel) - clinical applications for a novel paclitaxel delivery system. *Adv Drug Deliv Rev* 2009;61:785-794.
- [26] Bramfeldt H, Sarazin P, Vermette P. Characterization, degradation, and mechanical strength of poly(D,L-lactide-*co*- $\epsilon$ -caprolactone)-poly(ethylene glycol)-poly(D,L-lactide-*co*- $\epsilon$ -caprolactone). *J Biomed Mater Res A* 2007;83A:503-511.
- [27] Zhang Z, Ni J, Chen L, Yu L, Xu J, Ding J. Biodegradable and thermoreversible PCLA-PEG-PCLA hydrogel as a barrier for prevention of post-operative adhesion. *Biomaterials* 2011;32:4725-4736.
- [28] Petit A, Müller B, Meijboom R, Bruin P, van de Manakker F, Versluijs-Helder M, et al. Effect of polymer composition on rheological and degradation properties of temperature-responsive gelling systems composed of acyl-capped PCLA-PEG-PCLA. *Biomacromolecules* 2013;14:3172-3182.
- [29] Petit A, Müller B, Bruin P, Meijboom R, Piest M, Kroon-Batenburg LMJ, et al. Modulating the rheological and degradation properties of hydrogels composed of blends of PCLA-PEG-PCLA triblock copolymers and their fully hexanoyl-capped derivatives. *Acta Biomater* 2012;8:4260-4267.
- [30] Sandker MJ, Petit A, Redout EM, Siebelt M, Müller B, Bruin P, et al. *In situ* forming acyl-capped PCLA-PEG-PCLA triblock copolymer based hydrogels. *Biomaterials* 2013;34:8002-8011.
- [31] Ross TN, Kisiday JD, Hess T, McIlwraith CW. Evaluation of the inflammatory response in experimentally induced synovitis in the horse: a comparison of recombinant equine interleukin 1 beta and lipopolysaccharide. *Osteoarthritis Cartilage* 2012;20:1589-1590.
- [32] Gregory MH, Capito N, Kuroki K, Stoker AM, Cook JL, Sherman SL. A review of translational animal models for knee osteoarthritis. *Arthritis* 2012;2012:764621.
- [33] Goodrich LR, Nixon AJ. Medical treatment of osteoarthritis in the horse - a review. *Vet J* 2006;171:51-69.
- [34] Peyron JG. Intraarticular hyaluronan injections in the treatment of osteoarthritis: state-of-the-art review. *J Rheumatol Suppl* 1993;39:10-15.

- [35] Colen S, van den Bekerom MP, Mulier M, Haverkamp D. Hyaluronic acid in the treatment of knee osteoarthritis: a systematic review and meta-analysis with emphasis on the efficacy of different products. *BioDrugs* 2012;26:257.
- [36] Trigkilidas D, Anand A. The effectiveness of hyaluronic acid intra-articular injections in managing osteoarthritic knee pain. *Ann R Coll Surg Engl* 2013;95:545-551.
- [37] Brandt KD, Smith GNJ, Simon LS. Intra-articular injection of hyaluronan as treatment for knee osteoarthritis: what is the evidence? *Arthritis Rheum* 2000;43:1192-1203.
- [38] Reichenbach S, Blank S, Rutjes AW, Shang A, King EA, Dieppe PA, et al. Hyaluronan versus hyaluronic acid for osteoarthritis of the knee: a systematic review and meta-analysis. *Arthritis Rheum* 2007;15:1410-1408.
- [39] Jo S, Kim J, Kim SW. Reverse thermal gelation of aliphatically modified biodegradable triblock copolymers. *Macromol Biosci* 2006;6:923-928.
- [40] Bertone AL, Palmer JL, Jones J. Synovial fluid cytokines and eicosanoids as markers of joint disease in horses. *Vet Surg* 2001;30:528-538.
- [41] de Grauw JC, van de Lest CH, Brama PA, Rambags BP, van Weeren PR. *In vivo* effects of meloxicam on inflammatory mediators, MMP activity and cartilage biomarkers in equine joints with acute synovitis. *Equine Vet J* 2009;41:693-966.
- [42] de Grauw JC, van de Lest CH, van Weeren PR. Inflammatory mediators and cartilage biomarkers in synovial fluid after a single inflammatory insult: a longitudinal experimental study. *Arthritis Res Ther* 2009;11:R35.
- [43] Zhang Y, Huo M, Zhou J, Xie S. PKSolver: an add-in program for pharmacokinetic and pharmacodynamic data analysis in Microsoft Excel. *Comput Methods Programs Biomed* 2010;99:306-314.
- [44] Paulson SK, Kaprak TA, Gresk CJ, Fast DM, Baratta MT, Burton EG, et al. Plasma protein binding of celecoxib in mice, rat, rabbit, dog and human. *Biopharm Drug Dispos* 1999;20:293-299.
- [45] van Loon JP, de Grauw JC, van Dierendonck M, L'ami JJ, Back W, van Weeren PR. Intra-articular opioid analgesia is effective in reducing pain and inflammation in an equine LPS induced synovitis model. *Equine Vet J* 2010;42:412-419.

- [46] Zheng X, Baker H, Hancock WS, Fawaz F, McCaman M, Pungor EJ. Proteomic analysis for the assessment of different lots of fetal bovine serum as a raw material for cell culture. Part IV. Application of proteomics to the manufacture of biological drugs. *Biotechnol Prog* 2006;22:1294-1300.
- [47] Gawlitta D, van Rijen MH, Schrijver EJ, Alblas J, Dhert WJ. Hypoxia impedes hypertrophic chondrogenesis of human multipotent stromal cells. *Tissue Eng Part A* 2012;18:1957-1966.
- [48] Hosseininia S, Lindberg LR, Dahlberg LE. Cartilage collagen damage in hip osteoarthritis similar to that seen in knee osteoarthritis; a case-control study of relationship between collagen, glycosaminoglycan and cartilage swelling. *BMC Musculoskelet Disord* 2013;14:18.
- [49] Larsen SW, Frost AB, Østergaard J, Thomsen MH, Jacobsen S, Skonberg C, et al. *In vitro* and *in vivo* characteristics of celecoxib *in situ* formed suspensions for intra-articular administration. *J Pharm Sci* 2011;100:4330-4337.
- [50] Szekanecz Z, Koch A. Vascular involvement in rheumatic diseases: 'vascular rheumatology'. *Arthritis Res Ther* 2008;10:224.
- [51] Yehia SR, Duncan H. Synovial fluid analysis. *Clin Orthop Relat Res* 1975;107:1-24.
- [52] Gika HG, Theodoridou A, Michopoulos F, Theodoridis G, Diza E, Settas L, et al. Determination of two COX-2 inhibitors in serum and synovial fluid of patients with inflammatory arthritis by ultra performance liquid chromatography–inductively coupled plasma mass spectroscopy and quadrupole time-of-flight mass spectrometry. *J Pharm Biomed Anal* 2009;49:579-586.
- [53] Coxib and traditional NSAID Trialists' (CNT) Collaboration, Bhala N, Emberson J, Merhi A, Abramson S, Arber N, et al. Vascular and upper gastrointestinal effects of non-steroidal anti-inflammatory drugs: meta-analyses of individual participant data from randomised trials. *Lancet* 2013 Aug 31;382(9894):769-79 2013;382:769-779.

## Appendices

### Equation

**Equation A.1:** Theoretical number of methylene protons in PEG<sub>1500</sub> per mole,  $I_{PEG}$

$$I_{PEG} = 4 \times \left( \frac{M_{PEG}}{M_{EG}} \right) = 136 \quad \text{with } M_{PEG} = 1500 \text{ g/mol and } M_{EG} = 44 \text{ g/mol.}$$

**Equation A.2:** Number of methylene protons in PEG at 3.72-3.55 ppm,  $I_{3.6}$

This value was determined by adding an excess of TCAI to PEG<sub>1500</sub>. The formation of  $\text{Cl}_3\text{C-NH-C(O)-(O-CH}_2\text{-CH}_2)_n\text{-C(O)-NH-CCl}_3$  led to the formation of a new peak at 4.40 ppm ( $I_{4.4}$ , 4H,  $\text{Cl}_3\text{C-NH-C(O)-O-CH}_2\text{-CH}_2\text{-O-}$ ).

$I_{3.6} = 122$  for  $I_{4.4} = 4$ . This value is in agreement with the expected value of  $136 - 4 = 132$  H (as determined in Equation A.1.).

**Equation A.3:** Number of CL-CL bonds per mol PEG

$$n_{CL-CL} = I_{2.2} / 2 \quad \text{for normalized } I_{3.6} = 122.$$

**Equation A.4:** Number of CL-LA bonds per mol PEG

$$n_{CL-LA} = I_{2.3} / 2 \quad \text{for normalized } I_{3.6} = 122.$$

**Equation A.5:** Number of CL per polymer chain

$$n_{CL} = n_{CL-CL} + n_{CL-LA}.$$

**Equation A.6:** Number of LA per polymer chain

$$n_{LA} = I_{5.1} \quad \text{for normalized } I_{3.6} = 122.$$

**Equation A.7:** Molar ratio CL/LA

$$k = n_{CL} / n_{LA}.$$

**Equation A.8:** Number average molecular weight of PCLA

$$M_{n,PCLA} = n_{CL} \times 114 + n_{LA} \times 72.$$

**Equation A.9:** Weight CL content

$$CL(wt\%) = 100 \times \left[ \frac{(n_{CL} \times 114)}{M_{n,PCLA}} \right]$$

**Equation A.10:** Weight ratio PCLA / PEG

$$PCLA/PEG = \frac{M_{n,PCLA}}{M_{PEG}}$$

**Equation A.11:** Degree of Modification

$$DM(mol) = \frac{I_{CH_3-}}{3} \text{ for normalized } I_{3,6} = 122 \text{ with } I_{CH_3-} = I_{2.13} + I_{2.09} + I_{2.04}$$

**Equation A.12:** Number average molecular weight

$$M_{n,NMR} = M_{PEG} + M_{n,PCLA} + (x \times DM) \text{ with } x = 43$$

**Equation A.13:** Average length of the CL blocks

$$L_{CL} = (n_{CL-CL} / n_{LA-CL}) + 1$$

Chapter 6

**PK in horses**



## CHAPTER 7

# Summary and perspectives





## 1. Summary

The work described in this thesis is a part of the broader project, OAcontrol, which was financed by the Dutch public-private consortium Biomedical Materials (BMM). OAcontrol aimed at developing new treatments for osteoarthritis (OA). Within this project, the scope of this thesis work was to develop a drug delivery system for the local and sustained release of drugs into joints. During this development, many challenges needed to be overcome, which were related to the design of proper formulations for the delivery of the drugs of interest, and their efficacy and safety *in vivo*. A variety of injectable drug carriers have been developed to efficiently encapsulate and deliver drugs locally, for example, *in situ* forming depots. These systems are aimed at obtaining therapeutically effective concentrations of the encapsulated drug after local administration for prolonged times [1-5].

Amongst the polymers used to prepare those drug carriers, polyester/PEG block copolymers represent a large and various class of well-tolerated and biodegradable polymers with a broad range of physicochemical properties. They have been extensively investigated as biomedical materials for different applications such as use as implantable medical devices, in tissue engineering and in drug delivery. Amphiphilic polyester/PEG block copolymers form micellar suspensions in aqueous medium at low temperature. When these suspensions are brought to body temperature and above their critical gel concentration, they transform into viscoelastic hydrogels. Such systems have found clinical applications as *in situ* forming gels for drug delivery [6]. Interestingly, modification of the terminal hydroxyl groups of polyester-PEG-polyester copolymers allows modulation of the sol-to-gel transition temperature of these systems [7,8]. Therefore, one of the main themes of this thesis was to further understand the impact of this modification on rheological properties and degradation kinetics and to investigate whether such systems would enable local and sustained drug delivery in joints. In the studies described in this thesis, the non-steroidal anti-inflammatory drug (NSAID) celecoxib, which is used for the palliative oral treatment of OA, was chosen as the drug of choice.

**Chapter 1** provides an introduction to the challenges of OA therapy and an overview of temperature-responsive gelling systems made of polyester/PEG block copolymers. Particular attention is given to a subclass

of acylated poly( $\epsilon$ -caprolactone-*co*-lactide)-*b*-poly(ethylene glycol)-*b*-poly( $\epsilon$ -caprolactone-*co*-lactide) (PCLA-PEG-PCLA) triblock copolymers. Subsequently, the aim and outline of this thesis are presented.

In **Chapter 2**, the blending of a PCLA-PEG-PCLA triblock copolymer and its hexanoyl-capped derivative is described focusing on the temperature-responsive gelling behaviour and the modulation of rheological and degradation properties [9]. The cloud point of the blends was composition-dependent and could be tailored from 15 to 40 °C for blends containing 15 to 100 wt% uncapped polymer (and thus 85 to 0 % of the capped polymer). Aqueous systems with solid content between 20 and 30 wt% containing 15 to 25 wt% uncapped polymers showed a sol-to-gel transition temperature at 10-20 °C and are thus interesting injectable gels for drug delivery [10]. Complete degradation of these gels at pH 7.4 and 37 °C took ~100 days, independent of the blend ratio and the initial solid content. Interestingly, gel degradation is not due to chemical polymer hydrolysis but to polymer dissolution. The approach of blending uncapped and hexanoyl-capped polymers to prepare temperature-responsive gelling systems has however some limitations:

(i) the range of blending ratios, which results in temperature-responsive gelling systems, is rather narrow

(ii) temperature-responsive gelling systems prepared by this method quickly phase-separate at room temperature, which renders their handling difficult and might be detrimental for sustained delivery of water-soluble drugs as these drugs might preferentially partition in polymer-poor fractions and be released in a burst.

(iii) these systems dissolve in ~3-4 months, independent of the blending ratio and the initial solid content, whereas modulation of degradation time is highly desired to match the requirements of specific therapies.

To circumvent these shortcomings, the relationships between composition, PCLA microstructure, rheological and degradation properties are investigated in **Chapter 3** using a design of experiments [11]. Eight polymers with varying molecular weights of PCLA, caproyl/lactoyl ratios (CL/LA) and capped with either acetyl- or propionyl-groups were synthesized. Rheological and degradation/dissolution properties of aqueous systems composed of the polymers at 25 wt% concentration were studied. <sup>1</sup>H NMR analysis revealed

that the monomer sequence in the PCLA blocks was not fully random, resulting in relatively long CL sequences, even though transesterification was demonstrated by the enrichment with lactoyl units and the presence of PEG-OH end groups. Except the most hydrophilic polymer of acetyl-capped PCLA<sub>1400</sub>-PEG<sub>1500</sub>-PCLA<sub>1400</sub> with a CL/LA molar ratio of 2.5, all the polymers of 25 wt % in buffer were sols below room temperature and transformed into gels between room temperature and 37 °C, which makes them suitable as temperature-responsive gelling systems for drug delivery. Over a period of weeks at 37 °C, the systems containing polymers with long CL sequences (~8 CL units) and propionyl end-groups became semi-crystalline, as shown by X-ray diffraction analysis. Degradation of the gels by dissolution at pH 7.4 and 37 °C took 100-150 days for the amorphous gels and 250-300 days for the semi-crystalline gels. In conclusion, this chapter shows that changes in the polymer composition allow an easy modulation of both rheological and degradation properties.

To get more insight into the tolerability and biodegradation of *in situ* forming hydrogels made of acyl-capped PCLA-PEG-PCLA copolymers, polymers capped with triiodobenzoyl (TIB) groups were synthesized as a means to prepare radiopaque systems in **Chapter 4** [12]. TIB capping renders the gel radiopaque properties, enabling its *in vivo* visualization and quantification using micro-computed tomography ( $\mu$ CT). A gel containing TIB-capped polymer degraded *in vitro* (37 °C, pH 7.4) through dissolution over a period of ~20 weeks, and degraded slightly faster (~12 weeks) after subcutaneous injection in rats. This *in vivo* acceleration is likely due to active (enzymatic) degradation, shown by changes in polymer composition and molecular weight as well as by the presence of macrophages at the injection site. After intra-articular administration in rats, the visualized gel gradually lost signal intensity over the course of 4 weeks. Also, good cytocompatibility of an acetyl-capped polymer-based hydrogel was proven *in vitro* for erythrocytes and chondrocytes. Moreover, the intra-articular tolerability of this gel was demonstrated using  $\mu$ CT-imaging and histology, since both techniques showed no changes in cartilage quality and/or quantity.

In **Chapter 5**, the *in vitro* and *in vivo* properties and performance of a celecoxib-loaded hydrogel based on a fully acetyl-capped PCLA-PEG-PCLA triblock copolymer were investigated [13]. Mixtures of different compositions

of celecoxib and the acetyl-capped PCLA-PEG-PCLA triblock copolymer were added to buffer to yield temperature-responsive gelling systems. These systems containing up to 50 mg celecoxib per g gel were sols at room temperature and convert into immobile gels at 37 °C. *In vitro* release of celecoxib started after a ~10 days lag phase followed by a sustained release of ~90 days. Celecoxib release was shown to be mediated *in vitro* by polymer dissolution of the gels. *In vivo* (subcutaneous injection in rats) experiments showed an initial celecoxib release of 25 % of the loading during the first 3 days followed by a sustained release of celecoxib for 30-60 days. The absence of a lag phase and the faster release seen *in vivo* are likely due to the enhanced celecoxib solubility in biological fluids and active degradation of the gels by enzymes and/or macrophages, respectively. Finally, intra-articular tolerability of the 50 mg/g celecoxib-loaded gel was demonstrated using  $\mu$ CT-scanning, where no cartilage or bone changes were observed following injection into the knee joints of healthy rats. Thus, celecoxib-loaded acetyl-capped PCLA-PEG-PCLA hydrogels form a safe drug delivery platform for sustained intra-articular release.

To further evaluate the potential of the system for local drug delivery within the knee, the pharmacokinetics of celecoxib released from a gel after intra-articular administration in horses was studied in **Chapter 6** [14]. The gel was loaded with two dosages of celecoxib (50 mg/g and 260 mg/g), and sterilized by autoclaving without significant polymer hydrolysis. After intra-articular injection in joints of healthy horses, the gel induced a transient inflammatory response for 72 hours, which is similar to the control injection of Hyonate®, a commercially available hyaluronic acid gel used for intra-articular administration in horses. After injection of the gel loaded with the high dose celecoxib, the horses showed some slight signs of discomfort 24 hours after injection, which however completely disappeared 72 hours after injection. Importantly, there was no indication of damage of the cartilage. Celecoxib was detected in the joints at a concentration of 20  $\mu$ g/ml at 8 hours after injection and its concentration decreased progressively in 4 weeks. Celecoxib was also detected in plasma at concentrations of 150 ng/ml for 3 days after administration and thereafter dropped below the detection limit. These results show that the systems allow for sustained intra-articular levels of celecoxib for 4 weeks with only very low and short systemic

exposure to the drug, demonstrating that these injectable *in situ* forming hydrogels are promising vehicles for intra-articular administration of non-steroidal anti-inflammatory drugs.

## 2. Discussion and perspectives

The main topic of this thesis was the development and evaluation of an injectable *in situ* forming gel made of acylated PCLA-PEG-PLCA copolymers for the local and sustained release of celecoxib, which is to date the drug of choice for the treatment of OA (**Chapter 1**). As shown in this thesis, the advantageous properties of gels composed of acylated PCLA-PEG-PCLA copolymers is the straightforward preparation and the versatility in the rheological and degradation/release properties as well as ease of injection and good tolerability/biodegradability. Rheological and degradation/release properties can easily be modulated by the polymer composition and microstructure (**Chapter 2 & 3** [9,11]). The ease to modulate properties combined with the possibility of functionalizing the end groups with, for instance, iodine-containing groups allowing longitudinal imaging by computed tomography shows that the systems have potential for *in vivo* applications (**Chapter 4** [12]). Also, celecoxib is released from the gel in a sustained manner after subcutaneous injection in rats (**Chapter 5** [13]) and also locally after intra-articular injection in horses (**Chapter 6** [14]). The systemic exposure and duration is low and short and, plasma concentrations are a factor 150-330 lower than the levels in synovial fluid. This demonstrates clearly the potential of the system for local drug delivery with relatively high local drug concentrations and very low systemic leaching.

Thus, we have designed celecoxib-loaded gels with good tolerability after intra-articular administration in rats and horses as well the ability for local and sustained release of celecoxib for 4 weeks, which should allow less frequent administrations than the systems currently available for the intra-articular treatment of OA [15-17]. Based on human as well as veterinary clinical practice, one can expect to achieve therapeutically effective concentrations of celecoxib in the joint at 100-1000 fold lower total dosing levels than oral dosing. For comparison, typical oral delivery of Celebrex® is set at 200-600 mg/day celecoxib, whereas our system is currently set at 50 to 260 mg celecoxib per injection, with the potential to release the drug for

14 to 30 days. For a drug such as celecoxib, localized delivery has also great advantages to (i) limit the impact of side effects, and (ii) reduce or avoid drug-drug interactions and improve patient compliance issues, which are often an issue with elderly patients suffering from several comorbidities/chronic diseases and taking several drug treatments systemically.

However, further studies are required before this system can be brought to a clinical phase for the treatment of OA.

### *2.1. In vitro/in vivo correlation*

In Chapter 4 and 5 [12,13], the *in vitro* and *in vivo* degradation of unloaded systems ('placebos') and the release kinetics of celecoxib from a gel loaded with 50 mg/g celecoxib were studied. The degradation of the depots and release kinetics of celecoxib are different *in vitro* and *in vivo*. On one hand, the degradation of the depots is likely influenced by differences in gel depot geometry between *in vitro* and *in vivo* set-up as well as by the *in vivo* active (enzymatic) degradation. On the other hand, the release of celecoxib *in vivo* is also likely influenced by the enhanced celecoxib solubility in biological fluids (e.g., due to its high protein binding). It will therefore be important to gain knowledge to predict *in vivo* performance of the system by designing an *in vitro* model that better mimics *in vivo* conditions. Taking into account that the two main parameters that we identified as critical to influence *in vivo* degradation/release mechanism, are the active enzymatic degradation of the polymer and the enhanced solubility of celecoxib, one could consider adding esterases [18] and plasma proteins in the degradation/release medium used for the *in vitro* experiments to affect the degradation mechanism of the gels and the release of celecoxib. In parallel, an *in vitro* model with a flow-through cell could also serve to better mimic the *in vivo* situation [19,20].

### *2.2. Preclinical pharmacokinetics and pharmacodynamics studies*

Beyond the scope of this thesis, the efficacy of the local and sustained delivery of celecoxib into osteoarthritic joints needs to be investigated. However, the pathogenesis of OA is not fully understood, and thus there is neither a validated animal model available nor known biomarkers that can be used to study the pharmacodynamics of new treatments [21,22]. Therefore, it

is difficult to carry out preclinical studies to measure pharmacodynamics and thus to show efficacy in an animal model. So, it could be possible to go directly from preclinical safety and PK studies to Phase I studies in (horse) patients.

The approach described in this thesis was to design a new dosage form with a different route of administration and in a different dosage regimen for celecoxib, which is already commercially available as tablet under the trade name Celebrex® for the treatment of OA. Therefore, the designed celecoxib-loaded systems can be considered as “Supergenerics” [23]. This means that the required preclinical package can be simplified compared to that of a new drug. Hence, one could propose to perform comparative or even better cross-over pharmacokinetics studies, in which Celebrex® administration will be used as control. Likewise, the drug loading, injection volume and dose regimen could be adjusted to obtain celecoxib concentrations in the synovial fluid that match the concentration observed with Celebrex®. For such a study, the dog will be the animal model of choice as the correlation between celecoxib bioavailability in dogs and humans is known [24]. In addition, an efficacy study in patient horses or dogs, which are diagnosed with spontaneous OA [22], with lameness score as read out parameter, could also be considered. Nevertheless, this kind of study with patient animals is long lasting due to limitations in the recruitment of the animals and the pros and cons of such study need to be well defined in advance.

### 2.3. Preclinical safety studies

Polyester/PEG block copolymers are extensively investigated in the drug delivery field since there are made of well-accepted pharmaceutical excipients, even though controversial findings around the immunogenicity of PEG have been reported [25]. However, clinical experience with these copolymers is limited [6,26], and they are therefore considered as novel excipients. Hence a thorough safety package needs to be generated before a drug delivery system based on these polymers can be brought to the clinic [27-31]. For instance, a preclinical safety program should be composed of *in vitro* and *in vivo* studies to ensure the non-toxicity of the system [29,32].

#### 2.4. Quality by Design (QbD)

Quality by Design (QbD) is a systemic approach to pharmaceutical development, for which the international conference on harmonisation of technical requirements for registration of pharmaceuticals for human use (ICH) issued the guidelines Q8, Q9 and Q10. It means designing and developing formulations and manufacturing processes to ensure a science-based pharmaceutical quality assessment and a build-in quality of the product [33-35].

In the framework of this thesis, we pinpointed critical material attributes of the system that influence its performance like the CL sequence length, which is affected by the synthesis procedure (temperature, batch size), and which impacts the crystallization behaviour and thus the degradation time of the gel.

Amongst the various perspectives offered by *in situ* forming gels made of acyl-capped PCLA-PEG-PCLA triblock copolymers, the fact that no polymer chemical degradation *in vitro* is observed is remarkable. In the past decade, drug delivery system development has focused its attention on the design of biodegradable carriers, which often contain water-hydrolysable ester bonds. The consequences and advantages brought by this absence of chemical polymer degradation of the systems should be further explored.

The strategy that we followed in this thesis to thoroughly understand each property of the system, fits the requirements of the QbD approach. In future development steps to bring the system to the clinic, it will be important to continue identifying the manufacturing processes (e.g., scale-up of the synthesis, loading of the polymers with celecoxib, preparation of the system, dosage form, sterilisation, shelf-life and injection system for instance using pre-filled syringes [36]) with the same eagerness of understanding root causes of all data.

#### 2.5. Improvements for the next generation product

Besides, the studies needed to bring the system to the clinic, one should also investigate how to improve the performance of the system for further applications. Mainly, OA is a chronic disease, which progresses in time and thus, the patients need to be treated for their life expectancy. Multiple intra-articular injections can be deleterious for the integrity of the joints [15,37,38].



The system described and investigated in this thesis is already longer lasting than other systems but it is important to consider extending the release duration further. For instance, in Chapter 3 [11], we prepared gels with 9 months *in vitro* degradation duration. These long-lasting gels should be tested *in vivo* for their extended degradation and release duration, which would be a way to further lower the administration frequency.

Also, the gels of this thesis are very suitable for formulation and release of hydrophobic drugs. However, potential drug candidates, like biologics have in general good aqueous solubility. Therefore, further investigation is required to make the gels suitable for hydrophilic drugs. In Chapter 2 [9], we prepared gels that phase separated and are therefore likely less suitable as delivery vehicle of hydrophilic drugs including biotherapeutics. On the other hand, the systems described in Chapter 3, 4 & 5 [11-13] showed large gel windows without phase separation at 37 °C. These systems might be suitable for protein delivery, which remains to be further explored [39].

### 3. Conclusion

It can be concluded that *in situ* forming gels made of acyl-capped triblock copolymers described in this thesis, due to their easy to modulate properties, are attractive candidates for a broad range of drug delivery applications. We have shown in this thesis the proof of principle in both small and large animals to sustained and localized release by incorporating a ‘Block Buster drug’ into novel micelle-based injectable drug depots, which results in a ‘Supergeneric’ new dosage form with attractive clinical and commercial features. We believe that these systems can find their way towards clinical applications and, in particular for the local treatment of OA.

## References

- [1] Edwards SHR. Intra-articular drug delivery: the challenge to extend drug residence time within the joint. *Vet J* 2011;190:15-21.
- [2] Gulati N, Gupta H. Parenteral drug delivery: a review. *Recent Pat Drug Deliv Formul* 2011;5:133-145.
- [3] Wanakule P, Roy K. Disease-responsive drug delivery: the next generation of smart delivery devices. *Curr Drug Metab* 2012;13:42-49.
- [4] Gong C, Qi T, Wei X, Qu Y, Wu Q, Luo F, et al. Thermosensitive polymeric hydrogels as drug delivery systems. *Curr Med Chem* 2013;20:79-94.
- [5] Pillay V, Seedat A, Choonara Y, du Toit L, Kumar P, Ndesendo VM. A review of polymeric refabrication techniques to modify polymer properties for biomedical and drug delivery applications. *AAPS PharmSciTech* 2013;14:692-711.
- [6] Elstad NL, Fowers KD. OncoGel® (ReGel®/paclitaxel) - clinical applications for a novel paclitaxel delivery system. *Adv Drug Deliv Rev* 2009;61:785-794.
- [7] Jo S, Kim J, Kim SW. Reverse thermal gelation of aliphatically modified biodegradable triblock copolymers. *Macromol Biosci* 2006;6:923-928.
- [8] Yu L, Zhang H, Ding J. A subtle end-group effect on macroscopic physical gelation of triblock copolymer aqueous solutions. *Angew Chem Int Ed Engl* 2006;45:2232-2235.
- [9] Petit A, Müller B, Bruin P, Meyboom R, Piest M, Kroon-Batenburg LMJ, et al. Modulating rheological and degradation properties of temperature-responsive gelling systems composed of blends of PCLA-PEG-PCLA triblock copolymers and their fully hexanoyl-capped derivatives. *Acta Biomater* 2012;8:4260-4267.
- [10] Petit A, Bruin P, de Leeuw M, Meijboom R. Biodegradable compositions suitable for controlled release. Patent No. WO2012EP55998, 2012.
- [11] Petit A, Müller B, Meijboom R, Bruin P, van de Manakker F, Versluijs-Helder M, et al. Effect of polymer composition on rheological and degradation properties of temperature-responsive gelling systems composed of acyl-capped PCLA-PEG-PCLA. *Biomacromolecules* 2013;14:3172-3182.
- [12] Sandker MJ, Petit A, Redout EM, Siebelt M, Müller B, Bruin P, et al. In situ forming acyl-capped PCLA-PEG-PCLA triblock copolymer based hydrogels. *Biomaterials* 2013;34:8002-8011.

- [13] Petit A, Sandker M, Müller B, Meyboom R, van Midwoud P, Redout EM, et al. Celecoxib-loaded acetyl-capped PCLA-PEG-PCLA thermogels: *in vitro* and *in vivo* release behavior and intra-articular biocompatibility. Submitted
- [14] Redout EM, Petit A, van de Lest CH, Müller B, Meyboom R, van Midwoud P, et al. Sustained intra-articular release of celecoxib from *in situ* forming gels made of acetyl-capped PCLA-PEG-PCLA triblock copolymers in horses. Submitted
- [15] Hunter DJ. In the clinic. Osteoarthritis. Ann. Intern. Med. 2007;147:ITC18-1-ITC18-16.
- [16] Bahadır C, Onal B, Dayan V, Gürer N. Comparison of therapeutic effects of sodium hyaluronate and corticosteroid injections on trapeziometacarpal joint osteoarthritis. Clin Rheumatol 2009;28:529-533.
- [17] Larsen SW, Frost AB, Østergaard J, Thomsen MH, Jacobsen S, Skonberg C, et al. *In vitro* and *in vivo* characteristics of celecoxib *in situ* formed suspensions for intra-articular administration. J Pharm Sci 2011;100:4330-4337.
- [18] Seyednejad H, Gawlitta D, Kuiper RV, de Bruin A, van Nostrum CF, Vermonden T, et al. *In vivo* biocompatibility and biodegradation of 3D-printed porous scaffolds based on a hydroxyl-functionalized poly( $\epsilon$ -caprolactone). Biomaterials 2012;33:4309-4318.
- [19] Brown CK, Friedel HD, Barker AR, Buhse LF, Keitel S, Cecil TL, et al. FIP/AAPS joint workshop report: dissolution/*in vitro* release testing of novel/special dosage forms. AAPS PharmSciTech 2011;12:782-794.
- [20] Lee TW, Boersen NA, Yang G, Hui HW. Evaluation of different screening methods to understand the dissolution behaviors of amorphous solid dispersions. Drug Dev Ind Pharm 2013 (DOI: 10.3109/03639045.2013.807279).
- [21] Teeple E, Jay GD, Elsaid KA, Fleming BC. Animal models of osteoarthritis: challenges of model selection and analysis. AAPS J 2013;15:438-446.
- [22] Gregory MH, Capito N, Kuroki K, Stoker AM, Cook JL, Sherman SL. A review of translational animal models for knee osteoarthritis. Arthritis 2012;2012:764621.
- [23] Stegemann S, Klebovich I, Antal I, Blume HH, Magyar K, Németh G, et al. Improved therapeutic entities derived from known generics as an unexplored source of innovative drug products. Eur J Pharm Sci 2011;44:447.
- [24] Paulson SK, Vaughn MB, Jessen SM, Lawal Y, Gresk CJ, Yan B, et al. Pharmacokinetics of celecoxib after oral administration in dogs and humans: effect of food and site of absorption. J Pharmacol Exp Ther 2001;297:638-645.

- [25] Schellekens H, Hennink WE, Brinks V. The immunogenicity of polyethylene glycol: facts and fiction. *Pharm Res* 2013;30:1729-1734.
- [26] Lee JL, Ahn JH, Park SH, Lim HY, Kwon JH, Ahn S, et al. Phase II study of a cremophor-free, polymeric micelle formulation of paclitaxel for patients with advanced urothelial cancer previously treated with gemcitabine and platinum. *Invest New Drugs* 2012;30:1984-1990.
- [27] Osterberg RE, Demerlis CC, Hobson DW, McGovern TJ. Trends in excipient safety evaluation. *Int J Toxicol* 2011;30:600-610.
- [28] Steinberg M, Silverstein I. The use of unallowed excipients. *Int J Toxicol* 2003;22:373-375.
- [29] Baldrick P. Pharmaceutical excipient development: the need for preclinical guidance. *Regul Toxicol Pharmacol* 2000;32:210-218.
- [30] Robertson MI. Regulatory issues with excipients. *Int J Pharm* 1999;187:273-276.
- [31] Pifferi G, Restani P. The safety of pharmaceutical excipients. *Farmaco* 2003;58:541-550.
- [32] Zentner GM, Rathi R, Shih C, McRea JC, Seo M, Oh H, et al. Biodegradable block copolymers for delivery of proteins and water-insoluble drugs. *J Control Release* 2001;72:203-215.
- [33] Yu LX. Pharmaceutical quality by design: product and process development, understanding, and control. *Pharm Res* 2008;25:781-791.
- [34] McCurdy V. Quality by design. In: Houson I, editor. *Process Understanding: For Scale-Up and Manufacture of Active*, 2011. p. 1-16.
- [35] Suresh P, Basu PK. Improving pharmaceutical product development and manufacturing: impact on cost of drug development and cost of goods sold of pharmaceuticals. *J Pharm Innov* 2008;3:175-187.
- [36] Jezek J, Darton NJ, Derham BK, Royle N, Simpson I. Biopharmaceutical formulations for pre-filled delivery devices. *Expert Opin Drug Deliv* 2013;10:811-828.
- [37] Bellamy N, Campbell J, Robinson V, Gee T, Bourne R, Wells G. Intra-articular corticosteroid for treatment of osteoarthritis of the knee (Review). *Cochrane Database Syst Rev* 2006;19:CD005328.
- [38] Recommendations for the medical management of osteoarthritis of the hip and knee: 2000 update. *Arthritis Rheum* 2000;43:1905-1915.

- [39] Bruin P, Petit A, de Leeuw M, Piest M, Meijboom R. Biodegradable compositions suitable for controlled release. Patent No. WO2012EP55993, 2012.





## Appendices

**Nederlandse samenvatting**

**Résumé français**

**Curriculum vitae**

**List of publications**

**Acknowledgments**





## Nederlandse samenvatting

Het in dit proefschrift beschreven werk is onderdeel van een breder project, OAcontrol, dat werd gefinancierd door het Nederlandse publiek-private consortium Biomedical Materials (BMM). OAcontrol is gericht op het ontwikkelen van nieuwe behandelingen voor osteoartrose (OA). Binnen dit project was het doel van dit proefschrift om een afgiftesysteem te ontwikkelen voor de lokale en langdurige afgifte van medicijnen in het gewricht. Tijdens deze ontwikkeling moesten vele uitdagingen worden overwonnen, die gerelateerd zijn aan het ontwerp van de juiste formuleringen voor de afgifte van relevante geneesmiddelen en hun werkzaamheid en veiligheid *in vivo*. Verschillende injecteerbare geneesmiddeldragers zijn ontwikkeld om efficiënt geneesmiddelen in te sluiten en ze plaatselijk af te geven, zoals *in situ* vormende depots. Deze systemen zijn gericht op het verkrijgen van therapeutisch effectieve concentraties van het ingesloten geneesmiddel na lokale toediening gedurende lange tijd.

Onder de polymeren die gebruikt worden als basis voor deze geneesmiddeldragers, vormen polyester/PEG blokcopolymeren een grote en veelzijdige klasse van goed verdraagbare en biologisch afbreekbare polymeren met een breed scala aan fysisch-chemische eigenschappen. Zij zijn uitgebreid onderzocht als biomedische materialen voor diverse toepassingen, zoals implanteerbare medische materialen voor regeneratieve geneeskunde en de afgifte van geneesmiddelen. Amfifiele polyester/PEG blokcopolymeren vormen micellaire aggregaten in waterig milieu bij lage temperatuur. Wanneer deze aggregaten tot lichaamstemperatuur en boven hun kritische gel concentratie worden gebracht, transformeren ze in visco-elastische hydrogelen. Dergelijke systemen hebben klinische toepassingen gevonden als *in situ* vormende hydrogelen voor de afgifte van geneesmiddelen. Een interessant aspect is dat modificatie van de hydroxyl eindgroepen van polyester-PEG-polyester copolymeren de overgangstemperatuur van sol naar gel van deze systemen kan beïnvloeden. Daarom zijn de belangrijkste thema's van dit proefschrift de impact van deze invloed op de reologische eigenschappen en de afbraak-kinetiek van deze systemen te bestuderen en de mogelijkheden te onderzoeken om dergelijke systemen voor een lokale en gecontroleerde afgifte van geneesmiddelen in de gewrichten toe te passen. Het niet-steroïdale anti-inflammatoire geneesmiddel (NSAIG) celecoxib, dat voor

de palliatieve orale behandeling van osteoartrose wordt gebruikt, is gekozen als het geneesmiddel in de studies beschreven in dit proefschrift.

**Hoofdstuk 1** geeft een inleiding op de uitdagingen van de OA-therapie en een overzicht van temperatuurgevoelige hydrogelen gemaakt van polyester/PEG blokcopolymeren. In het bijzonder wordt aandacht gegeven aan een subklasse van geacyleerde poly( $\epsilon$ -caprolactone-*co*-lactide)-*b*-poly(ethyleenglycol)-*b*-poly( $\epsilon$ -caprolactone-*co*-lactide) (PCLA-PEG-PCLA) triblokpolymeren. Vervolgens worden het doel en de inhoud van dit proefschrift gepresenteerd.

In **Hoofdstuk 2** wordt de invloed van het mengen van een PCLA-PEG-PCLA triblokcopolymeer en zijn hexanoyl-eindgroep gefunctionaliseerde derivaten op het temperatuursafhankelijke geleergedrag en de modulatie van reologische en degradatie eigenschappen beschreven. Het vertroebelingspunt van de mengsels was afhankelijk van de mengverhouding en kon worden afgestemd tussen 15 en 40 °C voor mengsels die 15 tot 100 gewichts% eindgroep gefunctionaliseerd polymeer bevatten (en dus 85 tot 0 % van het ongefunctionaliseerd polymeer). Waterige systemen met een polymeergehalte tussen 20 en 30 gewichts% met 15 tot 25 gewichts% eindgroep gefunctionaliseerd polymeer vertoonden een sol-naar-gel overgangstemperatuur bij 10-20 °C en zijn dus interessant als injecteerbare gellen voor de afgifte van geneesmiddelen. De volledige afbraak van deze gellen bij pH 7,4 en 37 °C duurde ca. 100 dagen, afhankelijk van de mengverhouding en het initiële polymeergehalte. Interessant genoeg kwam de afbraak van de gellen niet door chemische polymeerhydrolyse maar door het oplossen van de polymeren. De aanpak van het mengen van ongefunctionaliseerde en hexanoyl-eindgroep gefunctionaliseerde polymeren om temperatuurgevoelige gellen te bereiden kent echter enkele beperkingen:

(i) de mengverhouding om temperatuurgevoelige gellen te bereiden is vrij smal

(ii) temperatuurgevoelige gellen bereid met deze werkwijze vertonen snel fasescheiding bij kamertemperatuur, wat hanteren lastig maakt en wat schadelijk kan zijn bij langdurige afgifte van water oplosbare geneesmiddelen omdat deze geneesmiddelen worden opgenomen in de polymeerarme fractie en dus initieel snel worden afgegeven.

(iii) deze systemen lossen op in ca. 3-4 maanden, afhankelijk van de mengverhouding en het initiële polymeergehalte, maar aanpassing van afbraakduur is zeer gewenst om de systemen op specifieke therapieën af te kunnen stemmen.

Om deze tekortkomingen te omzeilen, wordt de relatie tussen de samenstelling en de microstructuur van PCLA met de reologische en degradatie-eigenschappen onderzocht in **Hoofdstuk 3** via experimenteel ontwerpen. Acht polymeren met verschillende molecuulgewichten van PCLA, caproyl/lactoyl verhoudingen (CL/LA) en eindgroep gefunctionaliseerd met ofwel acetyl- ofwel propionyl-groepen werden gesynthetiseerd. Reologische en afbraak/oploseigenschappen van waterige systemen bestaande uit 25 gewichts% polymeren werden bestudeerd.  $^1\text{H}$  NMR analyse toonde aan dat de monomeersequentie in de PCLA-blokken niet volledig willekeurig was, waardoor er relatief lange CL sequenties optreden, ondanks dat transesterificatie werd aangetoond door de verrijking met lactoyl eenheden en de aanwezigheid van PEG-OH-eindgroepen. Behalve het meest hydrofiele polymeer, acetyl-eindgroep gefunctionaliseerd PCLA<sub>1400</sub>-PEG<sub>1500</sub>-PCLA<sub>1400</sub> met een CL/LA molverhouding van 2,5, vormden alle polymeren van 25 gewichts% in buffer sols onder kamertemperatuur en gelen tussen kamertemperatuur en 37 °C, waardoor ze geschikt zijn als temperatuurgevoelige systemen voor de afgifte van geneesmiddelen. Binnen enkele weken bij 37 °C werden de systemen met polymeren met lange CL sequenties (ca. 8 CL eenheden) en propionyl eindgroepen semi-kristallijn zoals bleek uit röntgendiffractie analyse. De afbraakduur van de gelen door oplossing bij pH 7,4 en 37 °C was 100 tot 150 dagen voor de amorfe gelen en 250 tot 300 dagen voor de semi-kristallijne gelen. Dit hoofdstuk toont dus aan dat het veranderen van de polymeersamenstelling een gemakkelijke manier is om de reologische en degradatie-eigenschappen van het systeem te beïnvloeden.

Om meer inzicht in de verdraagbaarheid en biologische afbraak van *in situ* vormende hydrogelen van acyl-eindgroep gefunctionaliseerd PCLA-PEG-PCLA copolymeren te krijgen, werden polymeren gefunctionaliseerd met triiodobenzoyl (TIB) eindgroepen om zo radiopaque systemen te bereiden in **Hoofdstuk 4**. TIB eindgroep functionalisering gaf de gel radiopaque eigenschappen, waardoor de *in vivo* visualisatie en kwantificatie met behulp

van micro-computertomografie ( $\mu$ CT) mogelijk was. Een gel die TIB-eindgroep gefunctionaliseerd polymeer bevat degradeerde *in vitro* (37 °C, pH 7,4) door oplossen gedurende ca. 20 weken en iets sneller (ca. 12 weken) na subcutane injectie bij ratten. Deze *in vivo* versnelling kwam waarschijnlijk door actieve (enzymatische) degradatie, zoals aangetoond door veranderingen in polymeersamenstelling en molecuulgewicht en door de aanwezigheid van macrofagen op de injectieplaats. Na intra-articulaire toediening bij ratten verloor de gevisualiseerde gel geleidelijk signaalintensiteit in de loop van 4 weken. Ook werd goede cytocompatibiliteit van een hydrogel gebaseerd op acetyl-eindgroep gefunctionaliseerd polymeer aangetoond *in vitro* voor erythrocyten en chondrocyten. Bovendien werd de intra-articulaire verdraagbaarheid van deze gel aangetoond middels  $\mu$ CT-beeldvorming en histologie, aangezien beide technieken geen veranderingen in kraakbeenkwaliteit en/of kwantiteit lieten zien.

In **Hoofdstuk 5** werden de *in vitro* en *in vivo* eigenschappen en prestaties van een celecoxib-geladen hydrogel gebaseerd op volledig acetyl-eindgroep gefunctionaliseerd PCLA-PEG-PCLA triblokcopolymeer onderzocht. Mengsels van verschillende samenstellingen van celecoxib en acetyl-eindgroep gefunctionaliseerd PCLA-PEG-PCLA triblokcopolymeer in buffer vormden temperatuurgevoelige systemen. Deze systemen met maximaal 50 mg celecoxib per gram gel waren sols bij kamertemperatuur en werden omgezet in gelen bij 37 °C. De *in vitro* afgifte van celecoxib begon na een vertragingfase van ca. 10 dagen, gevolgd door een gecontroleerde afgifte van ca. 90 dagen. Celecoxib afgifte werd *in vitro* gemedieerd door het oplossen van polymeer uit de gelen. *In vivo* experimenten (subcutane injectie bij ratten) toonden een celecoxib afgifte aan van ca. 25 % van de belading gedurende de eerste 3 dagen gevolgd door een vertraagde afgifte van celecoxib gedurende 30 tot 60 dagen. Het ontbreken van een vertragingfase *in vivo* en de snellere afgifte zijn mogelijk te verklaren door de verhoogde oplosbaarheid van celecoxib in biologische vloeistoffen en de actieve afbraak van de gelen door enzymen en/of macrofagen, respectievelijk. Tenslotte is de intra-articulaire verdraagbaarheid van een 50 mg/g celecoxib beladen gel aangetoond middels  $\mu$ CT-beeldvorming, waarbij geen kraakbeen of botveranderingen werden waargenomen na injectie in de kniegewrichten van gezonde ratten. Zulke acetyl-eindgroep gefunctionaliseerde PCLA-PEG-

PCLA hydrogelen geladen met celecoxib vormen dus een veilig geneesmiddelaafgiftesysteem voor langdurige intra-articulaire afgifte.

Om het potentieel van het systeem voor lokale afgifte in de knie verder te evalueren, werd de farmacokinetiek van de celecoxibgel na intra-articulaire toediening bij paarden onderzocht in **Hoofdstuk 6**. De gel werd beladen met twee doseringen celecoxib (50 mg/g en 260 mg/g), en gesteriliseerd door autoclaveren zonder significante polymeerhydrolyse. Na intra-articulaire injectie in gewrichten van gezonde paarden, induceerde de gel een tijdelijke ontstekingsreactie gedurende 72 uur, vergelijkbaar met de controle injectie van Hyonate®, een commercieel verkrijgbare hyaluronzuurgel voor intra-articulaire toediening bij paarden. Na injectie van de gel met de hoge dosis celecoxib vertoonden paarden lichte tekenen van ongemak 24 uur na injectie, die echter geheel verdwenen 72 uur na injectie. Belangrijk is dat er geen aanwijzingen voor beschadiging van het kraakbeen werden gezien. Celecoxib werd gedetecteerd in de synoviale vloeistof met een concentratie van 20 µg/ml 8 uur na injectie en de concentratie daalde geleidelijk in 4 weken. Celecoxib werd ook gedetecteerd in plasma met concentraties van 150 ng/ml gedurende 3 dagen na toediening, waarna de concentraties daalden tot onder de detectiegrens. Deze resultaten tonen aan dat gedurende 4 weken relevante intra-articulaire niveaus van celecoxib worden bereikt met slechts zeer lage en korte systemische blootstelling aan het geneesmiddel, waaruit blijkt dat deze injecteerbare *in situ* vormende hydrogelen veelbelovende systemen voor intra-articulaire toediening van niet steroïdale anti-inflammatoire geneesmiddelen zijn.

Het belangrijkste onderwerp van dit proefschrift was de ontwikkeling en evaluatie van een injecteerbare *in situ* vormende gel gemaakt van geacyleerde PCLA-PEG-PCLA copolymeren voor de lokale en langdurige afgifte van celecoxib, dat het meest geschikte geneesmiddel is voor de behandeling van osteoartrose (**Hoofdstuk 1**). Zoals in dit proefschrift is aangetoond, zijn de voordelige eigenschappen van deze gelen de eenvoudige voorbereiding en de veelzijdigheid van de reologische en afbraak/afgifte-eigenschappen, het gemak van injectie en de goede verdraagbaarheid/biologische afbreekbaarheid. Reologische en afbraak/afgifte-eigenschappen kunnen gemakkelijk gevarieerd worden via de polymeersamenstelling en microstructuur (**Hoofdstuk 2 & 3**). Het gemak om de systeemeigenschappen aan te passen gecombineerd met de

mogelijkheid van het functionaliseren van de eindgroepen met bijvoorbeeld jodium-bevattende groepen geeft potentieel voor *in vivo* longitudinale beeldvorming van de systemen door computertomografie (**Hoofdstuk 4**). Ook is celecoxib afgegeven uit de gel gedurende langere tijd na subcutane injectie bij ratten (**Hoofdstuk 5**) en alsmede plaatselijk na intra-articulaire injectie bij paarden (**Hoofdstuk 6**). De systemische blootstelling is laag en kort en de plasma concentraties zijn een factor 150 tot 330 lager dan de niveaus in de gewrichtsvloeistof. Dit toont duidelijk het potentieel aan van het systeem voor de lokale afgifte van geneesmiddelen met relatief hoge lokale concentraties van geneesmiddelen en zeer lage systemische blootstelling.

Zo hebben we gelen geladen met celecoxib ontworpen met een goede verdraagbaarheid na intra-articulaire toediening bij ratten en paarden en de mogelijkheid voor lokale en langdurige afgifte van celecoxib gedurende 4 weken, die minder frequent toegediend hoeven te worden dan de systemen die momenteel beschikbaar zijn voor de intra-articulaire behandeling van OA. Gebaseerd op de menselijke alsmede de veterinaire klinische praktijk, kan men therapeutisch effectieve concentraties van celecoxib in het gewricht verwachten met 100- tot 1000-voudig lagere totale dosering niveaus gedurende 4 weken, terwijl minder frequent toegediend hoeft te worden dan met de systemen die momenteel bestaan voor orale toediening. Ter vergelijking is een typische orale afgifte van Celebrex® ingesteld op 200-600 mg/dag celecoxib, terwijl ons systeem momenteel is ingesteld op 50 tot 260 mg celecoxib per injectie, met de potentie om het geneesmiddel af te geven voor 14 tot 30 dagen. Voor een geneesmiddel zoals celecoxib heeft gelocaliseerde afgifte ook grote voordelen: (i) beperking van de gevolgen van bijwerkingen, en (ii) verminderen of voorkomen van geneesmiddelinteracties met verhoogde patiënten compliance, wat vaak een probleem is bij oudere patiënten met comorbiditeit/verschillende chronische ziekten die het slikken van een aantal verschillende geneesmiddelen vereisen.

## Résumé français

Le travail décrit dans cette thèse fait partie du projet OAcontrol financé par le consortium public-privé néerlandais Biomedical Materials (BMM). OAcontrol visait à développer de nouveaux traitements de l'ostéoarthrose (OA). L'objectif de cette thèse y était de développer un système pour la délivrance locale et prolongée de principes actifs dans les articulations. De nombreux défis devaient être surmontés dont la conception de formulations appropriées pour la délivrance des principes actifs d'intérêt, et la démonstration de leur efficacité et de leur tolérance *in vivo*. Plusieurs systèmes injectables ont déjà été conçus et étudiés dans ce but, notamment des dépôts formés *in situ*.

Parmi les polymères utilisés pour préparer ces dépôts formés *in situ*, les copolymères à blocs polyester/PEG constituent une classe importante et diversifiée de polymères bien tolérés et dégradables avec un large éventail de propriétés physico-chimiques. Ils ont été largement étudiés comme matériaux biomédicaux pour différentes applications telles que dispositifs médicaux implantables, ou en tant que supports en ingénierie tissulaire et pour l'administration de principes actifs. Les copolymères à blocs à base de polyester/PEG amphiphiles forment des suspensions micellaires en milieu aqueux à basses températures. Lorsque ces suspensions sont portées à la température corporelle et au-dessus de leur concentration critique de gel, elles se transforment en hydrogels viscoélastiques. Ces systèmes ont trouvé des applications cliniques en tant que gels formés *in situ* pour la délivrance de principes actifs. Fait intéressant, la modification des groupes hydroxyles terminaux des copolymères polyester-PEG-polyester permet une modulation de la température de transition sol-gel de ces systèmes. Par conséquent, l'un des principaux thèmes de cette thèse était de mieux comprendre l'impact de cette modification sur leurs propriétés rhéologiques et leur cinétique de dégradation et de déterminer si ces systèmes permettraient l'administration locale et prolongée de principes actifs dans les articulations. Dans les études décrites dans la présente thèse, le principe actif anti-inflammatoire non stéroïdien (AINS), célécoxib, qui est utilisé pour le traitement oral palliatif de l'OA, a été choisi comme principe actif.

Le **Chapitre 1** présente une introduction aux défis de la thérapie de l'OA et un aperçu des systèmes gélifiants sensibles à la température composés de

copolymères à blocs de polyester/PEG. Une attention particulière est donnée à une sous-classe de copolymères triblocs acylés : les poly( $\epsilon$ -caprolactone-*co*-lactide)-*b*-poly(éthylène glycol)-*b*-poly( $\epsilon$ -caprolactone-*co*-lactide) (PCLA-PEG-PCLA).

Le **Chapitre 2** est consacré au mélange d'un copolymère tribloc de PCLA-PEG-PCLA avec son dérivé hexanoylé et aux effets sur la température de gélification et sur les propriétés rhéologiques et de dégradation. On a montré que l'apparition de turbidité dépend de la composition et varie entre 15 et 40 °C pour les mélanges contenant 15 à 100 % en poids de polymère hydroxylé (et donc de 85 à 0 % de polymère hexanoylé). Les systèmes aqueux avec des teneurs en polymère comprises entre 20 et 30 % en poids contenant 15 à 25 % en poids de polymère hydroxylé ont montré une température de transition sol-gel entre 10 et 20 °C et forment donc des gels injectables intéressants pour l'administration de principes actifs. La dégradation complète de ces gels à pH 7.4 et à 37 °C prend environ 100 jours, indépendamment du ratio de mélange et de la teneur initiale en polymère. Fait intéressant, la dégradation du gel n'est pas due à l'hydrolyse chimique du polymère, mais à la dissolution du polymère. L'intérêt de mélanger des polymères hydroxylés et hexanoylés pour préparer des systèmes gélifiants sensibles à la température est toutefois limité car :

(i) la gamme des compositions qui permet d'obtenir des systèmes gélifiants sensibles à la température est restreinte

(ii) les systèmes gélifiants thermosensibles obtenus par ce procédé montrent une séparation de phase rapide à température ambiante, ce qui rend leur manipulation difficile. Cette séparation de phase pourrait être préjudiciable à la prolongation de la délivrance de principes actifs hydrosolubles car de tels principes actifs pourraient se partitionner préférentiellement dans les fractions pauvres en polymères et être libérés très rapidement (burst effect).

(iii) ces systèmes se dissolvent en environ 3-4 mois, indépendamment du ratio de mélange et la teneur initiale en polymère, alors que la modulation de la durée de dégradation est fortement souhaitée pour remplir les exigences spécifiques des traitements.

Pour contourner ces inconvénients, l'effet de la composition et de la microstructure du PCLA sur les propriétés rhéologiques et sur la dégradation



ont été étudiées dans le **Chapitre 3**, en utilisant un plan d'expériences. Huit copolymères composés de PCLA de différentes masses moléculaires de PCLA et différents rapports capryl/lactyl (CL/LA) acylés avec des groupes propionyles ou des groupes acétyles ont été synthétisés. Les propriétés rhéologiques et la dégradation/dissolution de systèmes aqueux composés de ces polymères à une concentration de 25 % en poids ont été étudiées. Les analyses RMN  $^1\text{H}$  ont montré que la séquence des monomères dans les blocs PCLA n'était pas entièrement aléatoire, ce qui se traduit par des séquences de CL relativement longues, même si la transestérification est démontrée par l'enrichissement en unités LA et la présence de groupes terminaux PEG-OH. À l'exception du polymère le plus hydrophile composés de PCLA<sub>1400</sub>-PEG<sub>1500</sub>-PCLA<sub>1400</sub> acétylé avec un rapport molaire CL/LA de 2,5 tous les polymères à 25 % en poids dans du tampon étaient sous forme sol à des températures inférieures à l'ambiante et se transformaient en gels à des températures comprises entre la température ambiante et 37 °C, ce qui est favorable pour la délivrance de principes actifs. Après plusieurs semaines à 37 °C, les systèmes contenant des polymères avec de longues séquences de CL (environ 8 unités CL) et avec des groupes terminaux propionyles sont devenus semi-cristallins, comme l'a démontré l'analyse par diffraction aux rayons X. La dégradation des gels par dissolution à pH 7,4 et à 37 °C a duré 100 à 150 jours pour les gels amorphes et 250 à 300 jours pour les gels semi-cristallins. En conclusion, ce travail montre que des changements dans la composition des polymères permet une modulation facile de la thermosensibilité et de la dégradation.

Pour obtenir plus d'information sur la tolérance et la dégradation des hydrogels formés *in situ* à base de copolymères PCLA-PEG-PCLA acylés, un polymère a été acylé avec du triiodobenzoyl (TIB) afin de préparer des systèmes radio-opaques dans le **Chapitre 4**. Le groupe TIB donne des propriétés radio-opaques aux gels, ce qui permet leur visualisation *in vivo* et leur quantification à l'aide de micro-tomographie ( $\mu\text{CT}$ ). Un gel contenant un polymère acylé avec du TIB s'est dégradé *in vitro* (37 °C, pH 7,4) par dissolution sur une période d'environ 20 semaines et un peu plus rapidement (environ 12 semaines) après injection sous-cutanée chez le rat. Cette accélération *in vivo* est probablement due à une dégradation active (enzymatique), représentée par les changements dans la composition et la

masse moléculaire des polymères résiduels dans les explants ainsi que de par la présence de macrophages au site d'injection. Après administration intra-articulaire chez le rat, le gel visualisé par  $\mu$ CT a perdu progressivement son intensité de signal en 4 semaines. En outre, la bonne cytocompatibilité d'un hydrogel à base de polymère acétylé a été prouvée *in vitro* pour des érythrocytes et des chondrocytes. Aussi, la tolérance intra-articulaire de ce gel a été démontrée en utilisant l'imagerie  $\mu$ CT et l'histologie, puisque ces deux techniques n'ont révélé aucun changement dans la qualité et/ou la quantité du cartilage.

Dans le **Chapitre 5**, les performances d'un hydrogel à base de copolymère de PCLA-PEG-PCLA entièrement acétylé contenant du célécoxib ont été étudiés *in vitro* et *in vivo*. Des mélanges de différentes compositions en célécoxib et en copolymère ont été préparés dans un tampon pour obtenir des systèmes thermosensibles. Ces systèmes contenant jusqu'à 50 mg de célécoxib par g de gel étaient sous forme sol à température ambiante et transformés en gel immobile à 37 °C. La délivrance *in vitro* du célécoxib a commencé après une phase de latence d'environ 10 jours suivie d'une libération prolongée d'environ 90 jours. Le relargage de célécoxib a été démontré *in vitro* comme étant due à la dissolution du polymère. *In vivo* (injection sous-cutanée chez les rats), la délivrance du célécoxib a montré une libération initiale d'environ 25 % de la charge au cours des 3 premiers jours, suivie d'une libération prolongée de célécoxib de 30 à 60 jours. L'absence d'une phase de latence et la libération plus rapide observées *in vivo* sont probablement dues à la solubilité accrue du célécoxib dans les fluides biologiques et la dégradation active des gels par des enzymes et/ou des macrophages, respectivement. Enfin, la tolérance intra-articulaire du gel encapsulant du célécoxib à 50 mg/g, a été démontrée en utilisant l'imagerie  $\mu$ CT par l'absence de changement du cartilage ou des os après injection dans les genoux de rats sains. Ainsi, les hydrogels à base de PCLA-PEG-PCLA acétylés et encapsulant du célécoxib forment une plate-forme acceptable pour la délivrance intra-articulaire de ce principes actif.

Pour évaluer le potentiel du système de délivrance locale de principe actif dans le genou, la pharmacocinétique du célécoxib libérés d'un gel après administration intra-articulaire chez le cheval a été étudiée dans le **Chapitre 6**. Le gel a été chargé avec deux doses de célécoxib (50 mg/g et

260 mg/g), et stérilisé par autoclave sans hydrolyse significative du polymère. Après injection intra-articulaire dans les articulations de chevaux sains, le gel a induit une réponse inflammatoire transitoire pendant 72 heures, ce qui a aussi été observé après l'injection contrôle de Hyonate®, un gel d'acide hyaluronique disponible dans le commerce et utilisé pour administration intra-articulaire chez les chevaux. Après l'injection du gel contenant du célécoxib à la dose forte, les chevaux ont montré de légers signes d'inconfort 24 heures après l'injection, qui ont toutefois complètement disparus 72 heures après l'injection. Fait important, il n'y avait aucune indication de détérioration du cartilage montré par histologie. Le célécoxib a été détecté dans le fluide synovial à une concentration de 20 mg/ml 8 heures après l'injection et sa concentration a diminué progressivement en 4 semaines. Le célécoxib a également été détecté dans le plasma à des concentrations de 150 ng/ml pendant 3 jours après administration et par la suite a chuté en dessous de la limite de détection. Ces résultats montrent que les systèmes permettent des niveaux intra-articulaires soutenus de célécoxib pendant 4 semaines avec une exposition systémique au principe actif très faible et courte, ce qui démontre que ces hydrogels injectables formés *in situ* sont des véhicules prometteurs pour l'administration intra-articulaire de AINS.

Le thème principal de cette thèse était le développement et l'évaluation d'un gel injectable formé *in situ* à base de copolymères acylés de PCLA-PEG-PCLA pour la délivrance locale et durable de célécoxib, qui est à ce jour le principe actif de choix pour le traitement de l'OA (**Chapitre 1**). Comme le montre cette thèse, les avantages des gels composés de copolymères acylés de PCLA-PEG-PCLA sont une préparation simple et la polyvalence des propriétés rhéologiques et de dégradation/délivrance ainsi que la facilité d'injection et une bonne tolérance/biodégradabilité. Les propriétés rhéologiques et la dégradation/délivrance peuvent facilement être modulées par la composition des polymères et leur microstructure (**Chapitre 2 & 3**). La facilité de modulation des propriétés combinées avec la possibilité de fonctionnalisation des groupes terminaux avec, par exemple, des groupes contenant de l'iode qui permet l'imagerie par tomographie longitudinalement montre que les systèmes ont du potentiel pour des applications *in vivo* (**Chapitre 4**). En outre, le célécoxib est libéré à partir du gel d'une manière soutenue après l'injection sous-cutanée chez le rat (**Chapitre 5**) et aussi

localement après injection intra-articulaire chez le cheval (**Chapitre 6**). L'exposition systémique au célécoxib et sa durée sont faible et courte, et les concentrations plasmatiques sont un facteur 150 à 330 fois inférieures aux niveaux dans le liquide synovial. Cela démontre clairement le potentiel du système pour délivrance de principe actif avec des concentrations locales relativement élevées et une très faible exposition systémique.

Ainsi, nous avons conçu des gels chargés en célécoxib avec une bonne tolérance après administration intra-articulaire chez le rat et le cheval ainsi que la possibilité pour la délivrance locale de célécoxib pendant 4 semaines, ce qui devrait permettre des administrations moins fréquentes que les systèmes actuellement disponibles pour le traitement intra-articulaire de l'ostéoarthrose. Basé sur des données chez l'homme ainsi que sur la pratique clinique vétérinaire, on peut s'attendre à obtenir des concentrations thérapeutiques efficaces de célécoxib dans l'articulation avec des doses de 100 à 1000 fois plus faibles que pour une administration orale. A titre de comparaison, l'administration orale typique de Celebrex® est fixée de 200 à 600 mg de célécoxib par jour, alors que notre système est actuellement fixé de 50 à 260 mg de célécoxib par injection, avec la possibilité de délivrance du principe actif sur 14 à 30 jours. Pour un principe actif tel que le célécoxib, une délivrance locale a aussi de grands avantages pour (i) limiter l'impact des effets secondaires, et (ii) réduire ou éviter les problèmes d'interaction entre traitements et d'adhérence clinique, ce qui est souvent le cas avec les patients âgés souffrant de plusieurs comorbidités/maladies chroniques et qui prennent plusieurs traitements médicamenteux oraux.

## Curriculum vitae

Audrey Petit was born on June 5<sup>th</sup> 1980 in Baccarat, France. After an education in Classes Préparatoires in Chemistry, Biology, Physics and Earth Sciences, she entered the Ecole Nationale Supérieure de Chimie de Montpellier in 2003. Two year later, she carried out an one-year industrial internship at Octoplus, Leiden (The Netherlands) under the supervision of Dr. Delphine Ramos. The main theme of her work was to invent a process to prepare nanoparticles based on acrylated dextran for drug delivery. Thereafter, she worked as Erasmus student for one year at Utrecht Institute for Pharmaceutical Sciences (UIPS) in the Department of Psychopharmacology in the group of Prof.dr. Berend Olivier. There, she got familiar with *in vivo* techniques and she completed a research study on the effects of several neurotransmitters on the impulsive behaviour in mice, a project that was part of a broader research project on attention deficiency hyperactivity disorder (ADHD). After obtaining her Master's degree in Chemistry (Diplôme d'ingénieur) in 2005, she became Researcher at DSM, Geleen (The Netherlands) where is invented a drug delivery platform based on biodegradable urethane-containing microparticles and was awarded as DSM Inventor in 2007. In 2008, she joined Q-Chip, Cardiff (United Kingdom) as Delivery Scientist to supervise analytical activities related to the controlled drug delivery of peptides. In 2009, she joined Mike de Leeuw at Branching Tree, Maastricht (The Netherlands) to carry out a Biomedical Materials (BMM) project. This project became in 2010 the project of her PhD studies in a joint effort between Ingell Labs, Groningen (The Netherlands) and the Department of Pharmaceutics of UIPS under the supervision of Prof.dr.ir. Wim E. Hennink as well as Dr.ir. Tina Vermonden and Dr. Leo G.J. de Leede. The results of her doctoral work are presented in this thesis.

At present, Audrey works as Principal Investigator at MedinCell, Montpellier (France) in the development of a drug delivery platform based on PEG/PLA copolymers.



## List of publications

### Research articles

Everaldo M Redout\*, **Audrey Petit\***, Chris H van de Lest, Benno Müller, Ronald Meyboom, Paul van Midwoud, Tina Vermonden, Wim E Hennink, P René van Weeren. Sustained intra-articular release of celecoxib from *in situ* forming gels made of acetyl-capped PCLA-PEG-PCLA triblock copolymers in horses. Submitted. \* Authors with equal contribution.

Tim WGM Spitters, Dimitrios Stamatialis, **Audrey Petit**, Mike GW de Leeuw, Marcel Karperien. Delivery of small molecules from a drug delivery system into articular cartilage is dependent on synovial clearance and cartilage loading. Submitted.

**Audrey Petit\***, Marjan J Sandker\*, Benno Müller, Ronald Meyboom, Paul van Midwoud, Everaldo M Redout, Chris H van der Lest, Sytze J Buwalda, Leo GJ de Leede, Tina Vermonden, Robbert Jan Kok, Harrie Weinans, Wim E Hennink. Celecoxib-loaded acetyl-capped PCLA-PEG-PCLA thermogels: *in vitro* and *in vivo* release behavior and intra-articular biocompatibility. Submitted. \* Authors with equal contribution.

Marian J Sandker, **Audrey Petit\***, Everaldo M Redout, Michiel Siebelt, Benno Müller, Peter Bruin, Ronald Meyboom, Tina Vermonden, Wim E Hennink, Harrie Weinans. *In situ* forming acyl-capped PCLA-PEG-PCLA triblock copolymer-based hydrogels. *Biomaterials* 2013; 34:8002–8011. \* Authors with equal contribution.

**Audrey Petit**, Benno Müller, Ronald Meijboom, Peter Bruin, Frank van de Manakker, Marjan Versluijs-Helder, Leo G. J. de Leede, Albert Doornbos, Mariana Landin, Wim E. Hennink, Tina Vermonden. Effect of polymer composition on rheological and degradation properties of temperature-responsive gelling systems composed of acyl-capped PCLA-PEG-PCLA. *Biomacromolecules* 2013;14:3172-82.

**Audrey Petit**, Benno Müller, Peter Bruin, Ronald Meyboom, Martin Piest, Loes MJ Kroon-Batenburg, Leo GJ de Leede, Wim E Hennink, Tina Vermonden. Modulating rheological and degradation properties of temperature-responsive gelling systems composed of blends of PCLA-PEG-PCLA triblock copolymers and their fully hexanoyl-capped derivatives. *Acta Biomater* 2012;8:4260-4267.

*Other publications*

**Audrey Petit**, Mike de Leeuw, Leo GJ de Leede, Wim E Hennink. Injectable drug depots are coming of age for controlled delivery, IPI 2010 (<http://issuu.com/mark123/docs/ipi-summer-2010-ejournal>).

*Patents*

Peter Bruin, **Audrey Petit**, Mike de Leeuw, Martin Piest, Ronald Meijboom. Biodegradable compositions suitable for controlled release. EP20110002675 20110331.

**Audrey Petit**, Peter Bruin, Mike de Leeuw, Ronald Meijboom. Biodegradable compositions suitable for controlled release. EP20110002676 20110331.

Aylvin JAA Dias, Peter Bruin, **Audrey Petit**. Method for preparing polymeric matrices by radiation in the presence of sensitive pharmaceutical compounds, US2010068252 (A1).

Aylvin Dias, Mark J Boerakker, Jerome Lebouille, Tessa Kockelkoren, **Audrey Petit**. Particles comprising polymers with thioester bonds, WO2009EP55086 (A1).

Aylvin Dias, Bart JJM Plum, **Audrey Petit**, Tristan Handels. Microparticles comprising cross-linked polymer, WO2009040434 (A1).



Aylvin JAA Dias, **Audrey Petit**. Microparticles comprising cross-linked polymer, WO2007107358 (A1).

*Selected abstracts*

Marta Spis, Laurence Feraille, Sophie Antonelli, Nicolas Cimbolini, Pierre-Paul Elena, Georges Gaudriault, **Audrey Petit**. Biocompatibility of MedinGel biodegradable drug delivery system in the eye. ARVO, Orlando, USA, May 4-8, 2014 (poster).

Marjan J Sandker\*, **Audrey Petit\***, Peter Bruin, Ronald Meyboom, Michiel Siebelt, Wim E Hennink, Harrie H Weinans. Intra-articular drug delivery through an *in situ* gelling system. OARSI, Philadelphia, USA, April 18-21, 2013. Osteoarthritis Cartilage 2013;21;S63-S312. \* Authors with equal contribution (poster).

**Audrey Petit**, Benno Müller, Peter Bruin, Ronald Meyboom, Martin Piest, Tina Vermonden, Wim E Hennink. Modulating the rheological properties of hydrogels composed of blends of hydroxyl- and hexanoyl-PCLA-PEG-PCLA triblock copolymers. The 39th Annual Meeting & Exposition of the Controlled Release Society, Quebec, Canada, 14-18 July, 2012 (poster).

**Audrey Petit**, Benno Müller, Peter Bruin, Ronald Meyboom, Martin Piest, Leo GJ de Leede, Tina Vermonden, Wim E Hennink. Blends of hydroxyl- and hexanoyl-terminated PCLA-PEG-PCLA triblock copolymers: effect of mixing ratio on the rheological properties. 12th European Symposium on controlled drug delivery (ESCDD), Egmond aan Zee, The Netherlands, April 4, 2012 (poster).

**Audrey Petit**, Ronald Meyboom, Peter Bruin, Martin Piest, Leo GJ de Leede, Mike GW de Leeuw, Wim E Hennink. Injectable gels for the treatment of osteoarthritic knees. BMM/TeRM Annual Meeting, Ermelo, The Netherlands, May 24-25, 2011 (lecture).

**Audrey Petit**, Peter Bruin, Leo GJ de Leede, Mike GW de Leeuw, Seongbong Jo, Wim E Hennink. Injectable gels for the treatment of intervertebral disc diseases. BMM/TeRM Annual Meeting, Ermelo, The Netherlands, April 14-15, 2010 (poster).

**Audrey Petit**, Iris KM Cheung, Owen Shadick, Xiai Zhao, Daniel D Palmer. Production by Microfluidics of Monodisperse PLGA Microparticles for the Sustained Release of Leuprolide Acetate. 36th Annual Meeting & Exposition of the Controlled Release Society, Copenhagen, Denmark, July 18-22, 2009 (poster).

**Audrey Petit**, Tristan WYTH Handels, Bart JM Plum, Aylvin A Dias. Biodegradable Polyurethane (meth)acrylate microparticles as controlled drug delivery system. 35th Annual Meeting & Exposition of the Controlled Release Society, New York, USA, July 12-16, 2008 (lecture).

**Audrey Petit**, Tristan WYTH Handels, Bart JM Plum, Sjoerd van der Wal, Aylvin A Dias. Polyurethane (meth)acrylate microparticles as controlled drug delivery system of small molecules. Crossing Frontiers in Biomaterials and Regenerative Medicine, 8th World Biomedical Congress, Amsterdam, The Netherlands, May 28-June 1, 2008 (poster).

## **Acknowledgements**

Ohlala! Here we are 5th of April 2014, four weeks before the defence of my thesis and the last pages of my book to finish. The weather is getting good, the day are getting longer, the flowers are blooming, it will be soon the beginning of the bank holiday period and I get the opportunity to finalise one big chapter of my life. Indeed, this doctoral work was a big chapter that started five years ago, or perhaps even eleven years ago when I first came to The Netherlands to work on drug delivery systems (DDSs). So many amazing people met during that time that it is difficult to know how to start with the acknowledgements because as Einstein wrote in 'The world as I see it' (1949): 'A hundred times every day I remind myself that my inner and outer life depend on the labours of other men, living and dead, and that I must exert myself in order to give in the same measure as I have received and am still receiving'.

First of all, I believe I should thank Dr. Delphine Ramos, Dr. Leo LG de Leede that gave me the opportunity to specialize during my studies in DDS and made me meet Prof.dr.ir. Wim E Hennink and his acolyte Mies van Steenberghe. Or, perhaps I should start thanking Dr. Aylvin Dias, Dr Sjoerd van der Wal and Mike de Leeuw that gave me the tools and the spirit to invent a novel platform for DDS and the idea that I should carry out a doctoral work, 'a first own enterprise' as Aylvin describes it. But concretely, the most two important people without who this work would not be here: Mike and Wim.

Mike: I remember as if it was yesterday that we had this call five years ago to start this unusual adventure: BMM, the consortium you inspired, gave you the opportunity to participate, to properly launch InGell as well as to develop products in Orthopaedics, and you gave me in turn the opportunity to carry out my doctoral work. The idea was still vague, but our collaborator clearly chosen: the must and worldwide-known academic DDS expert/entrepreneur Wim.

Wim: how to thank for all you taught me! ... Besides what I still need to learn (e.g., stop making floppy mistakes), I learnt so much thanks to you. I knew since years that doing my doctoral work with you as promoter would be the best approach, but I did not realized at that time what it would mean. Now that I think about it I believe it can be summarized in a couple of take-

home messages: (i) stop making only observational work, (ii) interpret the data, (iii) be strict and don't let any details left. Also, I understand what Descartes described in 'Discourse on the method' and I hope you appreciated the 'clin d'oeil' on page 5 of this thesis (even though I felt obliged to keep it in French). The result of this extensive work with you as a coach is obvious: five papers, amongst which three in Biomaterials, hopefully. Thank you to allowing me to have team up with you and for all the time you have spent for the (at least) twenty editing of each chapter. One thing I still need to learn though is how to avoid making floppy mistakes. I know you taught me: 'no excuses, it is just impossible'. But, floppy mistakes in the lab remain the best way for filing patents, don't they? ... However, since Summer 2011, I understood thank to you that we needed to publish and thus produce with rigueur and Benno Müller came on time to help for that.

Benno: As Leo said you were the perfect trainee to come and work on my research or less politely the perfect 'slave' to generate the data for my thesis. You are the man in the shadow in this whole story but your data and your name are in all the papers of this work. You joined at the right time, I was busy since 1.5 years with the BMM projects, we had filed the patents, the experimental methods were developed and starting to get robust (after I repeated them all twice), it was time to really start working on publication. The outline of each chapter was ready, the data need to be produced 'only'. InGell was becoming InGell and the golden prison of Groningen was awaiting for me and your motivation to make the story happen. You made it, week after week you started to produce degradation and release data. Everything was running, you could perform the rheology measurements, starting to have more time to understand the technology. Just 6-month internship but the data for a thesis: thanks! Everything got ready on time to start the *in vivo* experiments in Rotterdam where Marjan was awaiting.

Marjan: a 50/50 collaboration in which you were responsible of the *in vivo* work and I was responsible of the *in vitro* work, but also a 50/50 time with 50 % of great time in front of the scanner trying to see this radiopaque gel and 50 % of the time of this endless editing of two papers. Thank you a lot for this productive input that allowed OAgel to be tested in horses by Everaldo.

Everaldo and Janny: Excuse my French, but I think the best part of the work with you was to get these f... stinky horse legs at the slaughter and spent Friday afternoon making them 'walked'... I don't think I will ever forget that time. Thanks!

This is without forgetting: Leo, Mies and Tina

Leo: in the small world of the (dutch) DDS, it was amazing when Mike told me five years ago that you were joining the InGell adventure.

Mies: always here, always making sure the apparatus are running, the methods correct, the memory of 25 years working with Wim and his many AIOs.

Tina: always discrete, smiling, collecting nicely grants; the opposite of Wim in many sense, but the right balance to work with him and publish great and greater papers. 'Shall you or I click on the 'submit' bottom?'

Many thanks to the three of you!

To the other co-authors of the work described in this thesis and, in particular Robbert Jan, Rene and Harrie: also a big thank for the expertise you brought to this work!

Also, dear Ingell team\*, dear Innocore team\*, dear UU team\*, and dear Polyvation team\*: thank you a lot for the positive spirit that made me succeed!

Et pour finir: chers amis et collègues de Vertical\*, de Montpellier, de Jacou et ma chère famille, je vous remercie du fond du cœur pour le support que vous m'avez apporté.

*\* Feliz, Neda, Sytze, Luis, Yang, Isil, Roy, Markus, Niels, Nathaniel, Martin, Myriam ×2, Ben, Avy, Amelie ×2, Luisa, Johan, Maarten, Arjen, Albert, Cristine, Rob, Jan, Ronald, Peter, Theo: Het was gezellig. Bedankt & tot ziens!*